

## Durham E-Theses

---

# *CO-PRODUCTION OF HYDROGEN, METHANE AND SILICA FROM RICE STRAW USING ANAEROBIC DIGESTION AND THERMAL TREATMENT PROCESSES IN AN INTEGRATED ENERGY SYSTEM*

EKWENNA, EMEKA, BONIFACE

### How to cite:

---

EKWENNA, EMEKA, BONIFACE (2022) *CO-PRODUCTION OF HYDROGEN, METHANE AND SILICA FROM RICE STRAW USING ANAEROBIC DIGESTION AND THERMAL TREATMENT PROCESSES IN AN INTEGRATED ENERGY SYSTEM*, Durham theses, Durham University. Available at Durham E-Theses Online: <http://etheses.dur.ac.uk/14300/>

### Use policy

---

The full-text may be used and/or reproduced, and given to third parties in any format or medium, without prior permission or charge, for personal research or study, educational, or not-for-profit purposes provided that:

- a full bibliographic reference is made to the original source
- a [link](#) is made to the metadata record in Durham E-Theses
- the full-text is not changed in any way

The full-text must not be sold in any format or medium without the formal permission of the copyright holders.

Please consult the [full Durham E-Theses policy](#) for further details.

---

Academic Support Office, The Palatine Centre, Durham University, Stockton Road, Durham, DH1 3LE  
e-mail: [e-theses.admin@durham.ac.uk](mailto:e-theses.admin@durham.ac.uk) Tel: +44 0191 334 6107  
<http://etheses.dur.ac.uk>

---

**CO-PRODUCTION OF HYDROGEN, METHANE AND SILICA FROM  
RICE STRAW USING ANAEROBIC DIGESTION AND THERMAL  
TREATMENT PROCESSES IN AN INTEGRATED ENERGY SYSTEM**

---

**EKWENNA EMEKA BONIFACE**

**A Thesis submitted for the degree of Doctor of Philosophy (PhD.)**



**Department of Engineering  
Ustinov College  
The University of Durham**

**November 2021**



## Abstract

The response to electricity inadequacies and waste management issues in Nigeria is projected to be achieved by designing and employing an integrated energy system in predominantly farm communities to complement the traditional fossil energy. Although the design of the energy unit encompasses detailed aims, the primary objective of the research study is "A solution to Nigeria's energy challenges with hydrogen and methane co-produced from pretreated rice straw in a three-stage anaerobic digestion process and to calculate the energy value of the produced biogas via the combined cooling, heat and power strategy". These research objectives were achieved using acidogenic and methanogenic processes in batch, semi-continuous and continuous systems after pretreating rice straw with mechanical and chemicals/agro-industrial wastes followed by a biological agent. At the same time, silica precursors were produced from the various RS digestate using a thermal procedure, while the energy assessments were done using data from the laboratory study and the literature. The research findings indicated that

- At acidogenesis stage, hydrogen yield was insignificant when chemical agents and agro-industrial wastes were employed alone. However, the daily H<sub>2</sub> production increased when the pre-treated (PT) RS residues were biologically hydrolysed with NaOH-PT samples (114 NmL H<sub>2</sub> g<sup>-1</sup> TS d<sup>-1</sup>) and PE-PT RS residues (103 NmL H<sub>2</sub> g<sup>-1</sup> TS d<sup>-1</sup>) having the highest values at steady states and raw RS producing the least (30 NmL H<sub>2</sub> g<sup>-1</sup> TS d<sup>-1</sup>).
- Mechanical and chemical/agro-industrial wastes pre-treatments followed by enzymatic hydrolysis of RS improved the daily specific methane production by 18%, 31.7% and 41.5% for HCL, PE and NaOH-PT RS residues than the raw RS (control) sample.
- In the methanogenesis phase, the methane production efficiency was 80% for NaOH, 75% for PE, 68% for HCL RS PT samples, while the control (raw RS) was 48%.
- Pre-treated and digested methanogenic RS ash samples contained amorphous silica materials confirmed by the scanning electron microscope, Energy-dispersive X-ray fluorescence spectrometer and X-ray diffraction results.

- Using the energy-integrated unit's PEIO data, the net energy (bio-methane, electricity, thermal and cooling) from Nigeria's RS annual yield was estimated. It was found that the net bio-methane at 1.6mpa ranged from 100 to 170 hm<sup>3</sup> if small scale processes were applied and 122 to 200 hm<sup>3</sup> when large scale operations were used. In the same vein, the predicted electricity produced in TWh available for use was within the range of 8.4 to 9.3. In addition, the net thermal energy available for use was between 12.7 to 13.4 TWh which gave 8.9 to 9.4 TWh of cooling fluid.
- Finally, whereas the *Firmicutes*, especially the *Clostridium*, *Ruminococcus* and *Thermoanaerobacterium* were the dominant microbial community in acidogenic digestates, the *Euryarchaeota* typified by *Methanobacterium*, *Methanosarcina* and *Methanosaeta* were the principal phyla for most methanogenic reactors

## Table of Contents

<b>Abstract</b> .....	<b>i</b>
<b>Table of Contents</b> .....	<b>iii</b>
<b>List of Tables</b> .....	<b>xi</b>
<b>List of Figures</b> .....	<b>xiv</b>
<b>List and Definition of Abbreviations</b> .....	<b>xviii</b>
<b>Declaration</b> .....	<b>xxiii</b>
<b>Acknowledgements</b> .....	<b>xxiv</b>
<b>Dedication</b> .....	<b>xxv</b>
<b>Chapter 1 Introduction</b> .....	<b>1</b>
1.1 Aims and Objectives of the study .....	11
1.2 Thesis Structure and Layout .....	13
<b>Chapter 2 Literature Review</b> .....	<b>16</b>
2.1 Nigeria Energy Scenario .....	16
2.2 Rice Straw .....	20
2.3 Pre-treatment Technologies for Lignocellulose Rice Straw .....	23
2.4 Polysaccharides Hydrolysis .....	27
2.5 Empty Oil Palm Fruit Bunches Ash (Potash) .....	30
2.6 Cassava-steep Wastewater .....	31
2.7 Corn-steep Liquor .....	33
2.8 Anaerobic Digestion and Dark Fermentation Processes .....	34
2.8.1 Microbiology, <i>Process and Biochemistry</i> .....	34
2.8.2 Hydrogen Production .....	37
2.8.3 Methane Production (Methanogenesis) .....	41
2.9 Factors that affect Anaerobic Digestion/Fermentation Process .....	42
2.9.1 Process Temperature .....	43

2.9.2	Process pH .....	44
2.9.3	Un-dissociated Acids .....	46
2.9.4	Nitrogenous Sources .....	47
2.9.5	Capable Seeded Sludge. ....	48
2.9.6	Carbon Sources .....	52
2.9.7	Phosphate Sources .....	54
2.9.8	Trace Elements .....	54
2.9.9	Organic and Hydraulic Overload .....	57
2.9	Biogas Enrichment and Upgrading Processes .....	59
2.9.1	Processes for Removing Hydrogen Sulphide from Biogas.....	59
2.9.1.1	Oxidation by <i>Thiobacilli</i> and biological filters .....	60
2.9.1.2	Iron sulphate complexes .....	60
2.9.1.3	Activated carbon sieve .....	61
2.9.1.4	Water scrubbing .....	61
2.9.2	Technologies for Removal of Water Vapour .....	62
2.9.3	Technologies for Removal of Carbon Dioxide .....	63
2.9.3.1	Physical Absorption .....	63
2.9.3.1.1	Water scrubbing .....	63
2.9.3.1.2	Pressure swing adsorption .....	63
2.9.3.1.3	Membrane separation .....	64
2.9.3.1.4	Cryogenic separation .....	64
2.9.3.2	Chemical Absorption .....	65
2.9.3.2.1	Scrubbing with alkali .....	65
2.9.3.2.2	Scrubbing with amine solvents .....	65
2.9.4	Biological Technology .....	66
2.10	Biogas as a Fuel for Combined Heat and Power Applications .....	67



2.11	Electricity Production Using Combined Heat and Power Systems .....	68
2.12	Absorption Chillers for CHP Systems .....	70
2.13	Rice Straw Ash as Silica Precursor .....	72
2.13.1	Silica extraction processes .....	74
2.14	Research Framework and Multigeneration Energy System .....	78
<b>Chapter 3</b>	<b>Materials and Methods .....</b>	<b>81</b>
3.1	RS Collection and Preparation .....	81
3.2	Agro-industrial Wastes Collection and preparation .....	81
3.2.1	Potash collection and preparation of potash extract .....	81
3.2.2	Corn seed collection and preparation of corn-steep liquor .....	83
3.2.3	Cassava collection and preparation of cassava-steep wastewater .....	84
3.3	Measurement of Lignocellulose Composition of Rice Straw .....	84
3.4	Determination of the Elemental Composition of Rice Straw and Biomass Samples.....	85
3.5	Analytical Determination of Carbon, Hydrogen, Nitrogen, Oxygen and Sulphur Content in Rice Straw and Seeded Sludge .....	86
3.6	Determination of Rice Straw Energy Value .....	87
3.7	Seed Sludge Collection and Preparation .....	88
3.7.1	Sludge collection and residual incubation .....	88
3.7.2	Sludge pre-treatment for bio-hydrogen production .....	89
3.7.3	Sludge acclimatisation.....	89
3.8	Experimental Procedures .....	89
3.8.1	Batch/ fed-batch fermentation process for hydrogen fermentation .....	89
3.8.2	Batch/ fed-batch fermentation process for methanogenesis .....	91
3.8.3	Continuous anaerobic fermentation process .....	92
3.8.4	Continuous anaerobic methanogenesis .....	93
3.9	Biogas Measurement and Specific Content Analysis .....	93

3.10	Analytical Assays and Measurements .....	95
3.11	Genetic Extraction and Microbial Community Analysis .....	96
3.12	Kinetic and Statistical Analyses .....	97
<b>Chapter 4</b>	<b>Enrichment of seeded sludge using agro-industrial wastes for biological hydrogen production .....</b>	<b>100</b>
4.1	Introduction .....	100
4.2	Materials and Methods .....	104
4.2.1	Digested Cattle Slurry Pre-treatment for Bio-hydrogen Production .....	104
4.2.2	Experimental Design of the Hydrogen Fermentation Process .....	105
4.3	Results and Discussion .....	106
4.3.1	Seeded Sludge Characterisation .....	106
4.3.2	Characterisation of Agro-industrial Wastes .....	107
4.3.3	Effects of Pre-Treatments Technologies on Fermentative Hydrogen Production .....	107
4.3.3.1	Hydrogen production on glucose reactors .....	107
4.3.3.2	Hydrogen production on sucrose digesters .....	110
4.3.3.3	Biogas/hydrogen yield and average hydrogen content of the reactor samples.....	113
4.3.4	Total Volatile Fatty Acids Production from various Digested Cow Slurry .....	115
4.3.5	Microbial Community Composition .....	117
4.4	Conclusion .....	122
<b>Chapter 5</b>	<b>Biological hydrogen production from unhydrolysed raw rice straw co-digested with digested cattle slurry .....</b>	<b>125</b>
5.1	Introduction .....	125
5.2.1	Experimental Procedures .....	129
5.2.3.1	Batch and semi-continuous AD processes.....	129
5.2.3.2	Continuous Anaerobic Fermentation Process .....	129
5.3	Results and Discussion .....	131

5.3.1	Enrichment of Seeded Sludge from Different Feeding Systems .....	131
5.3.2	Enrichment of Seeded Sludge for Hydrogen Producers Using Glucose and Sucrose .....	133
5.3.2.1	Enrichment using a fed-batch system .....	133
5.3.2.2	Enrichment using continuous system .....	136
5.3.3	Hydrogen Production from Unhydrolysed RS Using Enriched Seeded Sludge .....	139
5.3.4	Microbial Community Composition.....	141
5.4	Conclusion .....	145
<b>Chapter 6</b>	<b>A solution to Nigeria's energy challenges with hydrogen and methane co-produced from agro-industrial pre-treated rice straw in three-stage anaerobic digestion processes .....</b>	<b>147</b>
6.1	Introduction .....	147
6.2	Materials and Methods .....	150
6.2.1	Preparation of Rice Straw Hydrolysate .....	151
6.2.1.1	Acid pre-treatment of rice straw .....	151
6.2.1.2	Base pre-treatment of rice straw .....	151
6.2.1.3	Potash extract pre-treatment of rice straw .....	152
6.2.2	Enzymatic Hydrolysis .....	152
6.2.3	Lignin Determination Test .....	153
6.2.4	Detoxification of the Filtrate .....	153
6.2.5	Hydrogen Fermentation Process (Stage 1 Process) .....	154
6.2.5.1	Batch fermentation process .....	154
6.2.5.2	Continuous fermentation process .....	154
6.2.6	Methane Digestion Process (Stage 2 and 3 processes) .....	155
6.2.6.1	Utilization of effluents (organic acids) and pretreated RS residues for methane production .....	155
6.2.7	Energy Value, Electricity, and Thermal Generation from Pretreated RS samples .....	157
6.3	Results and Discussion .....	159

6.3.2	Preparation of RS Hydrolysate .....	159
6.3.2.1	Pre-treatments of RS and de-lignification .....	159
6.3.2.2	Rice straw hydrolysates detoxification .....	164
6.3.2.3	Enzymatic hydrolysis of rice straw samples .....	165
6.3.3	Hydrogen Fermentation Process (Stage 1 Process) .....	168
6.3.4	Production of Short-Chain Fatty Acids .....	172
6.3.5	Production of Methane from Acidogenic Effluents (Stage 2 Process) .....	174
6.3.6	Production of Methane from Pretreated RS Residues (Stage 3 Process) .....	177
6.3.7	Materials Balance of the Three-Stage Digestion Processes .....	182
6.3.8	Energy Value, Electricity and Thermal Generation from various RS Samples .....	186
6.3.9	Microbial Community Analysis .....	189
6.4	Conclusion .....	194
<b>Chapter 7</b>	<b>The production of nano-silica precursors from agro-industrial wastes leached and anaerobically digested rice straws .....</b>	<b>197</b>
7.1	Introduction .....	197
7.2	Materials and Methods .....	200
7.2.1	Digestate Preparation from Acidogenic and Methanogenic Reactors .....	200
7.2.2	Preparation of Leached RS Using Agro-Industrial Wastes .....	200
7.2.3	Silica Preparation from Various Digestates and Leached Rice Straw Residues .....	200
7.2.4	Analyses of Raw Rice Straw and Rice Straw Ash .....	201
7.3	Results and Discussion .....	202
7.3.1	Characterisation of Agro-Industrial Wastes .....	202
7.3.2	Characterisation and Thermal Analysis of Rice Straw Samples .....	202
7.3.3	Rice Straw Ash (silica) Characterisation .....	204
7.3.3.1	Morphological and physical appearance of silica materials .....	205
7.3.3.2	Scanning electron images of silica precursors .....	206

7.3.4	Chemical Analysis of Rice Straw Ash (Silica Materials) .....	208
7.3.5	X-ray Powder Diffractometer Pattern Analysis .....	211
7.4	Conclusion .....	214
<b>Chapter 8 The energy assessment of the digestion processes and other post digestion processes in the integrated energy system .....</b>		<b>216</b>
8.1	Background of study.....	216
8.2	Methods and Expectations .....	218
8.3	Description of Scenarios .....	220
8.3.1	Feedstock Scenarios .....	220
8.3.2	Energy Conversion Scenarios .....	221
8.4	Statistics of Primary Energy Flow .....	222
8.4.1	Energy demand in the collection and transportation of feedstock .....	222
8.4.2	Energy input in pre-treatment of feedstock .....	223
8.4.3	Energy demand in biogas plant operation .....	224
8.4.4	Energy Demand in Post Anaerobic Digestion Processes .....	225
8.4.4.1	Energy input in silica production process .....	225
8.4.4.2	Energy demand from biogas utilisation .....	226
8.4.4.3	Energy input from biogas enrichment .....	228
8.5	Energy Output .....	228
8.5.1	Energy yield from biogas production .....	228
8.5.2	Energy output from gasification of silica .....	229
8.6	Results and Discussion .....	230
8.6.1	Energy Input for Anaerobic Digestion Processes .....	230
8.6.2	Energy Demand for Post Anaerobic Digestion Processes .....	233
8.6.3	Energy Balance of the Anaerobic Digestion Processes .....	235
8.6.4	Energy Balance of the Integrated Energy System .....	237

8.6.5	Net Energy Production from Rice Straw Annual yield in Nigeria .....	240
8.7	Conclusion .....	244
<b>Chapter 9</b>	<b>Final remarks and recommendation for further research work .....</b>	<b>247</b>
9.1	Final Remarks .....	247
9.2	Summary of Research Outcomes .....	248
9.3	Recommendations and Observation .....	250
<b>Appendices</b>	<b>.....</b>	<b>254</b>
<b>References</b>	<b>.....</b>	<b>260</b>

## List of Tables

Table 1-1: Energy resource type and reserves in Nigeria .....	3
Table 2-1: Effects of ammonium nitrogen concentration in an AD process.....	47
Table 3-1: Elemental composition of potash, RS and seeded sludge (activated digested sludge (ADS) and digested cow slurry (DCS)) .....	82
Table 3-2: Characterization of cassava-steep waste water and corn-steep liquor .....	84
Table 3-3: Cyanogenic Glucosides at 4 <sup>0</sup> C and RT .....	84
Table 3-4: Ultimate analysis of RS and seeded sludge (ADS and DCS) .....	86
Table 4-1: Characterisation of raw and pretreated digested cow slurry .....	104
Table 4-2: Elemental composition of potash extract and various digested cow slurry .....	106
Table 4-3: Kinetic parameters of hydrogen production from various PT DCS .....	109
Table 4-4: The distribution of associated VFA concentrations from DCS samples .....	116
Table 5-1: Analytical Assays of raw RS and seeded sludge .....	129
Table 5-2: Production of SCFA and consumption of ammoniacal nitrogen from various reactors .....	139
Table 6-1: Physicochemical properties of raw RS and seeded sludge .....	150
Table 6-2: Characterisation of some PT RS residues and untreated RS .....	152
Table 6-3: Operational parameters of hydrogen and methane fermentation processes .....	155
Table 6-4: Data for calculation of energy equivalents, electricity and thermal yield .....	158
Table 6-5: Analysis of raw and various PT RS filtrates .....	163
Table 6-6: Analysis of enzyme PT RS Hydrolysates .....	167
Table 6-7: Hydrogen and biogas yield using hydrolysates from various PT RS residues .....	171
Table 6-8: VFA, SCOD and Nitrogen content of reactor effluents and methane sludge .....	174
Table 6-9: CH <sub>4</sub> and biogas yield using acidogenic effluents from various PT RS residues .....	176
Table 6-10: Gompertz data for the methane production from different PT RS residues .....	179
Table 6-11: The purified gas and biogas yield (m <sup>3</sup> H <sub>2</sub> /CH <sub>4</sub> tonne <sup>-1</sup> TS added d <sup>-1</sup> and m <sup>3</sup> tonne <sup>-1</sup> TS added d <sup>-1</sup> ) from different PT RS samples produced via CSABR .....	185

Table 6-12: The energy value of the produced gases (purified and raw biogas) in m <sup>3</sup> and kg biogas per tonne RS .....	186
Table 6-13: The electricity (KWh <sub>elect.</sub> ) and thermal energy (KWh <sub>thermal</sub> ) generation produced from the corresponding energy values at the different stages of process .....	188
Table 7-1: Characterisation of CSWWs and CSTL .....	202
Table 7-2: The solid/thermogravimetric analysis of leached RS, various PT Digestates and raw RS samples .....	203
Table 8-1: Characterisation of some PT RS residues and untreated RS .....	220
Table 8-2: Technical data of medium-scale wood gasification plant HKA 45 .....	221
Table 8-3: The primary energy for collection and transport of feedstock from sources .....	222
Table 8-4: The energy demand for the transport of feedstock and digestate from/to the biogas plant .....	223
Table 8-5: The primary inputs for the pre-treatment and sterilisation of feedstock .....	223
Table 8-6: Energy input in biogas plant operation .....	224
Table 8-7: Energy input in dewatering, drying and pelletisation of digestate .....	225
Table 8-8: Efficiency and corresponding energy demand for CHP generation .....	227
Table 8-9: Estimated heat losses in transmitting the heat to absorption chillers .....	227
Table 8-10: Energy input in biogas enrichment .....	228
Table 8-11: Energy from different PT RS digestates obtained during silica production .....	229



## List of Figures

Fig 1-1: Model design of the integrated energy system .....	12
Fig 1-2: Thesis structure and layout .....	14
Fig 2-1: Total primary energy supply (TPES) .....	16
Fig 2-2: Total final energy consumption .....	17
Fig 2-3: Electricity generation by fuel .....	18
Fig 2-4: Total electricity consumption .....	19
Fig 2-5: A cellulose molecule showing both the dimeric and monomeric unit .....	23
Fig 2-6: Effect of pre-treatment of lignocellulosic biomass .....	24
Fig 2-7: Oil palm fruit in the bunch (a), being de-fruited from the bunch (b) and an empty bunch (c) .....	29
Fig 2-8: Preparation of cassava wastewater from locally made fufu (a and b) .....	31
Fig 3-1: Representation of prepared RS with (A) 750 $\mu\text{m}$ sized and (B) 2cm-sized .....	81
Fig 3-2: A - CSTL extractions (the incubation was done for two days at RT) and B – PE preparation...83	
Fig 3-3: CSWW extraction preparation before incubation at RT (A) and under ice (B) .....	83
Fig 3-4: Cyanogenic glucosides determination (different levels of cryogenic glucoside for CSWW samples in days) .....	84
Fig 3-5: Sludge residual incubation (degassing) of seed sludge (ADS and DCS) for 30 days .....	89
Fig 3-6: Construction and assembling of a typical digester bottle (c) with the rubber bungs (a and b). The image "b" was used for feeding in fed-batch processes .....	90
Fig 3-7: Batch fermentation of AD and AF process in an automated stirred incubator system .....	91
Fig 3-8: A continuous stirred anaerobic bioreactor setting for AD and AF processes (1 L) .....	92
Fig 3-9: A continuous stirred anaerobic bioreactor setting for AD and AF processes (5 L) .....	93
Fig 4-1: Pictorial representation of the enrichment of seeded sludge using agro-industrial wastes for biological hydrogen production .....	103
Fig 4-2: Hydrogen production using glucose as substrates by various PT DCS .....	108

Fig 4-3: Hydrogen production using sucrose as substrates by various PT DCS .....	111
Fig 4-4: Biogas/hydrogen yield and average hydrogen content of the various DCS from glucose .....	113
Fig 4-5: Biogas/hydrogen yield and average hydrogen content of the various DCS from Sucrose .....	114
Fig 4-6: The relative abundance of top 25 most abundant microbial communities at genus and phylum level of pretreated DCS samples .....	118
Fig 5-1: Biological hydrogen production from unhydrolysed raw rice straw co-digested with sugar-enriched digested cattle slurry .....	128
Fig 5-2: Daily hydrogen production from untreated RS using heat-shocked DCS .....	131
Fig 5-3: Biogas yield and hydrogen contents from untreated RS using heat-shocked DCS .....	132
Fig 5-4: The enrichment of heat-shocked DCS with glucose as the medium using fed-batch mode .....	133
Fig 5-5: The enrichment of heat-shocked DCS using sucrose as the medium using fed-batch mode .....	135
Fig 5-6: Enrichment of heat-shocked DCS using glucose as substrates at steady-state .....	137
Fig 5-7: The enrichment of heat-shocked DCS using sucrose as substrates at continuous mode .....	138
Fig 5-8: The biogas and hydrogen accumulation from the enriched heat-shocked DCS using either glucose or sucrose as substrates .....	138
Fig 5-9: Daily hydrogen production and hydrogen accumulation from Untreated RS .....	140
Fig 5-10: The relative abundance of top 25 most abundant microbial communities at genus and phylum level of the various digestates .....	142
Fig 6-1: Hydrogen and methane co-production from agro-industrial pre-treated enzymatically enhanced rice straw in a three-stage anaerobic digestion process .....	149
Fig 6-2: Some of the chemical--PT RS samples before filtration and detoxification .....	150
Fig 6-3: De-lignification of some chemical-PT RS samples represented as percentage lignin loss .....	159
Fig 6-4: SEM micrographs of raw RS (1) and various PT RS (2: HCl, 3: PE, 4: NaOH, 5: CSTL and 6: CSWW) samples .....	160
Fig 6-5: some PT RS samples (A: 2mm sized RS; B: Milled RS; C: NaOH-PT RS; D: HCl-PT RS; E: CSWW-PT RS; F: PE Solid PT; G: PE-PT RS samples) .....	161

Fig 6-6: Detoxified or filtered samples of some PT RS hydrolysates A: HCl-PT; B: NaOH-PT; C <sub>1</sub> : Control, C <sub>2</sub> : PE-PT; D: CSWW-PT) .....	163
Fig 6-7: Cellulase activity at various concentrations and durations. ....	166
Fig 6-8: Representative of RS hydrolysates after enzyme hydrolysis .....	167
Fig 6-9: Daily hydrogen production (mL g <sup>-1</sup> sugar-utilized) and hydrogen content (%) from enzymatically PT RS residues via batch mode .....	169
Fig 6-10: Daily hydrogen production (mL g <sup>-1</sup> sugar-utilized) and hydrogen content (%) from enzymatically PT RS residues via CSABR .....	170
Fig 6-11: The associated VFA production after DF H <sub>2</sub> fermentation for continuous systems .....	172
Fig 6-12: Fed-batch methane production from acidogenesis effluents (stage 2) after 3 HRTs .....	173
Fig 6-13: Continuous methane production from acidogenesis effluents (stage 2) .....	175
Fig 6-14: Specific methane yield and cumulative biogas production from different PT RS residues ("a". NaOH, "b" PE, "c" HCl and "d" Raw RS) using batch processes .....	178
Fig 6-15: Daily methane yield and cumulative biogas production from different PT RS residues at steady states for 60days .....	181
Fig 6-16: RS mass balance analysis of the three-stage fermentation process with different PT technologies .....	183
Fig 6-17: The relative abundance of top 25 most abundant microbial communities at genus and phylum level from acidogenic and methanogenic reactors .....	191
Fig 7-1: Production of amorphous silica from pre-treated RS digestates from AD reactors and from agro-industrial wastes leached RS .....	199
Fig 7-2: Various dried digestates (A: CSWW-L RS; B: CSTL-L RS; C: Water-L RS; D: HCl-PT RS; E: PE-PT RS; F: NaOH-PT RS; G: Untreated-PT RS; H: Digestate from hydrogen rector and I: Raw RS) .....	201
Fig 7-3: RSA (silica) preparation from (A: CSWW-L RS; B: CSTL-L RS; C: Water-L RS; D: Untreated-PT RS; E: HCl-PT RS; F: PE-PT RS; G: Raw RS; H: NaOH-PT RS and I: Digestate from hydrogen rector) .....	204

Fig 7-4: SEM micrograph of the different RSA samples (A: Untreated-PT RS; B: CSTL-L RS; C: CSWW-L RS; D: HCl-PT RS; E: NaOH-PT RS; F: PE-PT RS; G: Water-L RS; H: Digestate from hydrogen reactor and I: Raw RS) .....	206
Fig 7-5: The elemental composition of silica samples (A: Untreated-PT RS; B: CSTL-L RS; C: CSWW-L RS; D: HCl-PT RS; E: NaOH-PT RS; F: PE-PT RS; G: Water-L RS; H: Digestate from hydrogen reactor and I: Raw RS) .....	207
Fig 7-6: The elemental spread of RSA samples (A: Untreated-PT RS; B: CSTL-L RS; C: CSWW-L RS; D: HCl-PT RS; E: NaOH-PT RS; F: PE-PT RS; G: Water-L RS; H: Digestate from hydrogen reactor and I: Raw RS) with silica ion having the most concentration .....	209
Fig 7-7: The XRD spectra of RSA samples (A: Untreated-PT RS; B: CSTL-L RS; C: CSWW-L RS; D: HCl-PT RS; E: NaOH-PT RS; F: PE-PT RS; G: Water-L RS; H: Digestate from hydrogen reactor and I: Raw RS) .....	212
Fig 8-1: Summary of the life cycle of the integrated unit studied. The arrows indicate the flow of the energy and mass material in the unit .....	218
Fig 8-2: A typical pellets sample for use in a gasifier .....	226
Fig 8-3: Total energy inputs of all the processes involved in hydrogen and methane production.....	230
Fig 8-4: The percentages of the energy inputs of all the processes involved in hydrogen and methane production .....	231
Fig 8-5: Total energy inputs of post AD processes from various PT RS samples .....	232
Fig 8-6: The percentages of the energy inputs required in post AD processes from different PT RS samples .....	234
Fig 8-7: The percentages of the PEIO of the AD processes for the various PT RS samples .....	235
Fig 8-8: The proportions of the energy balances of the integrated system .....	237
Fig 8-9: The proportions of the energy balances of the integrated system when bio-methane is the end-use product .....	238
Fig 8-10: The total useful energy products of post AD processes from the various RS feedstock .....	240

Fig 8-11: Predicted net bio-methane production (million cubic meters) at 1.6mpa from Nigeria's annual RS yield (14.1 million tonnes) of the various RS feedstock ..... 241

Fig 8-12a: The estimated net electricity, thermal and cooling fluid using CHP and gasifier of the various RS samples from Nigeria annual RS yield of 14.1 million tonnes..... 242

Fig 8-12b: Combined net electricity, thermal and cooling fluid of the various RS samples from Nigeria annual RS yield of 14.1 million tonnes ..... 243

## List and Definition of Abbreviations

AD	Anaerobic digestion
AF	Anaerobic fermentation
ADP	Adenosine diphosphate
ADS	Activated digested sludge
AFEX	Ammonia-based or ammonium fibre explosion
ASV	Amplicon sequence variant
ATP	Adenosine triphosphate
BMP	Biochemical methane potential
BGDB	Borosilicate glass Duran bottle (s)
CBM	Compressed bio-methane
CH <sub>4</sub>	Methane gas
CCS	carbon capture and storage
CHP	Combined heat and power
CCHP	Combined cooling, heat and power
C/N ratio	Carbon-to-nitrogen ratio
CoA-H	Coenzyme A
COD	Chemical oxygen demand
CO	carbon monoxide
CO <sub>2</sub>	Carbon dioxide
COD	Chemical oxygen demand
COP	Cooling coefficient of performance
CASBR	Continuous stirred anaerobic bioreactor
CSTL	Corn-steep liquor
CSWW	Cassava-steep waste water
CSTR	Continuous stirred tank reactor (s)

Cum	Cumulative volume (mL)
DCS	Digested cattle slurry
DADA	Divisive amplicon deionising algorithm
DF	Dark fermentation
DM	Digestate Mixture
DNA	Deoxyribonucleic acid
ED	Entner-Doudoroff
EDX	Energy-dispersive X-ray fluorescence spectrometer
EPFB	Empty palm fruit bunch
EMP	Embden-Meyerhof-Parnas
FAN	Free ammonia nitrogen
F/M	Food to microbial
FOS	in German <i>Fluchtige Organische Säuren</i> (TVFA expressed in mg HAc L <sup>-1</sup> )
FOS: TAC	Ratio of TVFA to total alkalinity (Ripleys ratio in English)
GC	Gas chromatography
GHG	Greenhouse gases
GW	Gigawatts
GJ	Gigajoules
Gwh	Gigawatts-hour
HCB	Hydrogen-consuming bacteria
HPB	hydrogen-producing bacteria
HHV	Higher heating value
HMF	5-hydroxymethyl-2-furaldehyde
HRT	Hydraulic retention time
H <sub>2</sub>	Hydrogen gas
H <sub>2</sub> S	Hydrogen sulphide

IRB	Iron-reducing bacteria
kWh	Kilowatts-hour
LAB	Lactic acid bacteria
LCB	lignocellulose biomass
LCFA	Long-chain fatty acid (s)
LBM	Liquefied bio-methane
LCV	Lower calorific value
LHV	Lower heating value
LiP	lignin peroxidase
LPG	Liquefied natural gas
MPE	Methane production efficiency
MSW	Municipal solid waste
Mt	Metric tonnes
Mtoe	Million tonnes of oil equivalent
MW	Megawatts
MWh	Megawatts-hour
NAD <sup>+</sup>	nicotinamide adenine dinucleotide ion
NRB	Nitrate-reducing bacteria
N mL	Millilitres in normal condition (gas volumes at 0 °C and an atmospheric pressure of 101.3 kPa) OLR Organic loading rate
ODM	Organic digested matter
PCR	polymerase chain reaction
PE	Potash extract
PEG	Polyethylene glycol
PEIO	Primary energy input to output
PFL	Pyruvate: formate lyase



PFOR	Pyruvate: ferredoxin oxidoreductase
PT	Pre-treated
PV	Photovoltaics
QIIME	Quantitative Insights into Microbial Ecology
RS	Rice straw
RSA	Rice straw ash
SEM	Scanning electron microscope
SBP	Specific biogas production (biogas yield) is expressed in N mL Biogas.g <sup>-1</sup> VS of substrate added
SRB	Sulphate-reducing bacteria
SCFA	short-chain fatty acid (s)
SHY	specific hydrogen yield expressed in N mL
SMP	Specific methane production expressed in N mL CH <sub>4</sub> .gVS.added per day
SMY	specific methane yield expressed in N mL or L
TAC	in German Totales Anorganisches Carbonate (total alkalinity buffer expressed as mg. L <sup>-1</sup> of CaCO <sub>3</sub> ).
TAN	Total ammoniacal nitrogen
TBMP	Theoretical biochemical methane potential
TCOD	Total chemical oxygen demand
TPES	Total primary energy supply
TOC	Total organic carbon
TVFA	Total volatile fatty acid(s)
TWh	Terawatts-hour
TS	Total solid
VFA	Volatile fatty acid (s)
VHP	Volumetric hydrogen production (N mL)

VHPR	Volumetric hydrogen production rate (N mL)
VHY	Volumetric hydrogen yield (N mL)
VMP	Volumetric biogas production expressed in N mL CH <sub>4</sub> .L <sup>-1</sup> reactor volume. D <sup>-1</sup> VS
	Volatile solids content (VS=TS + ash)
VS	Volatile solids
VSS	Volatile suspended solids
WLP	Wood-Ljungdahl pathway
XRD	X-ray diffraction

## **Declaration**

The work in this study is based on my research carried out at the Departments of Engineering in Newcastle University (Cassie building and Stephenson Building) and the University of Durham, England UK. It is imperative to state that no part of this thesis has been submitted elsewhere for any other degree or academic qualification, and it is all my work unless referenced to the contrary in the text.

## **Copyright © 2021 Emeka Boniface Ekwenna**

"The copyright of this thesis rests with the author. No quotations from it should be published without the author's prior written consent. Also, information derived from it should be acknowledged."

## Acknowledgements

Most pertinently, I offer thanksgiving to God Almighty for His insight and grace in accomplishing this research study through His Mother Mary and my patron saints, St Boniface and Louis Marie de Montfort. I want to express my heartfelt gratitude to the government of Nigeria through Niger Delta Development Commission (NDDC), Nigeria, for providing me with the opportunity to undertake this PhD research study. My appreciation goes to my supervisors Prof. Anthony Roskilly, Dr Paul Sallis, Dr Abdullah Malik and Associate Prof. Yaodong Wang, whose guidance and advice during this research study have been invaluable.

A special thanks to the laboratory technicians at the school of Civil Engineering and Geosciences and SWAN centre (Mechanical Engineering) at Newcastle and Durham Universities for their hard work to ensure that my samples were analysed and provided the necessary chemicals and laboratory equipment for this study.

I would also appreciate my amiable father, Mr Ahunanya Boniface Ekwenna, and my lovely and peaceful mother, Mrs Egojiuka Victoria Ekwenna, for their perpetual support, encouragement, and prayers, especially during the most challenging times of my research study. I also thank my wife Obianuju Esther Ekwenna, my siblings Tochi, Nkechi, Odinaka, Chidiebere, and my sweet cousin Ugochi for their love and support.

To my late sister Chinenye who modelled me with great personality and charisma, I emphatically thank you. This PhD is dedicated to you and souls in purgatory.

Lastly, I would like to thank my inlaws, friend Nkechi, and colleagues for their love, constant care, and motivation.

## Dedication

I dedicate this thesis

To God the Father Almighty  
Maker of heaven and earth  
The beginning and the end

To God the Son  
Christ the Redeemer, who is always present in the Holy Eucharist

To God the Holy Ghost  
My Sanctifier, for His inspirations

To Mother Mary  
For Her perpetual guidance and maternal providence

And to Sts. Louis-mariae de Monfort and Boniface  
My patron saints



## Chapter 1 Introduction

Nigeria to remain energy independent and maintain her status as the largest crude oil producer in Africa and 11<sup>th</sup> in the world as it has been predicted that her oil reserve will be finishing in the next 40 years (International Energy Agency (IEA), 2016 and Nigeria Energy Market Report (NEMR, 2021)); there is need for sustainable alternative energy. This renewable option will complement fossil energy, fulfil the Paris and Glasgow agreements on carbon-cut, and boost the agro-economy through agriculture investment. Nigeria has about 37.5 billion barrels of proven oil reserves and 187- 193 trillion cubic feet of proven natural gas reserves according to the Organisation of Petroleum Exporting Countries (OPEC), making Nigeria the second-largest gas producer (Nigerian Energy Support Programme (NESP), 2015; Emodi and Boo, 2015, Ugwoke *et al.*, 2020 and NEMR, 2021). The crude oil production is between 1.8 to 2.4 million barrels per d (mb/d), with a projection of 3 mb/d by 2025 (NESP, 2015 and NEMR, 2021). Ironically, this abundance of fossil energy has not positively affected the cumulative energy development of Nigeria in the power and gas sectors. There still exist inadequacy of electricity and queues in gas-stations weekly due to insufficiency of energy products (gas and petrol), lack of necessary electrical infrastructures and extensive national grid coverage and expertise in the management of energy,

Furthermore, according to the World Bank Doing Business 2015 Report, Nigeria is ranked 187 of 189 countries in the ease of getting electricity (NESP, 2015). It takes about an averagely of 260 days to get a permanent electricity connection, and once connected, the electricity supply is unstable, averaging less than eight hours daily. The insufficiency in electricity supply invariably affects business, especially sales leading to losses.

Historically, about 96% of the electricity of Nigeria comes from hydro systems and gas plants. These systems are archaic, poorly maintained, and often manned by unsuited professionals (Newsom, 2012; Oyedepo *et al.*, 2018 and IEA, 2020). Due to these reasons, electricity in Nigeria has remained within the capacity range of 6.0 to 8.2 GW, which is insufficient (Garba and Zangina, 2015, NESP, 2015, Nigerian Electricity Regulatory Commission (NERC), 2018 and NEMR, 2021). The electricity demand is

projected to be around 180 GW due to industrialisation and development. This prediction was made by the global minimum average electricity consumption per capita for emerging economies put at 500 kWh (Usman and Abbasoglu, 2015 and Oyedepo *et al.*, 2018). Over the years, fossil fuels, mainly crude oil, have been utilised to satisfy these energy demands (Dong *et al.*, 2019 and 2020 and Zhang *et al.*, 2020). However, the most striking debate in the energy and environmental sector is producing environmentally friendly energy due to oil pollution and rising atmospheric carbon emissions from fossil-based energy sources (Ajimi *et al.*, 2015, Ghimire *et al.*, 2015, Muritala *et al.*, 2019, Zhang *et al.*, 2020 and Banu *et al.*, 2022). Scientific researchers have widely accepted that this increase in CH<sub>4</sub> and CO<sub>2</sub> levels impact greenhouse gases negatively (Banu *et al.*, 2022). In 2018 alone, the global CO<sub>2</sub> emissions were at 408.52 ppm, the highest level recorded in more than 800 000 years (Edward *et al.*, 2021). Also, fossil fuel contributes to climate change, environmental issues, and deaths (IEA, 2016; Oyedepo *et al.*, 2018 and Edwards *et al.*, 2021). For example, according to a report by Milieudefensie (2011), more than 400 000 tonnes of oil have been spilt either by human errors or ageing facilities into creeks and soils of southern Nigeria in the last 30 years, with about 70% of the oil not yet been remediated or recovered. In the same vein, BBC bulletin report, Nigeria is referred to as the world oil pollution capital in their bulletin report on Niger Delta in 2010 (Duffield, 2010). These spills have led to numerous environmental and health issues such as atmospheric warming, cancer and even deaths (Edwards *et al.*, 2021). Therefore, energy production from fossil may no longer be sustainable.

The unconventional renewable energy sources such as wind, hydro, solar, geothermal and oceanic are not with issues as they are capital intensive and demand a considerable infrastructure layout. Nigeria's energy resources and their corresponding potentials are summarised in Table 1-1.

Hence, various ways of producing energy from cheap and renewable sources are being researched and developed. Biomass, which is biologically originated materials such as forestry, agriculture, and organic waste, is the fourth largest energy source after coal, oil, and natural gas (Salakkam *et al.*,



2019). Biomass is an up-and-coming renewable energy technology because of its readily available and renewability. The term renewable is the source of the energy ability to be ecologically sustainable in its harvesting, conversion, and application (Elbeshbishy *et al.*, 2017). Energy sources from biomass can be obtained by burning, combustion, gasification, and pyrolysis. However, more recently, interests have been directed towards the anaerobic digestion (AD) of biomass to produce more refined and cleaner fuels (biofuels) in the gaseous, liquid, or solid forms (World Energy Council, 2016). The near carbon neutrality, cheap availability of biomass materials globally, and the solution to environmental problems (Cheng *et al.*, 2011a, Jiang *et al.*, 2011, World Energy Council, 2016 and Salakkam *et al.*, 2019) conveys biomass AD technology as a good energy source for the future.

Table 1-1: Energy resource type and reserves in Nigeria (extracted from Sambo, 2018 and Oyedepo *et al.*, 2018).

S/No	Resource Type	Reserves (Natural Units)	Product Level (Natural Units)	Utilisation (Natural Units)
1	Light crude oil	37.06 billion bbl (as of 2017)	2.5 million barrels/day (as of 2014)	316, 000 bbl/day (as of 2015)
2	Natural gas	5.284 trillion CUM (as of 2017)	45.15 billion CUM (as of 2014)	26.86 billion CUM (as of 2015)
3	Coal and Lignite	2.734 billion tonnes	Insignificant	Insignificant
4	Tar sands	31 billion barrels of oil equivalent	-	-
5	Large hydropower	11, 250 MW	1, 938 MW (167.4 million MWh/day)	167.4 million MWh/day
6	Small hydropower	3, 500 MW	30 MW (2.6 million MWh/day)	2.6 million MWh/day
7	Solar radiation	3.5 – 7.0 kWh/m <sup>2</sup> /day (485.1 million MWh/day using 0.1% Nigeria land area)	Excess of 240 kWp of solar PV or 0.01 million MWh/day	Excess of 0.01 million MW <sub>p</sub> /day of solar PV
8	Wind	2 – 4 m/s at 10m height	-	-
9	Biomass:			
	Fuel wood	11 million hectares of forest and wood land	0.110 million tonnes/day	0.120 million tonnes/day
	Animal waste	245 million assorted in 2001	0.781 million tonnes of waste/day in 2001	Not available
	Energy drops & Agric residue	72 million hectares of Agric land and all waste lands	Excess of 0.256 million tonnes of assorted crops residues/day in 1996	Not available
10	Nuclear element	Not yet quantified	-	-

The biomass reserve in Nigeria is shown in Table 1.1. Nigeria has about 20 to 21 million cattle (Food and Agriculture Organization Corporate Statistical Database (FAOSTAT), 2017) and generates about 0.59 million tonnes of digested cattle slurry (DCS) daily and approximately 215 million tonnes of cattle slurry annually. Consequently, Nigeria currently produces around 15 million tonnes of rice straw (RS) per year (FAOSTAT, 2017). These agricultural wastes can be used to make energy products such as hydrogen and methane using AD processes and solve numerous environmental pollution. The higher

heating value (HHV) of RS is from 14.02 to 15.03 MJ/kg ( Nguyen *et al.*, 2016, Biswas *et al.*, 2017 and Maguyon-Detras *et al.*, 2020), while DCS is employed because it contains high levels of varying microorganisms that have the capability of hydrolysing lignocellulose (Ward *et al.*, 2008). The benefit of biomass notwithstanding has some limitations: low yield of energy products, socioeconomic impacts, and high capital cost of pre-treatments technologies.

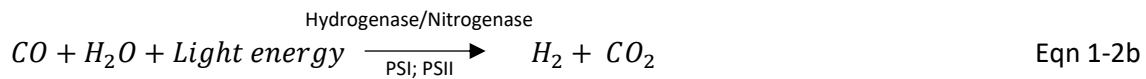
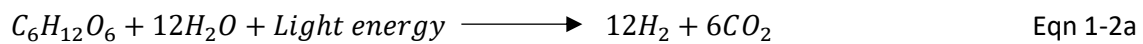
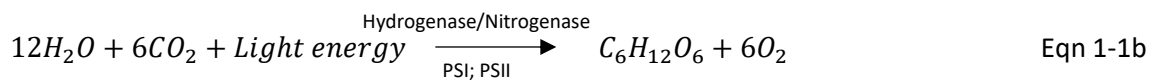
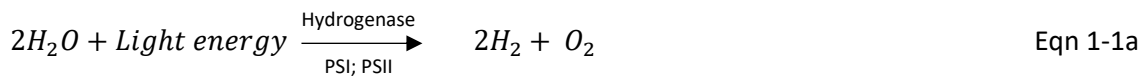
The conventional biogas processes have long been focusing on methane production. Nevertheless, in the past few years, hydrogen gas research and development have increased due to the positive attributes of hydrogen as an alternative low-carbon energy carrier (Edwards *et al.*, 2021 and Rosa and Mazzotti, 2022). The high energy content increased energy efficiency, and environmental friendliness of production is why hydrogen could be termed the future energy. Hydrogen is high in energy yield per molecule and has a calorific value of 142MJ/kg (Bharathiraja, 2016, Balachandar *et al.*, 2020 and Edwards *et al.*, 2021). In terms of energy content, hydrogen is 2.75 times that of any known hydrocarbon, and hydrogen combustion in cars is 50 times more efficient than gasoline (Van-Ginkel and Sung, 2001). In addition, hydrogen energy is clean and recyclable as the final product of its combustion is water vapour without CO, CO<sub>2</sub>, hydrocarbons and fine particles (Kotay and Das, 2008, Kothari *et al.*, 2008 and Ma *et al.*, 2021). The water vapour produced can be condensed and used for hydrogen production via renewable electrolysis or direct and indirect bio-photolysis. Hydrogen can also be used to decarbonise heavy carbon-emitting sectors such as transport, industries, power and heat generation – accounting for almost 90% of the world CO<sub>2</sub> emissions (IEA, 2020 and Edwards *et al.*, 2021). Furthermore, hydrogen is more preferred to methane as it has more industrial applications such as the generation of electricity in fuel cells or internal combustion engines (Pierra, 2006 and Edwards *et al.*, 2021); hydrogenation of edible oil, petroleum, coal and shale oil and synthesis of ammonia (Kothari *et al.*, 2012). Although costly, hydrogen can be stored as a metal hydride (Edwards *et al.*, 2021). Van-Ginkel and Sung (2001) stated that hydrogen transmission through gas pipelines would be more effective than transmitting electricity down the power lines.

Hydrogen as a promising energy carrier has some challenges yet to be resolved despite these outlined great benefits. For instance, hydrogen is more demanding to liquefy than methane and propane – these compounds are liquefied natural gas (LNG) constituents. Not only that, hydrogen being the lightest of all the elements, the volumetric energy density of hydrogen is much lower than other energy fuels, which implies that larger fuel tanks are required for vehicles running on hydrogen than petrol or diesel (Abasi and Abasi, 2011 and Dept of Energy, 2017). Moreover, the critical temperature of hydrogen is shallow, and there are issues relating to hydrogen leakage due to the smaller size and lightweight of hydrogen molecules (Kothari *et al.*, 2008). Then the problem with sustainable production and storage.

The fertiliser and petroleum industries at 50% and 37% are the most significant hydrogen users (Momirlan and Veziroglu, 2002). However, as stated by Das and Veziroglu (2001) and Winter (2005), sales of hydrogen have plummeted annually in the last five years by 10% due to the increased use of hydrogen in refineries for fuel quality. Furthermore, about 50 million tonnes of hydrogen are traded globally annually (Winter, 2005), and based on the national hydrogen program of the United States, Armor (1999) reported that the contribution of hydrogen to the US energy market would be within the range of 8 – 10% by 2025.

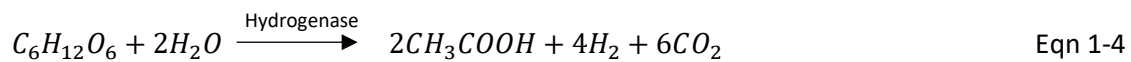
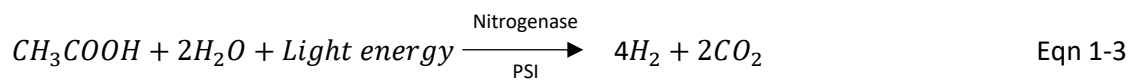
Conventionally, hydrogen can be produced in several ways, such as steam reforming of natural gas (40 - 48%) and heavy oils (30%), and gasification of heavy hydrocarbons or coal (18%) (Ghimire *et al.*, 2015; Nan-Qi *et al.*, 2016, Edwards *et al.*, 2021, Ma *et al.*, 2021 and Rosa and Mazzotti, 2022). Others, including nuclear electrolysis, biomass gasification, pyrolysis, and renewable electrolysis, constitute about 4% of the traditional hydrogen production. Even though low-carbon hydrogen production from conventional fuels is probable with carbon capture and storage (CCS) technology, also known as blue hydrogen (Edwards *et al.*, 2021), among the most worrying issues involved with conventional hydrogen technologies is lack of sustainability (Guo *et al.*, 2010) and emission of atmospheric carbon (as vast amount of fossil energy is required, leading to the liberation of about 2.5 to 5 tonnes of CO<sub>2</sub>

per tonne of hydrogen) (Abasi and Abasi, 2011 and Sharmila *et al.*, 2022). Other concerns are difficulty in getting pure hydrogen and the production of other undesirable energy products. Therefore, hydrogen should be produced from processes or sources that avoid or minimise CO<sub>2</sub> emissions to mitigate these concerns. The development of these processes has given rise to the biological research and study of hydrogen production that is less energy-intensive and environmentally friendly (Zhi and Wang, 2014, Zhang *et al.*, 2020, Ma *et al.*, 2021, Srivastava *et al.*, 2021, Rosa and Mazzotti, 2022 and Sharmila *et al.*, 2022). However, H<sub>2</sub> can also be produced from water utilising green electricity from solar or wind ("green" hydrogen).



According to Kapdan and Kargi (2006), Ghimire *et al.* (2015), Bharathiraja *et al.* (2016), Balachandar *et al.* (2020), Li *et al.* (2022) and Sharmila *et al.* (2022), hydrogen can be produced biologically by autotrophic and heterotrophic microorganisms. In autotrophic processes, which include the two photo-biological routes (direct (Eqn 1-1a and b) and indirect bio-photolysis (Eqn 1-2a - b) (Limongi *et al.*, 2021 and Li *et al.*, 2022), solar energy is directly transformed to hydrogen through a series of photosynthetic reactions that are carried by photosynthetic microbes such as algae - *Chlamydomonas reinhardtii* (Ghirardi *et al.*, 2000 and Limongi *et al.*, 2021), green algae - *Scenedesmus obliquus*, *Chlorella fusca* (Winkler *et al.*, 2002 and Jimenez-Llanos *et al.*, 2020), cyanobacteria (*Anabaena* sp, *Oscillatoria* sp, *Calothrix* sp (Pinto *et al.*, 2002 and Li *et al.*, 2022) and protists. Under heterotrophic conversions, hydrogen is produced simultaneously during the conversion of organic substrates to

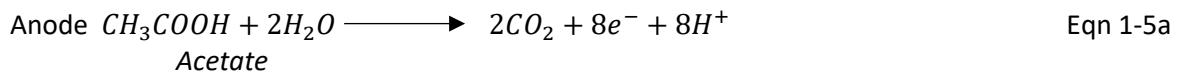
simpler organic compounds (Das and Verziroglu, 2008). The heterotrophic process is of two types 1) light/photo fermentation (Eqn 1-3) by photosynthetic bacteria: purple non-sulphur bacteria - *Rhodobacter Sphaeroides* (Kim *et al.*, 2006), *Rhodobacter capsulatus* (He *et al.*, 2005), *Rhodovulum Sulfidophilum W-1S* (Maeda *et al.*, 2003), *Rhodospirillum rubrum* and *Rhodopseudomonas palustris* (Barbosa *et al.*, 2001) and 2) dark fermentation (DF) (Eqn 1-4) by strict anaerobes – Clostridia, methylotrophs, rumen bacteria, methanogenic bacteria, archaea; facultative anaerobes – *Escherichia coli*, *Enterobacter*, *Citrobacter* and aerobes – *Alcaligenes* and *Bacillus* (Bundhoo and Mohee, 2016).



The two biological conversion processes have advantages over traditional hydrogen production methods in being carbon-neutral and can even aid environmental sanity (atmospheric carbon removal (Eqn 1-2b). Conversely, the major challenge of light-dependent conversion technologies is that yield output is relatively small, processes require controlled solar energy, and hydrogenase enzyme is oxygen labile (Balachandar *et al.*, 2020). It is affected by the free oxygen in the reaction processes. More so, colossal capital is required in financing photo bio-reactors.

Dark fermentation (DF), also called anaerobic fermentation (AF), is a series of biochemical reactions leading to energy products from incubating organic substrate with microbial inoculum in an oxygen-free environment (Adekunle and Okolie, 2015). DF is the most promising energy technology researched and is carbon-neutral. Depending on other environmental factors, it can produce a relatively high amount of hydrogen per gram of substrate (4 mol H<sub>2</sub> / mol of glucose). Compared to other methods, light is not required. Also, hydrogen gas produced can be linked directly to other processes and systems (e.g. fuel cells, internal combustion engines). Thus, there may be no need for energy storage and adsorption (Hossen *et al.*, 2015). In addition, organic acids produced could be

used as feeders in other energy processes, e.g. in photo-fermentation (Eqn 1-3), in microbial electrolysis cells for hydrogen production (Eqn 1-5a and b) and methane production (Eqn 1-6) using coupled fermentation system (hythane production) (Ueno *et al.*, 2007; Kim *et al.*, 2013, Jiang *et al.*, 2018 and Lusk *et al.*, 2018 and Srivastava *et al.*, 2021). More so, sludge – a mixed culture of *Clostridia* and other hydrogen producers-could easily be applied as inoculum (Kapdan and Kargi, 2006, and Xie *et al.*, 2010). The digestate too, which is rich in nitrogen, phosphorus, silicon and many other numerous microelements (Surendra *et al.*, 2014, Mirmohamadsadeghi and Karimi, 2018 and Bakar and Carey, 2020), could be used to enrich and regenerate the soil for growth in agricultural production or precursors for raw materials (e.g. silica) in industries (Guzman *et al.*, 2015). Additionally, DF can treat various organic waste, thereby offering cheap solutions to environmental waste management.



On the other hand, methane is a fuel gas produced conventionally by thermo-chemical, catalytic and biological processes. The catalytic procedure is commonly referred to as the Sabatier process. Usually, it involves reacting hydrogen with carbon monoxide or carbon dioxide at higher temperatures of 500 to 600°C under nickel catalysis (Aryal *et al.*, 2018 and Skov *et al.*, 2019). In the biological process, biogas rich with methane is produced anaerobically by the breakdown of biomasses (crop and plant debris, energy groups, animal manure, agricultural waste, municipal solid waste, using anaerobic digestion (AD) technology. The AD process is similar to the DF procedure, but while the AD process terminates in methanogenesis, the DF ends in acidogenesis, which is part of an AD digestion phase. Typically, the biogas produced from anaerobic digestion contains about 55 to 70% CH<sub>4</sub> (Munoz *et al.*, 2015 and Bharathiraja *et al.*, 2018), and It is this component, methane (which is also the main

component of natural gas), that has a calorific value. In addition to being an energy resource, methane is also a greenhouse gas 21 times by weight the global warming potential of CO<sub>2</sub> (Aryal *et al.*, 2018).

**Thus, a three-stage anaerobic digestion process that produces hydrogen and methane from RS co-digested with DCS is proposed in this research to maximise RS's energy value in the integrated energy system.**

Despite these mentioned benefits of hydrogen and methane, the RS AD process for biogas production is limited by RS rigid structure that is the low digestibility of its fibre content (Wei *et al.*, 2014 and Zhang *et al.*, 2020) and its high ash content of 15 – 20% (Menardo *et al.*, 2015). Hypothetically, it has been said that without pre-treatment of lignocellulose biomass, only 20% maximum sugar can be obtained from enzymatic hydrolysis (Dong *et al.*, 2019). Thus, effective and efficient pre-treatments are required to break the complex and heterogeneous matrix, increase surface area and create micropores on the lignocellulose material to enhance enzyme accessibility, hydrolysis, and cellulose degradation (Dong *et al.*, 2019 and Zhang *et al.*, 2020). Nonetheless, pre-treatment of lignocellulose biomass invariable increases biogas production cost and presents environmental hazards. So, ways and alternative means of pre-treating lignocellulose that are environmentally friendly and cost-effective are being studied. **Therefore, in this research thesis, agro-industrial wastes such as potash extracts (PE), cassava-steep wastewater (CSSW) and corn-steep liquor (CSTL) will be considered as a substitute for chemical pre-treatment agents for lignocellulose biomass.**

In addition to this, bio-hydrogen production is affected by the quality of seeded sludge in the DF process because seeded sludge contains diverse microorganisms that can produce hydrogen using the AD process (Srivastava *et al.*, 2021 and Sharmila *et al.*, 2022). However, hydrogen-consuming bacteria (HCB) and hydrogen-producing bacteria (HPB) in seeded sludge present a challenge of its use in the efficient production of hydrogen from organic matter. Untreated sludge generally produces a low H<sub>2</sub> yield of about < 1.0 mol H<sub>2</sub>/ mol of glucose (Wong *et al.*, 2014 and Yang *et al.*, 2020). This low hydrogen

production is due to the molecular hydrogen being utilised for energy by HCB (Li and Fang, 2007). The conventional approaches employed to enhance sludge solubilisation, enrich the hydrogen producers, and eliminate hydrogen consumers' activities are energy demanding and costly, especially in chemical purchases. The methods could also decimate some HPBs and hydrolytic microorganisms population and have related environmental issues (Zhu and Beland, 2006; Wong *et al.*, 2014 and Bundhoo and Mohee, 2016). **Thus in this thesis, research into less energy demanding and environmentally friendly options for HPB enrichment and digested cow slurry (DCS) pretreatment are also being investigated using agro-industrial wastes.**

**The research is further explored for nano-silica production from the RS digestate, mainly because solar photovoltaics (PV) are primarily produced from polysilicon.** When deployed to about 5% of Nigeria landmass, these PVs have the tendencies to generate an estimated value of 600 GW of electricity for Nigeria (Adebisi *et al.*, 2020). Even so, the initial financial requirement is substantial in the production of PVs, especially in the purification of silicons, which remains a limiting factor. Thus, cheaper sources of silicons are being studied. In addition, silica has a resourceful value and application, especially in the development of carbon/silica composites (Kumagai and Sasaki, 2009 and Mirmohamadsadeghi and Karimi, 2018), biocatalysts (Artkla, 2009, Azizi and Yousefpour, 2010), in the production of hydrogen and CO<sub>2</sub> capture materials and metallic ions adsorbents (Chen, 2010 and Liou and Yang, 2011).

Finally, the energy assessment and mass balance of the AD process in the integrated energy system **(designed to maximise employed biomass energy yield mainly from the three-stage anaerobic digestion process)** were determined and compared using the laboratory data and predicted energy values of the produced biomethane and biohydrogen from previous reviews.



## 1.1 Aims and Objectives of the Study

The research study offers solutions to energy and environmental issues, especially ravaging Nigeria's agricultural sector. The response is achieved by designing and employing an energy integrated system (Fig 1-1) in predominantly farm communities to complement the traditional fossil energy. The integrated unit entails using an anaerobic digestion process whereby tonnes of RS that constitute environmental pollution is pretreated using agro-industrial waste and enzymes, digested and converted to bio-hydrogen and bio-methane. Furthermore, instead of being employed for manure, the RS digestate produced from the AD process is utilised in nano-silica production for use in industries with further energy production in a gasifier. The certainty cements this exploration of nano-silica from biomass that silicon forms the backbone of most commercialised PV materials and has broader applications. Therefore, it offers a route for more green energy production.

Moreover, the produced biogas (either upgraded or raw) is used in the downstream processes for electricity and heat generation and natural gas substitutes. In contrast, most of the heat generated from the combined heat and power (CHP) plants was utilised via sorption chillers to provide air conditioning, refrigeration and process fluid cooling for industries. The spent heat usage maximised the integrated energy efficiency of the system as Nigeria is situated in the tropical climate zone, and as such, there is no need for district heating. Before the energy system design, studies were also done on critical factors affecting bio-hydrogen production. Finally, the system's energy assessment and mass balance are calculated to determine the system energy efficiency and stability.

Therefore, the above summary was accomplished by achieving the following objectives:

- ✚ Enrichment of seeded sludge using agro-industrial wastes for biological hydrogen production.
- ✚ The bio-hydrogen production from unhydrolysed raw rice straw co-digested with digested cattle slurry.

- ✚ A solution to Nigeria's energy challenges with hydrogen and methane co-produced from agro-industrial pre-treated enzymatically-enhanced rice straw in a three-stage anaerobic digestion process.
- ✚ The production of nano-silica precursors from agro-industrial wastes leached and anaerobically digested rice straw.
- ✚ The energy assessment of the digestion and post digestion processes in the integrated energy system

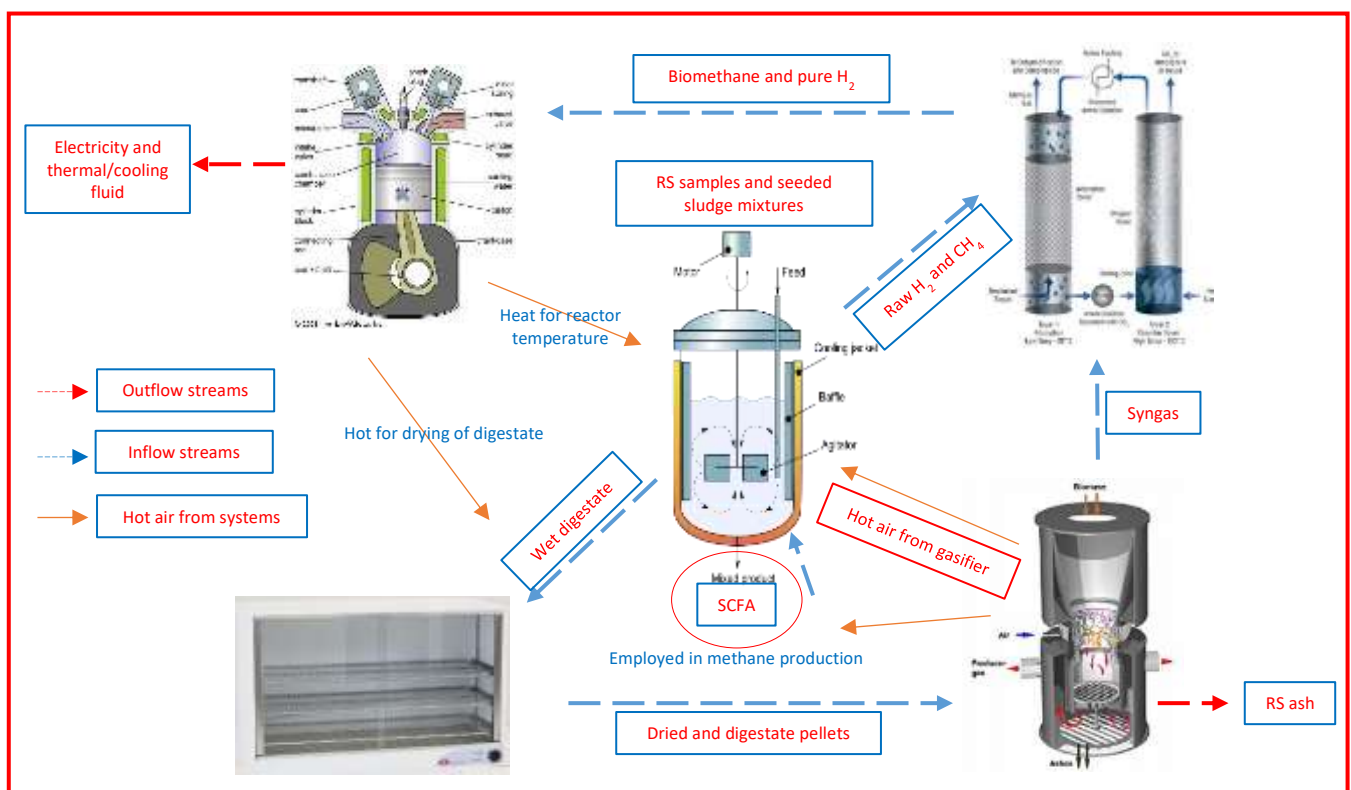


Fig 1-1: Model design of the integrated energy system

## 1.2 Thesis Structure and Layout

This thesis contains nine chapters (Fig 1-2), including the introduction (Chapter 1), which provided the research questions and objectives for this study and outlined the understanding of the concept of the study. Chapter 2 is the literature review that details the Nigerian energy crisis, nature and features of RS as an LCB, pre-treatment technologies for LCB, production of agro-industrial wastes and AD processes and factors that AD processes. The chapter also defines biogas purification processes, the generation of power, heat and cooling fluid from CHP plants, and RS ash as a precursor of silica. Following this is chapter 3, which is concerned with the methods and materials applied in the PhD research. Although this chapter covers all the experimental work done during the laboratory studies, some experiential chapters, mainly Chapter 6, which is more exclusive, also have a detailed methodology.

As mentioned previously, the thesis is summarised in Figure 1-1 titled "Model design of an integrated energy unit" (Fig 1-1), which is created mainly from Chapter 6. Before designing the energy system and research study in Chapter 6, experimental studies were also done on critical factors affecting biohydrogen production regarding DCS enrichment (Chapter 4) and biohydrogen production from unhydrolysed RS (Chapter 5). Subsequently, Chapter 7 examines silica production from a) agro-industrial leached RS samples and b) digested RS samples from Chapters 5 and 6. Chapter 8, "The energy assessment of the digestion and post digestion processes in the integrated unit", considered the energy balances of studied AD and silica production processes using RS as feedstock co-digested with DCS. So, it balances the energy demand of the operations of the whole unit with the energy output to determine the system's energy efficiency. Finally, Chapter 9 presents a detailed summary of the research outcomes and a critique of the significant research outcomes with suggestions and recommendations for future studies.

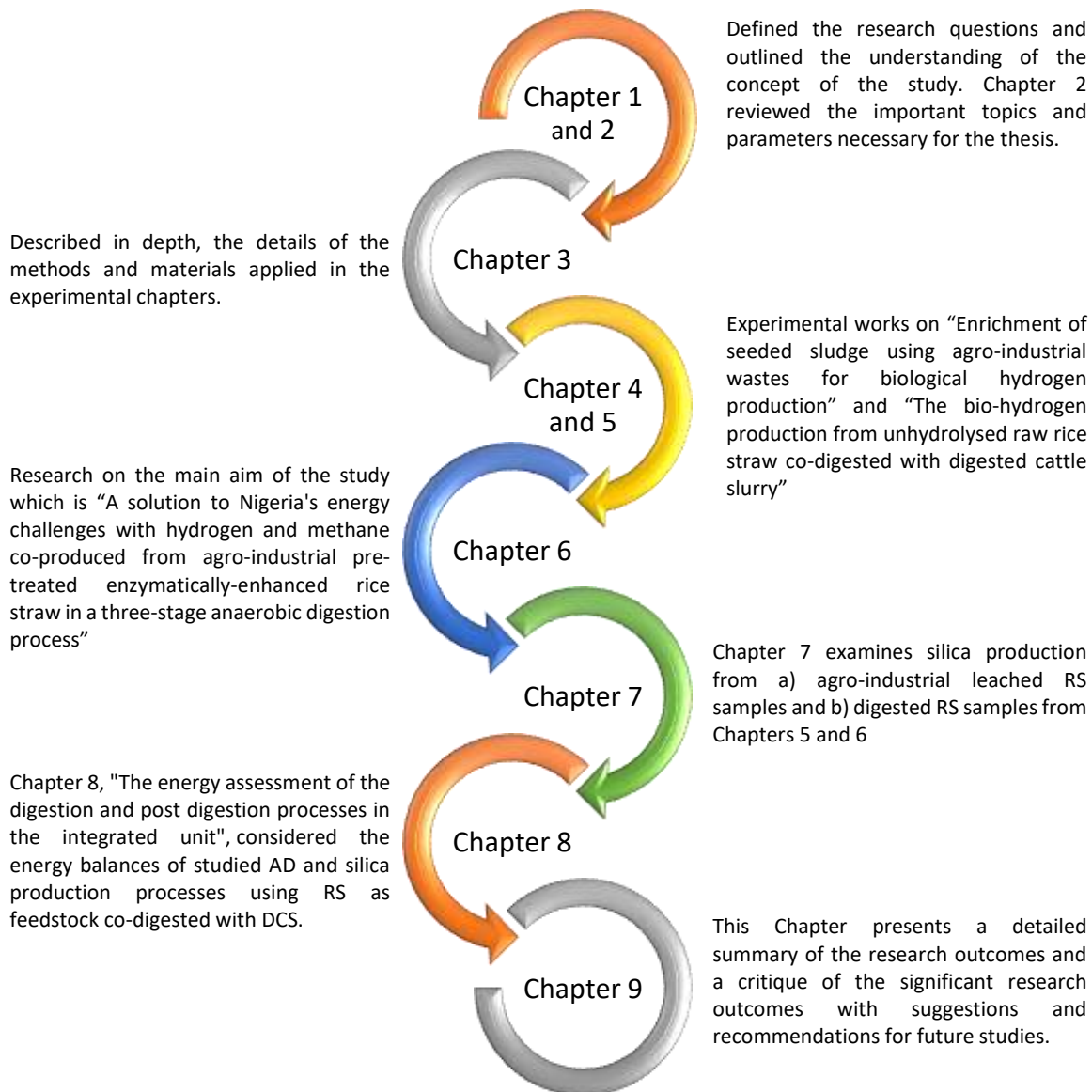


Fig 1-2: Thesis structure and layout



## Chapter 2 Literature Review

### 2.1 Nigeria Energy Scenario

The demand for energy in Nigeria has been growing rapidly due to economic and population growth. In 2015, Nigeria rebased its economy and became the largest economy in Africa. Consequently, the Nigerian population is at 191 million and 206 million by International Energy Agency (IEA) (2020) and World population reviews (2020). As a result, the Nigerian total primary energy supply (TPES) grew from about 65 million tonnes of oil equivalent (Mtoe) in 1990 to approx. 150 Mtoe in 2016 (IEA, 2016). The total primary energy supply within two decades in Nigeria shows that Nigeria, over the years, has depended upon biomass fuels and waste (Fig 2-1), which is due to scarcity and high cost of refined oil and natural gas and poor functioning refineries.

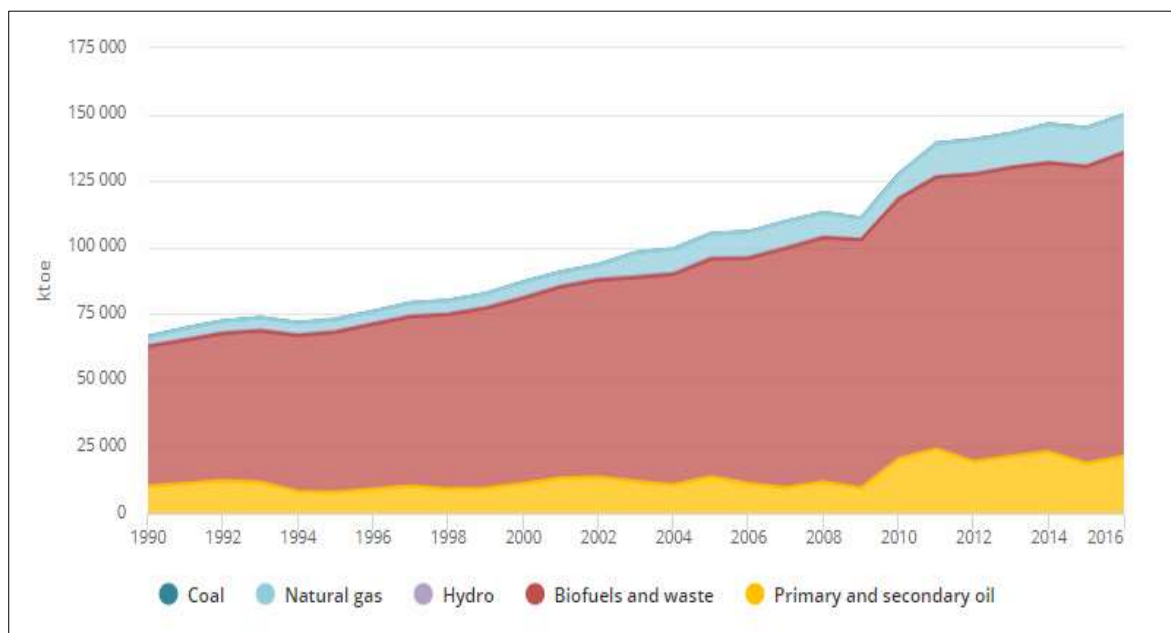


Fig 2-1: Total primary energy supply (TPES) (IEA, 2016)

Apart from fuels and waste, which make up 76% of TPES, others are natural gas (9.27%), primary and secondary oil (14.3%), coal (0.18%) and hydropower (0.32%) (IEA, 2016). Predictably, energy supply from oil and natural gas should be contributing more to the total energy supply in Nigeria based on the number of proven oil (37.5 billion barrels) and gas (187 - 193 trillion cubic feet) reserves (Nigerian

Energy Support Programme (NESP), 2015; Emodi and Boo *et al.*, 2015 and Ugwoke *et al.*, 2020). However, from these statistics, it is presumed that the average production of 1.8 to 2.4 million barrels of oil per day is mainly for export purposes (Nigerian National Petroleum Corporation, 2016). Nigeria imports its oil products, and 8.44 Mtoe of oil products was imported (NESP, 2015) in 2012 alone.

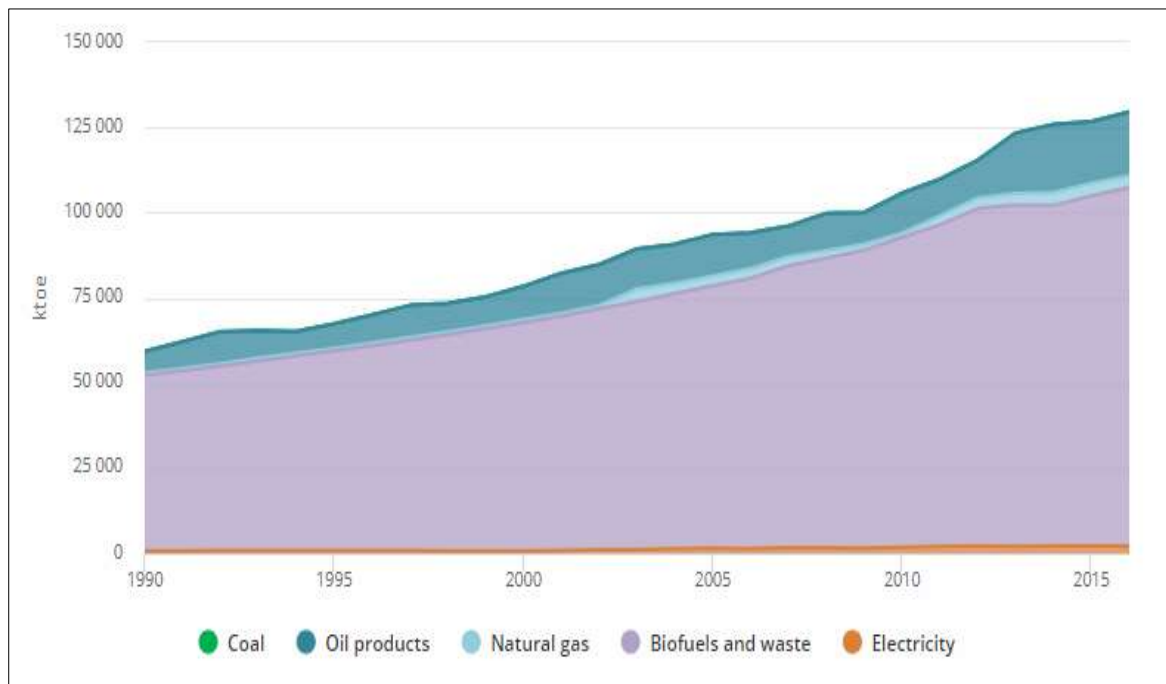


Fig 2-2: Total final energy consumption (IEA, 2016)

In addition, Nigeria's total energy consumption has risen from about 60 Mtoe in 1990 to approximately 130 Mtoe in 2016 (Fig 2-2). In energy supply, Nigeria heavily depends on biofuels and waste (81.18%) for its energy consumption, amounting to 105 Mtoe. Most of this energy is consumed for residential purposes, mainly for cooking. The remaining total energy consumption in 2016 is as follows coal (0.18%), electricity (1.68%), natural gas (2.63%) and primary and secondary oil (14.5%). The growing dependence on wood fuel for energy needs is primarily due to the lack of electricity (Oyedepo *et al.*, 2018) and the high cost of processed energy products. This over-reliance on biomass fuel and waste for energy has changed the country's vegetation and increased desertification and deforestation, leading to severe flooding and other environmental issues (Zubairu *et al.*, 2015 and Oyedepo *et al.*, 2018). In the same vein, firewood and waste as the significant energy consumption source have

contributed to greenhouse gases (GHG), notably anthropogenic CH<sub>4</sub>, CO<sub>2</sub>, CO and NO<sub>x</sub> and volatile organic acids, a precursor of ozone. These gases affect the ozone layer and are among the significant causes of climate change, environmental pollution and death (IEA, 2016 and Oyedepo *et al.*, 2018). The generation of gases is due to the predominant use of cooking methods from an open fire with remarkably low thermal efficiency. According to IEA (2016), Nigeria emission has spiked from 28.06 metric tonnes (Mt) CO<sub>2</sub> in 1990 to 85.99 Mt CO<sub>2</sub> in 2016 with 0.46 t CO<sub>2</sub> emission per capita.

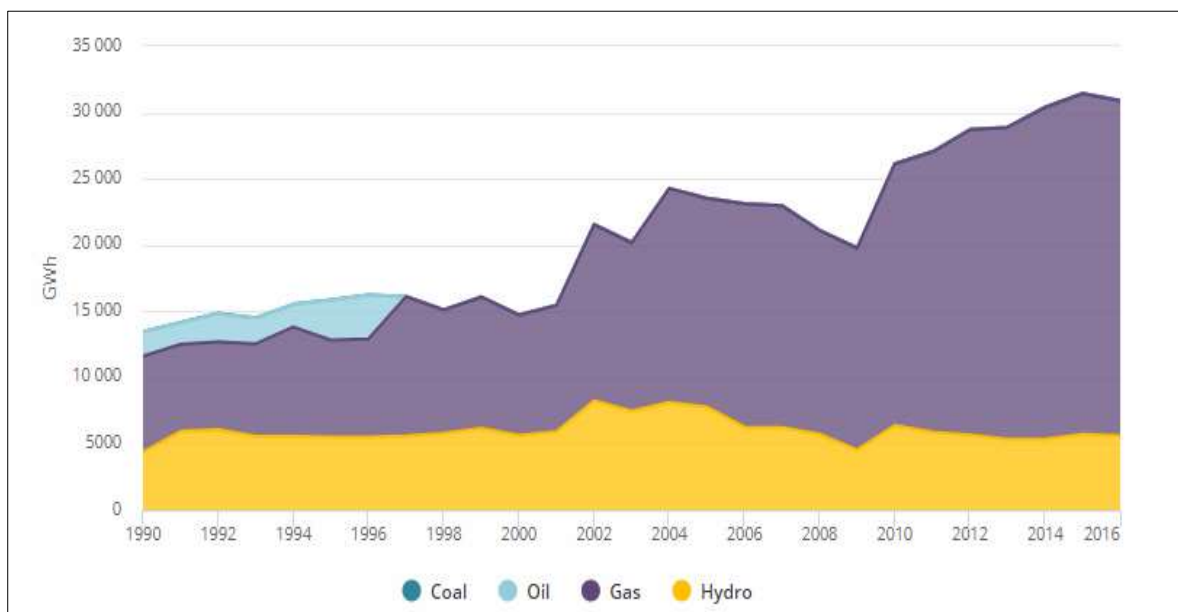


Fig 2-3: Electricity generation by fuel (IEA, 2016)

NESP (2015) reported four primary power generation options in Nigeria in electricity generation. They are transmission-based off-grid generation, on-grid generation, embedded generation and captive generation. If more than 1MW of electricity is generated, detailed approval licenses are required for transmission-based off-grid, on-grid, and embedded, while captive generations only require the Nigerian Electricity Regulatory Commission permit. In captive generations, the generated electricity is entirely consumed by the producing generator, while off-grid generation external off-takers (schools, estates), which usually are granted distribution licenses, are required for additional electricity consumption (Federal Ministry of Power (FMP), 2015). Conversely, in embedded generation, an external distribution company transmits the generated electricity to the grid and lastly, all power



plants evacuate their power to the national transmission grid (FMP, 2015). Nigeria total power generation is a mixture of all the options detailed above. Since there is little or no statistics on the other transmission generations for both off-grid generation, embedded generation and captive generation, the data provided by NERC is mainly for power plants connected to the transmission grid (NESP, 2015).

The data provided by the IEA (2016) indicated that electricity generation in Nigeria has risen from 13.8 TWh in 1990 to 30.9 TWh in 2016 based on statistics obtained within the last two decades. At the moment, the use of gas-powered plants contributes about 81.9% of electricity generation (25.3 TWh) while the remainder, 18.1%, comes from the three hydro-powered plants (5.6 TWh) (Table 2-3). These generating power stations are connected to 27 grids in the Nigeria electricity supply industry (NESI) (Oyedepo *et al.*, 2018 and NESI, 2020).

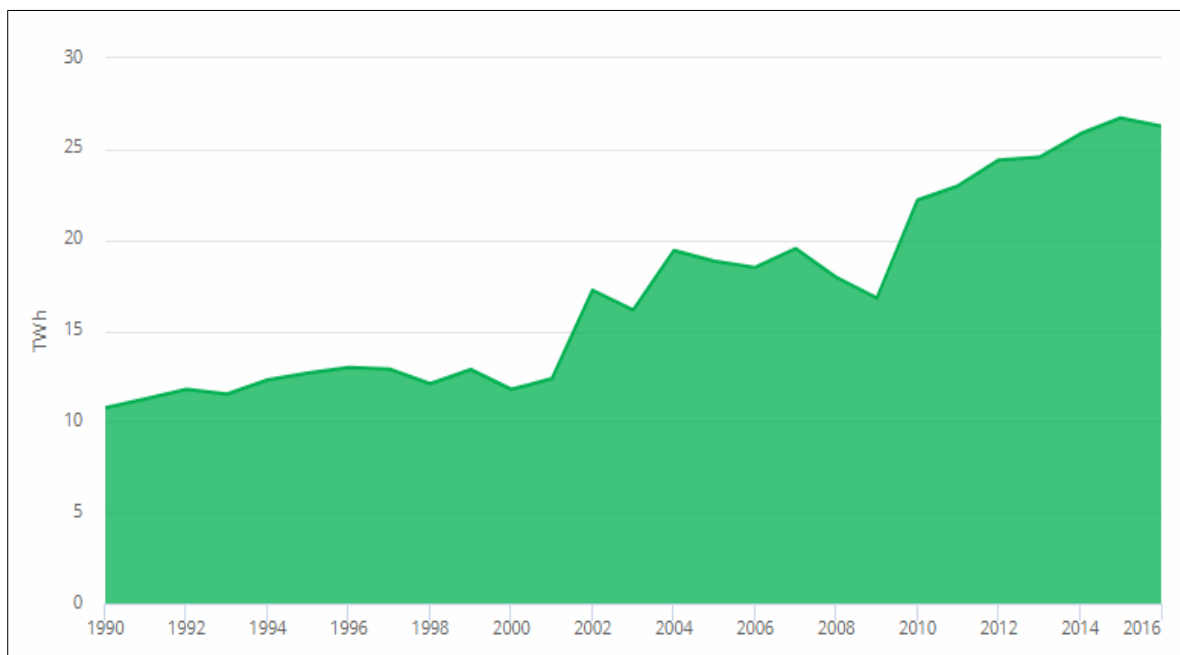


Fig 2-4: Total electricity consumption (IEA, 2016)

Although the installed capacity of electricity generation in Nigeria is around 19.8 GW (19.4 GW for on-grid generators, 0.31 GW for off-grid generators and 0.05 GW for embedded generators), the available generating capacity is 6.5 to 8.2 GW (NESP, 2015, Nigerian Electricity Regulatory Commission (NERC),

2018) and worsening. NERC, in their quarterly bulletins, reported the peak generation of 5 162 MW which was attributed to drop in power generation, load rejection across the power distribution companies, transmission to grid line constraints, unavailability of gases, water shortages, and grid constraints (NERC, 2018)

Under the two-decade period, the total electricity consumption of Nigeria grew from 10.77 TWh in 1990 to 26.26 TWh in 2016 (Fig 2-4), while the electricity consumption per capita was relatively constant from 1990 (110 kWh) to 2016 (140 kWh) (IEA, 2016). At 140 kWh per capita in 2016, Nigeria trail significantly behind other developing nations in electricity per capita. Ghana's electricity per capita consumption is 403 kWh, about three times higher than Nigeria, while South Africa stands at 4.36 MWh (Oyedepo *et al.*, 2018), about 31 times Nigeria's electricity per capita. The highest value ever documented was 156 kWh in 2012. The same year, the detailed electricity consumption by economic sectors shows that residential has the highest consumption rate per capita (57.8%) while the industrial sector is 15.8% and others 26.3% (IEA, 2016). Going by the global minimum average electricity consumption per capita for emerging economies put at 500 kWh, Nigeria would require 180 GW of electricity for full power. The estimated demand is significantly miles away from the current electricity production (Usman and Abbasoglu, 2015 and Oyedepo *et al.*, 2018).

## **2.2 Rice Straw**

Rice straw (RS), the stem/vegetative part of rice plant (*Oryza sativa* or *Oryza glaberrima*) removed during rice harvest, is among other lignocellulose materials biomass be used for biogas and bio-hydrogen production. Rice straw is the most abundant waste globally, accounting for almost 782 million tonnes in annual supply (Food and Agricultural Organisation (FAO), 2018), resulting from rice being the third most important crop after barley and wheat in terms of total crop production (Biswarup *et al.*, 2016). RS is the fourth most important crop after sorghum, millet and maize in Nigeria (Kosemani *et al.*, 2020). Rice is a popular crop in many agricultural economic-dependent countries like China, India, Thailand, Indonesia, Taiwan, Vietnam, and Brazil. According to a report from FAO (2017

and 2018), Nigeria produces approximately 6.8 million tonnes of rice annually, which has lately increased due to the diversification of the economy, especially in the agriculture sector.

In rice harvesting and processing, RS makes more of the yield (twice the yield) of rice paddy (Yuan, 2002). Rice straw is locally used as fuel for domestic purposes, in paper making industries, animal feeds constitution, and raw materials to fabricate average density fiberboards and bricks (Hiziroglu *et al.*, 2008 and Rodriguez *et al.*, 2008). At the same time, many are disposed of by burning or left open unattended on the field, thereby causing environmental pollution (atmospheric bio-methane) and degradation. This unhealthy environmental practice can be avoided by employing RS as a carbon nutrient for bioenergy production via the AD process. In addition, the high cellulose and hemicellulose content that can be easily fermentable sugars, its' readily and globally available, and composition of other important microelements make rice straw potential feedstock for hydrogen, methane and silica production (Wattanasiriwech *et al.*, 2010; Guzman *et al.*, 2015, Biswarup *et al.*, 2016 and Thao *et al.*, 2019 and Dong *et al.*, 2020).

There are many works of literature on the use of RS for biogas production (Lo *et al.*, 2010; Lei *et al.*, 2010; Chang *et al.*, 2011; Chen *et al.*, 2012a; He *et al.*, 2014; Ghimire *et al.*, 2015; Mernardo *et al.*, 2015; Mustafa *et al.*, 2016 and Kannah *et al.*, 2019). Dong *et al.*, 2020 obtained 72.5 mL H<sub>2</sub>/g-pretreated RS in their work on High-solid pre-treatment of rice straw at cold temperature using NaOH/Urea for enhanced enzymatic conversion and hydrogen production. Additionally, the specific methane yield of 325.76 NmL CH<sub>4</sub>/gVS was obtained from microwave pretreated RS, which was higher than the untreated one 230 NmL CH<sub>4</sub>/gVS (Kainthola *et al.* 2019). In the pre-treatment conditions of rice straw for simultaneous hydrogen and ethanol fermentation by mixed culture, Biswarup *et al.* (2016) produced 771mL/L of volumetric hydrogen 1776 mg COD/L of ethanol. Also, Liu and his companions working on bio-hydrogen production evaluation from rice straw hydrolysate by concentrated acid pre-treatment in both batch and the continuous system showed that bio-hydrogen

gas could be produced from rice straw (Liu *et al.*, 2013). Furthermore, 58% of stable hydrogen content was achieved by Kim *et al.* (2012) in their work on hydrogen production by anaerobic co-digestion of rice straw and sewage sludge. Hydrogen and methane gas were co-produced by Kim *et al.* (2013) using two-staged systems in the research study on hydrogen and methane production from untreated rice straw and raw sewage sludge under thermophilic anaerobic conditions. In addition to this, Guzman *et al.* (2015), in their work on the valorisation of rice straw waste, have shown that rice straw could produce amorphous silica, which can serve as a cement substitute in civil constructions, raw materials in ceramics and glass industries. Similar work was documented by Wattanasiriwech *et al.* (2010) on the production of amorphous silica nanoparticles from rice straw with microbial hydrolysis pre-treatment.

As stated above, the main constituents of rice straw are the cellulose (40 - 50%), hemicellulose (25 - 30%) and the aromatic compound - lignin (12- 18%) (Sangnark and Noomhorm, 2004, Chen *et al.*, 2012b and Shah *et al.*, 2015), while the remaining inorganic components (10 - 15%) is mainly of ash and little of the extractive materials (Guzman *et al.*, 2015 and Bakar and Carey, 2020). However, like any lignocellulose biomass (LCB) material, the most significant rice straw limitation for energy production that needs to be resolved before rice straw can be hydrolysed and used for bio-hydrogen production is the de-lignification and deconstruction of its rigid structure (Wei *et al.*, 2014). This difficulty in hydrolysis is brought by the fermentable polysaccharide sugars (hexose and pentose) being encased by a non-fermentable lignin polymer (Kumar *et al.*, 2013 and 2015 and Lee *et al.* 2014). Similarly, LCB can resist degradation due to their cells walls, which confers hydrolytic stability and structural robustness (Kratky and Jirout, 2011). The structural robustness is owing to the crosslinking of the polysaccharide's sugars (cellulose and hemicellulose) among themselves using  $\beta$ -1, 4 – glycosidic bonds and with the complex aromatic polymer (lignin) through ester and ether linkages (Kumar *et al.*, 2013 and 2015). Therefore, it is pertinent to detach the cellulose from the lignin first

and realign the ultrastructural components to increase the surface area to a final particle size of 0.2 – 2mm (Kratky and Jirout, 2011) for effective solubilisation through pre-treatments.

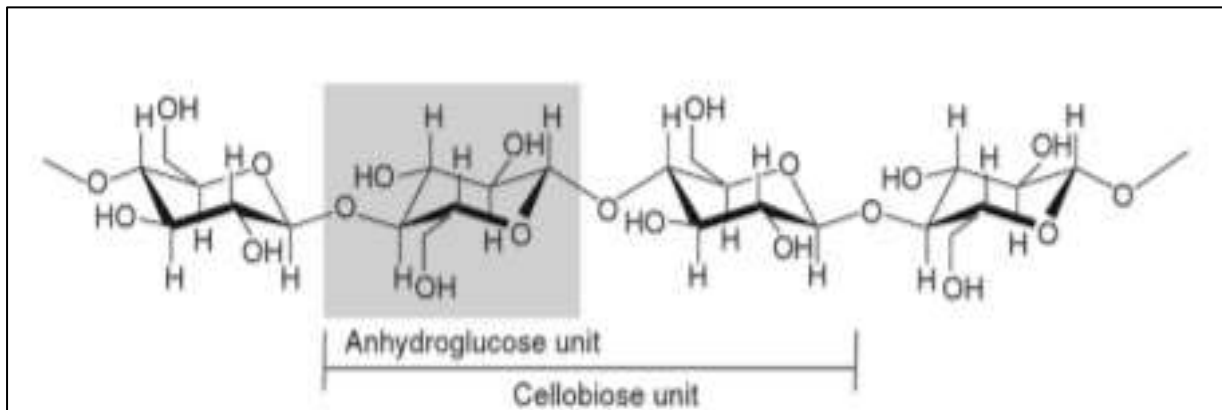


Fig 2-5: A cellulose molecule showing both the dimeric and monomeric unit (Kumar *et al.*, 2009)

The cellulose ( $C_6H_{10}O_5$ )<sub>n</sub>, (Fig 2-5), the principal structural constituent of plant cell walls that provide structural support, is the most abundant renewable organic resource (Chen *et al.*, 2016). Even though hemicellulose ( $C_5H_8O_4$ )<sub>n</sub> offers support for the plant's cell wall, it is a complex carbohydrate with a lower molecular weight than cellulose (Dahlquist, 2013). On the other hand, lignin is the most abundant non-sugar component of the biomass. As defined by Chen *et al.* (2012b) and Wei (2016), lignin is a polyphenyl aromatic tri-dimensional compound that is composed of monolignol monomers such as *p*-coumaryl alcohol, coniferyl alcohol, and sinapyl alcohol and linked together via dehydrogenation (alkyl-alkyl, alkyl-aryl and aryl-aryl ether bonds) in varying proportions. Lignin masked the hollo-cellulose to protect from microbial attack and provide structural support (Lee *et al.* 2014 and Jorgenssen *et al.*, 2007). Thus, lignin is the main barrier to the breakdown of lignocellulose biomass.

### 2.3 Pre-treatment Technologies for Lignocellulose Rice Straw

Lignocellulose biomass (LCB) pre-treatments aim to remove the lignin component, disrupts the bonds of cellulose and hemicellulose, improve the surface area of the LCB and create micropores on the lignocellulose material (Fig 2-6). In addition, the pre-treatments will make it more accessible to microbial attack, enzyme hydrolysis and cellulose degradation (Cheng *et al.*, 2011a; Chen *et al.*, 2011

and 2017; Dong *et al.*, 2019 and Salakkam *et al.*, 2019). Numerous pre-treatments methods have been employed to overcome the challenge presented by lignin and the structural robustness of LCB. The pre-treatment methods, according to Mosier *et al.* (2005) and Cheng *et al.* (2011a) and Salakkam *et al.* (2019), are widely classified as chemical (alkali, acids, oxidative agents (ionic), organic solvent (organosolv), salts (metal chlorides) and plasma); physical/mechanical (microwave irradiation, ultrasonic, grinding, milling sonification) and physicochemical (steam explosion @160-260°C, hot water treatment and ammonium fibre explosion).

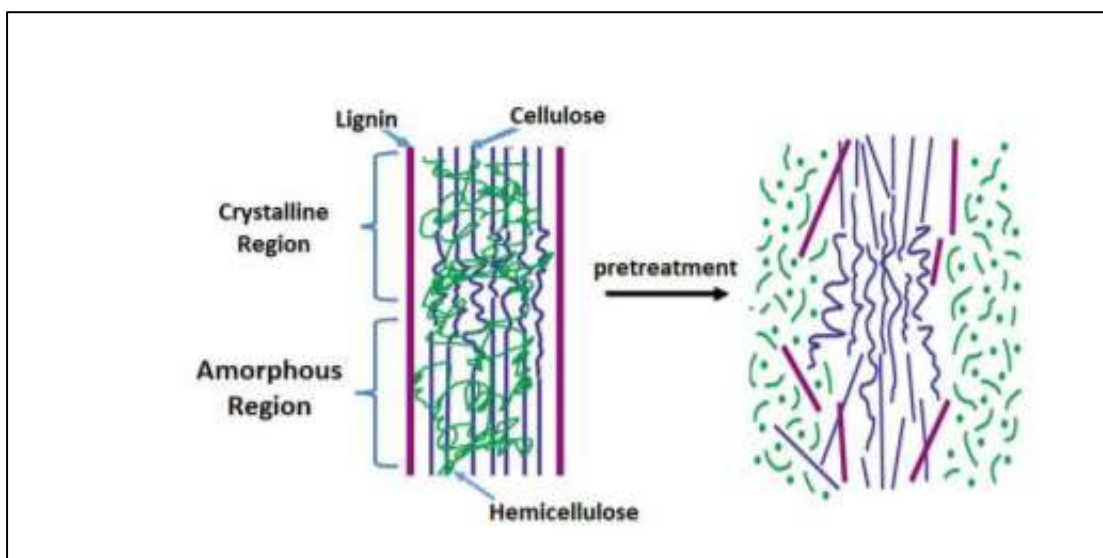


Fig 2-6: Effect of pre-treatment of lignocellulosic biomass (Mosier *et al.*, 2005)

In chemical pre-treatment, chemicals such as acids, alkalis, ionic liquids, organic acids, acetyl-salicylic acid are used mainly for bonds cleavages, precipitates formations, oxidation, and in the dissolution of complex polymers (Cheng *et al.*, 2011a; Chen *et al.*, 2017 and Mohapatra *et al.*, 2017). Acids, e.g.HCl, could hydrolyse cellulose and hemicellulose by attacking the  $\beta$ , 1-4 glucosidic bonds of lignocellulose, whereas lignin is degraded when alkali is applied. Alkalis such as  $\text{Ca}(\text{OH})_2$ , NaOH, KOH and  $\text{NH}_4\text{OH}$  are mainly employed to cleave the ester and ether bonds in lignin and hemicellulose, enhancing lignin porosity and susceptibility to microbial attack (Chen *et al.*, 2017 and Mohapatra *et al.*, 2017). Ionic liquids are charged salts that form hydrogen bonds with a cellulose hydroxyl group of LCB; thus, they form precipitates (Chen *et al.*, 2017 and Salakkam *et al.*, 2019). They also tend to dissolve lignin

polymer. Organic solvents, when employed, are used to amplify the pore size, thereby increasing the surface area of cellulose and can also be used to cleave the linkage of lignin ester bonds (Salakkam *et al.*, 2019).

In physical pre-treatment, the highly crystalline and robust lignocellulose structure is disordered to increase the surface area to hydrolysis and microbial breakdown (Cheng *et al.*, 2011a). Whereas grinding reduces the biomass materials into small particles, milling is used to produce a fine particle. Thermal pre-treatment has double objectives – lignocellulose pre-treatment and sterilisation. In the LCB pre-treatment, the bonds of lignin and hemicellulose and the bonds in crystalline cellulose are degraded by applying heat ranging from 50-250°C to lignocellulose feedstock (Hendriks and Zeeman, 2009). In microwave irradiation, like any other irradiation process, non-ionising electromagnetic radiation with wavelengths ranging from 1 mm to 1 m located between 300 and 300 000 megahertz (MHZ) is applied, which causes the swelling and fragmentation of LCB (Salakkam *et al.*, 2019). In ultrasound pre-treatment, the decomposition of lignin and hemicellulose is brought by the reactive H<sup>+</sup> and OH<sup>-</sup> radicals and increment in pressure produced by cavitation within the plant cells and liquid regions with the plant (Rodriguez *et al.*, 2017).

Physical and chemical pre-treatment methods can be combined to enhance lignin removal and cellulosic link cleavages to increase hydrolysis efficiency. For example, in the steam explosion process, after the subjection of LCB to the high pressure of 0.69 – 4.83 MPa and temperature of about 160-260°C for a few seconds, the saturated steam that is generated enters the biomass and swells the cell wall of the biomass resulting in the disruption and release of hexoses and pentose sugars (Cheng *et al.*, 2011b, Chen *et al.*, 2017 and Salakkam *et al.*, 2019). Ammonia-based or ammonium fibre explosion (AFEX) process is the same as a steam explosion; however, the lignocellulose is exposed to liquid ammonia under high pressure of 250-300 psi and temperature of about 60-100°C for a few minutes (Sun *et al.*, 2016). The immediate pressure release causes crystalline cellulose fragmentation, increasing the enzymatic hydrolysis (Salakkam *et al.*, 2019).

These pre-treatments technologies, notwithstanding their apparent advantages, are costly, require a considerable amount of energy, washing-up requirement, produce toxic and inhibitor compounds (phenolic compounds from lignin and furan derivative like furfural and 5-hydroxymethyl-2-furaldehyde (HMF) from hemicellulose) that lowers the activity of microbes and other biocatalysts (Bundhoo *et al.*, 2015; Schroyen *et al.*, 2015 and Jeonsson and Martins, 2016). Furthermore, some of these pre-treatments negatively affect the sugar monomers' yield (Zhang *et al.*, 2007 and Ren *et al.*, 2010), present difficulty in recovering and disposing of used chemicals, taking time, and creating carbon emissions, negating the intentions of the whole process generally. However, there are improvements to these concerns, and two or more pre-treatments methods can be employed to reduce cost and energy. In this regard, the writer will explore the application of agro-industrial wastes as a substitute for alkaline and acid pre-treatments.

The biological pre-treatment method, which uses a microorganism or microbial parts or products to pre-treat LCB, has been widely used as its operation is milder than the traditional physical and chemical pre-treatments (Cheng *et al.*, 2011a; Kuhad *et al.*, 2013 and Rodriguez *et al.*, 2017). Microorganisms used are mainly fungi (white rot, brown rot and soft rot) known for their unique ligninolytic system (Kuhad *et al.*, 2013; Gai *et al.*, 2014, Shah *et al.*, 2015 and Rouches *et al.*, 2016). *Cyathus stercoreus*, *Phanerochaete chryosporium*, *Ceriporia lacerate*, *Ceriporiosis subvermispora*, and *Pleurotus ostreatus* are among the most employed white rot (Hassan *et al.*, 2018). Other ligninolytic microbes include bacteria, actinomycetes, cyanobacteria and other fungus species (Kuhad *et al.*, 2013). As reported by Wan and Li (2012), these fungus species are effective in de-lignification of lignocellulose biomass with their ligninolytic/oxidative enzymes such as laccase, lignin peroxidase (LiP) and manganese peroxidase (MnP). The application of these enzymes directly to the rice straw has been documented (Sindhu *et al.*, 2016) to reduce the long pre-treatment duration of biological treatment. Nevertheless, the production of most of these enzymes is still on the lab scale and have high-cost requirements. Arguably, using a mixed microbial culture can be efficient as participating



microbes benefit mutually. However, slow solubilisation of complex carbon compounds, production of unwanted products and growth of hydrogen consuming methanogens are associated with mixed culture.

After the pre-treatments, the newly released polysaccharides are hydrolysed to simple monosaccharides. Lastly, the simple sugars are fermented to hydrogen or methane, with the digestate further processed through combustion technologies to yield other valuable products like silica and biochar or employed as manure.

#### **2.4 Polysaccharides Hydrolysis**

Kumar *et al.* (2009) and (2016) report on the research and development perspectives of lignocellulose-based bio-hydrogen production, stated that only a smaller percentage of microorganisms with cellulolytic capability could enzymatically hydrolyse cellulose polysaccharides, which is a homopolymer containing glucose as the only monomer. In furtherance, he reported that the most crucial step of cellulose hydrolysis is to cleave the  $\beta$ -1, 4 linkages existing between two close glucose molecules placed repeatedly throughout the cellulose chain. The cellulase enzyme's uniqueness does this action, among other enzymes, in degrading the insoluble carbon polymer - cellulose (Wilson, 2011). These groups of enzymes that work differently but synergistically are classified as endo-cellulases (also known as endoglucanase), exo-cellulases (or exoglucanases), and cellobiohydrolase (also called  $\beta$ -glucosidase) (Juturu and Wu, 2014). First, the endo-glucanase binds randomly to the cellulose polysaccharides chain and cleaves the molecule into smaller oligomeric fragments. Next, the oligomeric polymer is split into cellobiose (dimeric) molecules by exo-glucanase (Wei *et al.*, 2014), and finally, cellobiohydrolase is needed to solubilise the dimeric sugar to monomeric and consumable glucose (Kuhad *et al.*, 2016) (Fig 2-5). It is important to note that cellobiose serving in a regulatory capacity acts as a potent inhibitor for exo-cellulases (exo-glucanases) and can bring complete inhibition at a 2% concentration within the system cellulosome (Andric *et al.*, 2010).

The application of a mixture of cellulase enzymes, mainly  $\beta$ -glucosidase, has been observed to have synergistic effects, and this has been described as more profitable than a single class of cellulase enzyme (Wilson, 2011). Typically, cellulase producing microorganisms make two kinds of cellulases: aerobes secrete an extracellular enzyme complex – cellulosome; while the other produced by anaerobes is a multi-enzyme cellulase complex (Tsavkelova and Netrusov, 2012). There are wide varieties of microorganisms that can naturally produce cellulase enzymes, including bacteria, fungi, actinomycetes, and yeast (Kuhad *et al.*, 2016). It is recently reported that it is not only microorganisms that produce cellulases, but some insects, molluscs, nematodes, and protozoa can do it (Kuhad *et al.*, 2016). However, only relatively few could produce a high amount of cellulase required at a commercial scale, and none can make all the three cellulases for complete crystalline cellulose solubilisation (Sukumaran *et al.*, 2005). Due to their higher cellulase productivity and the ability to make thermostable cellulases presently, thermophilic cellulolytic fungi have been widely used (Kuhad *et al.*, 2016). It is also paramount to mention that mesophilic and psychrophilic cellulolytic microorganisms have been well documented (Sattar *et al.*, 2016a). Psychrophilic cellulolytic microbes are becoming more interesting because of their potential to be used in industrial and cold applications. For example, Lu *et al.* (2011) produced hydrogen using *Geobacter psychrophilus* at 9°C using microbial cell electrolysis. Nonetheless, as Kasana and Gulati (2011) reported, most works on isolated cold cellulase-producing microorganisms are not true psychrophiles but facultative psychrophiles that can grow at 30–35 °C.

In structure and composition, hemicellulose is more complicated than cellulose. This complexity is because hemicellulose is a heteropolymer and constitutes sugar monomers such as glucose, xylose, mannose, galactose, rhamnose, arabinose and sugar acids like methyl-glucuronic and galacturonic acids, which can adhere to each other at random (Perez *et al.*, 2002). Hemicellulose includes xylan, arabinoxylan, glucuronoxylan, xyloglucan and glucomannan (Van-Dyk and Pletschke, 2012). Also, in terms of the degree of solubilisation, hemicellulose is easier to hydrolyse than cellulose. In carbon

hydrolysis, hemicellulose requires many enzymes, such as endo-xylanase, acetyl xylan esterase,  $\beta$ -xylosidase, endo-mannanase,  $\beta$ -mannosidase,  $\alpha$ -L-arabinofuranosidase,  $\alpha$ -glucuronidase, ferulic acid esterase,  $\alpha$ -galactosidase, and a p-coumaric acid esterase, due to the complex composition (Singh *et al.* 2010). Van-Dyk and Pletschke (2012) state that these enzymes are grouped into two: a) depolymerising enzymes, which cleave the backbone, and b) the other enzyme removes substituents that may hinder the work of depolymerising enzymes. Among the hemicellulose enzymes mentioned, the major hemicellulose-degrading enzymes are endo-xylanase and endo-mannanase (Singh *et al.*, 2010), and many species of fungi and bacteria (*Thermoanaerobacter mathranii* A3N), including *Actinomyces*, have been reported to produce these kinds of enzymes (Beg *et al.*, 2001).

After the hydrolysis of the polysaccharides, the free monomers could be further subjected to bioconversion for biofuels and other valuable products (Nanda *et al.*, 2013), the only challenge being that the pentose sugars are difficult to ferment. However, some microorganisms, e.g. *Bacillus firmus*, *Geobacter metallireducens*, can utilise pentoses as carbon substrate (Prakasham *et al.*, 2010). Besides, xylose is more preferred to glucose due to its higher hydrogen yield potential per substrate (Prakasham *et al.*, 2010). Therefore, research studies are growing on the need to either employ such organisms, augment the traditional glucose fermenters, or use biological tools to genetically modify traditional fermenters' metabolic pathways (glucose consuming bacteria).



Fig 2-7: Oil palm fruit in the bunch (a), being de-fruited from the bunch (b) and an empty bunch (c)

## 2.5 Empty Oil Palm Fruit Bunches Ash (Potash)

The potash, which is widely available in Nigeria and used as a soil fertiliser (Mohammad *et al.*, 2012), is made locally as a left-over char (ash) from utilising the oil palm empty fruit bunches as a source of heat energy for cooking (Yusoff, 2006) (Fig 2-7c). The oil palm (*Elaeis guineensis*) takes its origin from the Gulf of Guinea in West Africa and is a tropical plant that does well in warm climates (Fig 2-7a and c). Oil palm in Nigeria is grown mainly in the south-eastern part of the country to produce edible cooking oil and a valuable economic plant as the oil can be exported or used in diesel production esterification processes (Chang, 2014). The high oil yield of about 4.87 t ha<sup>-1</sup> per year is 1.0 times higher than soybean oil, 8.0 times greater than sunflower and 6.5 times more than rapeseed in yield. (Tye *et al.*, 2011 and Chang, 2014). In oil palm processing and extraction, empty palm fruit bunch (EPFB) is among the palm biomass produced in abundance (4.42 t ha<sup>-1</sup> per year), with 1.0 tonne of EPFB biomass generated for every 1.0 tonne of palm oil produced alongside other wastes such as palm fibres (0.7 tonnes), palm kernels (0.3 tonnes) and palm shells (0.3 tonnes) (Dalimin, 1995 and Kelly-Yong *et al.*, 2007). The EPFB itself, which accounts for almost 20% of the fresh fruit bunch weight (Mohammad *et al.*, 2012), is a bulk brown residue (Fig 2-7c) at oil palm mills after the palm fruits (Fig 2-7b) have been removed and processed.

Apart from being used as local fertiliser, the ash (potash) produced after combustion from the EPFB (Mohammad *et al.*, 2012) is also used locally as insecticides and washing plates. The filtrate obtained after filtration of the mixture of the ash with water is slippery to touch, giving an impression that it is an alkali (Udoetok, 2012) and is darkish brown depending on the amount of water used in the mixture. This filtrate is evaluated for pre-treatment of RS and sludge enrichment for hydrogen production. The application of PE as a biomass pre-treatment agent stems from the notion that PE is used as a food softener in meal preparation in Eastern Nigeria. PE is generally added while cooking dry seeds and hard meats to quicken the tenderness and shorten cooking time.

The proximate analysis of EPFB fibres reported by Chang (2014) showed that ash content (%) is within the range of 1.30 – 13.65 and can be a good source of raw material in silica production. Furthermore,

the work of Udoetok (2012) on the characterisation of ash made from oil palm fruit bunches found out that EPFB ash contains varying amounts of heavy metals (chromium, zinc, calcium, potassium, sodium and magnesium) and anions (phosphate, nitrate, sulphate and chloride), which in varying quantities, are essential metals required for microbial growth. Hence, EPFB ash or extract supplementation in the anaerobic digesters may be a good alternative for trace elements in AD processes.



Fig 2-8: Preparation of cassava wastewater from locally made fufu (a and b)

## 2.6 Cassava-steep Wastewater

Cassava (*Manihot esculenta Crantz*), according to a report by the Federal Ministry of Agriculture and Natural Resources Nigeria (FMANN) (2006) and Howeler (2020), was brought into Central Africa from South (Latin) America in the sixteenth century by the Portuguese voyagers. They continued that the formerly enslaved people probably introduced cassava into southern Nigeria as they returned to Nigeria from South America through Sao Tome and Fernando Po's islands. Cassava is a dicotyledonous plant that belongs to the plant Euphorbiaceae family (Bassam, 2010). Cassava, one of the essential crops in Nigeria, is the most widely cultivated crop in the southern part of the country and irrefutably, the most grown crop by every household, which is due to ease of cultivation, high carbon and calorie

content, and ease of conversion to many different forms of food products (Cushion *et al.*, 2009). Currently, Nigeria is the largest cassava producer with an estimated annual output of over 34 to 59.5 million tonnes of cassava tuber roots (FMANN, 2006, FOASTAT, 2018, Muchie and Baskaran, 2012 and Ghosh, 2017). Moreover, studies revealed that cassava plays a significant role in the local communities' economy in southern Nigeria and is increasingly growing to other country zones.

The raw roots and leaves, which are not palatable, contain varying cyanide compounds (cyanogenic glucosides: linamarin and lotaustralin) harmful to humans and animals (FMANN, 2006; Okunnade and Adekalu, 2013). As mentioned before, the raw cassava is processed mainly in many forms in Nigeria to improve consumption, increase the shelf life of the products, make transportation and marketing more manageable and reduce the cyanide content (Cushion *et al.*, 2009, Atuluegwu and Egwuonwu, 2011 and Oyeyinka *et al.*, 2020). The most common traditional processing methods, which include boiling, steaming, slicing, grating, soaking or seeping, fermenting, roasting, pressing, drying, and milling, give pitiable products quality and yield (Oyeyinka *et al.*, 2018 and 2020). However, there has been an improvement in increasing yield output and quality through modern technology (FMANN, 2006). During cassava processing leading to tissue damage, the cyanogenic glucosides are hydrolysed by an endogenous enzyme – linamarase to respective cyanohydrins and further to hydrogen cyanide known to be very toxic to animals and humans (FMANN, 2006). Among the traditional processing methods, fermentation is the most popular in the rural communities in Nigeria. Fermentation can be done under the presence of air (aerobic or sun–drying) or the absence of air (anaerobic).

In anaerobic fermentation, small-sized or whole roots cassava are placed in water for 3-5 days in a jar or airtight plastic containers (Fig 2-8a and b). This process is followed by other approaches depending on the cassava processed products required (garri, fufu, or abacha chips (African salad)). As stated earlier, cassava tissue damage will occur during the fermentation, leading to rapid hydrolysis of the cyanogenic glucosides, efficiently reducing both the free and residue cyanide in the processed products. For illustration, Hahn (2006) reported that fermentation in water is more efficient for

reducing the cyanide of roots, and about 70-95 per cent of cyanide is said to be removed from the fresh cassava roots after three days of fermentation in water.

The fresh spent water used for the fermentation steeping cassava-steep wastewater (CSWW) (Fig 2-8) is very acidic and toxic because of the high amount of hydrogen cyanide, relative amount of organic acids, and degrading enzymes, particularly  $\beta$ -glucosidase (FMANN, 2006 and Okunnade and Adekalu, *et al.*, 2013). Based on O-Thong *et al.* (2011), about 5.0 – 7.0 L of wastewater (including CSWW) is produced from 1.0 kg of fresh roots, which means that the wastewater from cassava processing can be in millions of litres depending on the amount of raw cassava processed. This also means that about 295 - 413 million cubic meters of CSWW are produced annually in Nigeria (Nigeria produces about 59.5 million tonnes of cassava annually (FOASTAT, 2018). If not appropriately treated, the water also constitutes environmental challenges due to cyanide and organic compounds (Okunnade and Adekalu *et al.*, 2013). CSWW may also have a redox effect as it has been found that human sludge is reduced in a filled pit toilet (latrines) that predominantly abound in the local communities of Nigeria. This research studied the redox effect of CSWW as a potential pre-treatment agent for RS and seeded sludge. Also, the potential of CSSW as an enrichment agent for HPB in seeded sludge and as a chelating agent in removing metallic impurities in RS ash employed in silica production is explored.

## **2.7 Corn-steep Liquor**

Corn-steep liquor (CSTL) is the wastewater that is generated during the steeping of corn as a prerequisite for the fractionation of corn components in the wet-milling process. In the steeping process, the counter-current water flow and the addition of a small amount of sulphuric acids to inhibit the growth of moulds and other undesirable organisms with the dried corn are involved (Hull *et al.*, 1996). The steeping is generally done in tanks at varying temperatures ranging from 20 - 55 °C over approximately 1 – 3 days. Depending on the corn product of choice, the details of the process vary among different industries. In the steeping processes, the pattern is that the new, dried corn is

coarsely crushed and imbued into the tanks that contain the sulphuric-added steep water. As a result, the volume of steep-water generated in the corn wet-milling is much, and the residual water contains varying amounts of complex mixtures of carbohydrates, amino acids, peptides, organic compounds, heavy metals, inorganic ions, and *myo*-inositol phosphates, giving CSTL a high chemical oxygen demand (Steven *et al.*, 1996 and Wang *et al.*, 2016). Therefore, CSTL is proposed as an optimum substrate for microbial growth. It can also serve as an excellent feedstock in bio-hydrogen/methane production as it offers almost all the necessary nutrients. CSTL organic acid constituent may produce a similar effect to weak acids on biomass as a pre-treatment agent. Zhao *et al.* (2010), in their research study on methane production from rice straw pretreated by a mixture of acetic and propionic acid, were able to find that methane production from RS was enhanced by dilute organic acid pre-treatment. Hence, the research experiment evaluated the effectiveness of CSTL as a pre-treatment agent for RS and an enrichment agent for HPB in seeded sludge and as a chelating agent in removing metallic impurities in silica production.

Even though there are no available statistics in Nigeria regarding the amount of CSTL generated, many industries using corn as raw materials abound, and these companies make litres of corn wastewater. Having said that and using available statistics from China, more than 20 million tonnes of corn starch wastewater is produced by over 600 companies (Vera *et al.*, 2015).

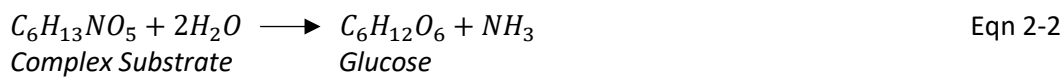
## **2.8 Anaerobic Digestion and Dark Fermentation Processes**

### **2.8.1 Microbiology, Process and Biochemistry.**

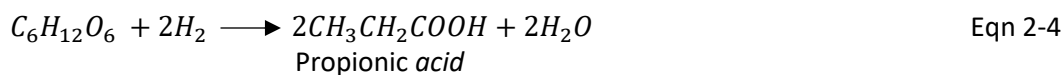
The anaerobic fermentation processes can be described as a synergistic process of four serially different stage processes: hydrolysis, acidogenesis, acetogenesis, and methanogenesis (Khan *et al.*, 2017b). The AF process comes after disintegrating the organic composite materials into individual polymers (Campanaro *et al.*, 2016), and each step is carried out by a distinct functional group or community of microorganisms (Yu and Schanbacher, 2010).



In the hydrolysis stage, catalysed by the extracellular hydrolytic enzymes (such as xylanases, cellobiases, cellulases, amylases, proteases and lipases), insoluble organic materials such as polysaccharides, proteins and fats present in feedstocks are transformed or broken down to soluble derivatives (sugars, amino acids and fatty acids) by facultative or strictly anaerobic bacteria (e.g., *Clostridium* spp) (Weiland, 2010; Angelidaki *et al.*, 2011 and Khan *et al.*, 2017b) (Eqn 2-1 and 2-2).

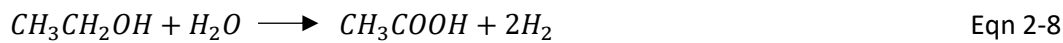
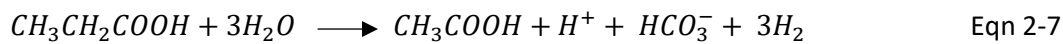


Kinetically, for substrates such as simple sugars and starch, the hydrolysis stage can be remarkably rapid while the hydrolysis process is slow and often the major rate-limiting step of the AD process for insoluble lignocellulose substrates (Adney *et al.*, 1991; Mata-Avarez *et al.*, 2014 and Mason and Stuckey, 2016).



In acidogenesis step, also referred to as the hydrogen production stage, the resulting monomers of hydrolytic products such as unsaturated fatty acids, glycerol, monosaccharides and amino acids are converted into short-chain fatty acids (SCFA), gases (hydrogen and carbon dioxide), acetic acids and alcohols (Eqn 1-4, 2-3 to 2-6) (Yu *et al.*, 2010; Angelidaki *et al.*, 2011; Khan *et al.*, 2017b and An *et al.*, 2020b) by another community of facultative and strictly anaerobic bacteria (e.g. *Bacteroides*,

*Clostridium*, *Butyribacterium*, *Propionibacterium*, *Pseudomonas* and *Ruminococcus*). Acetate is the major SCFA formed. Other SCFA produced include propionate, butyrate, formate, lactate, isobutyrate, valerate and succinate with small quantities of alcohols (e.g. ethanol and glycerol). Whereas lactate, propionate or acetate/butyrate/caproate are produced via acetyl-CoA enzyme by fermentation of glucose either by the Embden-Meyerhof-Parnas (EMP) or Entner-Doudoroff (ED) pathways, acetate, ammonia and hydrogen gas are liberated by fermentation of mixed amino acids using the Stickland reaction (Angelidaki *et al.*, 2011). This step proceeds rapidly and can lead to AD failure due to SCFA accumulation when substrates containing large amounts of soluble carbohydrates (simple sugars and starch) are digested at high organic loading rates (Yu *et al.*, 2010).



In the acetogenesis phase, the SCFA with three or more carbons and other products (alcohols and long-chain fatty acids from lipid hydrolysis) of the two preceding steps cannot be consumed directly by the methanogens. Instead, they are converted into acetic acids with the evolution of gases, mainly H<sub>2</sub> and CO<sub>2</sub> (Eqn 2-7 to 2-8) (Khan *et al.*, 2017b) by a unique community of strictly anaerobic bacteria known as syntrophic acetogens. However, hydrogenotrophic methanogens must exist with the syntrophic acetogens to rapidly consume the H<sub>2</sub> produced by the syntrophic acetogenesis through an interspecies transfer of hydrogen. This mutual relationship is because the oxidation of SCFA and alcohols under fermentative conditions are thermodynamically unfavourable (De Bok *et al.*, 2005). Acetate is also produced via the reduction of CO<sub>2</sub> using the reductive acetyl CoA or Wood-Ljungdahl pathway (WLP) (Angelidaki *et al.*, 2011).

The most significant syntrophic acetogens in anaerobic digesters are *Syntrophomonas wolfei* utilises butyrate, and *Syntrophobacter wolinii*, which oxidises propionate. The syntrophic acetogens grow slowly with a generation time of more than one week, and as a result, the solid retention time in

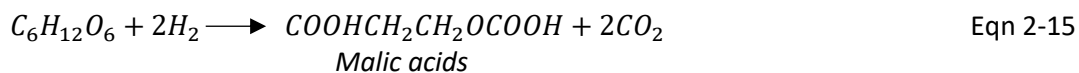
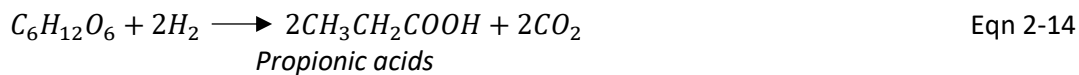
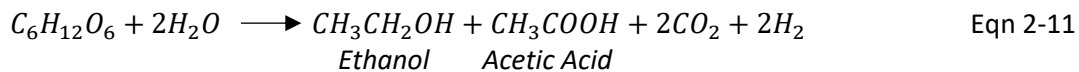
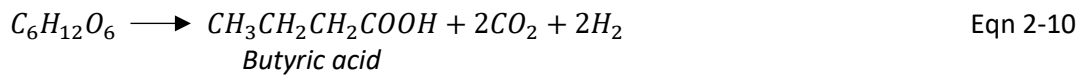
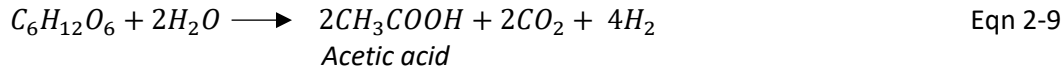
anaerobic digesters has to be long enough (e.g. 15 days or longer) to sustain and retain enough syntrophic acetogens (Angelidaki *et al.*, 2011). Therefore, syntrophic acetogenesis can be the rate-limiting step in an AF process and is mainly encountered during an AD process where the organic loading rate is too high, and the production of non-acetic SCFA is too much for the community of syntrophic acetogens. Lastly, the acetic acids produced are consumed by the methanogens to methane with carbon dioxide's evolution. The methanogenesis stage is discussed below.

### **2.8.2 Hydrogen Production**

Anaerobic digestion, which requires low energy inputs, and little mixing, has been commonly researched with biogas or methane as the final products. Other intermediary products are hydrogen gas, carbon dioxide and volatile acids are produced by acidogens. However, hydrogen gas is quickly consumed while the volatile acids can be converted into methane by the hydrogen-consuming bacteria (Van-Ginkel and Sung, 2001). Therefore, if the end step or methanogenesis were to be prevented by inhibiting hydrogen-consuming bacteria, intermediary products such as SCFA and gases will accumulate in the reactor due to the high activity of the acidogens. In other words, the organic substrate is converted to organic acids, mainly acetic acids and butyric acids, with the evolution of hydrogen gas and no further conversion of these volatile acids to methane are preferred (Argun *et al.*, 2017). To achieve this inhibition, an enrichment procedure using either chemical agents (Chloroform, extreme acids or alkali) or physical (heat-shock, irradiation) inhibit non-spore-forming bacteria (which are mainly HCB) while the spore-forming bacteria (mostly the HPB) will survive.

Hypothetically, at room temperature, the breakdown of 1mol of glucose yields 12 mol of hydrogen gas but based on reaction stoichiometry, fermentation of 1 mol of glucose into the most common products acetic (Eqn 2-9), and butyric acids (Eqn 2-10) yields 4 mol and 2 mol hydrogen gas respectively. That is 498mL H<sub>2</sub>/g hexose and 249mL H<sub>2</sub>/g hexose for acetic and butyric routes, respectively, at 25°C. However, due to the formation of acetic and butyric acid mixture in the ratio of

3:4, the practical yield of hydrogen is mostly around 2.0 – 2.5 mol H<sub>2</sub>/ mol of glucose (Kapdan and Kargi, 2006).



Thus, only less than half of glucose is utilised for hydrogen production, and glucose degradation might follow other biochemical routes without hydrogen production (Hallenbeck, 2009). The formation of these products makes sense as they are essential in forming adenosine triphosphate (ATP), a high energy molecule necessary for the growth and survival of organisms and necessary for redox balance maintenance of the fermentation process (Hallenbeck *et al.*, 2012). Under some conditions, the organic products ethanol and acetate are produced (Eqn 2-11), lowering the stoichiometric yield to 2 mol of H<sub>2</sub> for 1 mol of glucose (Hallenbeck, 2009). Similarly, the metabolic routes leading to ethanol (Eqn 2-12) and lactic acids (Eqn 2-13) produced by *Clostridium barkeri* (Khanal *et al.*, 2003) are non-hydrogen forming, while propionic acid (Eqn 2-14) and malic acid (Eqn 2-15) are the hydrogen-consuming end product of a fermentative process.

Traditionally in anaerobic fermentation processes for hydrogen production, carbon-containing monosaccharides are broken down in the absence of oxygen by the hydrogen-producing microorganism, typically of strict anaerobes (*Clostridia* (*C. butyricum*, *C. thermolacticum*, *C. pasteurianum*, *C. paraputrificum* M-21 and *C. bifermentans*) (Kapdan and Kargi, 2006), facultative anaerobes of genus *Enterobacteriaceae* (*Escherichia coli*, *Enterobacter* (*Enterobacter aerogenes*, *Enterobacter cloacae* ITT-BY), *Citrobacter*), *Thermoanaerobacterium* (*T. Thermosaccharolyticum* and *Desulfotomaculum geothermicum*), methylotrophs, rumen bacteria, methanogenic bacteria and archaea) (Shin *et al.*, 2004; Kapdan and Kargi, 2006 and Li and Fang, 2007). It has also been reported that some aerobes such as *Aeromonas* spp, *Pseudomonas* spp, *Vibro* spp, *Alcaligenes* and *Bacillus* can also produce hydrogen (Kapdan and Kargi, 2006; Li and Fang, 2007).

In dark fermentation processes, soluble sugars are broken down to pyruvate by hydrogen-producing bacteria through the glycolytic pathways using the action of nicotinamide adenine dinucleotide ion (NAD<sup>+</sup>) producing adenosine triphosphate (ATP) from adenosine diphosphate (ADP) and the reduced form of nicotinamide adenine dinucleotide (NADH) (Li and Fang, 2007). Then, the produced pyruvate is further broken down to acetyl coenzyme A (acetyl-CoA) through two possible pathways: formate (pyruvate: formate lyase (PFL)) route or the reduced ferredoxin (pyruvate: ferredoxin oxidoreductase (PFOR)) pathway (Holladay *et al.*, 2009) depending on the type of seeded culture utilized.

In the PFL pathway, the anaerobic conversion of pyruvate by coenzyme A (CoA-H) action gives rise to the production of acetyl-CoA and formate (Das and Veziroglu, 2001 and Hallenbeck, 2009). The formate is then converted to H<sub>2</sub> and CO<sub>2</sub> by the actions of formate hydrogen lyase under acidic conditions (Das and Veziroglu, 2001 and Hallenbeck, 2009). Under the PFOR routes, the pyruvate is oxidised by ferredoxin oxidase (Fd<sub>ox</sub>) and coenzyme A to acetyl-CoA, ferredoxin reductase (Fd<sub>red</sub>) and CO<sub>2</sub>, with subsequent reduction of H<sup>+</sup> ions by Fd<sub>red</sub> to H<sub>2</sub> and Fd<sub>ox</sub> (Hallenbeck and Benemann, 2002 and Nath and Das, 2004).

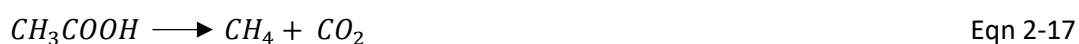
The acetyl-CoA generated in both PFL and PFOR pathways gives rise to the formation of end products such as acetate, butyrate, butanol, ethanol (Li and Fang, 2007 and Ntaikou *et al.*, 2010) with a yield of ATP while any residual NADH produced can be re-oxidised to H<sub>2</sub> (Ntaikou *et al.*, 2010 and Bundhoo and Mohee, 2016) depending on the end-product. For instance, no residual NADH will be reduced to H<sub>2</sub> if the end-products are either butyric or ethanol (Ntaikou *et al.*, 2010), which means that a maximum of 4 mol H<sub>2</sub> can be produced from 1 mol of glucose if the end-product is acetic acid, while a maximum of 2 mol H<sub>2</sub> is made from a mol of glucose if butyric acid is the end-product (Turker *et al.*, 2008 and Bundhoo and Mohee, 2016). Nevertheless, in practical situations and as stated earlier, hydrogen yield is lower than 4 mol per glucose since both acetate and butyrate exist as a mixture of end-products.

Organisms that lack the PFOR pathway but only have the PFL pathways cannot produce hydrogen from NADH and hence, are limited to the production of 2 mol H<sub>2</sub>/ mol of glucose with the evolution of carbon dioxide (CO<sub>2</sub>). In comparison, those with the PFOR pathways can produce hydrogen from NADH oxidation using either one or more of the several different hydrogenases making roughly 2 – 4 mol H<sub>2</sub>/ mol of glucose (Hallenbeck *et al.*, 2012). The different hydrogenases include the NADH-dependent, the Fd-dependent hydrogenases and bifurcating NADH-Fd dependent hydrogenase. For example, in Fd-dependent hydrogenase, ferredoxin is reduced through the NFOR (NADH: ferredoxin oxidoreductase) (Hallenbeck *et al.*, 2012).

In the process of disposing of excess electrons through the activity of the hydrogenases, molecular hydrogen is produced and under anaerobic conditions, that is, in the absence of oxygen, protons (H<sup>+</sup>) can act as electron acceptors to counterbalance the electrons generated by the oxidation of organic substrate giving rise to hydrogen production (Das and Veziroglu, 2001).

### 2.8.3 Methane Production (Methanogenesis)

Hypothetically, at standard temperature and pressure, methane yield from cellulose and hemicellulose are 415 and 424 mL-CH<sub>4</sub>/gVS with a methane content of 50% (Li and Khanal, 2016). As discussed earlier, if the methanogenesis were to be prevented by inhibiting hydrogen-consuming bacteria, intermediary products such as SCFA and gases would accumulate in the reactor due to the high activity of the acidogens. However, under normal circumstances, the final phase of the AF process proceeds to methanogenesis, which involves converting C<sub>1</sub> methylated compounds, acetate and H<sub>2</sub>/CO<sub>2</sub> to methane mainly by the *Archaea* in an anorexic environment (Gerardi, 2003 and Angelidaki *et al.*, 2011). Methanogens are fastidious and strict anaerobes that belong to the phylum *Euryarchaeota* (Angelidaki *et al.*, 2011). The three main methanogenic pathways utilize the WLP for methane production (Angelidaki *et al.*, 2011; Borrel *et al.*, 2016; Vanwonterghem *et al.*, 2016 and Aryal *et al.*, 2018). The pathways are a) Hydrogenotrophic methanogenesis – where CH<sub>4</sub> is produced via the reduction of CO<sub>2</sub> by H<sub>2</sub> (Eqn 2-16); b) by the utilization of other C<sub>1</sub> substrates (e.g., methanol and methylamines), also known as the methylotrophic pathway, which involves the oxidation of C<sub>1</sub> compounds to generate electrons required for the production of three molecules of methane (Costa and Leigh, 2014 and Aryal *et al.*, 2018). Hydrogenotrophic methanogens account for one-third of the total methane produced and are mainly found in the genera *Methanobacterium*, *Methanospirillum*, *Methanobrevibacter*, *Methanococcus*, *Methanomicrobium*, *Methanoculleus*, *Methanogenium* and *Methanothermobacter* pathways (Gerardi, 2003; Angelidaki *et al.*, 2011; Lever, 2016 and Vanwonterghem *et al.*, 2016).



In the last methanogenic pathway, c) Methane is also produced from acetate's direct utilization by acetoclastic methanogens (Eqn 2-17). In this pathway, also termed acetotrophic (acetoclastic), acetate compound is split into a methyl group for methane generation and a CO, which is oxidized to generate the required reducing power (Aryal *et al.*, 2018). Methane produced from acetate accounts for two-thirds of the total methane because, as stated previously, under normal circumstances, acetate is the principal end product of the acidogenesis step in all anaerobic fermentation processes (Angelidaki *et al.*, 2011). The dominant species of acetoclastic methanogens are within the genera *Methanosaeta* and *Methanosarcina*. While some species of *Methanosarcina* can use C<sub>1</sub> substrates, *Methanosaeta* is obligate acetoclastic methanogens (White, 2000). The unique cofactor, F<sub>420</sub>, autofluorescent at a wavelength of 420 nm (Gorris and Van-der Drift, 1994 and Yu and Schanbacher, 2010), is in all methanogens and more in hydrogenotrophic methanogens. The cofactor appears blue when viewed microscopically. Most methanogens grow slowly, especially the acetoclastic methanogens (the generation time of *Methanosaeta* is 3.4 – 9 days) due to low energy yield from the methanogenesis pathway (Gerardi, 2003). However, because the low energy yield of the methanogenesis process forces it to run rapidly, methanogenesis is not a rate-limiting step.

## **2.9 Factors that affect Anaerobic Digestion/Fermentation Process**

Generally, for processes undergoing anaerobic digestion or fermentation, some factors may influence or inhibit the microbial growth leading to either failure or stability of the AD/DF process (Chen *et al.*, 2008 and Rajagopal *et al.*, 2013). For example, AD process instability can arise from issues relating to process pH, the temperature variation, digester feeding, inadequacies of essential inorganic salts/metallic ions, presence of inhibitory and toxic substances, non-capable degrading microbial consortia, hydraulic retention time, poor bio-reactor design and approach employed in the digestion processes (Drosg, 2013 and Ghimire *et al.*, 2015). These factors are discussed extensively below.



### 2.9.1 Process Temperature

Even though there are no significant variations in specific methane yields from mesophilic to thermophilic temperatures, the reactor temperature is critical and may affect process stability. The microbial community is more diverse and stable when the AD process operates at mesophilic than thermophilic temperatures (Ward *et al.*, 2008 and Appels *et al.*, 2011). Nevertheless, functioning at thermophilic temperatures is pertinent to achieving shorter hydraulic retention times desired features of an optimised AD process; most AF technology facilitates increased organic loading rates (Bocher *et al.*, 2008). Similarly, the operating temperature depends on the hydrogen-producing organisms, and many documentations on these organisms are available (Jung *et al.*, 2011). The substrate biodegradability rate, the hydrogen-producing enzymes activity, and H<sub>2</sub> producers' metabolism are significantly influenced by temperature (Elbeshbishy *et al.*, 2017). The metabolic routes can even shift by the influence of the operating temperature as different microorganisms become predominant at different temperatures (Elbeshbishy *et al.*, 2017). Increasing the temperature of DF reactors within a normal temperature range has been found to increase the yield of hydrogen since the activity of H<sub>2</sub> consumers are suppressed at high operating temperature (Saady, 2013). Based on the numerous reports on bio-hydrogen and methane production, mesophiles are favoured at a temperature of 37°C, 55°C for thermophiles and 70 - 80°C for hyper-thermophiles (Jung *et al.*, 2011 and Sattar *et al.*, 2016b). Even though thermophiles can yield higher hydrogen than mesophilic microorganisms, the hydrogen production rates per volume are still lesser due to slow microbial growth and lower cell masses (Foglia *et al.*, 2006). Thus, there may be a need to use a membrane bioreactor to sustain the high concentration of cell density for constant hydrogen production from lignocellulosic biomass at such a high temperature. However, it is expensive to maintain such a high temperature.

Since the operating temperature can control the by-products spectrum, it is crucial to maximise the temperature to shift the metabolic pathways towards yielding hydrogen routes (acetate and butyrate production) and away from hydrogen consuming pathways (alcohol or solvent production) (Vijayaraghavan and Soom, 2006). Although the variation of by-products due to temperature changes

is not consistent due to different mixed-seed culture communities, Wang and Wan (2008b) reported that as temperature increased from 20°C to 35°C, the ethanol concentration increased and reduced as the temperature is amplified from 35°C to 55°C. In contrast, butyrate was the predominant by-product at 37°C and acetate at 55°C (Yu *et al.*, 2002).

### 2.9.2 Process pH

The pH is considered as the most critical and sensitive operating parameter for maximum yield of hydrogen as it can also shift the by-products spectrum, affects the microbial community structure, regulate the intracellular metabolic functions such as the hydrogenase activity and further increases ammonia toxicity due to rise in the concentration of free ammonium nitrogen (FAN) (Temudo *et al.*, 2007, Chen *et al.*, 2008; Wang and Wan, 2008b; Guo *et al.*, 2010 and De Gioannis *et al.*, 2014). The pH of a solution is defined generally as the negative logarithm of the hydrogen ion concentration ( $H^+$ ). The pH value of <6.3 inhibits methanogens' activities under both mesophilic and thermophilic conditions, whereas homoacetogens are deactivated at a pH of 5.5 under thermophilic conditions (Luo *et al.*, 2011). More so, extreme pH (<4.5 and >11) favours solvent production (Van-Ginkel and Logan, 2005) and inhibits methanogens. Furthermore, hydrogen production metabolic pathways could be affected as strong acidic pH (<4.0) directly reduces the hydrogenase activity (Dabrock *et al.*, 1992) and other intracellular metabolic functions activities due to the formation of acidic and alcoholic metabolites that can penetrate the microbial cell membrane (Elbeshbishy *et al.*, 2017). So, there should always be a balanced pH value not to affect the iron-containing hydrogenase enzyme and inhibit hydrogen-consuming bacteria activities.

Anaerobic fermentation usually gives rise to acidic products, resulting in the more extended lag/exponential phase, which variably decreases the fermentation medium's initial pH (Sinha and Pandey, 2011). The drop in pH is maintained by adjusting the initial pH using a pH meter base/acid after different periods or using automatic pH controllers (Yasin *et al.*, 2011). The broad range of pH 4.5 to 8 is being reported in batch studies (Collet *et al.*, 2004; Kapdan and Kargi, 2006 and Guo *et al.*,

2010), whereas the pH 5.0 – 6.5 is recorded as the optimum for bio-hydrogen generation (Khanal *et al.*, 2003, Zhang *et al.*, 2007 and Antonopoulou *et al.*, 2010) using rice straw co-digested with sewage sludge. Regardless of the initial pH, most research indicated that the final pH in AF hydrogen production ranges between 4.0 – 4.8 due to organic acid production, which diminishes the medium's buffering capacity (Khanal *et al.*, 2004; Kapdan and Kargi, 2006). The initial pH of 4.0 – 4.5 is said to cause more extended lag periods, such as 20 h (Liu and Shen, 2004), whereas high initial pH of 9.0, which negatively affects hydrogen production yield, decreases lag time (Zhang *et al.*, 2003).

Similarly, the type of organic acids produced is affected by operating pH. For example, more butyric acid is produced at a pH of 4.0 – 6.0, while both acids (butyric and acetic acids) will be equal in concentration at pH 6.5 – 7.0 (Fang and Liu, 2002). In contrast, the propionate production pathway, the hydrogen consumption route, increases at neutral or alkaline pH > 7 (Lee *et al.*, 2009).

Methane production operates on a narrow pH range of 6.5 to 8.5, and the AD process could fail if the pH falls below 6.0 or rises above 8.0 (Ward *et al.*, 2008 and Weiland, 2010). Since hydrogen (produced at the acidogenic stage) and methane (generated at the acetogenic and methanogenic phase) operates at different pH values, a two-stage bioreactor design may increase process stability in an AD (Nasir *et al.*, 2012 and Peña Muñoz and Steinmetz, 2012).

On the other hand, the AD reactor contents' ability to resist changes in the pH brought about by the acids produced during the degradation process is defined as alkalinity value or the system's buffering capacity (Federation, 2007 and Von Sperling and De Lemos Chernicharo, 2005). These buffering effects are mainly provided by bicarbonate from CO<sub>2</sub>, a by-product of an AD process (Van Haandel and Van Der Lubbe, 2007). It is vital to mention that under certain circumstances, CO<sub>2</sub> can be solubilised in water to form carbonic acid (Eqn 2-18), along with VFA contributing to the reduction of pH in an AD process (Schon, 2010), which affect the activities of methanogens (Khanal, 2011). Studies have shown that to maintain the pH of an AD process above 6.8, bicarbonate alkalinity should be above 1000 mg/L CaCO<sub>3</sub>, while for large scale AD plants, the bicarbonate alkalinity is maintained between 1000 – 5000

mg/L CaCO<sub>3</sub> (Federation, 2007 and Khanal, 2011). Nonetheless, for a more stable AD process with a pH range of 7.0 – 7.2, Andreoli (2007) suggested bicarbonate alkalinity levels between 4000 - 5000 mg/L CaCO<sub>3</sub>.



### 2.9.3 Un-dissociated Acids

As stated hitherto, in producing bio-hydrogen via DF of glucose, acetate and butyrate are the primary soluble metabolites, and these volatile fatty acids (VFA) may ultimately reflect the hydrogen production efficiency in DF processes. Nonetheless, some of these VFA are precursors of many essential compounds required to maintain biomass (Wong *et al.*, 2014). However, over-accumulation of these soluble organic acids can inhibit the hydrogen and methane producers' intracellular functions with propionate the most inhibitory SCFA to the AD process at concentrations > 5 mg/L (Oreopoulou and Russ, 2006). The inhibition of metabolic functions is perhaps due to the rise in ionic strength or inhibition by un-dissociated acids (Ciranna *et al.*, 2014 and Srikanth and Mohan, 2014). The un-dissociated acids at low extracellular pH less than the PK<sub>a</sub> values of organic acids (the PK<sub>a</sub> values for acetate and butyrate are 4.75 and 4.8, respectively) may penetrate microbial cell walls (Ciranna *et al.*, 2014). Once inside the cell, the soluble metabolites dissociate and release protons (cations) at higher intracellular pH, adversely affecting microbial metabolism and growth by decreasing the intracellular pH. Moreover, the accumulation of the anions (A<sup>-</sup>) increases the osmolarity of the cytoplasm and the cell turgor pressure (Elbeshbishy *et al.*, 2017). In addition to this, the decrease in intracellular pH may activate the hydrogen-consuming pathways for solvent production and deplete the intracellular ATP

as more protons will be required to balance the intracellular pH, thereby reducing substrate inhibition and biomass growth (Khanal *et al.*, 2004).

In buttressing inhibition due to un-dissociated acids, Wang *et al.* (2008) studied the effects of various concentrations from 0 – 300mM of externally organic acids (acetate, butyrate and propionate). They found that inhibition started at a concentration above 50mM, while substrate utilization and bio-hydrogen production were stopped entirely at 300mM. A similar result was obtained by Van Ginkel and Logan (2005) when 60mM of either acetate or butyrate was externally added. They also observed that internally produced VFA by the fermenting microbial consortia are more inhibitory than externally added, and at 19mM, concentrations of self-produced un-dissociated acids have been found to stop hydrogen production and activate solvent production. In contrast, in the work of Intanoo *et al.* (2014) on optimization of separate hydrogen and methane production from cassava wastewater using a two-stage up-flow-anaerobic sludge blanket reactor (UASB) system under thermophilic operation, they established that the VFA-inhibition level in HPBs is around 8800 mg/L while for methane-producing bacteria it is 350 mg/L.

Table 2-1: Effects of ammonium nitrogen concentration in an AD process (Von Sperling and De Lemos Chernicharo, 2005)

Ammonia concentration (N, mg /L)	Impacts
50 – 200	Beneficial
200 - 1000	No adverse effect
1500 – 3000	Inhibitory at pH 7.4 to 7.6
Over 3000	Toxic at pH > 7.6

#### 2.9.4 Nitrogenous Sources

Nitrogen is an essential building block precursor of enzymes and other cellular constituents of typical AD microorganisms. However, inhibition of AD processes could occur if ammonia nitrogen or carbon to nitrogen ratio is higher than usual (Argun *et al.*, 2008). In the application of animal wastes (CS) for

the AD process, the principal cause of inhibition of fermentative function at pH >7.4 is nitrogen sources ( $\text{NH}_4^+$ -N/L) at a range of 1.5 – 4.0g owing to degradation of ammonia-containing compounds such as amino acids, urea and proteins (Guo *et al.*, 2010, Rajagopal *et al.*, 2013 and Chen *et al.*, 2014). Adverse interference with intracellular pH, increase of microbial cellular energy requirement, and deactivation/ inhibition of essential enzymes involved in AD or AF processes have been identified as the significant causes of hydrogen/methane production inhibition due to high ammonium nitrogen (Bisaillon *et al.*, 2006). Ammonium concentration at a too low or excessive concentration in a digester impacts the optimal performance of an AD process (Table 2-1) (Poltronieri and D'urso, 2016). The two forms of inorganic ammonia nitrogen present in an aqueous solution in a reactor are the free ammonia ( $\text{NH}_3$ ) and the ammonium ion ( $\text{NH}_4^+$ ), which together constitute the total ammoniacal nitrogen (TAN) (Chen *et al.*, 2008). The inhibition due to nitrogen is mainly from the non-ionised form of nitrogen ( $\text{NH}_3$ ) that can penetrate the microbial cell wall freely, causing a proton and  $\text{K}^+$  deficiency at higher  $\text{pK}_a$  value and temperature (Kayhanian, 1999; Lin *et al.* 2013; Drog, 2013 and Chen *et al.*, 2008; 2014;). The  $\text{pK}_a$  value for free ammonia at 37°C is 9.25, and interesting dark fermentation for bio-hydrogen production is done at acidic pH values (Elbeshbishy *et al.*, 2017) while methane formation at neutral pH. Therefore, nitrogen inhibition in hydrogen/methane production may involve other mechanisms not necessary from free ammonia. Conversely, the other form – ionized ammonium-directly inhibits enzymes involved in AD processes (Kayhanian, 1999 and Drog, 2013). The nitrogen inhibition effects can be reduced by gradual acclimatization and dilution of feedstock (Elbeshbishy *et al.*, 2017). For instance, Salerno *et al.* (2006) reported that continuous bio-hydrogen production is feasible at high ammonia nitrogen concentration (7.8 g N/L) gradually increased from a lower nitrogen concentration (0.8g N/L).

### **2.9.5 Capable Seeded Sludge**

In the application of capable microbial consortia, co-cultures perform better in de-lignification of lignin, solubilisation of cellulose and hemicellulose, and the complete fermentation of pentoses and

hexoses to the use of pure culture (Pachapur *et al.*, 2015). However, even though single microbial species produce a relatively high hydrogen yield, it is not sustainable (Ren *et al.*, 2008). More so, mixed cultures offer advantages to the participating organisms in sudden environmental changes and nutrient shocks (Brener *et al.*, 2008). In this regard, activated seeded sludge is the most widely used and preferred. Readily available sludge contains over 70% of co-cultures of *Clostridium* and other hydrogen-producing organisms (Fang *et al.*, 2006). All the same, the use of activated sludge has a significant challenge. Activated sludge, besides containing HPB, also consists of a ranging number of HCB and other microorganisms that rival HPB for nutrients (Bundhoo and Mohee, 2016). These organisms could also alter the biochemical pathway of hydrogen production, thereby reducing the net bio-hydrogen yield. Hydrogenotrophic methanogens, homoacetogens, lactic acid bacteria (LAB), sulphate-reducing bacteria (SRB), nitrate-reducing bacteria (NRB), propionate producers, iron-reducing bacteria (IRB) and other hydrogen consuming microbes are among the non-hydrogen producers (Guo *et al.*, 2010 and Saady, 2013). Almost all studied methanogens that belong to the first group of methanogenic *Archaea* classified based on the utilization of three different substrates are hydrogenotrophic, which means that they can produce methane through reduction of CO<sub>2</sub> with H<sub>2</sub> or formate (Kampmann *et al.*, 2012), as discussed previously. These hydrogenotrophic methanogens, the main HCB in activated sludge, present a challenge in that the hydrogen produced during the DF process is consumed in methane production, resulting in lower bio-hydrogen yield (Saady, 2013).

Homoacetogenic bacteria are strict anaerobes that can produce acetate by growing autotrophically, heterotrophically or mixotrophically on various substrates (Henderson *et al.*, 2010 and Saady, 2013). On autotrophic mode, acetate is produced by reducing CO<sub>2</sub> with H<sub>2</sub> as the electron donor while heterotrophic homoacetogens utilise organic substrates viz. sugars to produce acetate as the end-product among others (such as succinate and lactose (Guo *et al.*, 2006 and 2010). In the mixotrophic mode, soluble organic substrates and hydrogen are consumed to produce acetate (Henderson *et al.*, 2010 and Saady, 2013). The presence of any of these homoacetogens in activated sludge will result in

inhibition of bio-hydrogen yield in the DF process via the following mechanism: a) the reduction of  $\text{CO}_2$  with  $\text{H}_2$  by the autotrophic reduces the yield of bio-  $\text{H}_2$ , while b) the utilization of organic substrates by the heterotrophic homoacetogens to produce acetate will lower the quantity that will be available for bio-hydrogen production (Saady, 2013). In the work of Siriwongrungsom *et al.* (2007) on homoacetogenesis as the alternative pathway for  $\text{H}_2$  sink during thermophilic anaerobic degradation of butyrate under suppressed methanogenesis, they found out that any  $\text{H}_2$  produced was consumed instantly to methane via homoacetogenesis. Lastly, c) acetate production by the homoacetogens increases acetate concentration, which directly inhibits the DF process for bio-hydrogen production by altering the metabolic pathways, among others (see above on inhibition by un-dissociated acids).

Propionate is a hydrogen-consuming end product of the anaerobic process as  $\text{H}_2$  is used as an electron donor by propionate producers (Saady, 2013). Consequently, propionate can be produced from the degradation of lactate and consumption of NADH by some propionate producers, e.g. *Clostridium propionicum* and *Clostridium homopropionicum*. The effect of propionate production is a decrease in hydrogen yield resulting from hydrogen consumption for propionate and NADH utilisation. Propionate is also inhibitory to the DF process, as discussed under un-dissociated weak acids.

Sulphur reducing bacteria are strict anaerobes and, under anaerobic conditions, can reduce sulphates to sulphides ( $\text{S}^{2-}$ ) during fermentation of much sulphur-containing feedstock, mainly organic wastes (food waste) (Barton and Fauque, 2009). However, cattle slurry has low sulphur levels since cattle feedings are mostly grasses high in carbon content and low in protein (Triolo *et al.*, 2013 and Westerholm *et al.*, 2016). Partial or complete oxidation of soluble organic substrates to acetic acid and  $\text{CO}_2$  or complete oxidation to  $\text{CO}_2$  and  $\text{HCO}_3^-$  can occur together with sulphate reduction (Chen *et al.*, 2008). A high amount of sulphide above 100 mg/L is toxic to hydrogen producers, substrate-degrading and fermenting microorganisms, SRB, acetotrophic and hydrogenotrophic methanogen (Koch *et al.*, 2010; Westerholm *et al.*, 2016 and Elbeshbishy *et al.*, 2017). A high sulphide concentration may also



form insoluble metal sulphides, thereby lowering the bio-availability of essential macronutrients (Dhar *et al.*, 2012; Bundhoo and Mohee, 2016 and Elbeshbishy *et al.*, 2017). Nonetheless, the most lethal to fermenting microbes is the sulphide's unionised form ( $H_2S$ ), which can easily penetrate the microbial cell membrane and denature proteins by forming complexes between polypeptide chains (Lens *et al.*, 1998). Unfortunately, since the DF process for hydrogen production is at acidic pH ( $pH < 6$ ), where most dissolved sulphide exists as  $H_2S$ , hydrogen producers are highly susceptible to inhibition by sulphide. The  $pK_a$  value for  $H_2S$  is 6.9 (Elbeshbishy *et al.*, 2017). Acclimatization, supplementation of metallic ions, e.g. iron to form complexes (Dhar *et al.*, 2012) and enrichment using sulphide oxidizing microbes (*Thiobacillus denitrificans*) (Chouari *et al.*, 2015) have been found to mitigate the inhibitions caused by a high concentration of sulphide. The sulphide oxidizing microbes oxidise the sulphide to sulphate using nitrate as an electron acceptor.

On the other hand, lactic acid bacteria are renowned for their anti-microbial activities, which may inhibit hydrogen-producing microorganisms (Lee *et al.*, 2013, Sikora *et al.*, 2013 and Gomes *et al.*, 2015). The change of fermentative medium pH through lactic acid production by *Lactobacillus* sp from carbon-based substrates produces anti-microbial products, e.g. hydrogen peroxide and secretion of polypeptide antibiotics (bacteriocins) are the mechanisms LAB can inhibit hydrogen production. LAB compete with HPB for pyruvate and NADH in lactic acid production, resulting in decreased hydrogen yield. The produced lactic acid inhibits DF processes by contributing to the concentration of undissociated acids or changes in operating pH. Wang and Zhao (2009) affirmed the inhibiting effect from lactic acid when they reported a decrease in bio-hydrogen yield from 0.071 to 0.049  $m^3/kg$  as the amount of lactic acid grew from 2345.6 to 4456.6. Nonetheless, lactic acid in micro-concentrations has enhanced bio-hydrogen output (Wang *et al.*, 2010).

Nitrate reducing bacteria are among the most populous microorganisms in a mixed culture due to the abundance of proteinous organic content commonly associated with diverse cultures. The autotrophic NRB are the ones that are among the HCB, as the use of  $H_2$  as an electron donor in

producing ammonia (Khanal, 2008). Therefore, the inhibition to the DF process for hydrogen is due to the utilization of hydrogen for ammonia and increased ammonia level, which is also inhibitory above a specific threshold (Bundhoo and Mohee, 2016).

With the ability of the *Clostridium* and most HPB to form spores and survive in harsh conditions, seeded sludge can be pre-treated by exposure to a higher temperature, UV radiations, extremely pH values and other hazardous or toxic compounds (O-Thong *et al.*, 2009 and Sattar *et al.*, 2016a). In contrast, methanogens, homoacetogens, LAB, SRB, NRB and other non-hydrogen producers cannot survive and are deactivated (Oh *et al.*, 2003). Generally, heat treatment is commonly employed owing to ease of operation (Fang *et al.*, 2006). Nevertheless, it is paramount to state that it has been observed that many spore-forming HCB exist and may survive the pre-treatments conditions, while many non-spore-forming HPB and hydrolytic microorganisms are inactivated or repressed after such pre-treatments (Singh and Wahid, 2014 and Bundhoo *et al.*, 2015). In affirmation of this, Oh *et al.* (2003) reported a decrease in hydrogen production from anaerobic fermentation of glucose due to spore-forming homoacetogens activities (*Clostridium aceticum* and *Clostridium thermoautotrophicum*), which possibly were consuming the produced H<sub>2</sub> for acetic acid production. Similar observations were made by Pendyala *et al.* (2012) from homoacetogens *Bacteriodes fragilis*, *Eubacterium aerofaciens*, and methanogen *Methylophilus methylotrophs*, propionate producer *Propionibacterium acnes* after various pre-treatments.

Additionally, though depending on the type of pre-treatments employed, it has been reported that the concentration of heavy metals in pre-treated sludge tends to increase compared to raw sludge, and these heavy metals are known to be inhibitory to fermenting organisms (Guo *et al.*, 2008).

### **2.9.6 Carbon Sources**

In the AD process, the primary substrate is carbohydrate substances, precisely simple sugars (glucose and xylose) and polysaccharides (starch and cellulosic materials). Also, protein, fat, and oil-containing

substrate have been recorded as suitable substrates. As reported previously, the most important organic acids produced during hydrogen production by anaerobic fermentation of polysaccharides are mainly acetic acids, butyric acid, and propionic acids. The formation of these organic acids is dependent on the type of feedstock employed. For instance, accumulation of lactic acids was observed when lactose and sucrose-containing polysaccharides were used as substrate (Collet *et al.*, 2004), whereas methane was produced when sewage sludge was used as substrate (Wang *et al.*, 2003).

In the AD process, as specified by Kim *et al.* (2012), proper carbon to nitrogen (substrate concentration) is essential for any substrate of choice for efficient degradation, increment in process stability and hydrogen yield, since anaerobic fermenting microbes consume carbon 25 – 30 times faster than nitrogen (Kalil *et al.*, 2008). Although there is no agreed ratio as a wide range of optimum C/N ratios of 5 – 200 has been recorded in the literature for DF for bio-hydrogen owing to differences in temperature, microbial consortia, temperature and substrate; the desired C/N ratio for efficient bio-hydrogen production that has been widely used is 25. In Hills and Roberts's work, as cited by Kim *et al.* (2012), the C/N ratio of 35 – 118 was used in the anaerobic digestion of lignocellulose biomass. Most nitrogen components were from organic waste such as sludge, while the lignocellulose biomass has a high carbon content. Similarly, Kim *et al.* (2004) reported that bio-hydrogen production is enhanced when food waste is co-digested with sewage sludge. In co-digestion of rice straw and sewage sludge at a C/N ratio of 25, Kim *et al.* (2012) were able to produce optimum bio-hydrogen in their work on hydrogen production by anaerobic co-digestion of rice straw and sewage. Biswarup and colleagues, in their work on pre-treatment conditions of rice straw for simultaneous hydrogen and ethanol fermentation by mixed cultures; were able to establish that 100g rice straw/L (at C/N ratio 25) was the best concentration for maximum yield of sugars in the experimented range of 75 -250g rice straw/L (Biswarup *et al.*, 2016). Nitrogen inhibition threshold can be diluted if either the amount of the carbon or the nitrogen content of the feedstock is co-fermented with another feedstock that is lower in the amount of either of the carbon or nitrogen content in the main stock to achieve the desired ratio (Kalil *et al.*, 2008).

### 2.9.7 Phosphate Sources

Phosphate containing compounds are pH buffers for microbial metabolism and major inorganic compounds essential for the effective functioning of fermentative microbial metabolism (Lin and Lay, 2004). It has been found that maintaining proper optimal phosphate concentration influence significantly hydrogen and methane production by reducing the duration of the lag phase, hydrogen production rate and AD process (Lin and Lay, 2004 and Zhou *et al.*, 2013). To confirm this, Lin and Lay (2004) reported that  $K_2HPO_4$  concentration at 600 mg/L produced the highest hydrogen yield while 30% below or above this concentration lowers the hydrogen production by 40%. Although affected by other nutrient and metal ions such as nitrogen and iron, the recommended optimum ratio for C/P is 130 (Hawkes, 2002 and Argun *et al.*, 2008).

### 2.9.8 Trace Elements

Trace metallic ions at low concentration are essential for cellular growth, proper functioning of enzymes (where they act as cofactors) and other metabolic activities involved in the AD process (Weiland, 2010; Karlsson *et al.*, 2012; Westerholm *et al.*, 2012 and Triolo *et al.*, 2013). Nonetheless, inhibition of the anaerobic digestion process could occur at a high concentration of these metal ions, which may have been sourced from the inoculum to be employed or substrates (Elbeshbishy *et al.*, 2017). The inhibition occurs in several mechanisms such as inhibition of the transport of essential nutrients and ions, intracellular accumulation of metals leading to dissipation of ATP due to metal pumping and destruction of membrane function and structure (Lemire *et al.*, 2013 and Le and Nitisoravut, 2015). Consequently, inhibition of these metal ions may be influenced by the metal ions' chemical attributes such as the pH, concentration of organic matters, and chelating agents (Elbeshbishy *et al.*, 2017). The element "iron" is of great focus as it is essential in hydrogen production (Hawkes *et al.*, 2002). The hydrogenase enzyme responsible for hydrogen evolution from sugar monomer requires reduced ferredoxin to be oxidised, and this compound is usually  $Fe^{2+}$  complexed (Kapdan and Kargi, 2006). Hence, external iron addition might be necessary for hydrogen production.

In the same vein, the iron-sulfur protein – ferredoxin is involved in (1) pyruvate oxidation to acetyl-CoA and CO<sub>2</sub> under the PFOR pathway in DF processes for H<sub>2</sub> production, (2) acts as an electron carrier, (3) in proton reduction to molecular hydrogen in anaerobic fermentative hydrogen production where they assist in the formation of hydrogenase and (4) reduction of inhibition due to sulphide (Lee *et al.*, 2001 and Bao *et al.*, 2013). The effects of iron on the growth and development of hydrogen producers, hydrogenase and the rate of hydrogen production were affirmed by Vaňáčová *et al.* (2001) when they demonstrated that iron could induce metabolic changes to both Fe-S and non-Fe-S proteins operating in hydrogenase. The inorganic salt, FeCl<sub>3</sub>, has been reported to improve hemicellulose hydrolysis into oligomeric and monomeric sugars with enormous xylose and xylotriose production (Lopez-Linares *et al.*, 2009).

Similarly, Liu and Shen (2004) reported that about 10mg/L iron concentration was optimum in batch hydrogen production by *Clostridium pasteurianum* from a starch substrate. Furthermore, it is documented that FeCl<sub>3</sub>, when used in combination with dilute acid, enhances the enzymatic solubilisation of lignocellulose by altering the matrix structure (Liu *et al.*, 2009). Nevertheless, the culture is likely to form cell clumps that could hamper mass transfer, have distorted cell structure, and negatively affect the cells' physiological characteristics and higher iron concentration (Chin *et al.*, 2003). The range of 20-25 mg/L for pure cultures has been shown to favour the hydrogen production rate (Alalayah *et al.*, 2009). Conversely, a yield of 2.73 mol of hydrogen per glucose was achieved at 1600 mg/L of iron concentration (Alshiyab *et al.*, 2008).

The light metallic ion calcium, sodium and magnesium are essential for the proper function of metabolic activities and microbial growth at a moderate concentration, while higher concentrations can slow down growth or inhibit fermentative microorganisms (Soto *et al.*, 1993). Sodium (Na<sup>+</sup>) is essential in building the Na-K-ATP enzyme pump required to transfer nutrients like glucose inside a microbial cell to hasten the fermentation reaction (Fox and Pohland, 1994). Also, the Na<sup>+</sup> gradient created by adding sodium ions enhances Fd<sub>ox</sub> reduction by NADH, thereby resulting in a higher yield of Fd<sub>red</sub> (Lee *et al.*, 2012). However, environmental osmotic pressure could induce bacterial

inactivation and possible death due to increased sodium concentration (Fox and Pohland, 1994). Furthermore, inhibition to H<sub>2</sub> yield due to other metabolites' formation resulted from a change in the metabolic pathway because of increased Na<sup>+</sup> concentration (Kim *et al.*, 2009). Cao and Zhao (2009) recommended that to achieve high hydrogen yield, sodium concentration should be < 20 g/L, while at higher sodium concentration (28.70 g/L), the process was slowed down, and hydrogen yield reduced. Extracellular polysaccharides, which play a crucial role in biofilms formation, has calcium as a principal constituent. The polysaccharides are necessary for cell granulation, retention and sedimentation (Morgan *et al.*, 1991). In addition, calcium is essential in spore formation and the making of other extracellular polymer materials like capsules. Calcium is also required as a co-enzyme for alpha-amylase and many proteases (Wang *et al.*, 2007). The reported range for optimum use reported in the literature is 0-150mg/L (Chang and Lin, 2006). The addition of 5.4 mg/L of Ca<sup>2+</sup> concentration has been reported to improve significantly bio-hydrogen production (Lee *et al.*, 2004). Conversely, a high calcium concentration could reduce the surface area leading to a decrease in mass transfer and can affect the extracellular structures.

Magnesium is essential for many intracellular functions and metabolic reactions and is present in cell walls and membranes. It is a cofactor of numerous enzymes involved in kinases, phosphatases and synthetases reactions (Wang *et al.*, 2007), where they are needed to build cellular proteins. The range of 0-200mg/L has been identified as the optimum for hydrogen production (Alshiyab *et al.*, 2008), while a high concentration of Mg<sup>2+</sup> could accelerate glycolysis (Elbeshbishy *et al.*, 2017).

As with all media supporting microorganism growth, essential mineral salts must be present to boost the organisms' metabolic and catabolic activities. Nonetheless, in varying quantities during AD and AF processes, many other trace elements such as manganese, cobalt, molybdenum, copper, zinc chromium, cadmium, and barium are required to boost enzyme catalytic actions (Bundhoo and Mohee, 2016). In addition, nickel micro-addition in fermentation and digestion processes is essential

as Ni-Fe hydrogenase is involved under the PFL pathway for bio-hydrogen production from formate (Hallenbeck *et al.*, 2012). However, trace element deficiency is rare in an AD system as animal slurries, and seeded sludges usually contain sufficient concentrations (Drosg, 2013).

### **2.9.9 Organic and Hydraulic Overload**

Process inhibition can occur when organic solids fed in a reactor exceed the degradation capacity of the microbial community, thereby leading to a decrease in the production of hydrogen, increase in the yield of VFA, a shift towards solvent production, reduction in the volumetric reactor products and microbial access to biomass (Levin *et al.*, 2004; Ward *et al.*, 2008; Drosg, 2013 and Neshat *et al.*, 2017). Similarly, hydraulic overload is directly related to the amount of organic substrate degraded by the cells per unit time and is defined as the ratio between the fermenter volume and the feed flow rates (Drosg, 2013). The inhibition for each process pathway could occur when the operating retention times are so short that it does not support the individual growth rates of degrading microorganisms leading to washing out. In general, HPB prefers short retention times against SCFA and LCFAs degraders and methanogens, which prefer longer retention times due to their prolonged growth rates (Angelidaki *et al.*, 1999 and Liu *et al.*, 2008). The maximum specific growth rates ( $\mu_{\max}$  d<sup>-1</sup>) of some bacteria and archaeal groups within the AD process are 6.38, 5.10, 1.0, 0.67, 0.60, 0.55, 0.53 and 0.49 d<sup>-1</sup> for amino acid degraders, glucose acidogens, carbohydrate and protein hydrolysis, butyrate degraders, methanogens, LCFA degraders, lipolytic and propionate degraders respectively (Angelidaki *et al.*, 1999). Thus in hydrogen production, a combination of the pH 5.5 and HRT of 3 days may be optimum for product yield using glucose as a medium (Liu *et al.*, 2008). This rate is different for AD plants, which must function at retention times that are beyond the growth rates of most microbial communities, which is usually 15 -30 days at mesophilic conditions and 10-20 days at thermophilic conditions (Angelidaki *et al.*, 2011 and Westerholm *et al.*, 2016). The extended retention times are because the wash-out of slow-growing bacteria participating in the AD process can limit biogas production (Drosg, 2013).

Furthermore, the shorter hydraulic retention times (HRT) in fermentation processes result from a chemical reaction that is thermodynamically unfavourable, leading to production and accumulation of VFA at longer HRT (Li, 2009). Hawkes *et al.* (2002) reported that for a liquid-type substrate, the optimal HRT is 8-12 h, while a longer optimal HRT is required to treat solid-type substrate as a hydrolysis step is needed.

In addition to this, hydrogen production is influenced by the partial pressure of hydrogen in a bioreactor. Hydrogen partial pressure, defined as the mass transfer of hydrogen from the liquid to the gaseous phase, is expedited by the lower pressure in the headspace (Bastidas-Oyanedej *et al.*, 2012 and Beckers *et al.*, 2015). Therefore, if the hydrogen concentration in the liquid phase increases because of high pressure in the headspace, the oxidation of ferredoxin becomes less favourable, and the reduction of ferredoxin takes place, resulting in decreased production of hydrogen gas (Chong *et al.*, 2009). In the DF process, the enzyme hydrogenase catalyses the reversible oxidation and reduction of ferredoxin, which could be a regulatory mechanism that HPB has evolved. Hence, enzyme hydrogenase might be negatively affected by high hydrogen pressure. In a continuous system, the produced hydrogen must be liberated to de-pressure the headspace to continue producing hydrogen optimally.

The OLR, as stated by Schon 2020) is calculated as shown in Eqn 2-19.

$$OLR = \frac{Q.C}{V} = \frac{C}{HRT} \quad \text{Eqn 2-19}$$

Where

OLR is the organic loading rate measured in KgVS.m<sup>-3</sup> d<sup>-1</sup> or KgCOD.m<sup>-3</sup> d<sup>-1</sup>.

Q is the influent flow rate measured in m<sup>3</sup>.d<sup>-1</sup>, and V is the reactor volume in m<sup>3</sup>

C is the concentration of volatile solids in the substrate measured in KgVS.m<sup>-3</sup> or KgCOD.m<sup>-3</sup>

The SRT is the same as the HRT in a continuous system without recirculation. In contrast, SRT is usually higher than HRT in AD reactors that use solids recycling (De Lemos Chernicharo, 2007 and Schon, 2010).



## 2.9 Biogas Enrichment and Upgrading Processes

Whereas biogas produced via the DF process typically contains (v/v) 50% to 60% H<sub>2</sub> and 40% to 60% CO<sub>2</sub>, methane, made through the AD pathway, contains (v/v) 55% to 70% CH<sub>4</sub> and 30% to 45% CO<sub>2</sub>. In addition, other minor impurities such as H<sub>2</sub>S (0 – 10, 000 ppm), N<sub>2</sub> (0-3% (v/v)), O<sub>2</sub> (0 -1%(v/v)), water vapour (5 -10% (v/v) or higher at thermophilic temperatures), NH<sub>3</sub> (0 -200 mg/m<sup>-3</sup>) and siloxanes (0 - 41 mg/m<sup>-3</sup>) and dust can also be present with either gases (Munoz *et al.*, 2015; Pellegrini *et al.*, 2015; Qyyum *et al.*, 2020 and Lai *et al.*, 2021).

Both gases can be combusted for heat and energy generation. However, the presence of these gases, especially CO<sub>2</sub> and impurities, diminish the thermal energy value of biogas (for biogas with 60-65% methane content, the lower calorific value (LCV) is within 20-25 MJ/m<sup>3</sup>, while the energy content (LCV) of methane is 36 MJ/ m<sup>3</sup> at STP), increase the storage space requirement, make it uneconomical to compress and transport to longer distances, induce solid accumulation on plants equipment, corrode gas pipelines and damage power plants (Kapdi *et al.*, 2005; Olugasa *et al.*, 2014; Angelidaki *et al.*, 2018; Qyyum *et al.*, 2020 and Lai *et al.*, 2021). In addition to this, biogas impurities reduce the density and Wobbe index (WI) of biogas (JIn *et al.*, 2017 and Aryal *et al.*, 2018). These biogas contaminants also cause an increment in air emissions and health hazards. Thus, there is a need to remove the unwanted gases and impurities from biogas and upgrade it to pure hydrogen/biomethane before applying them for power and heat generation.

Generally, the biogas enrichment processes are classified into chemical, physical, and biological. Each method used alone or combined is unique for removing one or a group of gases/impurities. For this section, “biogas” referred to individual methane and hydrogen-containing gas samples.

### 2.9.1 Processes for Removing Hydrogen Sulphide from Biogas

Naturally, H<sub>2</sub>S is removed first from biogas because of its unpleasant odour and highly corrosiveness. Depending on the sulphate substrates, minor quantities of mercaptans produced during anaerobic fermentation are equally removed along with H<sub>2</sub>S (Angelidaki *et al.*, 2018). Even though low

concentrations of H<sub>2</sub>S can cause severe corrosion in gas pipelines, in biogas conversion systems and biogas plants, about 1000 to 2000 ppm are generated from animal manure (Krich *et al.*, 2005). H<sub>2</sub>S is poisonous and hazardous to the environment since combustion is converted to sulphur dioxide (Olugasa *et al.*, 2014), which is toxic. H<sub>2</sub>S and organic sulphides can be removed by biological H<sub>2</sub>S oxidation (that is, the removal of H<sub>2</sub>S in the digester from the crude biogas using air injected into the digester biogas holder), the addition of Iron chloride to the digester influent, water scrubbing, lime scrubbing, reaction with iron oxide or hydroxide, use of activated-carbon filter beds and biological removal on a filter bed (Hagen *et al.*, 2001, Sun *et al.*, 2015 and Qyyum *et al.*, 2020). The mentioned processes are detailed below.

#### 2.9.1.1 Oxidation by *Thiobacill* and biological filters

Typically, when air/oxygen is mixed with biogas that collects on top of the digester, sulphides in the biogas are oxidised to elementary hydrogen and sulphur by *Thiobacilli* microorganism (Krich *et al.*, 2005 and Qyyum *et al.*, 2020). Hence, H<sub>2</sub>S concentration is reduced to less than 50 ppm. This same principle is applied in biological filters where H<sub>2</sub>S is removed from biogas using membranous filters coated with *Thiobacillus*. In the same vein, digestate dominated by *Thiobacilli* on its surface can be used as a biological filter for H<sub>2</sub>S adsorption and removal (Krich *et al.*, 2005 and Abatzoglou and Boivin, 2009). In both cases, as with water scrubbing, the biogas mix with 4% to 6% air, and the biological filters meet in a counter-current flow. Thus, the biological filter bed offers the required surface area for scrubbing and the oxidising bacteria's attachment.

#### 2.9.1.2 Iron sulphate complexes

Iron Sulphate salt particles can be formed when iron chloride reacts with H<sub>2</sub>S, and the addition of Iron chloride to the digester influent can be very effective in reducing high H<sub>2</sub>S levels (Krich *et al.*, 2005; Abatzoglou and Boivin, 2009 and Qyyum *et al.*, 2020). Similarly, H<sub>2</sub>S reacts with iron hydroxides or oxides to form iron sulfide. This endothermic process is often called “iron sponge” as biogas is passed

through iron oxide pellets commonly known as rust-covered wool to remove H<sub>2</sub>S (Kohl and Nelson, 1997 and Abatzoglou and Boivin, 2009).

#### 2.9.1.3 Activated carbon sieve

Hydrogen sulphide is scrubbed off using activated carbon impregnated with potassium iodide in pressure-swing adsorption systems where the H<sub>2</sub>S is loosely adsorbed in the carbon sieve under the pressure of about 100 – 115 psi (Krich *et al.*, 2005 and Angelidaki *et al.*, 2018). The adsorption system uses four filters synchronously, and the release of pressure allows the impurities to desorb and release from the carbon sieve. The process, which requires a temperature of 50 – 70°C, adsorbs CO<sub>2</sub> and water vapour. The adsorption process is made better by adding air to the biogas, which then oxidises the H<sub>2</sub>S to elementary sulphur and water (Krich *et al.*, 2005). The activated carbon then adsorbs the sulphur.

#### 2.9.1.4 Water scrubbing

The most widely employed technology for biogas cleaning and upgrading is water scrubbing (Angelidaki *et al.*, 2018). The contaminants H<sub>2</sub>S and CO<sub>2</sub> from biogas can be removed using a water scrubbing mechanism because these gases have increased solubility in water than methane and hydrogen. According to Henry's law, the gram of H<sub>2</sub>S, H<sub>2</sub>, CH<sub>4</sub> and CO<sub>2</sub> dissolved in 100g of water at 1 atm, and RT is 0.385, 0.00016, 0.0023 and 0.169, respectively (Kaye and Laby, 1986; Abatzoglou and Boivin, 2009; Budzianowski *et al.*, 2017 and Angelidaki *et al.*, 2018). The theory shows that water scrubbing can effectively and selectively remove H<sub>2</sub>S because it is more soluble in water than carbon dioxide. The process of water scrubbing will be explained further under CO<sub>2</sub> removal technologies.

Nevertheless, the major problem with this method is that H<sub>2</sub>S desorbed after contact can create environmental issues. Chemicals like NaOH and CaO can be added to water to enhance the scrubbing capabilities for both H<sub>2</sub>S and CO<sub>2</sub> removal (Krich *et al.*, 2005 and Abatzoglou and Boivin, 2009), which is due to the chemical reaction of the NaOH and the H<sub>2</sub>S, which increases the physical absorption

capacity of the water. Hence, the addition of NaOH results in lower volumes of operating water and reduced pumping demands. However, this reaction forms sodium sulphide and sodium hydrogen sulphide, which are insoluble and not regenerated.

### **2.9.2 Technologies for Removal of Water Vapour**

The gas produced via the AD process is usually saturated with water vapour because biogas from fermentation reactors are generally collected from the headspace above a liquid surface or semi-solid substrate. Although the quantity of saturated water vapour in biogas depends on temperature and pressure, biogas at 41°C, 32°C, and 4°C contains 10%, 5%, and 1% water vapour volume, respectively (Olugasa *et al.*, 2014; Munoz *et al.*, 2015 and Angelidaki *et al.*, 2018). Apart from affecting biogas calorific value, water vapour must be removed from biogas to prevent the water vapour condensing within the systems, which can cause corrosion and clogging. Corrosion within the gas systems can occur if the H<sub>2</sub>S has not been removed from the biogas. The impurity H<sub>2</sub>S reacts with the water vapour to form sulfuric acid (H<sub>2</sub>SO<sub>4</sub>), which is known to be very corrosive (Krich *et al.*, 2005). Similarly, carbonic acid (H<sub>2</sub>CO<sub>3</sub>), which is formed when water vapour reacts with CO<sub>2</sub>, is also corrosive at a pH near 5.0.

Various techniques can be applied to remove condensation from a pipe, including tees, U-pipes, or siphons, where condensate drains is placed at all the low points in the piping to remove condensation. Other devices used to remove water include demisters, cyclones, moisture traps and water traps (Qyyum *et al.*, 2020). In addition, the refrigeration process is used to remove excess water vapour at the dew point that was not removed from the downstream condensation, and the dew point of biogas is about 2°C (Krich *et al.*, 2005).

Other means of water vapour removal includes adsorption and absorption at elevated pressures. In adsorption technology, water vapour is removed via adsorption on SiO<sub>2</sub>, activated carbon or molecular sieves, which can be regeneration by applying heat or pressure adjustment (Sun *et al.*, 2015). Water vapour can also be absorbed using glycol solutions or hygroscopic salts (Qyyum *et al.*, 2020).

### 2.9.3 Technologies for Removal of Carbon Dioxide

As stated before, CO<sub>2</sub> constitute the primary contaminant of biogas and the following technologies used in the removal of CO<sub>2</sub> from natural gas in petrochemical industries are applied for CO<sub>2</sub> removal from biogas. The processes include physical (water scrubbing, absorption, pressure swing adsorption, and cryogenic separation) and chemical (scrubbing with amines and glycols (such as Selexol™) and chemical membrane separation).

#### 2.9.3.1 Physical Absorption

##### 2.9.3.1.1 Water scrubbing

Carbon dioxide is more soluble in water than methane and hydrogen and can be removed using water scrubbing (Qyyum *et al.*, 2020). However, when water scrubbing is used for CO<sub>2</sub> removal, the biogas pressure is raised (150 - 300 psig) to ease the solubility processes (Krich *et al.*, 2005 and Bauer *et al.*, 2013). The scrubbing process usually is achieved with a two-stage compressor process, where the raw pressurised biogas passes in from the bottom of the column and goes upward, and the freshwater introduced at the topmost of the column flows downward over a packed bed (Bauer *et al.*, 2013 and Qyyum *et al.*, 2020). The packed bed, usually a high-surface-area plastic media, ensures efficient contact between the water and the gas phases in a counter-current absorption process (Ryckebosch *et al.*, 2011). Therefore, the water-saturated with CO<sub>2</sub> is continuously withdrawn from the bottom of the column, while the purified gas saturated with about 95% methane content exits from the top.

##### 2.9.3.1.2 Pressure swing adsorption

Contaminants, mainly CO<sub>2</sub> and H<sub>2</sub>O from raw biogas, can be removed by passing the raw gas through a column filled with a molecular sieve such as activated carbon, silicates and alumina at elevated pressures (Sircar, 2002 and Qyyum *et al.*, 2020). This process, called pressure swing adsorption (PSA), separates different gases from raw biogas based on the molecular characteristics and affinity towards the adsorbent materials (Angelidaki *et al.*, 2018). Using the approach which involves using several

columns, typically four with a pore size of 3.7 Å, CO<sub>2</sub> and H<sub>2</sub>O preferentially are adsorbed under high pressure (4-10 bars), while CH<sub>4</sub> will pass through (the molecular size of CH<sub>4</sub> is 3.8 Å, while that of CO<sub>2</sub> is 3.4 Å) (Krich *et al.*, 2005 and Augelletti *et al.*, 2017). As a result, CO<sub>2</sub> is allowed to enter into the matrix of the absorbent material, while CH<sub>4</sub> is not permitted to enter but passes through the interstitial spaces (Patterson *et al.*, 2011).

#### 2.9.3.1.3 Membrane separation

This technique works because some raw gas constituents are retained when transported through a thin selective membrane while others pass through. The process done under pressure uses a selective membrane that allows preferential passage of one of the gases (Baker, 2012 and Khan *et al.*, 2017a). The most commonly used selective membrane separating CH<sub>4</sub> from H<sub>2</sub>S and CO<sub>2</sub> is acetate-cellulose polymer and polyimide membranes (Baker, 2012 and Angelidaki *et al.*, 2018). However, Yousef *et al.* (2021) was reported using polyethersulfone membranes under different pressures and temperatures on CO<sub>2</sub>/N<sub>2</sub>, CO<sub>2</sub>/H<sub>2</sub> and CO<sub>2</sub>/CH<sub>4</sub> selective performance.

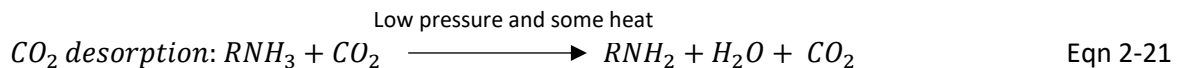
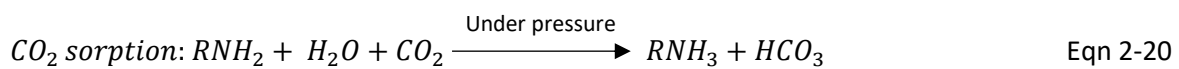
#### 2.9.3.1.4 Cryogenic separation

This purification approach works on the principle that gases have different temperature-pressure domains. The process involves a gradual decrease of the biogas temperature to separate the liquefied CH<sub>4</sub> from other impurities (Munoz *et al.*, 2015 and Khan *et al.*, 2017a). These contaminants, such as CH<sub>4</sub> and CO<sub>2</sub>, liquefies at different temperature-pressure domains and are better explained by the differences in the boiling points at 1 atm (CH<sub>4</sub> has -161.5°C, while CO<sub>2</sub> is -78.2°C) (Khan *et al.*, 2017a). Thus it will be possible to purify biogas using this approach. Because cryogenic separation brings about the recovery of pure methane in the liquid state, it might be worth considering if the end objective is to produce liquefied biomethane (LBM), a product equivalent to liquefied natural gas (LNG). In this case, the refrigeration process involved in cryogenic separation is integrated with LBM production's cooling process (Krich *et al.*, 2005).

### 2.9.3.2 Chemical Absorption

#### 2.9.3.2.1 Scrubbing with alkali

The CO<sub>2</sub> from raw gas can be absorbed and removed using suitable bases resulting in a neutralization reaction (Bajracharya *et al.*, 2009 and Olugasa *et al.*, 2014). The alkali (NaOH, KOH and Ca (OH)<sub>2</sub>) have all been proposed for use in chemical scrubbing, and the absorption can be enhanced by agitation (Olugasa *et al.*, 2014). The absorption rate is increased by the concentration of the solution and the normality with NaOH most rapid at normality 2.5 to 3.0 (Kapdi *et al.*, 2005).



(R represents the remaining organic component of the molecule)

#### 2.9.3.2.2 Scrubbing with amine solvents

This approach is based on the very high selectivity of amines for CO<sub>2</sub>. Organic amines such as monoethanolamine (MEA), diethanolamines (DEA), and diglycolamines (DGA) are employed as CO<sub>2</sub> absorbers at slightly elevated pressures of 150 psi (Krich *et al.*, 2005; Khan *et al.*, 2017a and Angelidaki *et al.*, 2018) (Eqn 2-20). Regeneration is by heating and reducing the amines' pressure to drive off the absorb CO<sub>2</sub> (Eqn 2-21). The general chemical equations below represent the principle of amine scrubbing (Krich *et al.*, 2005), which involves raw biogas at 1 -2 bars entering the absorber unit from the bottom of the tank while the amine solution flows from the top in a counter-current way. The regeneration of the resultant CO<sub>2</sub> amine solution is done in the stripping unit under low pressure and heat (Khan *et al.*, 2017a and Angelidaki *et al.*, 2018).

Amine scrubbing is a quality rather than a quantity process compared with water scrubbing as it ensures that only CO<sub>2</sub> is absorbed completely, thereby minimising the volume of the process

(Angelidaki *et al.*, 2018). However, the drawback is that the procedure can be intricate when compared to water scrubbing.

#### 2.9.4 Biological Technology

Although these technologies are still early, they have been experimentally proven, sustainable, and cost-effective to upgrade biogas. In addition to this, a biological methanation is an attractive option for biogas enrichment compared to other purification methods as it is both green (as H<sub>2</sub>S, CO<sub>s</sub> are consumed), cost-effective and low energy demanding (Roy *et al.*, 2016 and Khan *et al.*, 2017a). The biological method is generally classified into chemoautotrophic and photosynthetic (Angelidaki *et al.*, 2018). Whereas it has been stated earlier that CO<sub>2</sub> does not have energy value, and its presence reduces the thermal value of biogas, H<sub>2</sub>S produces corrosive solutions (see section 2.9.1). Thus, the significant advantage of biological technology is that the CO<sub>2</sub> is converted from non-energy yielding to other energy value forms (CH<sub>4</sub>) under mild experimental conditions that contribute significantly to biogas' general value.

In chemoautotrophic biogas upgrading technology, CH<sub>4</sub> is produced based on the action of hydrogenotrophic methanogens (such as *Methanobacterium*, *Methanoculleus*, *Methanomicrobium*) that can utilize H<sub>2</sub> and reduce CO<sub>2</sub> to CH<sub>4</sub> (Eqn 2-16) (Agnessens *et al.*, 2017).

The biological processes can occur *in-situ*, where the H<sub>2</sub> is injected inside a biogas reactor to reduce the endogenous CO<sub>2</sub> produced in the anaerobic reactor and be converted to CH<sub>4</sub> by the action of autochthonous methanogenic *Archaea* (Bassani *et al.*, 2015 and Kougias *et al.*, 2017). On the other hand, in *ex-situ*, both CO<sub>2</sub> are provided from external sources (syngas, industrial waste gas) in an anaerobic digester containing hydrogenotrophic methanogens resulting in their subsequent conversion to CH<sub>4</sub>. Both concepts are affected by pH, oxidation of VFA and solubilisation of H<sub>2</sub> to the liquid phase (Bastonnee *et al.*, 2002 and Tirunehe and Norrdahl, 2016).



Like chemoautotrophic methods, the biological process can be catalysed by phototrophic organisms (algae such as cyanobacteria and microalgae), and methane recovery can reach up to 97% on the reactor and selected algal species (Angelidaki *et al.*, 2018). Moreover, the phototrophic biogas upgrading process not only removed CO<sub>2</sub>, but H<sub>2</sub>S removal is additionally achieved (Abatzoglou and Boivin, 2009 and Toledo-Cervantes *et al.*, 2016).

Other biological methods of biogas upgrading can be achieved through microbial electrochemical methods. Typically, in microbial electrolysis cell (MEC), electrons released from the oxidation of soluble organics by bacteria can combine with protons and be reduced to generate H<sub>2</sub> in the cathode (Lu and Ren, 2016; Khan *et al.*, 2017a and Aryal *et al.*, 2018) and this H<sub>2</sub> can be used for biogas upgrading by combining with external CO<sub>2</sub> for the production of CH<sub>4</sub> (Cheng *et al.*, 2009).

## **2.10 Biogas as a Fuel for Combined Heat and Power Applications**

Biogas can be used to substitute natural gas or liquefied petroleum gas by burners and boilers to produce heat and steam (Su *et al.*, 2018). However, most standard commercial available burners will not work when biogas is used directly. The inability of the burners to work is because gas must flow into the combustion in the precise stoichiometric ratio with air at any given fuel gas feed pressure, and since biogas has high CO<sub>2</sub> content during combustion if it flows through the burner orifice at the same pressure use for feeding methane or propane, the fuel-to-air ratio is insufficient to ensure flame stability (Krich *et al.* 2005). The solution is to either adjust the commonly available burners or use a biogas burner that operates parallel with the natural gas burners regardless of the fuel used; airflow is kept constant (Krich *et al.*, 2005). In both cases, the burner orifices are set such that a proper amount of gas is fed to the burner to meet combustion stoichiometry. Nonetheless, vital factors to consider are the combustor's capability to handle the increased volumetric throughout the lower-energy biogas, flame stability, and the corrosive impact of raw biogas on the burner equipment (Krich *et al.*, 2005).

## 2.11 Electricity Production Using Combined Heat and Power Systems

Fuels such as natural gas, gasoline, oil, diesel fuel, propane, coal, wood, wood waste, and biomass can produce electricity via conventional power generation plants or CHP plants (Infield and Freris, 2020). Nonetheless, energy efficiency in a conventional power plant is low (35-40 %), and the waste heat is often disposed to rivers, lakes, oceans or the atmosphere (Pilavachi, 2002, Sipilä, 2016 and Hengeveld *et al.*, 2020). For instance, the UK average fossil-fuel electricity generator system has an efficiency of around 40% (this is different from electricity supplied from fossil fuels which in the year 2020 stood at 56.9% (UK Energy in Brief, 2021)) and the remaining 60% of the energy is lost mostly as heat via cooling towers and very slightly from electricity transmission (Pilavachi, 2002, Sipilä, 2016 and Hengeveld *et al.*, 2020). In contrast, the heat liberated during co-generation systems (CHP) can be used as working fluid or rather process heat for onsite use such as drying of digestates (Hengeveld *et al.*, 2020) or procedures involving heating in industries, for district heating and in cooling using absorption chiller unit for combined cooling heat and power (CCHP) systems (Ahmadi *et al.*, 2013 and Keshavarzzadeh *et al.*, 2019). In summary, CHP is defined as the recovery and the application of waste heat from power generation, and this involves three stages: power generation, heat recovery and heat use. A CHP plant's overall energy efficiency is increased to about 70-90 % or even more by utilising the heat (Pilavachi, 2002, Rabiou *et al.*, 2012, Ahmadi *et al.*, 2013, Magbanki *et al.*, 2013, Su *et al.*, 2018, Keshavarzzadeh *et al.*, 2019 and Amaral *et al.*, 2020). In the UK, the overall conversion efficiency of primary fuel to electricity and heat is around 75% using correctly sized and well-designed packaged CHP, which implies that for every 100 units of fuel, about 30 units of electricity and 45 units of thermal energy will be generally produced from a packaged CHP (Peacock and Newborough, 2008 and Dong *et al.*, 2009). Depending on the demand of energy output, efficiency and prime mover, CHP applications can be categorised either as large scale (above 100MWe), small scale (50 KWe – 1MWe) and microscale (5 - 50 KWe). Although CHP requires initial significant capital investment outlay, reduction of CO<sub>2</sub> and energy bills and offer of financial incentives as electricity from CHP qualifies as “Good Quality” are the benefits associated with it (De Paepe *et al.*, 2006, Peacock and Newborough,

2008 and Dong *et al.*, 2009). Also, cogeneration systems can be cost-effective as the life span can be more than 20 years.

In the CHP plant, the principal components are the prime mover (engine), which provides the mechanical motive power, an electricity generator, a heat recovery system, and a control system. If the CHP provides chilled water, the heat recovery system may be coupled with absorption chillers. There are five main types of CHP prime mover: internal combustion engines, steam turbines, gas turbines, combines-cycle gas turbines and other new and emerging technologies such as Stirling engines, fuel cells and Organic Rankine Cycles (ORCs) (Sipila, 2016).

While the motive power in internal combustion engines is provided by the traditional spark-ignition engines used mainly in cars and small generators, the motive force for gas turbines comes from a turbine driven by a steady stream of burning fuel (Lantz, 2012). This thermodynamic cycle is called the Brayton Cycle. In the Brayton cycle, the combustion chamber and gas turbine are flowed through by a mix of air and burning gases in the proper stoichiometric ratio, and the exhaust gases from the turbines are recovered primarily by using heat the district heating water. Gas turbines are fast to start and stop and require less maintenance but have lower electrical efficiencies than internal combustion engines.

In steam turbines, the motive power comes from a turbine driven by a steady stream of high-pressure steam generated in a boiler. The efficiency can be maximised when the steam is condensed and pumped back to the boiler as hot water below the boiling point. The thermodynamic cycle is the Rankine Cycle. In Rankine Cycle, which is the most widely used technology for electricity generations from fuels (Dong *et al.*, 2009), the gas boils water to steam in a boiler, and the steam continues to flow and drive a turbine. The turbine is usually connected to a generator that produces electricity, converting mechanical energy to electrical energy. The waste heat generated from condensing the utilised steam is used to heat the district heating water systems while the condensed water is then recirculated to the steam boiler as feedwater.

The combined cycle gas systems combine a gas-turbine cycle (CCGT) and a steam-turbine cycle and have a very high power efficiency (55%) than either of the processes when used individually (Dong *et al.*, 2009). In CCGTs, after power is generated, as outlined above from a gas turbine, the high-temperature exhaust gases from a gas turbine are used for high-pressure steam production, which then passes through the steam turbine to generate more power (Dong *et al.*, 2009). CCGTs are usually used in large scale power production.

Although other new and emerging technologies such as Stirling engines, fuel cells, and ORCs have high electricity efficiencies, they are capital intensive (Dong *et al.*, 2009 and Sipila, 2016). Stirling engine is similar to a steam engine in that all its heat flows in and out via the engine wall. However, the Stirling engine uses a permanently enclosed gaseous fluid such as helium or air as its working fluid, unlike the steam engine that uses water in its liquid and gaseous phases. The motive power is created by the difference in temperature of the working fluid brought about by the general cycle in all heat engines, such as compressing cool gas, heating the gas, expanding the hot gas and cooling the gas. In the same vein, electricity and heat can be generated by electrochemically oxidizing fuel, often catalysed by a transition metal or acid solution or reactions carried out at a high temperature using a fuel cell. Lastly, ORCs, working fluid other than water with either a lower or higher boiling point, can generate electricity and heat using the same principle as a steam turbine (Dong *et al.*, 2009 and Sipila, 2016). This implies that ORCs can use low-grade heat such as water heat from conventional CHP or boilers to generate electricity using a working fluid with a lower boiling point.

### **2.12 Absorption Chillers for CHP Systems**

Chillers provide air conditioning, refrigeration and process fluid cooling in commercial buildings, shopping outlets, hospitals and industrial plants. Vapour compression and sorption are the two basic types of chiller cycles. The cycle is powered using reciprocating or centrifugal compressors driven by electric motors, natural gas engines, and steam turbines in vapour compression chillers. The sorption chillers are either absorption or adsorption driven by the thermal energy produced directly from an

integrated fired burner or hot water, steam, or combustion exhaust (Bruno *et al.*, 2009, Sun *et al.*, 2012, and US Dept of Energy, 2017). Absorption chillers usually operate with low-grade heat from various industrial processes or thermal energy from combustion exhaust (Sun *et al.*, 2012, Ahmadi *et al.*, 2013 and US Dept of Energy, 2017) and use a binary of different refrigerants and absorbents to meet a range of site cooling needs. For instance, water (which has refrigeration temperature above 0°C) serving as refrigerant and lithium bromide as absorbent is used to provide chilling fluid of 4.4°C or higher, while for lower temperature, ammonia/water can be used as refrigerant/absorbent, respectively (Jaruwongwittaya and Chen, 2010).

The absorption chiller cycle is based on the same principle as the vapour compression cycle. However, the prime mover, typically an electric motor and compressor in the vapour cycle compression cycle, is replaced with a thermal compressor system in absorption chillers (US Dept of Energy, 2017). The thermal compressor system comprises the top chamber (the generator and the condenser) and the lower chamber containing the absorber, the solution pump, and the evaporator. The system also has a heat exchanger that transfers heat from the concentrated lithium bromide to lithium bromide and water solution (Ahmadi *et al.*, 2013). The system works in the same principle with a mechanical compressor in a vapour compression chiller which takes low pressure/low-temperature refrigerant vapour from the evaporator and delivers high pressure/high-temperature refrigerant vapour to the refrigerant condenser (US Dept of Energy, 2017). Nonetheless, a thermal compressor uses an absorbent fluid to chemically bond with the refrigerant vapour (essentially compressing it by changing phase from a gas to a liquid) instead of directly condensing the refrigerant vapour using a large amount of mechanical energy.

Typically, the dilute or weak absorbent solution and refrigerant in absorption chillers are easily pumped from the absorber to the generator through the heat exchanger using a relatively small electric pump. In comparison, the refrigerant is separated from the absorber/refrigerant solution using thermal energy in the form of waste hot water in the generator while the concentrated absorber (lithium bromide) travels back to the absorber through the heat exchanger. The hot refrigerant vapour

then migrates to the condenser, cooled down into a liquid that further flows down to the evaporator through a small orifice at low pressure. This sudden pressure drop will cause the refrigerant to flash and drop temperature into the cold water of about 4°C for cooling purposes. Subsequently, the concentrated lithium bromide solution strongly attracts the excess refrigerant (water) vapour from the evaporator resulting from temperature differences in the cooling fluid application. This intense attraction process which causes the low pressure in the evaporator is exothermic. Hence, the heat is given off, and this residual water vapour in the absorber chamber is condensed back to liquid to mix with the absorbent, and the cycle continues. Generally, the overall performance of an absorption cycle depends heavily on the thermodynamic properties of the working fluids (Sun *et al.*, 2012).

### **2.13 Rice Straw Ash as Silica Precursor**

RS can be used as a natural source for silica production (Khosand *et al.*, 2012; Permatasari *et al.*, 2016 and Mirmohamadsadeghi and Karimi, 2018), as its inorganic component, rice straw ash (RSA), is about 10 -15% by weight (Agbagla-Dohnani *et al.*, 2001; Sangnark and Noomhorm, 2004 and Bakar and Carey, 2020). Moreover, these inorganic constituents are rich in silica, silicon compounds, alkali and alkaline earth metals (Agbagla-Dohnani *et al.*, 2001 and Guzman *et al.*, 2015).

Silicon is generally made for industrial purposes through synthesis despite being the most readily available component after oxygen in the earth's lithosphere (Permatasari *et al.*, 2016). The various silica sources can be obtained naturally from quartz sand, rock, clay and volcanic soil, phytoplankton, rice husk, straw, and silica in crystalline and amorphous forms (Barik *et al.*, 2008 and Mirmohamadsadeghi and Karimi, 2018). The amorphous silica form is the most widely used as it is highly reactive, whereas the crystalline silica is hard, chemically inert and has a high melting point (Chandrasekhar *et al.*, 2003 and Mirmohamadsadeghi and Karimi, 2018). Silica has a versatile commercial value as it could be used as raw materials for numerous industrial processes ranging from ceramics making, fillers, electronic components, adsorbents, biomedicine, catalysts, drug delivery systems, thermal insulators, rubber, glass and chromatography (Londeree, 2002; Hao *et al.*, 2006;

Adam *et al.*, 2008; Azizi and Yousefpour, 2010; Liou and Yang, 2011, Ghorbani *et al.*, 2013; Permatasari *et al.*, 2016 and Nandiyanto *et al.*, 2020). In elemental form, silica can be used as a component for building material and in vitreous form, it can be employed in glass wires and optical element manufacturing (Londeree, 2002 and Patel *et al.*, 2017). Silica in amorphous form is also used as a thickening and absorbent agent in cosmetic products, in toothpaste as an abrasive agent, as a matting and thickening agent in ink production and as an anti-corrosion agent in preventing metal corrosion (Chen *et al.*, 2013; Patel *et al.*, 2017 and Nandiyanto *et al.*, 2020). More so, silica materials could be employed in the near future in the development of more advanced materials such as carbon/silica composites, soluble silicates, silicon carbides, silicon nitride, elemental silicon, and magnesium silicide and alloys (Chandrasekhar *et al.*, 2003; Kumagai and Sasaki, 2009 and Mirmohamadsadeghi and Karimi, 2018), biocatalysts (Artkla, 2009, Azizi and Yousefpour, 2010), in the production of hydrogen and CO<sub>2</sub> capture materials and metallic ions adsorbents (Chen, 2010 and Liou and Yang, 2011).

Conventionally, silica precursors that are used commercially are alkoxysilane compounds such as tetraethylorthosilicate (TEOS), sodium silicate and tetramethylorthosilicate (TEMS) (Permatasari *et al.*, 2016), which are produced mainly from quartz and sol-gel process (Patel *et al.*, 2017 and Nandiyanto *et al.*, 2020). Recently, sodium silicate has been used in the industrial production of nano-silica (Affandi *et al.*, 2009). Conversely, due to the high-temperature requirement, high-cost implications, health challenges and death associated with the production or from these compounds, there have been renewed efforts on sourcing silica in cheap, safer and environmentally friendly (Fadhulloh *et al.*, 2014; Permatasari *et al.*, 2016; Patel *et al.*, 2017; Hadraimi *et al.*, 2020 and Nandiyanto *et al.*, 2020).

Among the cheap source of silica are agricultural wastes, which include but are not limited to rice husk (Adam *et al.*, 2008, Umeda and Kondoh, 2008 and 2010, Athinarayanan *et al.*, 2015 and Askaruly *et al.*, 2020), rice straw (Wattanasiriwech *et al.*, 2010; Khorsand *et al.*, 2012; Lu and Hsieh, 2012; Mirmohamadsadeghi and Karimi, 2018 and Bakar and Carey, 2020), wheat straw (Chen *et al.*, 2010), corn cob (Shim *et al.*, 2015 and Velmurugan *et al.*, 2015) and bagasse (Vaibhav *et al.*, 2015 and Sapawe

*et al.*, 2016). The silicon materials extracted from this agricultural waste could produce nano-silica with high porosity and surface area (Liou and Yang, 2011 and Bakar and Carey, 2020). Additionally, agricultural wastes are considered a good source for silica production because of their low cost, high silica content, comparable silica quality, high energy content, fine-sized amorphous material and environmental friendly (Patel *et al.*, 2017).

Silica is formed in some tropical plant organisms as a direct competition between more photosynthetic C4 plants and lesser C3 plants, e.g. rice, that may have led the latter to have evolved in the uptake of silica (Van Soest, 2006 and Bakar and Carey, 2020) which is absorbed in the form of water-soluble silicic acid (orthosilicate (Si(OH)<sub>4</sub>). Although orthosilicate does not have the buffering capacity in plant metabolism as it exists in the un-ionised form (Van Soest, 2006), the silica acid is saturated, leading to eventual polymerisation into soluble polysilicic acids, which are then deposited on the plant cell walls (Van Soest, 2006 and Bakar and Carey, 2020) as amorphous silica. This polymerisation is because the pKa value of silica is 9.8 – 11.8 in the plant sap.

### 2.13.1 Silica extraction processes

There are many documentations on the extraction processes of silica from agricultural waste. According to Fadhlulloh *et al.* (2014) and Patel *et al.* (2017), these processes are generally grouped into three main approaches: chemical, thermal and biological or microbial extraction methods. Typically, the structure, composition and morphology of silica derived from agricultural biomass are strongly influenced by the extraction method employed (Soltani *et al.*, 2015). In the thermal extraction process, agricultural biomass is valorised to ash in muffle furnace, fixed bed furnace, inclined step-grate furnace, cyclonic furnace, fluidised bed reactor, rotary kiln or tubular reactor (Patel *et al.*, 2017). The significant drawbacks of using thermal technology are longer reaction time, hot spot formation and insufficient complete carbon oxidation due to lack of free-flowing air (Patel *et al.*, 2017). Lu and Hsieh (2012) produced amorphous silica nano-disks using pyrolysis at 575<sup>o</sup>C and dissolution, followed by precipitation using NaOH and H<sub>2</sub>SO<sub>4</sub>, respectively. In the same vein, nano-silica materials were

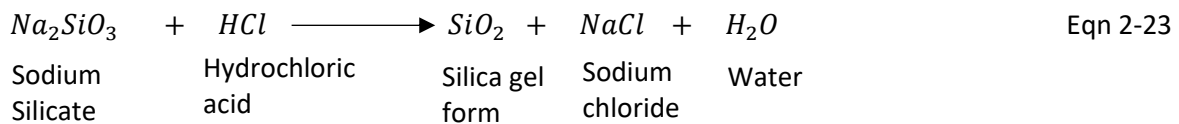
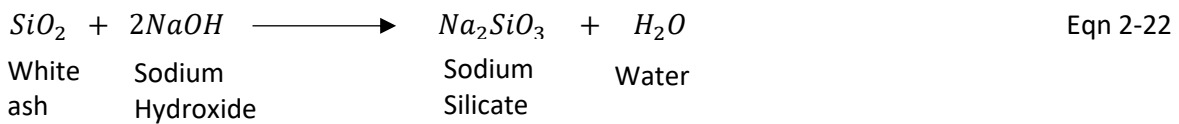


effectively produced from wheat straw by thermal treatment at a heating rate of 10<sup>0</sup>C/min at 400<sup>0</sup>C, 500<sup>0</sup>C, 600<sup>0</sup>C and 700<sup>0</sup>C, after initial combustion at a temperature of 500<sup>0</sup>C for 8 hours (Chen *et al.*, 2010).

However, before these extraction methods, acid leaching is paramount to remove/reduce the impurities and increase the surface area of silica, thereby improving the quality (Kongmanklang and Rangriwatananon, 2015). These impurities (metals and organic compounds) are converted to their respective individual ions after acid treatment (Vaibhav *et al.*, 2015). In the research experiment of Bakar *et al.* (2016) on high purity amorphous silica production from rice husk, they suggested that high purity silica can be produced by controlled combustion after acid treatments. In their research work, leaching of rice husk with sulphuric acid and hydrochloric acid was carried out before combustion at 500<sup>0</sup>C to 900<sup>0</sup>C for 2hr to obtain pure silica. They stated that acid treatments could eliminate metallic impurities such as iron, manganese, calcium, sodium, potassium, and magnesium, influencing silica colour and purity before combustion. Bakar and Carey (2020) also produced nano-biosilica from RS using alkaline hydrolysis pre-treatment.

Similarly, Rafiee *et al.* (2012) reported using 1M of HCl in silica production from rice husk and obtained silica with improved surface area. In addition to this, a wheat straw sample was leached by applying 5M sulphuric acid in the ratio 1:10 (g ml<sup>-1</sup>) with constant stirring at 1000rpm under room temperature (RT) for 24 h preceding to heating treatment at different temperatures and the time in a furnace (Ahmad-Alyosef *et al.*, 2015). Nonetheless, the use of strong acids in leaching has a cost implication, create negative impacts on the environment, and its corrosive nature has gained interest in the employment of weaker acid (citric or lactic acid or acetic acid), which are readily available, environmentally friendly and harmless (Umeda and Kondoh, 2008; 2010). Thus, Umeda and Kondoh (2010) reported silica production with a purity of 99% using citric acid as a leaching agent and hydrolysis process at temperatures above 200<sup>0</sup>C to extract pure silica from rice husk. In detailing further, they explained that metal impurities could be removed from rice husk through a chelate reaction between the metal and the carboxyl group of the citric acid.

Compared to the most straightforward extraction process is burning in the open air. However, as Della *et al.* (2002) reported, desirable characteristics of silica such as the high reactivity of the surface area and amorphousness may be lost. In addition, crystalline silica such as cristobalite or tridymite reported causing debilitating lung disease known as silicosis after continuous exposure may be formed at a prolonged-firing temperature above 500°C (Della *et al.* 2002). It has also been reported that these crystalline forms reduce the reactivity of silica in the synthesis of downstream industrial products such as zeolites used widely as adsorbents and biocatalysts (Della *et al.* 2002 and Bakar *et al.* (2016).



Alternatively, as documented by Kalapathy *et al.* (2000) and (2002); Zaky *et al.* (2008) and Patel *et al.* (2017), chemical extraction method can be used to produce high purity nano-silica from rice straw ash using an alkaline agent followed by acid neutralisation or use of other chemical agents such as toluene, ethanol or ionic liquids. Alkaline extraction involves dissolving of the rice straw or rice husk ash in an alkali (NaOH) at 100°C for 1.0 h under constant stirring followed by precipitation of sodium silicate using acid solutions (1N HCl) at pH 7.0 (Eqn 2-22 and 2-23) (Kalapathy *et al.*, 2000 and 2002 and Patel *et al.*, 2017).

The base method is because amorphous silica solubility is high at pH>10 and very low at pH < 10 (Kalapathy *et al.* 2000 and 2002). Ionic liquid has been employed by Chen *et al.* (2013) for silica production from agricultural wastes. The limitation to chemical extraction is the corrosiveness of the solutions, high-cost implication, complexity of the processes in silica recovery, and difficulty in the complete elimination of the by-products trapped in the nano-silica pores Na<sub>2</sub>SO<sub>4</sub> or NaCl.

The biological (microbial) method, which is cleaner and environmentally friendly, involves breaking the organic part of the agricultural biomass by microorganisms or their part (enzymes). (Esteves *et al.*, 2009) and leaving the silica component. In this way, the biomass's organic component decreases while the inorganic constituents increase before subjection to the thermal process. Thus the time duration required with the expected thermal extraction process is reduced. In a published report by Wattanasiriwech *et al.* (2010) on an experiment on the production of amorphous silica nanoparticles from rice straw with microbial hydrolysis pre-treatment, they affirmed the reviews of other researchers on silica extraction using microbial hydrolysis technique after saccharification. They subsequently proposed that the residual rice straw substrate contain a large amount of amorphous silica after sugar hydrolysis. They further stated that silica produced from such a technique is better as the desired properties are preserved.

In the same way, Rohatgi *et al.* (1987) obtained a high inorganic material ( $\text{SiO}_2$ ) and decreased organic matter from microbial fermentation of rice husk using white-rot fungi species (*Cyathus*) for 60days, followed by drying at  $80^\circ\text{C}$  and sieving to a prescribed size before combustion at  $450^\circ\text{C}$ . Mirmohamadsadeghi and Karimi (2018) also reported the production of amorphous silica from RS digestate produced via dry anaerobic digestion (AD). However, there are few reports on this attractive possibility. The biological method perhaps is not a direct conventional method for silica production but a process that aids in producing quality and amorphous silica. First, this idea is because hydrolytic organisms degrade the biomass's organic components. Secondly, the residual metallic ions (impurities) are consumed during the microbial hydrolytic and AD processes to support numerous metabolic activities and finally, the free organic acids produced during the digestion process act as a leaching agent for the metallic impurities. Therefore, no need for pre-leaching as suggested above. The microbial activity leaves the remaining organic component of the lignocellulose material intact, which can now be subjected to combustion for silica production. Therefore, the biological method can preserve the quality of the silica and lower the temperature and time consumed in silica production.

## 2.14 Research Framework and Multigeneration Energy System

Typically, hydrogen, methane, electricity, thermal energy systems, and even silica are produced, planned, and operated individually. Nevertheless, there are increasing coupling, interactions, and interdependencies between the systems in modern times, which offers a cost-effective means of utilizing large volumes of variable renewable energy in the energy system (El-Emam and Dincer, 2018 and Koirala *et al.* 2021). Multigeneration (poly-generation), an energy system that produces numerous useful outputs from single or several primary energy inputs such as biogas, increases energy efficiency and sustainability while conserving the environment (Ahmadi *et al.*,2013). Thus, integrating several energy systems would increase the energy output by effectively utilizing system waste streams (El-Emam and Dincer, 2018). In a multigeneration system, the biogas ( $H_2$  and  $CH_4$ ) produced in an AD process is used to produce electricity, heat and cooling fluid through CCHP technology, while the digestate from the AD system is employed for silica production in a thermal procedure. Thus, the valuable products of poly-generation systems such as biogas, heating, cooling, drying, electricity and even freshwater, which are primarily in-demand in residential and rural areas, specifically in the farm, are obtained using this technology (El-Emam and Dincer, 2018). Therefore, the technology would benefit Nigeria, especially in the rural areas that lack infrastructure for electricity, as most of the energy produced is used within the community. Also, the improved energy efficiency and output of integrated energy systems would complement and support the growing demand for energy, particularly electricity. Recall that generated electricity in Nigeria is within the capacity range of 6.5 to 8.2 GW, insufficient for the country (Garba and Zangina, 2015, NESP, 2015 and NERC, 2018). On the other hand, the projected energy demand is around 180 GW. Hence, designing an integrated energy system, especially for rural settlers, significant contributors to Nigeria energy consumption, is believed to improve energy inadequacies and reduce GHG gases from firewood and fossil sources.

The challenges and research gaps relating to methane, hydrogen and silica production from RS have been mentioned and discussed extensively in the experimental chapters. Furthermore, the generation

of electricity and thermal energy from CCHP using biogas is reviewed by Bruno *et al.* (2009), Su *et al.* (2018) and Koirala *et al.* (2021). In addition, Wang *et al.* (2015) published an article on energy and exergy analyses of an integrated CCHP system with biomass air gasification.

In the same vein, using agro-industrial wastes - PE, CSSW and CSTL, as pre-treatment agents for RS, DCS enrichment, and leaching agents for chelating inorganic elements during silica production is novel, as there is no known published work, is discussed and investigated in the empirical chapters.



## Chapter 3 Materials and Methods

### 3.1 RS Collection and Preparation

The RS used in the study was collected from Xiamen University, China and was used as feedstock. The rice straw was chopped into 2mm pieces and washed thoroughly three times with tap water before placing it in an electric oven at 70 °C until dry. Then, the sized-medium RS was milled with a grinder, sieved through 750 µm and stored in a sealed plastic container at room temperature until use (Fig 3 - 1a and b). Finally, the proximate and ultimate analysis of the rice straw was done as described below. The composition of RS (dry basis) was determined to be 39.5% cellulose, 30.5% hemicellulose, 17% lignin and 13% others.



Fig 3-1: Representation of prepared RS with (A) 750 µm sized and (B) 2cm-sized

### 3.2 Agro-industrial Wastes Collection and Preparation

#### 3.2.1 Potash collection and preparation of potash extract

The potash or ash from empty palm fruit was collected from a heap of burnt empty palm bunches (Fig 2-7) at a palm oil processing factory in Anara Town, Imo State, Nigeria. The potash extract (PE) was prepared by mixing 500g of potash with 1L of deionised water (1:2 ratio). The mixture was appropriately stirred and allowed to settle at room temperature for 48 h. After the incubation, the potash mixture was vacuum-filtered using Whatman filter paper (0.45µm), and the residue was rinsed

with 500 mL of distilled water to bring the total ratio of potash to distilled water to 1:3. The pH of the filtrate was observed to be  $11.05 \pm 0.25$ , which is highly alkaline. The PE colour was deep brown (Fig 3-2a), and then the PE was kept at refrigerating temperature of 4°C after the metal analysis was done using ALPHA standard (2005) (Table 3-1).

Table 3-1: Elemental composition of potash, rice straw and seeded sludge (activated digested sludge (ADS) and digested cow slurry (DCS))

Cations	Potash (mg/g)	RS (mg/g)	ADS (mg/L)	Raw DCS (mg/L)
Calcium	557.50	45.30	208.65	205.00
Magnesium	346.42	3.48	206.88	200..18
Sodium	280.22	2.22	66.22	76.22
Potassium	5041.55	119.35	375.08	365.88
Zinc	4.37	0.36	2.97	2.00
Nickel	0.29	9.27	0.20	0.20
Aluminium	113.45	1.15	21.95	15.87
Iron	113.18	47.89	131.37	135.13
Manganese	16.37	5.56	5.26	4.26
Copper	10.35	0.26	3.11	2.75
Lead	<0.05	<0.05	<0.05	<0.05
Silicon	81.32	10.87	1.21	1.00
Arsenic	0.16	0.05	1.10	0.56
Chromium	0.23	0.21	0.29	0.29
Strontium	0.13	0.09	3.74	2.89
Barium	0.70	0.28	0.47	0.50
Selenium	1.58	0.2	0.71	0.67
Anions				
Chloride	366.80	NA	NA	NA
Nitrite	16.90	NA	NA	NA
Bromide	4.43	NA	NA	NA
Sulphur	137.50	NA	27.09	25.00
Nitrate	1.25	NA	NA	NA
Phosphor	201.50	15.01	NA	NA

NA: Not available



### 3.2.2 Corn seed collection and preparation of corn-steep liquor

The corn was purchased from an African Shop located at Westgate Road, Newcastle Upon Tyne, UK. The corn-steep liquor (CSTL) was prepared to represent the ones obtainable in Nigeria's corn-based industries. The dried corn was coarsely crushed and imbued into plastic containers containing sulphuric-added deionised water (0.1%) for two days at room temperature, with the wastewater changed every 24 h (Fig 3-2a). The wastewater termed corn-steep liquor was placed in a container and kept at a temperature of -25 until use. The organic acid content and the COD of the CSTL were done before use (Table 3-2).



Fig 3-2: A - CSTL extractions (the incubation was done for two days at RT) and B – PE preparation

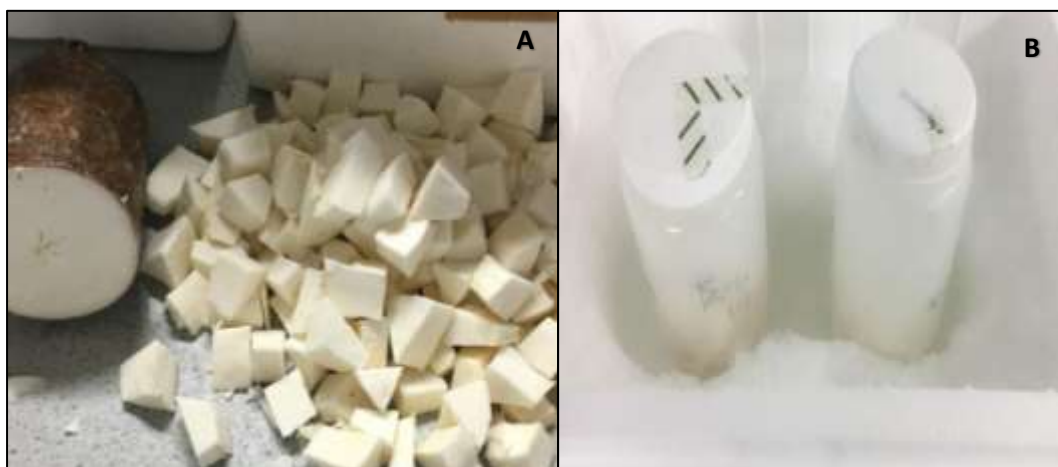


Fig 3-3: CSWW extraction preparation before incubation at RT (A) and under ice (B)

Table 3-2: Characterization of cassava-steep waste water and corn-steep liquor

Sample	Acetic Acid (mg/L)	Butyric Acid (mg/L)	Formic Acid (mg/L)	Lactic Acid (mg/L)	Total COD (mg/L)	Soluble COD (mg/L)	pH
CSWW at 4°C	44.49	932.87	NA	NA	4880.00	1040.00	3.85
CSWW at RT	2329.89	2679.71	NA	NA	13640.00	5680.00	3.81
CSTL	1595.32	1201.69	NA	NA	7520.00	3600.00	3.45

NA: Not available

### 3.2.3 Cassava collection and preparation of cassava-steep wastewater

Fresh cassava roots tubers were purchased from a Hutchinson fruits shop located at Fenham Newcastle Upon Tyne, UK. The cassava-steep wastewater (CSWW) was generated as the wastewater used in a) anaerobic fermentation of small-sized peeled cassava (Fig 3-3a) after incubation in water for 4.0 days in airtight plastic containers and b) the anaerobic fermentation under ice cubes kept at 4°C for 3.0 days (Fig 3-3b) to reduce or prevent the loss of the active compound (glucosidic cyanosides) (Fig 3-4) and other organic compounds therein. The cryogenic glucosides organic acid content (Table 3-3) and the COD of the CSWW were done prior to use (Table 3-2).



Fig 3-4: Cyanogenic glucosides determination (different levels of cryogenic glucoside for CSWW samples in days)

Table 3-3: Cyanogenic Glucosides at 4°C and RT

CSWW Extract	CSWW Cyanogenic glucosides (mg/L)		
	Day 1	Day 2	Day 3
CSWW @ RT	8	0	0
CSWW @ 4°C	20	27	27 - 30

### 3.3 Measurement of Lignocellulose Composition of Rice Straw

The cellulose, hemicellulose, lignin and ash components of the RS were determined using the method reported by Lo *et al.* (2010). In summary, about 10mg of thoroughly dried RS was placed in test tubes

containing 1.0  $\mu\text{l}$  of 72% (w/w) sulphuric acid. The reaction mixtures were stirred continuously using a glass rod in an ice-cold water bath and then transferred to a water bath set at 30 $^{\circ}\text{C}$  under continuous stirring for 1.0 h. Subsequently, the acid hydrolysis reaction was ended by placing the tubes in an ice-cold water bath. Next, the sulphuric acid in the tubes was diluted to 4% by transferring all the supernatants to 125 mL serum bottles containing 84 mL of distilled water while the solid residues were rinsed with 50 mL deionised water and used for lignin and ash analysis. The diluted solutions were well mixed and 1.0 mL transferred to anaerobic pressure bottles. The bottles were autoclaved at 121 $^{\circ}\text{C}$  for 1.0 h, after which; the hydrolysates were collected and neutralised to pH 6.0 using calcium carbonate. Later, the concentration of pentose (hemicellulose) and hexose (cellulose) sugars were measured using HPLC. Finally, the solid residues containing the lignin plus ash were wholly dried and recorded as  $W_A$ . Subsequently, the dried solid residues were placed in a furnace at 550 $^{\circ}\text{C}$  for 24 h and recorded as  $W_B$ . The difference between  $W_A$  and  $W_B$  was the lignin content, while  $W_B$  was the ash content.

### **3.4 Determination of Elemental Composition of Rice Straw and Biomass Samples**

The procedure was done using a modified description of Nielsen (2017). The wet ash process involved the digestion of 1 g of a dried and ground sample of RS biomass and about 1.0 mL of seeded sludge in a conical flask placed in a fume cupboard. Approximately 10 mL of each of the concentrated  $\text{H}_2\text{SO}_4$  and  $\text{HNO}_3$  acids were then poured inside the flasks. Following this, the biomass and acids mixture was placed on a hot plate and heated at 120 $^{\circ}\text{C}$  for 15 minutes. During this heating process, effervescence occurred along with the release of  $\text{NO}_2$  gas depicted by reddish-brown gas production. The addition of acids sustains the digestion process until all the biomass is entirely digested, evidenced by the formation of a light-yellow solution. At this juncture, no further release of  $\text{NO}_2$  gas. Afterwards, the digested mixture was transferred to a 50 mL standard volumetric flask and was made up to 50 mL using de-ionised water. A sample from this diluted solution was used for the determination of its elemental composition using inductively coupled plasma atomic emission spectrometer (Vista-MPX)

with CCD, detector, Newcastle University, UK, under the analytical process outlined in the Standard Methods for the Examination of Water and Waste Water 20<sup>th</sup> Edition (APHA 3120C) (ALPHA standard, 2005). The anions composition of the PE sample were analysed using High-Performance Liquid Chromatography (HPLC) Thermo-scientific DIONEX AQUION, Newcastle University, UK. The biomass elemental composition analysis was done in triplicates and presented in Table 3-1.

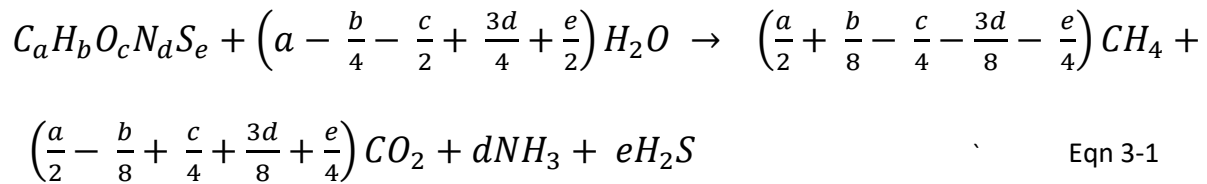
Table 3-4: Ultimate analysis of rice straw and seeded sludge (ADS and DCS)

Biomass	Carbon (%)	Hydrogen (%)	Nitrogen (%)	Oxygen (%)	Sulphur (%)	Others (%)	C/N ratio
RS	42.76	6.30	0.68	44.70	0.15	5.56	63:1
ADS	34.44	3.77	2.98	NA	0.58	NA	12:1
DCS	38.54	3.99	2.92	NA	0.65	NA	13:1

NA: Not available

### 3.5 Analytical Determination of Carbon, Hydrogen, Nitrogen, Oxygen and Sulphur Content in Rice Straw and Seeded Sludge

The carbon, hydrogen, nitrogen, and sulphur contents of the sludge and RS were analysed using the Perkin-Elmer 2400 CHNS Elemental Analyzer, Newcastle University, from 1.0g of the individual biomass, while the oxygen content of each biomass in the same quantity was measured using Thermo Elemental Analyzer (NA 2000) by Elemental Microanalysis Laboratory, UK. The data obtained were measured to an accuracy of  $\pm 1\%$  (Table 3-4) and used in producing the stoichiometric formula, particularly for RS using the modified Buswell equation (Eqn 3-1). Whereas the constants “a, b, c, d and e” were obtained by dividing their various corresponding elements (%) (Table 3-4) with their molar mass, the molar ratios which gave the chemical formula of RS were achieved by dividing the individual constants with the least constant value. The values of RS ultimate analysis were also used to calculate theoretical biochemical methane potential (TBMP) using Eqn 3-2 (Achinas and Euverink, 2016).



$$\text{TBMP (NmL CH}_4 \text{ g VS}^{-1}) = \frac{22.4 * \left(\frac{a}{2} + \frac{b}{8} - \frac{c}{4} - \frac{3d}{8} - \frac{e}{4}\right)}{12.017a + 1.0079b + 15.999c + 14.0067d + 32.065e} \quad \text{Eqn 3-2}$$

### 3.6 Determination of Rice Straw Energy Value

The higher heating value of raw RS and raw RS digestate was determined using Oxygen Bomb Calorimeter Parr 1341 from Newcastle University. About 0.50 g of the respective samples were measured, pelletized, and placed on the combustion crucible of the bomb head, held by the electrodes containing about 10cm of a nichrome ignition wire. The ignition wire was then wrapped around the electrode cautiously to avoid touching the combustion crucible and form a loop into it and above the pellets. The bomb head was carefully placed on the bomb cylinder that is supported by the bomb bracket. Following this, the bomb cylinder was screwed tightly after a few drops of distilled water from the calorimeter bucket had been added. The bucket contains a specific quantity (1600 mL) of distilled water that was employed in the experiment. The bomb is then pressurised at 30 atm with oxygen gas and submerged carefully inside the calorimeter bucket circular bottom already placed in an insulated container. The electrodes were inserted into the terminal sockets of the bomb after a stream of continuous gas bubbles were checked. The lid with the stirrer was then used to cover the calorimeter, and the stirrer turned to ascertain that it was running freely before the drive belt was attached to the pulleys. Following this, the temperature sensor attached to the data logger is inserted into the port on the cover lid. Finally, the data produced is recorded via a Pico PT-104 (PT100) data logger connected to a computer after igniting the switch. The exact process was first done with benzoic acid that has a known heat of combustion of -26.454 KJ/g to determine the heat capacity of the calorimeter ( $C_{cal}$ ) from Eqn 3-3a. The heat of combustion (higher heating value (HHV)) rounded up to MJ kg<sup>-1</sup> of RS was

also calculated using Eqn 3-3a and b, while the HHV was converted to lower heating value (LHV) in MJ kg<sup>-1</sup> using Eqn 3-4 (Nguyen *et al.*, 2016).

The heat released on combustion of (pellets sample + ignition wire) = Heat absorbed by (water + calorimeter), which is the same as

$$\Delta_c H^0 m_s + \varepsilon = m_w C_{H_2O} \Delta T + C_{cal} \Delta T \quad \text{Eqn 3-3a}$$

Which can be re-written as

$$\Delta_c H^0 = \frac{(m_w C_{H_2O} \Delta T + C_{cal} \Delta T) - \varepsilon}{m_s} \quad \text{Eqn 3-3b}$$

Where

$\Delta_c H^0$  is the heat combustion of the sample (KJ g<sup>-1</sup>)

$m_s$  is the mass of the sample (g)

$\varepsilon$  is the heat of combustion of the wire (-9.6J/cm) and length of burnt nichrome wire (cm)

$m_w$  is the mass of water (g)

$C_{H_2O}$  is the specific heat capacity of water (4.184 J g<sup>-1</sup> °C<sup>-1</sup>)

$C_{cal}$  is the heat capacity of the calorimeter (J g<sup>-1</sup> °C<sup>-1</sup>)

$\Delta T$  is the temperature differences (°C)

$$LHV = HHV - 0.212 * H - 0.0245 * M - 0.008 * Y \text{ (MJ kg}^{-1}\text{)} \quad \text{Eqn 3-4}$$

Where  $H$ ,  $M$ , and  $Y$  are the percentages of hydrogen, moisture, and oxygen from RS, respectively.

### 3.7 Seed Sludge Collection and Preparation

#### 3.7.1 Sludge collection and residual incubation

The sludge employed were activated digested sludge (ADS) and digested cattle slurry (DCS). They were collected from Cockle Park Farm, Newcastle University, Newcastle Upon Tyne, UK, which processes cattle and pig slurry and then stored at 4°C until future use. Before use, the sludge was incubated for degassing for 30 days (Fig 3-5) at 37°C and 55°C to remove any remaining indigenous biomass.



Fig 3-5: Sludge residual incubation (degassing) of seed sludges (ADS and DCS) for 30 days

### 3.7.2 Sludge pre-treatment for bio-hydrogen production

The DCS was sieved through a 2.0mm screen to filter out solid particles and make them homogenous. Afterwards, pre-treated to deactivate hydrogen consumers as prescribed by Fan *et al.* (2004), Nathao *et al.* (2013) and Biswarup *et al.* (2016). The pre-treatment was done as follows - the sludge was boiled at 100 °C for 1 hr and afterwards acclimatized.

### 3.7.3 Sludge acclimatization

Before laboratory study, the pre-treated DCS and ADS were acclimatized using the substrates of interest for a specific duration. For example, heat-shocked DCS was acclimatized for 24 h with glucose, sucrose and RS hydrolysates at pH 5.5 + 0.2 and temperature 55°C while the ADS was acclimatized with VFA or various RS samples for a week and 30 days respectively at pH 7.0 + 0.1 and temperature 37°C. After the sludge acclimatization, analytical tests were done before the commencement of various research experiments.

## 3.8 Experimental Procedures

### 3.8.1 Batch/ fed-batch fermentation process for hydrogen fermentation

After acclimatization, the Heat-shocked DCS were tested for their capabilities to produce hydrogen using soluble substrates (glucose and sucrose) preceding application on various RS PT hydrolysates.

The batch cultivation was done using 500 mL grade 3.3 borosilicate glass Duran bottles (BGDB) (VWR 215-1594) with a working volume of 400 mL and a food to microbial (F/M) ratio of 0.75. Rubber bung 29mm (Fischer Scientific 11582922) was drilled, and a 1 mL syringe with Luer lock was inserted to facilitate the biogas collection route. The rubber stopper attached to the syringe was then used to create an airtight seal at the lid of each of the BGDB (Fig 3-6a). In the fed-batch systems, a second opening slightly bigger in diameter (7.5 – 8mm) for feeding inlet was made on the rubber bungs and connected using a tube (Fig 3.6b). The fermentations were done in triplicates in an automated stirred incubator system (Fig 3-7) with an initial pH of 5.8. Nonetheless, the operational pH of 5.5 was maintained using 5M HCl and 5M NaOH. The cultivation temperature of the incubator system was 55°C, while the rotational speed was done at 120 rpm. The carbon to nitrogen (C/N) ratio was maintained at 25, and the reactor mixture was supplemented with a 5% mineral medium. The mineral medium contained the following per litre: (NH<sub>4</sub>HCO<sub>3</sub> 6.72 g; KH<sub>2</sub>PO<sub>4</sub> 0.125 g; Na<sub>2</sub>HPO<sub>3</sub> 5.24 g CaCl<sub>2</sub> 0.3 g; MgCl<sub>2</sub>·4H<sub>2</sub>O 0.1 g; FeSO<sub>4</sub>·7H<sub>2</sub>O 0.025 g; CoCl<sub>2</sub>·6H<sub>2</sub>O 0.0001 g; ZnSO<sub>4</sub>·7H<sub>2</sub>O 0.0024 g; CuSO<sub>4</sub>·5H<sub>2</sub>O 0.005g, peptone 0.75 g; distilled water 1000 mL).

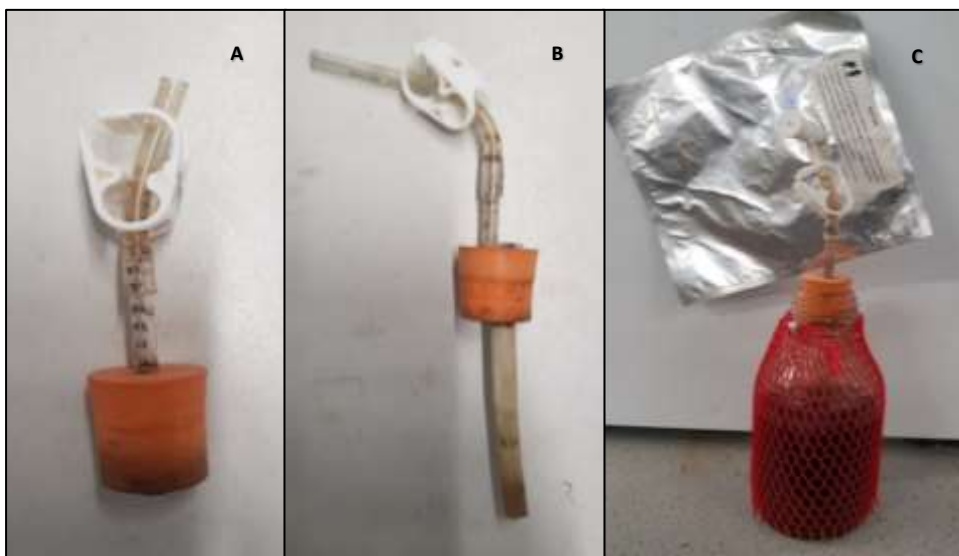


Fig 3-6: Construction and assembling a typical digester bottle (c) with the rubber bungs (a and b). The image “b” was used for feeding in fed-batch processes



The reactors were flushed with nitrogen for 3 minutes. Finally, biogas was collected daily in a 500 mL Supel™-Inert Multi-Layer Foil Gas Sampling Bag with Thermogreen® LB-2 Septa equipped with screw cap Valve (SCV) purchased from Sigma-Aldrich UK connected to the syringe gas take-off of the reactors through PVC tube. At the same time, a plastic sheath net was placed around each prepared BGDB to minimise projectile travel in the event of explosion due to in build of pressure within the reactor (3-6c). The total biogas volumes produced by each CSABR were measured daily, and the hydrogen content (%) was determined as detailed in Section 3.9.



Fig 3-7: Batch fermentation of AD and AF process in an automated stirred incubator system

### 3.8.2 Batch/ fed-batch fermentation process for methanogenesis

The procedure was the same as described above under acidogenesis with variations in the condition of cultivation. The food to microbial (F/M) ratio was 0.4, whereas the batch process was also done in triplicates in an automated stirred incubator system with an initial pH of  $7.1 \pm 0.2$ . The temperature of the incubator system was kept at  $37^{\circ}\text{C}$ , and the rotational speed was done at 100 rpm. The pH of 7.0 was maintained using 5M HCl and 5M NaOH. The total biogas volumes produced by each BGDB were measured daily, and the methane content (%) was determined as described in Section 3.9.

### 3.8.3 Continuous anaerobic fermentation process

In the continuous stirred anaerobic bioreactor (CSABR) set-up, six (Fig 3-9) or eight (Fig-3-8) Quickfit® glass anaerobic bioreactor each of 1 or 5-litre capacity (Sigma-Aldrich, UK) consisting mainly the gas inlet/outlet system, the feeding mechanism and stirrers that are controlled automatically by an adjustable electric motor. A working volume of 900 mL or 4.8 L was employed, and the bioreactors were incubated in a water-filled bath at 55°C using an automatic heating system (Grant, T100) (Fig 3-8 and 9). This temperature was also sustained by covering the top of the water bath with spongy-like foams. The CSABR was seeded with Heat-shocked and acclimatised DCS sludge while the headspace of the individual bioreactors was flushed with nitrogen for 3 minutes to provide an oxygen-free condition. The automatic overhead stirrers were set at 120 rpm for uniformity in digestate mixing. The CSABR fermentation conditions were similar to the previous batch acidogenesis conditions in section 3.8.1. Each reactor was connected to a 1L Supel™-Inert Multi-Layer Foil gas bag for daily gas sampling, while the total biogas volumes produced by each CSABR were measured daily, and the hydrogen content (%) determined as described in Section 3.9.

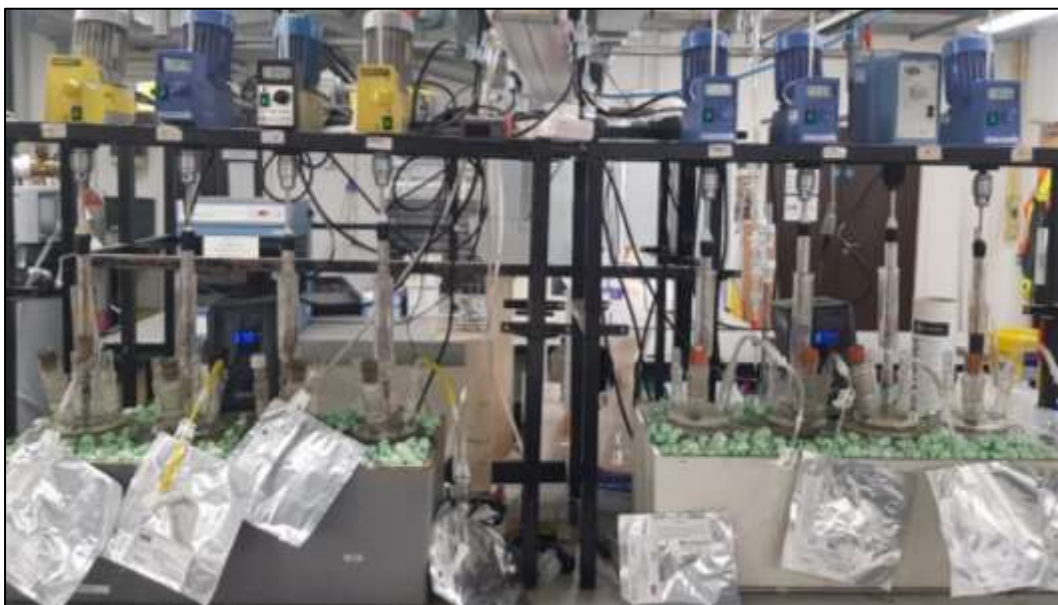


Fig 3-8: A continuous stirred anaerobic bioreactor setting for AD and AF processes (1 L)

### 3.8.4 Continuous anaerobic methanogenesis

The CSABR set-up was the same as in section 3.8.3. Nonetheless, the Quickfit® glass anaerobic bioreactor employed was six, and the cultivation conditions were similar to the batch methane process outlined in section 3.8.2. Each bioreactor was 5L (Fig 3-9), while the working volume was 4.8L. The nitrogen flushing was done for 5 minutes, and the total biogas volumes produced by each CSABR were measured daily. Lastly, the methane content (%) was determined as described in Section 3.9.



Fig 3-9: A continuous stirred anaerobic bioreactor setting for AD and DF processes (5 L)

### 3.9 Biogas Measurement and Specific Content Analysis

The collected biogas was measured to determine the volume of biogas produced using either 100 mL SGE 100MR-LL-GT or 1 L SGE Jumbo syringe 1000MAR-LL-GT purchased from Sigma-Aldrich, UK. At the same time, the CH<sub>4</sub> or H<sub>2</sub> content was analysed by injecting 100, 80, 60, 40 and 20 µL volumes of a known standard percentage of either of the gases into using thermal conductivity detector gas chromatography-Trace GC Ultra (Thermo Scientific, UK) with argon as the carrier gas for hydrogen, and Carlo Erba HRGC 5160 GC equipped a flame ionization detector with helium as the carrier gas for methane using 100 µL SGE Gas Tight Syringe with Luer Lock (Sigma-Aldrich, UK). The gas area peaks were captured using Trace GC Ultra software and plotted against the respective percentage of either CH<sub>4</sub> or H<sub>2</sub> content in each µL of known standard injected into the GC. Following this, a straight-line

graph is drawn from this plot, which produced the equation of a straight line ( $y = MX + c$ ); where  $y$  represents the respective gas areas as captured by the GC software and  $x$  is the known gas content (%),  $m$  is the slope of the graph and  $c$  is a constant. By applying this equation, the gas contents of the unknown reactor biogas were calculated by substituting the area ( $y$ ) produced in the GC after injecting with a 100  $\mu\text{L}$  syringe. Afterwards, the respective percentage of hydrogen or methane was then extrapolated by finding the corresponding value of  $x$  related to  $y$ , multiplied by the total volume of biogas to determine the actual volume of hydrogen/methane produced. However, before the later process, the AD process is typically a wet procedure, which gives rise to vapour pressure that affects the concentration and total volume of biogas. Therefore, there is a need to normalise the volumes of biogas at STP (that is, specific biogas production (SBP) using Eqn 3-5 and hydrogen or methane content (specific methane production (SMP) using Eqn 3-6 if the gases are measured in the humid state (Verein Deutscher Ingenieure (VDI) 4630, 2006). In addition to this, the extrapolated biogas contents (%) were subjected to headspace correction using Eqn 3-7 since inert gas in the headspace at the commencement of the fermentation test caused a dilution of the biogas (VDI 4630, 2006).

$$V_0^{tr} = V \cdot \frac{(P - P_w) \cdot T_0}{P_0 \cdot T} \quad \text{Eqn 3-5}$$

Where

$V_0^{tr}$  is the volume of the dry gas in the state in NmL

$V$  is the volume of the gas in the gas bag in mL

$P$  is the pressure of the gas phase at the time of reading in hPa

$P_w$  is the vapour pressure of the water corresponding to the ambient (room) temperature, in hPa

$P_0$  is the normal pressure, 1013 hPa

$T_0$  is the normal temperature, 273k

$T$  is the temperature of the biogas, which is equivalent to the ambient room in K

$$C_{CH_4}^{dry} = C_{CH_4}^{moist} \frac{P}{P - P_w} \quad \text{Eqn 3-6}$$

Where

$C_{CH_4}^{dry}$  is the CH<sub>4</sub> or H<sub>2</sub> content in the dry, measured in % by volume  
 $C_{CH_4}^{moist}$  is the CH<sub>4</sub> or H<sub>2</sub> concentration in the moist gas, measured in % by volume  
 $P$  is the pressure of the gas phase at the time of reading, measured in hPa  
 $P_w$  is the vapour pressure of water as a function of the temperature at the ambient space, measured in hPa.

$$C_{korr} = C_{t_2}^{tr} + (C_{t_2}^{tr} - C_{t_1}^{tr}) \frac{V_K}{V_B} \quad \text{Eqn 3-7}$$

Where

$C_{korr}$  is the correct concentration of the biogas components in the dry gas, in % by volume  
 $C_{t_2}^{tr}$  is the measured concentration of biogas components in the dry gas, in % by volume  
 $V_K$  is the headspace volume, measured in mL  
 $V_B$  is the volume of the biogas produced, measured in mL  
 $t$  is the time of measurement ( $t_2 > t_1$ )

### 3.10 Analytical Assays and Measurements

The measurement of total solids (TS), volatile solids (VS), volatile suspended solids (VSS)), the alkalinity test, ammoniacal nitrogen (NH<sub>4</sub>-N) and chemical oxygen demand (COD) were measured according to standard methods 2540 B, 2320, 4500 and 5220 B respectively (ALPHA standard, 2005), while the reducing sugar concentrations (glucose) were measured using the 3, 5 – dinitrosalicylic acid colourimetry (DNS) method. Whereas the concentration of metabolites (volatile fatty acids (VFA), such as acetate, butyrate, formate and propionate were determined using High-Performance Liquid Chromatography (HPLC) Thermo-scientific DIONEX AQUION equipped with Dionex IonPac™ ICE-ASI columns, the reducing sugar concentrations mainly from the measurement of lignocellulose composition were analysed using high-performance liquid chromatography (HPLC) (Shimadzu LC-10AT Liquid Chromatography, equipped with a COREGEL 87H3, and refractory index detector, RID) at 37 with C. 0.005 N of sulfuric was used as the carrier phase at the flow rate of 0.6 mL/min. The total organic carbon was determined using the Total Organic Carbon Analyser (TOC-5050A SHIMADZU), and

the cyanogenic contents of the CSWW samples were determined using Quantofix Cyanide Kit from SIGMA-ALDRICH, UK. Finally, the microstructure of pre-treated RS residues and raw RS were observed before using a scanning electron microscope (SEM) HITACHI NEXUS.

### **3.11 Genetic Extraction and Microbial Community Analysis**

The samples for microbial analysis were taken at the end of individual experiments of Chapters 4, 5 and 6 and stored at -20°C in a sterile 50 mL centrifuge tube (VWR, 525-0402) before genomic DNA extraction. The DNA extraction was performed using the FastDNA<sup>™</sup> SPIN Kit for Soil (MP Biomedicals LLC., 116560200) and according to the manufacturer's protocol except for the sample preparations where 500 µL of seeded sludge or digestate was used. In addition, a blank tube containing 500 µL of microbiological grade sterilised water (Microzone, UK) was also used as the control to checkmate the presence or absence of kit contaminants. After the genomic DNA extraction, the DNA concentrations and quality were determined using Qubit<sup>®</sup> 2.0 Fluorometer. The samples DNA quantity and specificity were also improved by following the cleaning protocol of QIAquick<sup>®</sup> Nucleotide Removal Kit (Qiagen, 2016) and ensuring the acceptable range of 1.8 to 2.2 for the DNA quality ratios 260:280 and 260:230 is sustained. The samples were then stored at -20°C until when ready for genomic sequencing. For the sequencing, about 100 µL of the various DNA extracts were placed in PCR tubes and sent to NU-OMICS laboratory, Northumbria University, UK, where the polymerase chain reaction (PCR) amplification, library preparation and high-throughput 2 X 250 amplicon sequencing of the V4 region of the 16S rRNA gene using the Illumina MiSeq Personal Sequencer Protocol (Kozich *et al.*, 2003) were carried out. Whereas the amplicon sequencing of taxonomic marker genes such as the 16S rRNA gene in bacteria provides an efficient characterization of bacteria communities (Callahan *et al.*, 2016b), the PCR process involves the amplification of the extracted DNA V4 hypervariable region of 16S rRNA using the universal reverse primer 806R (GGACTACHVGGGTWTCTAAT) and the forward primer 515F (GTGCCAGCMGCCGCGGTAA) primers to analyse the bacterial and archaeal communities respectively (An *et al.*, 2020b).

After sequencing from each sample was completed from Illumina MiSeq, the raw sequence data (FastQ files) obtained were denoised and quality filtered using DADA2, which is a publicly-available R package (<https://github.com/benjjneb/dada2>) that extends and improves the DADA model (Callahan *et al.*, 2016a). The quality filtration involves the trimming and truncating of low-quality regions, especially the first 10 bases for both forward and reversed reads, often known to contain pathological errors (Callahan *et al.*, 2016b). The reads in each sample were then dereplicated by the “derep” function in DADA2 to identify the unique amplicon sequence variants (ASV) from redundant sequences contained in the data set. Whilst the chimeric sequences from each sample were removed from each sequence, the non-chimeric sequences from the samples were taxonomical assigned using MIDAS 2.0 reference database (Callahan *et al.*, 2016a; Rognes *et al.*, 2016 and Tabraiz *et al.*, 2021) within the Quantitative Insights Into Microbial Ecology (QIIME2) pipeline (<https://qiime2.org/>) (Caporaso *et al.*, 2010). Afterwards, a feature table used for data visualization and statistical analysis was produced containing the unique ASVs and their relative abundance per each sequenced DNA digestate sample. The statistical analysis, especially the Local Contributions of Beta Diversity (LCBD), which was a comparative indicator of the degree of the uniqueness of digestate samples in reference to local community composition, was conducted on these data to generate figures and pictographs using the MicrobiomeSeg in R packages (SSekagiri *et al.*, 2017) built from existing packages such as vegan (Oksanen *et al.*, 2007), phyloseq (McMurdie and Holmes, 2013) and DESeq2 (Love *et al.*, 2014).

### **3.12 Kinetic and Statistical Analyses**

The biogas (H<sub>2</sub> and CH<sub>4</sub>) produced was determined from the equations according to Lee *et al.* (2010) (Eqn 3-8), while the integrated energy model of the research study (Fig 1-1) is the graphical summary of the whole structural plan of the research study. The kinetic model for biogas (H<sub>2</sub> and CH<sub>4</sub>) production rate and accumulations were determined using a modified Gompertz equation (Eqn 3-9) and Matlab software (MATLAB R2016a), while the data was analysed using the statistical Excel software (Microsoft Corporation, USA). The R software packages (R version 3.3.2; R Core Team, 2013)

were employed for the statistical microbial analysis as discussed above. The values presented were based on a 5% statistical significance level, and results were shown within  $\pm 2$  S.D.

$$H = \frac{(PV_1 - PV_2)}{A} \quad \text{Eqn 3-8}$$

Where H (mL CH<sub>4</sub> or H<sub>2</sub>/sugar-added or gVS) is the CH<sub>4</sub> or H<sub>2</sub> production; PV<sub>1</sub> (mL) is the volume of potential daily CH<sub>4</sub> or H<sub>2</sub> production from adding the sugar or RS; PV<sub>2</sub> (mL) is the volume of possible daily CH<sub>4</sub> or H<sub>2</sub> production from control, and A (g) is added sugar (TS) or RS (gVS).

$$H(t) = P \cdot \exp \left\{ -\exp \left[ \frac{R_m \cdot e}{P} (\lambda - t) \right] \right\} \quad \text{Eqn 3-9}$$

Where H (t) is the cumulative H<sub>2</sub> production (mL); P is the H<sub>2</sub> production potential (mL); R<sub>m</sub> is the maximum H<sub>2</sub> production rate (mL/d); e is 2.71828; λ is the lag phase time (d), and t is the fermentation time (d).





## Chapter 4    Enrichment of seeded sludge using agro-industrial wastes for biological hydrogen production

### 4.1    Introduction

Biological hydrogen production is affected, among other factors, by the quality of seeded sludge in the dark fermentation (DF) process, which is because seeded sludge contains diverse populations of microorganisms that can produce hydrogen using the anaerobic digestion (AD) pathway. Thus, the main benefits in the use of seeded sludge over pure cultures are its affordability, and that bacteria genera participate in synergistic interactions with other microbes, and its resistance and adaption to environmental stresses (Li and Fang, 2007; Pendyala *et al.*, 2012, Wong *et al.*, 2014; Singh and Wahid, 2015 and Bundhoo *et al.*, 2015). However, hydrogen consuming bacteria (HCB) existing together with hydrogen-producing bacteria (HPB) in seeded sludge present a challenge of its (seeded sludge) use in the efficient production of hydrogen from organic matter as untreated sludge generally produce a low H<sub>2</sub> yield of about < 1.0 mol H<sub>2</sub> / mol of glucose (Wong *et al.*, 2014 and Yang *et al.*, 2020). The low production of H<sub>2</sub> is because molecular hydrogen is used for energy by HCB (Li and Fang, 2007), producing other products such as methane. In mixed cultures, hydrogen yield is within the range of 0.28 and 0.57 mol H<sub>2</sub> mol<sup>-1</sup> glucose from the 4 mol H<sub>2</sub> mol<sup>-1</sup> glucose that is biologically possible under DF technology, which perhaps is a direct consequence of hydrogen consumption by HCB (Hallenbeck and Gosh, 2009).

Several conventional methods to enhance sludge solubilisation, enrich the hydrogen producers and eliminate the activities of hydrogen consumers using either chemical agents (chloroform, extreme acids or alkali) or physical procedures (heat-shock, ultrasonication, irradiation, aeration) or a combination of both have been evaluated or reviewed (Cai *et al.*, 2004; Fan *et al.* 2004; Mu *et al.*, 2007; Kim and Shin, 2008; Ren *et al.*, 2008; Wang and Wan, 2008a; O-thong *et al.*, 2009; Chang *et al.*, 2011; 2008; Nathao *et al.* 2013; Saady, 2013; Wong *et al.*, 2014; Alemahdi *et al.*, 2015; Biswarup *et al.* 2016; Sattar *et al.*, 2016a, Liu *et al.*, 2020; Mockaitis *et al.*, 2020 and Yang *et al.*, 2020). Generally, the

Heat-shock condition ranged from 80 to 121°C with the duration of exposure between 15 and 120 mins in the literature (Mu *et al.*, 2007; Ren *et al.*, 2008 and Chang *et al.*, 2011). In addition, for acid and alkaline enrichment, the pre-treatment is done by subjecting the seeded sludge to extreme pH values; that is, for acid PT, the pH is adjusted to 2 – 4 while for base enrichment, the pH is altered to 11 – 12 (Cai *et al.*, 2004; Show *et al.*, 2007, Mu *et al.*, 2007 and Chang *et al.*, 2011). However, these traditional approaches are energy demanding, require high-cost overlay, especially in chemicals purchase, affect the synergistic interactions of sludge microbes, decimate some HPB and hydrolytic microorganisms' population and have related environmental issues (Zhu and Beland, 2006; Wong *et al.*, 2014 and Bundhoo and Mohee, 2016).

Research into less energy demanding and environmentally friendly options have been reported. For example, Chen and his colleague started hydrogen fermentation from untreated acclimatised sewage sludge using glucose and sucrose substrates (Chen and Lin, 2001). They obtained a hydrogen yield of 1.63 mol H<sub>2</sub>/ glucose when glucose was used as the substrate and a hydrogen yield of 4.45 mol H<sub>2</sub>/ sucrose when sucrose was employed as the feeder in less than 60 days of incubation. Nevertheless, the accumulation of volatile fatty acids, mainly acetic acid and butyric acid, from both sugar substrates and the use of soluble sugars for enrichment could have cost implicative. Kim *et al.* (2012) reported that untreated sludge at C/N ratio 25, hydrogen production was 33% higher than heat-treated, with a stable hydrogen content of 58% in their work on hydrogen production by anaerobic co-digestion of rice straw (RS) and sewage sludge. They adduced the reason for the low yield of hydrogen from heat-repressed sludge from inhibition of microbial community that could be involved in the decomposition of rice straw for bio-hydrogen production. The problem with this study is reduced utilisation of biomass brought from the recalcitrant nature of RS and low hydrogen yield (18 mL H<sub>2</sub>/g-added straw) that was reported as the maximal cumulative hydrogen yield (Kim *et al.*, 2012). Much recently, although the maximum hydrogen yield increased from 7.96 to 19.40 mL H<sub>2</sub>/gVS after waste activated sludge (WAS) was pre-treated by freezing in the presence of nitrite (Liu *et al.*, 2020); this approach

might be both cost and energy-intensive. Furthermore, the added nitrite could be easily converted to ammonia, affecting fermentation. Similarly, Yang *et al.* (2020) reported that a combination of  $\text{K}_2\text{FO}_4/\text{PH 9.5}$  could promote hydrogen yield from WAS. While it is true that potassium ferrate is non-polluting to the environment and an oxidant, the procedure can affect the total cost of the fermentation.

A more promising and green approach is proposed, which is novel to the best of the writer's knowledge. It entails the application of agro-industrial waste materials – potash extract (PE), cassava-steep wastewater (CSWW) and corn-steep liquor (CSTL) as alternative materials that can enrich the level of HPB and inhibits the population of HCB in digested cow slurry (DCS).

The PE contains some heavy metals (Udoetok *et al.*, 2012) that can be utilised to inhibit or slow down hydrogenotrophic microbes' activities in seeded sludge. More so, highly alkaline PE can enhance sludge solubilisation and create extreme alkaline conditions for HCB, while HPB will form spores and survive. Similarly, CSWW and CSTL are highly acidic due to the concentration of SCFA. The SCFA could also produce the same effects as pre-treatment with HCl on enriching HPB in seeded sludge. **Thus, in this research study, a) agro-industrial wastes were investigated as cheap and less energy-demanding techniques for enhancing HPB in DCS for maximum hydrogen production. In addition, b) Microbial community diversity after pre-treatments and acidogenic processes were also examined.**

## Graphical Introduction

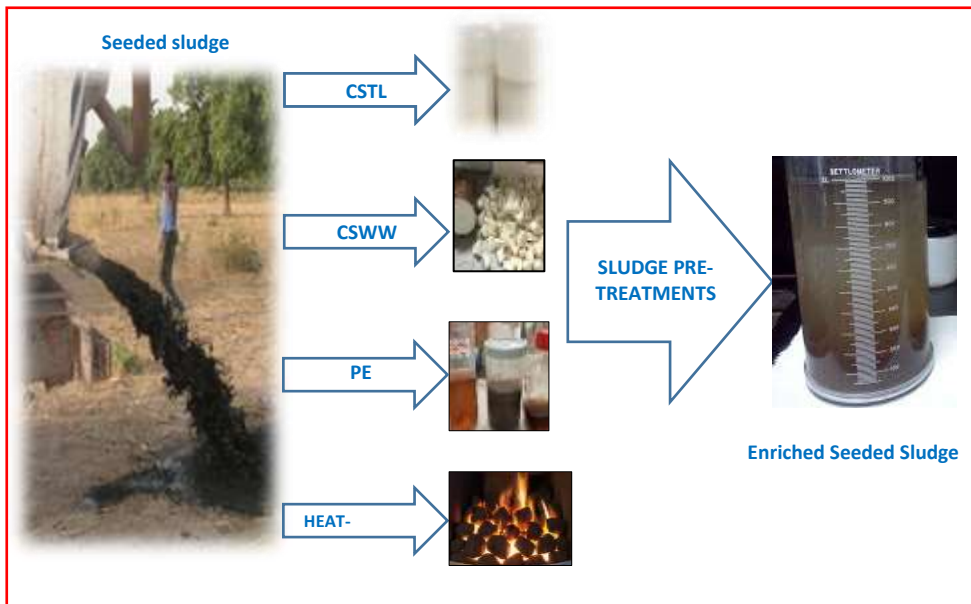


Fig 4-1: Pictorial representation of the enrichment of seeded sludge using agro-industrial wastes for biological hydrogen production.

## 4.2 Materials and Methods

### 4.2.1 Digested Cattle Slurry Pre-treatment for Bio-hydrogen Production

The DCS was sieved through a 2.0mm screen to filter out impurities and afterwards pre-treated to deactivate hydrogen consumers using the agro-industrial wastes (PE, CSTL, and CSWW) as pre-treatment agents. The pre-treatments were done by incubating the DCS at extreme pH values using each local waste. DCS enrichment using either CSTL or CSWW was performed by altering the DCS's pH with either CSTL or CSWW to  $3.53 \pm 3.0$  and incubating for 48 hours on a magnetic stirrer at 200 rpm. The CSTL/ CSWW PT DCS was acclimatised for a certain period (7 days). Before use, the pH adjusted to  $5.7 \pm 0.3$  using 5M NaOH.

Similarly, in the enrichment of DCS with PE, a revised O-Thong *et al.* (2009) revised protocol was employed - the DCS was adjusted to pH  $11.26 \pm 0.4$  with PE and then mixed at 200 rpm for 24 h. The PE-PT DCS was acclimatised for a month, and the pH was adjusted to pH  $5.7 \pm 0.2$  using 5M HCl before application. As a positive control and for comparison purposes, the traditional heat-shock process was also employed as defined in Chapter 3 Section 3.7.2.

Before the laboratory study, the pre-treated inocula were acclimatised using glucose or sucrose under stated laboratory conditions for 3 or 4 days, respectively, at pH 5.5 and a temperature of 55°C before solid characterization was done (Table 4-1) (See Chapter 3 Section 3.7.3).

Table 4-1: Characterisation of raw and pretreated digested cow slurry

Substrate	TS (g/mL)	TSS (g/mL)	VS (g/mL)	VSS (g/mL)	Ash (g/mL)	VS (%)	Ash (%)	NH <sub>4</sub> <sup>+</sup> -N (g/L)	Alkalinity (mg CaCO <sub>3</sub> L <sup>-1</sup> )	Moisture Content	SCOD (mg L <sup>-1</sup> )
DCS	0.095	0.069	0.073	0.052	0.022	77	23	0.30	4014.50	95.00	520.00
PE-PT DCS	0.045	0.036	0.030	0.021	0.015	67	33	0.19	3015.00	96.00	1760.00
CSTL-PT DCS	0.014	0.010	0.011	0.006	0.003	79	21	0.15	2030.00	97.10	1160.00
CSWW-PT DCS	0.010	0.008	0.010	0.007	0.000	100	0	0.16	2540.00	98.50	4680.00

#### **4.2.2 Experimental Design of the Hydrogen Fermentation Process**

The acidogenesis design and process were as outlined in Chapter 3 Section 3.8.1, and the incubation was done for 3.0 days when glucose was employed as the substrate and 4.0 days when sucrose was used as the medium. The digesters were labelled as CSTL, CSWW, PE-PT DCS and Heat-shocked DCS, reflecting their respective agents applied during DCS pretreatments, while the control reactors were identified as untreated DCS. The total biogas volumes produced by each borosilicate glass Duran bottles (BGDB) were measured daily, and the hydrogen concentration (%) was determined as described in Chapter 3, Section 3.9.

## 4.3 Results and Discussion

### 4.3.1 Seeded Sludge Characterisation

The physicochemical attributes of the seeded sludge employed in the study are characterised in Table 4-1. The carbon /nitrogen ratio of the seeded sludge was within the acceptable range of 5 – 200 (Kim *et al.*, 2012). The DCS pH was 8.56. After DCS pre-treatments, the elemental composition of PE and the various pretreated DCS sludge (Table 4-2).

Table 4-2: Elemental composition of potash extract and various digested cow slurry

Cations	PE (mg/L)	PE-PT DCS (mg/L)	CSTL-PT DCS (mg/L)	CSWW-PT DCS (mg/L)	Heat-shock DCS (mg/L)	Raw DCS (mg/L)
Calcium	1957.84	630.13	256.00	270.93	208.65	205.00
Magnesium	1246.41	670.48	223.39	179.77	206.88	200..18
Sodium	280.22	182.22	89.05	75.05	66.22	76.22
Potassium	8741.55	2919.35	607.31	639.39	375.08	365.88
Zinc	44.37	6.33	3.26	4.62	2.97	2.00
Nickel	0.49	0.27	0.23	0.24	0.20	0.20
Aluminium	513.89	115.34	27.19	20.36	21.95	15.87
Iron	913.08	427.56	149.96	147.77	131.37	135.13
Manganese	26.37	5.56	6.57	4.83	5.26	4.26
Copper	10.48	2.3	3.46	2.78	3.11	2.75
Silicon	41.32	14.75	1.3	1.70	1.21	1.00
Arsenic	0.36	0.21	0.21	0.21	1.10	0.56
Chromium	0.63	0.21	0.18	0.27	0.29	0.29
Lead	<0.05	<0.05	<0.05	<0.05	<0.05	<0.05
Strontium	13.19	3.07	3.87	4.34	3.74	2.89
Barium	0.70	0.28	0.41	0.39	0.47	0.50
Selenium	5.88	3.28	0.21	19.41	0.71	0.67
Anions						
Chloride	766.86	60	Na	Na	Na	Na
Nitrite	26.09	Na	Na	Na	Na	Na
Bromide	4.43	Na	Na	Na	Na	Na
Sulphur	274.90	98.48	25.88	21.71	27.09	25.00
Nitrate	2.50	Na	Na	Na	Na	Na
Phosphor	1.50	Na	Na	Na	Na	Na



It can be seen from Table 4-2 that pre-treating DCS with PE increased the concentration of metal ions, especially the earth metals, even the 30 day adaption period when compared with the distribution of ions from other PT DCS and raw DCS. This augmentation with earth metals, especially potassium, magnesium and calcium, will directly create unfavourable conditions for microorganisms' metabolic activities, especially the HCB. Also, PE pre-treatment ensures the growth of HCB is inhibited while HPB, though also affected by the increased levels of metal ions, will survive and form spores.

#### **4.3.2 Characterisation of Agro-Industrial Wastes**

The elemental concentrations (cations and anions) of PE in Table 4-2 shows that the earth metals - potassium (8.74 g/L), calcium (1.96.g/L), and magnesium (1.25 g/L) were the highest among the cations, while chloride (0.77 g/L) was the highest among the anions. These results were slightly consistent with the outcome reported by Udoetok *et al.* (2012) on potash extracts. It can be said based on the elemental composition of PE in Table 4-2 that it can be used as a buffer depending on the aims and circumstances. In the same vein, Table 3-2 illustrated the chemical attributes of CSWW and CSTL. In both samples, the pH was within 3.0 and 4.0, which is acidic. The acidity is due to organic acids that are predominantly acetic and butyric acid. In addition to this, both samples also have high chemical oxygen demand (COD) concentrations, mainly from carbohydrates or starch molecules.

#### **4.3.3 Effects of Pre-Treatments Technologies on Fermentative Hydrogen Production**

##### **4.3.3.1 Hydrogen production on glucose reactors**

After acclimatisation, the enriched seeded sludge, CSTL, CSWW and PE-PT DCS were tested for their capabilities to produce hydrogen using glucose or sucrose. Heat-pre-treatment at 100°C for 1.0 h was used as the control, and the following conventional method was applied. The hydrogen production using glucose or sucrose as substrates by various PT DCS is illustrated in Fig 4-2 and 4-3. Whereas the hydrogen production profile was modelled from the Gompertz equation and presented in Table 4-3, the figures showed hydrogen production activities from all the samples, including the positive control,

the seeded sludge without pre-treatment. Similarly, the R-square value of 0.999 indicated that the fermentation processes were stable and efficient (Table 4-3) in all the reactors.

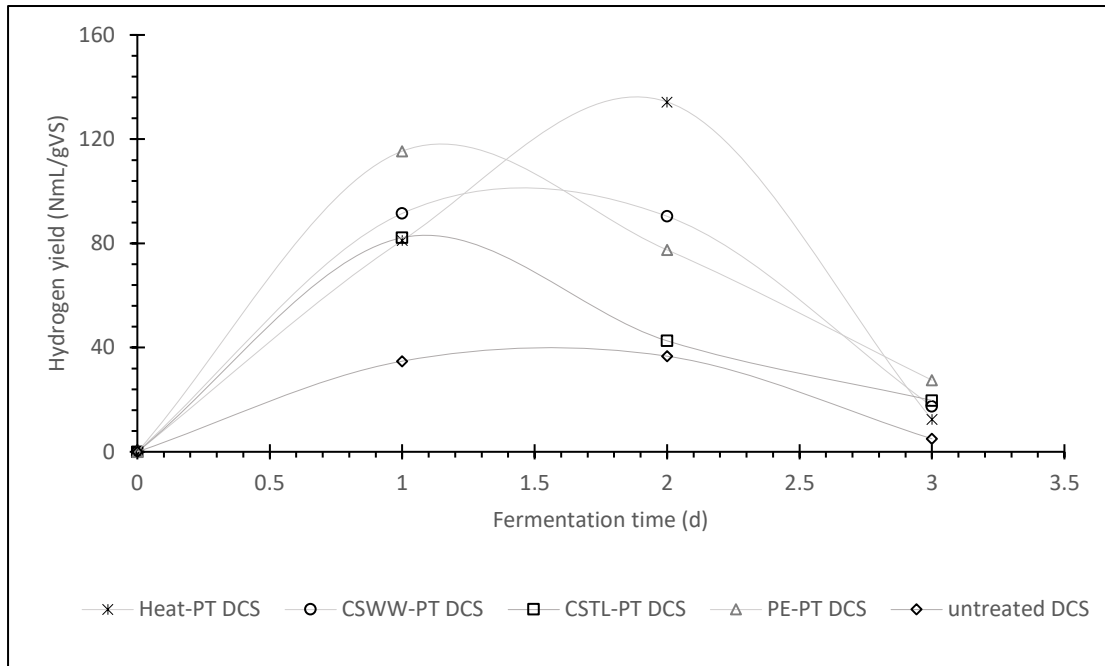


Fig 4-2: Hydrogen production using glucose as substrates by various PT DCS

However, the results showed that the cumulative and the hydrogen production rate from the various PT DCS was far higher than that of the untreated DCS sludge using glucose (Fig 4-2) and sucrose (Fig 4-3) substrates, which tallies with Wang and Wan (2008a) findings. The high hydrogen production indicated that these pre-treatments could inhibit HCB while preserving the activities of HPB in DCS, unlike untreated DCS, where the volume of daily hydrogen production and accumulation is reduced. The variation in volumetric hydrogen production (VHP) is due to the utilisation of molecular hydrogen for energy by HCB (Li and Fang, 2007). When glucose was the medium, the Heat-shocked DCS produced the most daily hydrogen of  $135 \text{ NmL H}_2 \text{ g}^{-1} \text{ VS}$  on the second day compared to other PT DCS, followed by PE-PT DCS, which gave the highest daily hydrogen of  $115 \text{ NmL H}_2 \text{ g}^{-1} \text{ VS}$  within 24 h (Fig 4-2). The Heat-shock DCS reactor also had the highest hydrogen accumulation of  $229 \text{ NmL H}_2 \text{ g}^{-1} \text{ VS}$ , followed by PE-PT DCS digester, which has  $222 \text{ NmL H}_2 \text{ g}^{-1} \text{ VS}$  as the volumetric hydrogen yield (VHY) (Table 4-3). In contrast, other PT DCS (CSWW and CSTL-PT) and untreated DCS (control) gave 202, 143

and 77 NmL H<sub>2</sub> g<sup>-1</sup> VS as the VHY, respectively. These findings also agreed with Wang and Wan (2008a) and Mu *et al.* (2007). They demonstrated that the hydrogen yield from the Heat-shocked seeded sludge was the highest among all the tested samples in their study. Nevertheless, agro-industrial PT DCS have shortened lag phases from 0.2 (5.0 h) to 0.4 (10 h) days (Table 4-3) when compared to the Heat-shocked DCS (Fig 4-2) when glucose is used as the medium. The high hydrogen production and the shortened lag phases, mainly PE-PT DCS, could be due to trace elements in PE-PT DCS (especially potassium, iron, manganese, cobalt, copper, zinc chromium, and barium) favouring acidogenesis, hence, more evolution of hydrogen gas (He *et al.*, 2018). The high accumulation of ions in the PE extracts can act as a soluble buffer, thereby maintaining the effects of total volatile fatty acids (TVFA) in the fermentation medium, ensuring the traditional function of fermentative microbial metabolism (Lin and Lay, 2004 and Elbeshbishy *et al.*, 2017). In the same vein, the presence of soluble monosaccharides and other organic constituents in CSWW and CSTL-PT DCS can act as start-up substrates for fermentative hydrogen and other biochemical productions such as bio-alcohols, organic acids production by HPB and HCB (Escaramboni *et al.*, 2018 and Chen *et al.*, 2020). On the other hand, the extended lag phase from heat-repressed sludge could be from the inhibition of some microbial communities involved in the start-up of the hydrogen production process (Kim *et al.*, 2012).

Table 4-3: Kinetic parameters of hydrogen production from various PT DCS

PT DCS	Gompertz Data							
	$P$ (NmL H <sub>2</sub> g <sup>-1</sup> VS)		$\lambda$ (d)		$R_m$ (mL d <sup>-1</sup> )		R-Square	
	Glucose	Sucrose	Glucose	Sucrose	Glucose	Sucrose	Glucose	Sucrose
Heat	229	374	0.7	0.7	240	223	0.999	0.999
PE	222	349	0.2	0.7	144	268	0.998	0.999
CSWW	202	287	0.4	0.5	151	142	0.999	0.999
CSTL	143	283	0.2	0.8	97	226	0.998	0.999
Untreated	77	185	0.5	0.7	67	108	0.999	0.999

Furthermore, the shortened lag phase also recorded in untreated DCS (Table 4-3) could be due to microbial consortia that perform better in hydrogen fermentation in terms of adaptation and

tolerance to sudden changes in the environment and nutrient shocks (Brener *et al.*, 2008). Like agro-industrial pre-treated DCS, this mixed seeded sludge might share the same physiological benefits as Heat-shocked DCS (Kim *et al.*, 2012). Even so, hydrogen is rapidly consumed by HCB in untreated sludge for energy in metabolic activities (Li and Fang, 2007). Additionally, HCB in untreated sludge could alter hydrogen production's biochemical pathway to short-chain fatty acids (SCFA), solvent, and alcohol production, thereby reducing net bio-hydrogen yield (Guo *et al.*, 2010; Saady, 2013 and Bundhoo and Mohee, 2016). This alteration of metabolism is confirmed by the highest daily VHP of 37 NmL H<sub>2</sub> g<sup>-1</sup> VS by the untreated DCS sample produced on the second day (Fig 4-2) and the microbial community composition (Fig 4-6). Other PT DCS (CSWW-PT DCS and CSTL-PT DCS) had lower daily VHP of 92 and 82 NmL H<sub>2</sub> g<sup>-1</sup> VS, respectively, when compared to Heat-shock and PE-PT DCS (Fig 4-2)

Using the kinetic parameters derived from Gompertz Eqn (3-9) (Table 4-3), the maximum hydrogen production rate of 240 mL/d was obtained from Heat-shocked DCS digester, followed by CSWW-PT DCS (151 mL d<sup>-1</sup>), PE-PT DCS (144 mL d<sup>-1</sup>), and CSTL-PT DCS (144 mL d<sup>-1</sup>) when glucose was used as the energy source. The least hydrogen production rate of 67 mL d<sup>-1</sup> was observed from untreated DCS. These results differ from the outcomes attained by Chang *et al.* (2011). They obtained a maximum hydrogen rate of (21.02 mL h<sup>-1</sup> (504.48 mL d<sup>-1</sup>) from Heat-shocked sludge. The difference could be from the mode of heat treatment of sludge, source of activated sludge applied, and gas measurement time. While Chang and co experiment was monitored hourly, gases from this study were measured daily for four days.

#### 4.3.3.2 Hydrogen production on sucrose digesters

The result of hydrogen production using sucrose as the carbon source was different from fermentation with glucose as a medium (Fig 4-3). The lag phase attained when sucrose was employed as the medium was almost the same in all the PT DCS digesters except for CSWW-PT DCS (Table 4-3). This development is contrary to the lag phase when glucose was used as the substrates and can be

explained by the different solubility rates of the two carbohydrates in the reactor. The highest daily hydrogen production peaks were recorded in all laboratory reactors on the second day, with the highest peak of 211 NmL H<sub>2</sub> g<sup>-1</sup> VS recorded at the PE-PT DCS reactor (Fig 4-3). The subsequent highest hydrogen production peak was obtained from a Heat-shocked DCS sample with 199 NmL H<sub>2</sub> g<sup>-1</sup> VS as the highest peak value reflecting the daily hydrogen production. The values of 185 and 131 NmL H<sub>2</sub> g<sup>-1</sup> VS were obtained as the highest daily hydrogen productions for CSTL-PT and CSWW-PT DCS samples, while for untreated DCS, 97 NmL H<sub>2</sub> g<sup>-1</sup> VS was produced as the highest daily hydrogen production value.

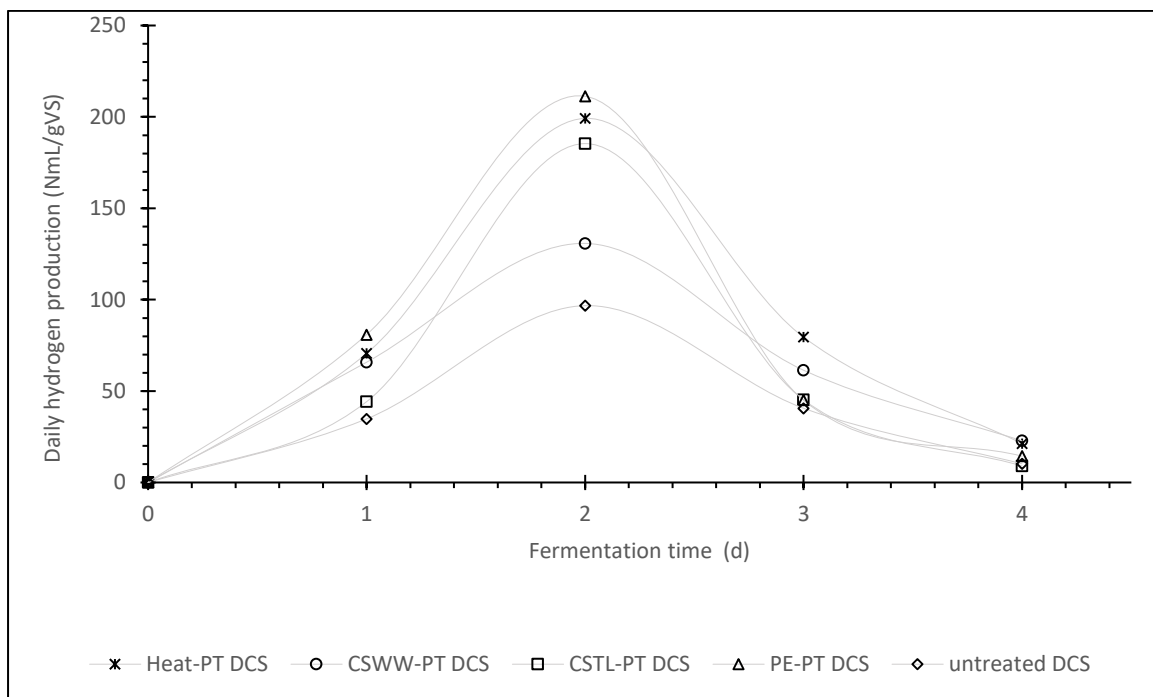


Fig 4-3: Hydrogen production using sucrose as substrates by different PT DCS

In contrast, the highest hydrogen accumulation of 374 NmL H<sub>2</sub> g<sup>-1</sup> VS was achieved from the Heat-shocked DCS reactor, followed by PE-PT DCS reactor digester, which had 349 NmL H<sub>2</sub> g<sup>-1</sup> VS as the VHY compared CSWW, CSTL-PT and untreated DCS. The other PT DCS and control gave 287, 283 and 185 NmL H<sub>2</sub> g<sup>-1</sup> VS as the VHY, respectively (Table 4-3). The result obtained agreed with the review of Ren *et al.* (2008) and studies of Fan *et al.* (2004), Nathao *et al.* (2013), and Biswarup *et al.* (2016) on Heat-shock processes for seeded sludge enrichment.

The mechanism or strategy for PE on sludge enrichment is not fully understood. However, it is believed that suppression could be from the extreme alkaline condition of the PE and the presence of earth and trace metals, particularly potassium and calcium. The alkaline state could accelerate sludge solubilisation and inhibition of methanogenesis and other HCB (Cai *et al.*, 2004; Zhang *et al.*, 2018 and Yang *et al.*, 2020). Furthermore, the presence of these earth metals (Table 3-2) could lead to the formation of earthy salts such as potassium ferrate that can lyse the microbial cells of HCB, causing the release of essential nutrients required for metabolism and hydrogen fermentation (He *et al.*, 2018 and Yang *et al.*, 2020). More so, PE contains trace elements that support acidogenesis (He *et al.*, 2018.) and hydrogen fermentation processes. The element "iron" is of great focus as it is essential in anaerobic fermentation for hydrogen production (Hawkes *et al.*, 2002). The hydrogenase enzyme responsible for hydrogen evolution from sugar monomer requires reduced ferredoxin to be oxidised, and this compound is usually Fe<sup>2+</sup>complexed (Kapdan and Kargi, 2006). In the same vein, the iron-sulfur protein - ferredoxin (Fd) is involved in (1) pyruvate oxidation to acetyl-CoA and CO<sub>2</sub> under the PFOR pathway in DF processes for H<sub>2</sub> production, (2) acts as an electron carrier, (3) in proton reduction to molecular hydrogen in anaerobic fermentative hydrogen production where they assist in the formation of hydrogenase and (4) reduction of inhibition due to sulphide (Lee *et al.*, 2001 and Bao *et al.*, 2013). Potassium ions in high PE concentration could also complement the proton and K<sup>+</sup> deficiency caused by increased free ammonia levels (Kayhanian, 1999 and Drog, 2013). Thus, the hydrogen fermentation process is stabilised. The presence of these earth metals in PE also has flocculation abilities paramount for formations of biological linkages at cellular levels, separation and disintegration at sludge levels, and oxidation of organic compounds (Morgan *et al.*, 1991; Sharma *et al.*, 2015; He *et al.*, 2018 and Yang *et al.*, 2020). These physiological activities are essential for AD processes.

The result of the hydrogen production rate affirmed the outcome of Heat-shocked DCS digester as the highest daily hydrogen producer when glucose was the substrates and the result of PE-PT DCS digester

as the highest daily hydrogen producer when sucrose was used as the carbon source (Table 4-3). The highest maximum hydrogen production rate of 268 mL/d was observed from the PE-PT DCS digester, followed by CSTL-PT DCS (226 mL d<sup>-1</sup>), Heat-shock DCS (223 mL d<sup>-1</sup>), and CSSW-PT DCS (142 mL d<sup>-1</sup>). Untreated DCS gave the least hydrogen production rate of 108 mL d<sup>-1</sup>. The disparities in the reactor samples in terms of hydrogen yield, daily hydrogen production, and hydrogen production rate when either of the substrates was employed as the medium could not be explained, but it is presumed that glucose is more metabolised easily than sucrose, which is also confirmed from the degradation profiles (Fig 4-2 and 4-3). Therefore, heat-shocked HPB is much more reactivated under glucose medium than sucrose, favouring PE-PT DCS owing to the presence of trace elements (Table 4-2) (He *et al.*, 2018).

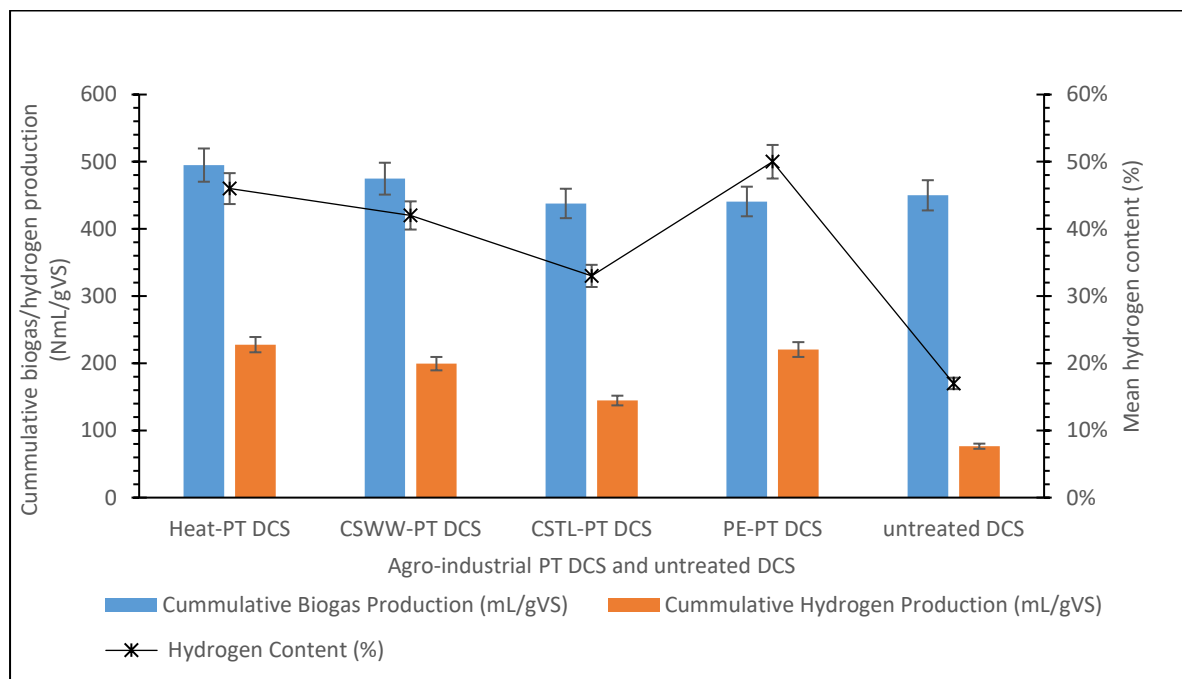


Fig 4-4: Biogas/hydrogen yield and average hydrogen content of the various DCS from glucose

#### 4.3.3.3 Biogas/hydrogen yield and average hydrogen content of the reactor samples

The result of the biogas/hydrogen yield and average hydrogen content of the various DCS from glucose (Fig 4-4) and sucrose (Fig 4-5) is presented herein. At a mean hydrogen content of 46%, the Heat-shocked DCS produced the highest biogas and hydrogen accumulation of 494 NmL g<sup>-1</sup> VS and 228 NmL H<sub>2</sub> g<sup>-1</sup> VS correspondingly when glucose was employed as substrates (Fig 4-4). Similarly, when sucrose

was the carbon source, Heat-shocked DCS, at average hydrogen content of 55%, produced the highest biogas and hydrogen accumulation of 674 NmL g<sup>-1</sup> VS and 371 NmL H<sub>2</sub> g<sup>-1</sup> VS, respectively (Fig 4-5). Nonetheless, the PE-PT DCS with an average hydrogen content of 52% had the highest biogas accumulation of 676 NmL g<sup>-1</sup> VS in all the enriched samples (Fig 4-5) when sucrose was used as the substrates. The VHY of 220 and 352 NmL H<sub>2</sub> g<sup>-1</sup> VS of glucose and sucrose, respectively, from PE-DCS reactors, were comparably close with Heat-shock DCS outcomes. Untreated DCS had the most negligible cumulative hydrogen production (77 and 182 NmL H<sub>2</sub>g<sup>-1</sup>VS) and the mean hydrogen content (17 and 28%) when glucose and sucrose were applied as carbon sources, respectively (Fig 4-4 and 4-5).

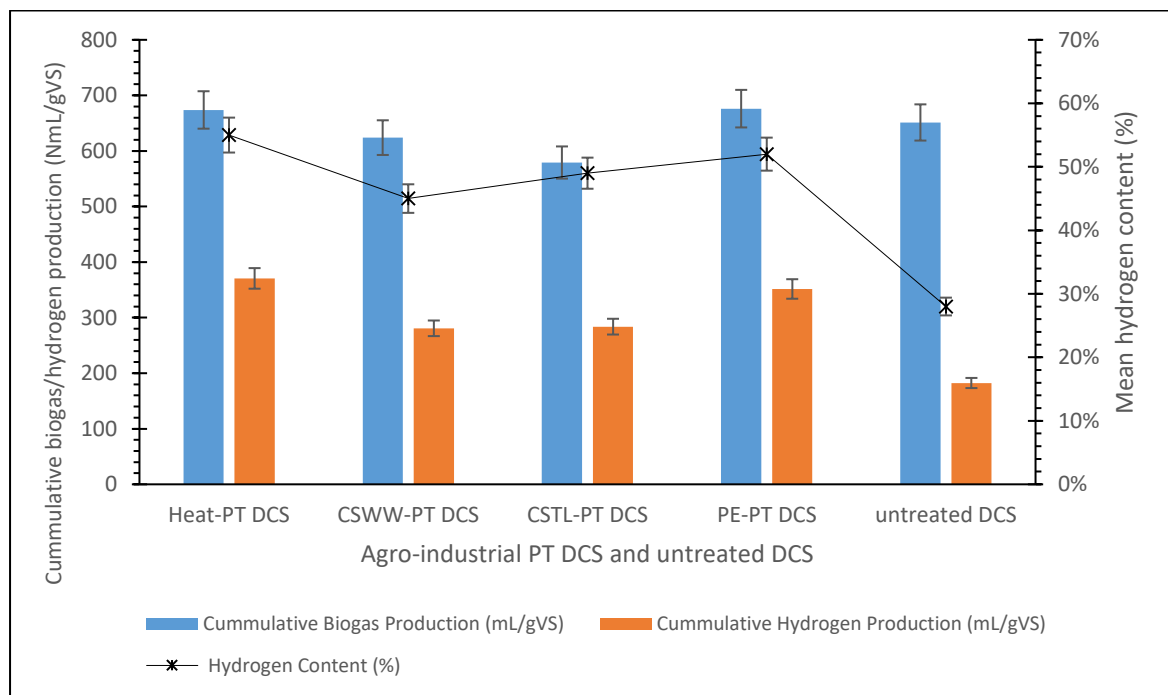


Fig 4-5: Biogas/hydrogen yield and average hydrogen content of the various DCS from Sucrose

While CSWW-PT DCS digester with mean hydrogen content (42%) produced 199 NmL H<sub>2</sub> g<sup>-1</sup> VS as the cumulative hydrogen yield, the CSTL-PT DCS digester, which has mean hydrogen content (33%), generated the hydrogen yield of 145 NmL H<sub>2</sub> g<sup>-1</sup> VS when glucose was the medium (Fig 4-4). On the other hand, in sucrose reactors, CSTL-PT DCS samples had a little higher hydrogen content (49%) and hydrogen yield of 284 NmL H<sub>2</sub> g<sup>-1</sup> VS than CSSW-PT DCS samples, which had mean hydrogen content



(45%) and hydrogen yield of 281 NmL H<sub>2</sub> g<sup>-1</sup> VS (Fig 4-5). Compared to heat-shocked DCS, the hydrogen yield and the average hydrogen content of other agro-industrial PT DCS were lower in glucose and sucrose fed reactors (Fig 4-4 and 4-5). However, the biogas yield from all the pre-treated DCS and the untreated except CSTL-PT DCS using sucrose as a medium was approximately within the same range for glucose and sucrose systems.

The close volumetric biogas production of agro-industrial PT DCS with Heat-PT DCS shows that the fermentation process was excellent and stable despite disparities in hydrogen content values and hydrogen yield (Fig 4-4 and 4-5). The lower biogas yield obtained from CSTL-PT DCS digesters could be from liberated hydrogen consumption, where molecular hydrogen could serve as an energy source for some HCB (Li and Fang, 2007). This argument is also confirmed from the low mean hydrogen content achieved from some agro-industrial PT DCS and shifting fermentation pathways following lactic and solvent production (Table 4-4) (Coelho *et al.*, 2010). Furthermore, it is believed that the mechanisms of action for CSWW and CSTL-PTs which are 1) suppressing microbes with weak acids, mainly acetic acids, and 2) from nutrient shock due to the presence of carbohydrates, and as such, there will be more evolution of VFA (Table 4-4) will lead to the production of more biogas. Thus, CSWW and CSTL can create an unfavourable environment for acidogenic microorganisms. However, HCB can survive and further alter the acidogenic pathway. In affirmation of this perspective, Saady (2013) reported that HCB in seeded sludge could rival HPB for nutrients, and HCB can alter the biochemical pathways, thereby reducing net hydrogen yield and production of unwanted products. On the other hand, Heat-shocked and PE-PT DCS could produce higher mean hydrogen content because the various pre-treatments could repress HCB, while HPB survives the harsh treatments.

#### **4.3.4 Total Volatile Fatty Acids Production from various Digested Cow Slurry**

Typically, bio-hydrogen is produced during the acidogenic stage in an AD process (Chang *et al.*, 2011 and Bundhoo *et al.*, 2015) together with SCFA and CO<sub>2</sub>. The hydrogen production rate was also affirmed by producing various VFA (Table 4-4). Thus, TVFA concentration from the different PT DCS

reactors is a valuable indicator for monitoring hydrogen fermentation. Table 4-4 illustrates the distribution of associated VFA concentrations from DCS samples. It can be seen from the table that there was increased production of VFA in CSWW-PT DCS and PE-DCS, which could be due to more carbohydrate compounds in CSWW, which were degrading either during acclimatisation or along with the added substrates.

On the other hand, the metallic ions content in PE (Table 4-2) could have influenced the accumulation of VFA in PE-PT DCS. Whereas acetic and butyric acid accounted for the most soluble fermentation products, butyrate was almost twice the acetate amount in the fermentation products for glucose and sucrose. The more butyrate concentration shows that the fermentation process was primarily due to the butyric-acid type pathway (Mu *et al.*, 2007 and Chang *et al.*, 2011). Although the result was consistent with findings for acids and base pre-treatments by Mu *et al.* (2007) and Li *et al.* (2007), the established pathway was different for various methods applied by Ren *et al.* (2008), where acetate-type fermentation pathway was recorded to be the most dominant in all samples.

Table 4-4: The distribution of associated VFA concentrations from DCS samples

Sludge Enrichments	Acetic (mg/L)		Butyric (mg/L)		Formic (mg/L)		Lactic acid (mg/L)	
	Glucose	Sucrose	Glucose	Sucrose	Glucose	Sucrose	Glucose	Sucrose
Heat-shock DCS	520.00	698.57	748.68	969.72	2.85	2.83	Na	Na
CSTL-PT DCS	788.90	988.60	1061.34	1241.34	Na	105.70	180	340
CSWW-PT DCS	848.80	1048.80	2567.01	2707.01	Na	101.50	185	350
PE-PT DCS	722.03	992.04	1149.15	1249.15	Na	40	90	150
Untreated DCS	435.80	546.70	578.90	795.00	Na	60	Na	25
Raw DCS (cont.)	320.15		205.00		Na		Na	

The production of formate was insignificant in glucose samples. However, when sucrose was applied as a carbon source, there was a minimal concentration of formic acids, with CSTL and CSWW having about 102 – 106 mg/L levels indicating a continuous hydrogen fermentation process from dissolved but complex carbohydrates molecules contained in CSTL and CSWW-PT DCS.

Furthermore, the gradual increase in the formation of lactate in both the glucose and sucrose reactors (especially from CSTL-PT and CSWW-PT DCS) (Table 4-4), which is in agreement with the findings of O-Thong *et al.* (2011), could either be from a) the consumption of liberated hydrogen and alteration of hydrogen fermentative pathways by HCB especially methanogens or b) nutrient shock (Coelho *et al.*, 2010; Saady, 2013 and Elbeshbishy *et al.* 2017). This argument is confirmed by the relative abundance of the most dominant microbial community at genus and phylum level (Fig 4-6), where the most principle genus *Ruminococcus* products (H<sub>2</sub>, acetate, and CO<sub>2</sub>) are easily used as substrates for methanogens.

Additionally, lactic acid bacteria (LAB) are known for their anti-microbial activities, which are inhibitory to HPB (Lee *et al.*, 2013, Sikora *et al.*, 2013 and Gomes *et al.*, 2015) and affect the yield of hydrogen production. Therefore, the change of fermentative medium pH caused by the produced lactic acid and anti-microbial products such as hydrogen peroxide and polypeptide antibiotics (bacteriocins) can inhibit hydrogen fermentation pathways.

#### **4.3.5 Microbial Community Composition**

The microbial diversity after the fermentation process was investigated with the bacteria community's relative abundance and taxonomic distribution in each sample analysed at the genus and phylum levels (Fig 4-6). It can be seen from the graph that a total of 25 phyla across all samples were identified, with 24 phyla classified and 1 unclassified. *Firmicutes* were the most dominant phylum accounting for ~70 to 100% in the pretreated samples, followed by *Actinobacteria* (~1 to 15%), *Chloroflexi* (~1 to 5%), *Proteobacteria* (~1 to 4%) and *Bacteroidetes* (~1 to 3%). Heat-shocked DCS also contains *Planctomycetes* (~1%). In addition, PE-PT DCS digestates had *Thermotogae* (3.5%), which produces hydrogen, acetate and CO<sub>2</sub> from sugar. *Thermotogae* produces sulphide in the presence of sulphur compounds or hydrogenotrophic sulphate-reducers such as *Desulfovibrio Vulgaris* (An *et al.*, 2020b). This argument is definite as PE contains varying amounts of sulphur (Table 4-2). While most of the mentioned phylum are well-known hydrogen producers from simple to complex substrates producing

varying fatty acids, *Planctomyces* and *Chloroflexi* are known for degrading organic matter, especially ammonia (Suominen *et al.*, 2021). The high population of *Firmicutes* across pretreated samples compared to the control could be from the impacts of the DCS pre-treatments, which enriched the hydrogen producers and eliminated the activities of hydrogen consumers before submissions to acidogenic fermentation.

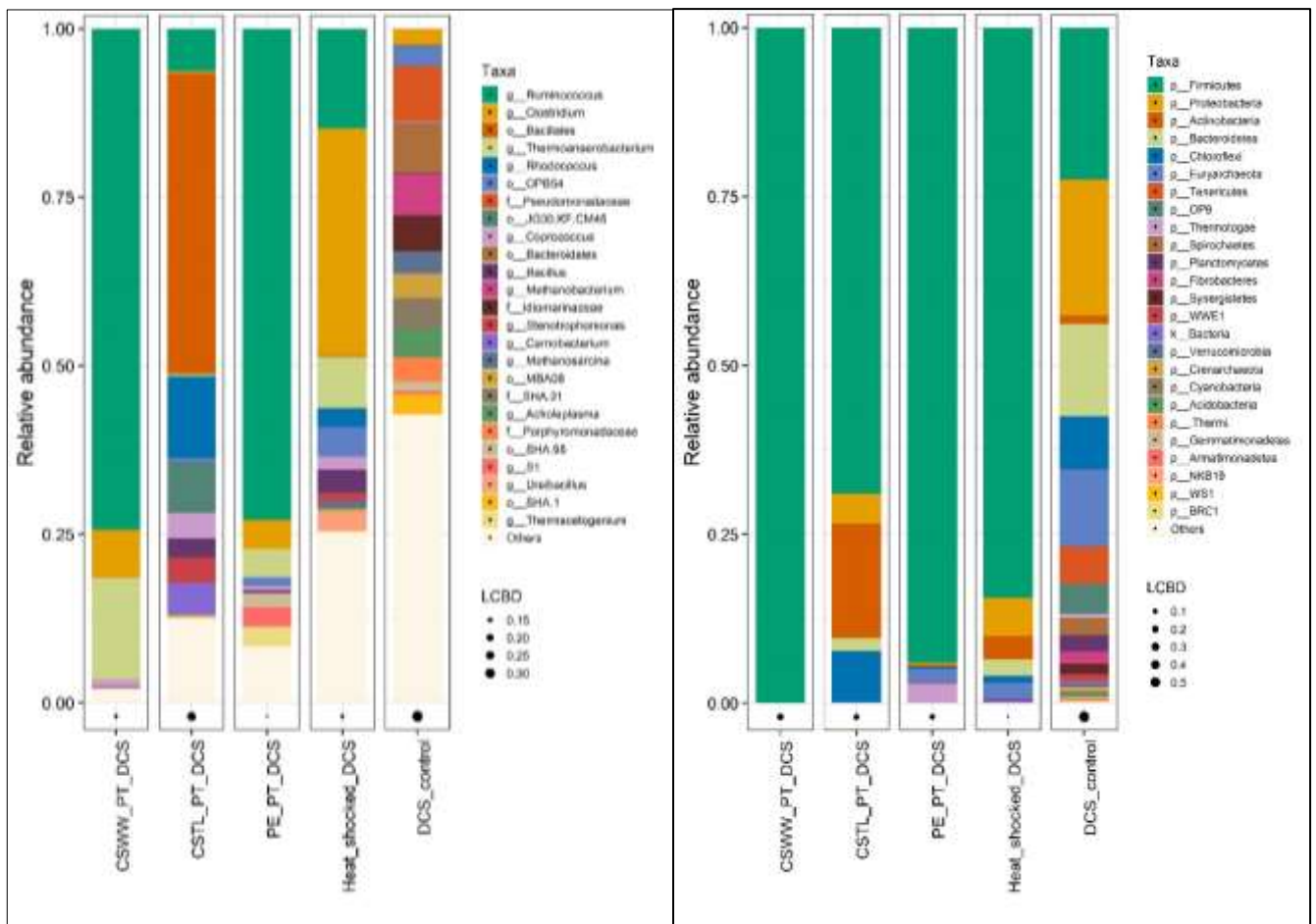


Figure 4-6: The relative abundance of the top 25 most abundant microbial communities at the genus and phylum level of pretreated DCS samples. While the bars correspond to taxa that are most dominant within the sample, the black points whose diameter relate to the magnitude of the LCBD value of the digestates that is higher LCBD mean the sample has more unique species than others.

In contrast, the control DCS sample had *Firmicutes* (~20%) and *Actinobacteria* (~20%) as the most principle phylum, followed by *Bacteroidetes* (~12%), *Euryarchaeota* (~10%), *Chloroflexi* (~5%), *Actinobacteria* (~4%), *Spirochaetes* (~2.5%), *Planctomyces* (~2%), *Fibrobacteres* (~2%) and others (~1

to 1.5%). The uneven distribution in microbial composition in the control samples compared to pretreated samples affirmed the effectiveness of DCS pre-treatment in the hydrogen fermentation process. Furthermore, the high inhabitants of HCB observed in the microbial configuration in the DCS control digestates confirmed the reason untreated DCS produce lower hydrogen yield than DCS enriched either by physical or chemical methods.

The enriched DCS samples' microbial community was dominated by *Ruminococcus*, *Bacillales*, *Clostridium*, *Thermoanaerobacterium* and *Rhodococcus* at the genus level. Other notable genera were *Bacillus* and *Coprococcus* (Fig 4-6). The identified genera were reported among the HPB by Shin *et al.* (2004), Kapdan and Kargi (2006) and Li and Fang (2007). While the optimal growth temperature of the reported organisms were mesophiles and thermophiles, *Thermoanaerobacterium* is a strict hyperthermophilic bacteria, which, though it thrives better at a temperature above 70°C, have adapted to the operating temperature of 55°C.

In contrast, *Bacillales*, *Bacteroidales*, *Methanobacterium*, *Idiomarinaceae*, *Acholeplasma*, *Methanosarcina*, *Clostridium*, *Thermoacetogenium* and *Carnobacterium* were among the most dominant communities in control DCS digestates.

The genera *Ruminococcus* and *Coprococcus* found in the mammalian gut can degrade recalcitrant substrates producing varying SCFA (Biddle *et al.*, 2013). The organisms, notably *Ruminococcus*, also played a role in cellulose and cellobiose degradation to hydrogen, acetic acid and CO<sub>2</sub>, providing direct soluble substrates for methane production (An *et al.*, 2020b). This idea explained why CSWW-PT reactors, populated by HPB (Fig 4-6), still produced low hydrogen yield than PE and Heat-shocked DCS. Many thermophilic *Clostridium* grows optimally at 55 to 65°C and can degrade a broad complex of carbohydrates such as cellulose, hemicellulose and xylans producing hydrogen and SCFA (Liczbinski and Borowski, 2021). The most popular *Clostridium* is *C. buytricum*, *C. thermolacticum*, *C. pasteurianum*, *C. paraputrificum* M-21 and *C. bifermentans* (Kapdan and Kargi, 2006).

Additionally, the order *Bacillales* that *Geobacillus* and *Thermobacillus* represent are facultative endospore-forming bacteria that can degrade lignocellulose under aerobic and anaerobic conditions employing highly thermostable enzymes such as  $\alpha$ -amylase and  $\beta$ -xylosidase (Liczbinski and Borowski, 2021). Another most dominant genus, *Thermoanaerobacterium*, can utilize complex substrates such as xylan, starch, cellulose, hemicellulose and its degraded products and transform them to acetic acids, hydrogen and CO<sub>2</sub> at an optimal temperature of 65 to 70 °C (Lusk *et al.*, 2018 and Liczbinski and Borowski, 2021). This knowledge explains why *Thermoanaerobacterium* was the second most abundant genus in CSWW-PT DCS. The CSWW employed in the DCS pretreatment has a high amount of COD, mainly of starch related compounds (Table 3-2). More so, even though there was no alcohol detection in all the reactors, it has been reported that *Thermoanaerobacterium* may contribute to ethanol production during AD processes (An *et al.*, 2018). The genus *Rhodococcus* which belongs to the family *Nocardiaceae* and phylum *Actinobacteria* is widely used to produce bioactive compounds such as antibiotics, anticancer drugs and immunosuppressive agents from polypeptides, alkaloids and fatty acids (Elsayed *et al.*, 2017). The production of these bioactive compounds, it is believed, come with the generation of hydrogen, and as such, *Rhodococcus* is an active HPB, although the level of hydrogen liberated from substrates may not be as high as those produced from more popular HPB. The genus *Bacillus*, which also belong to the phylum *Firmicutes* is known to produce hydrogen and fatty acids from the consumption of a wide variety of substrates in aerobic conditions (Kapdan and Kargi, 2006; Li and Fang, 2007 and Patel *et al.*, 2017).

The genus *Ruminococcus* was the most principle bacteria in CSWW (~75%) and PE-PT DCS (~73%) (Fig 4-6). On the other hand, *Bacillales* (~45%) and *Clostridium* (~35%) were the predominant genera in CSTL-PT and Heat-shocked DCS, respectively. Their various pre-treatments could explain the differences in the most abundant bacteria across the enriched samples. In CSWW and PE enrichments, the *Ruminococcus* is popular in the stomach of rumen animals, and thus the digested cattle slurry strived better when enriched with CSWW and PE. In contrast, in Heat-shocked DCS, the genus

*Clostridium* was able to survive better the heat treatment applied while the HCB, as seen in DCS control samples and other HPB, were eliminated, inactivated or reduced in population. Even so, there was no unequivocal explanation on the increased dominance of *Bacillales* in CSTL-PT DCS; they may have been favoured more than the other HPB during CSTL DCS enrichment processes due to the presence of assimilable and soluble substrates.

#### 4.4 Conclusion

The effectiveness of applying agro-industrial waste materials as alternative materials that can enrich the level of HPB and inhibits the population of HCB in DCS was examined. Based on the result obtained, it is concluded that agro-industrial waste materials can enrich HBP in DCS. Although Heat-shock DCS produced the highest daily VHP of 135 NmL H<sub>2</sub> g<sup>-1</sup> VS on the second day when compared to other PT DCS using glucose as substrates, it is followed by PE-PT DCS, which gave the highest daily VHP of 115 NmL H<sub>2</sub> g<sup>-1</sup> VS but at a shorter time (24 h). The other PT DCS - CSWW-PT DCS and CSTL-PT DCS had lower daily VHP of 92 and 82 NmL H<sub>2</sub> g<sup>-1</sup> VS, in that order, while the untreated DCS had 37 NmL H<sub>2</sub> g<sup>-1</sup> VS as its highest daily VHP.

Similarly, when sucrose was the medium, the highest peaks were recorded in all the laboratory reactors on the second day, with the highest daily VHP of 211 NmL H<sub>2</sub> g<sup>-1</sup> VS achieved at the PE-PT DCS digesters. This outcome is followed by Heat-shock DCS samples with 199 NmL H<sub>2</sub> g<sup>-1</sup> VS as the highest daily VHP. The 185 and 131 NmL H<sub>2</sub> g<sup>-1</sup> VS values were obtained as the highest daily VHP for CSTL-PT and CSWW-PT DCS samples, respectively, while for untreated DCS, 97 NmL H<sub>2</sub> g<sup>-1</sup> VS was produced as the highest daily VHP.

In relation to hydrogen accumulation, the Heat-shock DCS produced the highest VHY of 229 NmL H<sub>2</sub> g<sup>-1</sup> VS when glucose was employed as substrates and 374 NmL H<sub>2</sub> g<sup>-1</sup> VS when sucrose was used as the carbon source. PE-PT DCS digesters produced almost the same effects as Heat-shock DCS. They gave hydrogen accumulation of 220 NmL H<sub>2</sub> g<sup>-1</sup> VS for glucose and 352 NmL H<sub>2</sub> g<sup>-1</sup> VS for sucrose digesters. In contrast, there was much variation from the other agro-industrial PT DCS about the hydrogen yield from both substrates even though the biogas accumulation from all the pre-treated DCS and the untreated (except for CSTL-PT DCS with sucrose as the medium) were almost within the same range for both feeding systems.

The mechanism of PE, CSTL, and CSWW on sludge enrichment is not fully understood. However, it is believed that suppression of PE could be from the extreme alkaline condition of the PE and the presence of earth and trace elements, particularly potassium, magnesium, calcium, and iron. In the



same vein, the strategy of microbial inhibition from CSWW and CSTL-PTs could be from the high concentration of SCFA and nutrient shock. Whereas acetic and butyric acid accounted for the most soluble fermentation products, butyrate was almost twice the acetate fermentation products for glucose and sucrose, which shows that the fermentation process was mainly due to the butyric-acid type pathway.

Finally, after the various DCS PT studies, the dominant phylum *Firmicutes* represented by the *Clostridium* and *Ruminococcus* were the most abundant bacteria compared to the untreated DCS (control), which was diverse.



## Chapter 5 Biological hydrogen production from unhydrolysed raw rice straw co-digested with digested cattle slurry

### 5.1 Introduction

The high cellulose and hemicellulose content of rice straw (RS) that can be easily fermentable sugars, its' readily and globally availability, inexpensiveness and composition of essential microelements makes RS potential feedstock for hydrogen (Wattanasiriwech *et al.*, 2010; Guzman *et al.*, 2015, Biswarup *et al.*, 2016, Thao *et al.*, 2019 and Dong *et al.*, 2020). Nonetheless, the biological hydrogen production via dark fermentation (DF) technology is affected, among other factors, by the complex, recalcitrant and lignified nature of RS, which has restricted its hydrolysis and prevents the easy accessibility of fermentable sugars by HPB (Lynd *et al.*, 2005 and Zhang *et al.*, 2020). So, there is a need to detach the cellulose and hemicellulose from lignin first and re-align the ultrastructural components to increase the surface area for effective solubilisation through various pre-treatments (Kratky and Jirout, 2011). However, these pre-treatments, especially the application of chemicals, are cost and energy-intensive, tend to produce fermentation inhibitors and contaminate the environment. Moreover, pre-treating RS before application to an anaerobic digestion (AD) system can make biological approaches unsustainable and complicated. Therefore, producing hydrogen biologically using anaerobic fermentation without pre-treatment of raw RS is considered in this study.

Chen *et al.* (2012a) was able to produce hydrogen from RS in their published article on thermophilic dark fermentation of untreated RS using mixed cultures and obtained the value of 24.8 NmL H<sub>2</sub>/g TS as the peak hydrogen yield from RS concentration of 90 g TS/L with particle size 0.297 mm using heated sludge. Similarly, Kim and colleagues reported the production of 0.74 mmol H<sub>2</sub>/g VS with 58% stable hydrogen content though there was an evolution of high methane gas from RS using untreated sludge at a carbon/nitrogen ratio of 25 (Kim *et al.*, 2012). Additionally, in their research on hydrogen and methane production from untreated RS and raw sewage sludge under thermophilic anaerobic

conditions using a two-stage system, Kim *et al.* (2013) obtained H<sub>2</sub> accumulation of 21 ml/g VS with stable H<sub>2</sub> content of about 60.9%. Furthermore, Alemahdi *et al.* (2015) produced the highest bio-H<sub>2</sub> yield of 14.54 ± 0.29 ml H<sub>2</sub>/g VS from their research on enhanced mesophilic bio-hydrogen production of raw rice straw and activated sewage sludge by co-digestion. However, even though the hydrogen content from the above studies was relative within the reported values, the volume of H<sub>2</sub> yield produced from untreated RS was low and fermentation pathways inefficient, compared with the theoretical hydrogen yield from RS via the AD system, which is 301 Nml H<sub>2</sub>/g TVS (Cheng *et al.*, 2011a).

The reduced yield could be from the incomplete conversion of RS biomass by the hydrogen-producing bacteria (HPB) due to the recalcitrant nature of RS. Hence, insufficient concentrations of soluble sugars. In addition to this, hydrogen-consuming bacteria (HCB) will quickly adapt to the fermentation system than HPB in the seeded sludge as the rigid structural moieties of RS typically require more time to hydrolyse - there are no sugar monomers or easily accessible substrates for consumption by the hibernated HPB. Conventionally, bio-hydrogen is produced during the acidogenic stage in an AD process (Bundhoo *et al.*, 2015), with glucose as the limiting factor. Therefore, the absence of fermentable sugars from RS will depopulate the HPB and ensure the dominance of HCB that evolve from consuming short-chain fatty acids (SCFA) in the medium. The increased HCB population will eventually change metabolic pathways from hydrogen to methane and organic acids or solvents production even when sugars are being released from RS substates. Biological hydrogen production from untreated RS using sugar enriched digested cow slurry (DCS) is suggested to tackle these challenges.

In this hypothesis, DCS is employed because it contains high levels of varying microorganisms that have the capability of hydrolysing lignocellulose (Brener *et al.*, 2008 and Ward *et al.*, 2008), and the enrichment of HPB is done with either glucose or sucrose with the gradual addition of untreated RS during the adaptive stage. The sugar enrichments and steady but continuous removal of effluents before the anaerobic fermentation may ensure the availability of soluble consumable sugar

monomers for the growth and dominance of HPB and hydrolytic microflora. The supremacy of hydrogen-producers and lignocellulose biomass degraders is because they prefer short retention times than SCFA and long-chain fatty acids (LCFA) degraders and methanogens, which prefer longer retention times due to their slow growth rates (Angelidaki *et al.*, 1999 and Liu *et al.*, 2008). Hence, most HCB are washed-out during short HRTs. The maximum specific growth rates ( $\mu_{\max}$  d<sup>-1</sup>) of some bacteria and archaeal groups within the AD process are 6.38, 5.10, 1.0, 0.67, 0.60, 0.55, 0.53 and 0.49 for amino acid degraders, glucose acidogens, carbohydrate and protein hydrolysis, butyrate degraders, methanogens, LCFA degraders, lipids degraders and propionate degraders respectively (Angelidaki *et al.*, 1999). Therefore, in hydrogen production, a combination of pH 5.5 and short HRTs may be optimum for product yield using glucose as a medium (Liu *et al.*, 2008). This rate is different for AD plants, which must function at retention times that are beyond the growth rates of the microbial communities, which is usually 15 -30 days at mesophilic conditions and 10-20 days at thermophilic conditions (Angelidaki *et al.*, 2011 and Westerholm *et al.*, 2016). The extended retention times are because the wash-out of slow-growing bacteria participating in the AD process can limit biogas production (Drosg, 2013). Hence, in this thesis, a) the feasibility of producing hydrogen biologically from untreated RS through dark fermentation method using glucose or sucrose enriched seeded sludge and b) the characterisation of the microbial communities in the employed seeded sludge, which are the research objectives, is investigated.

## Grahical Introduction

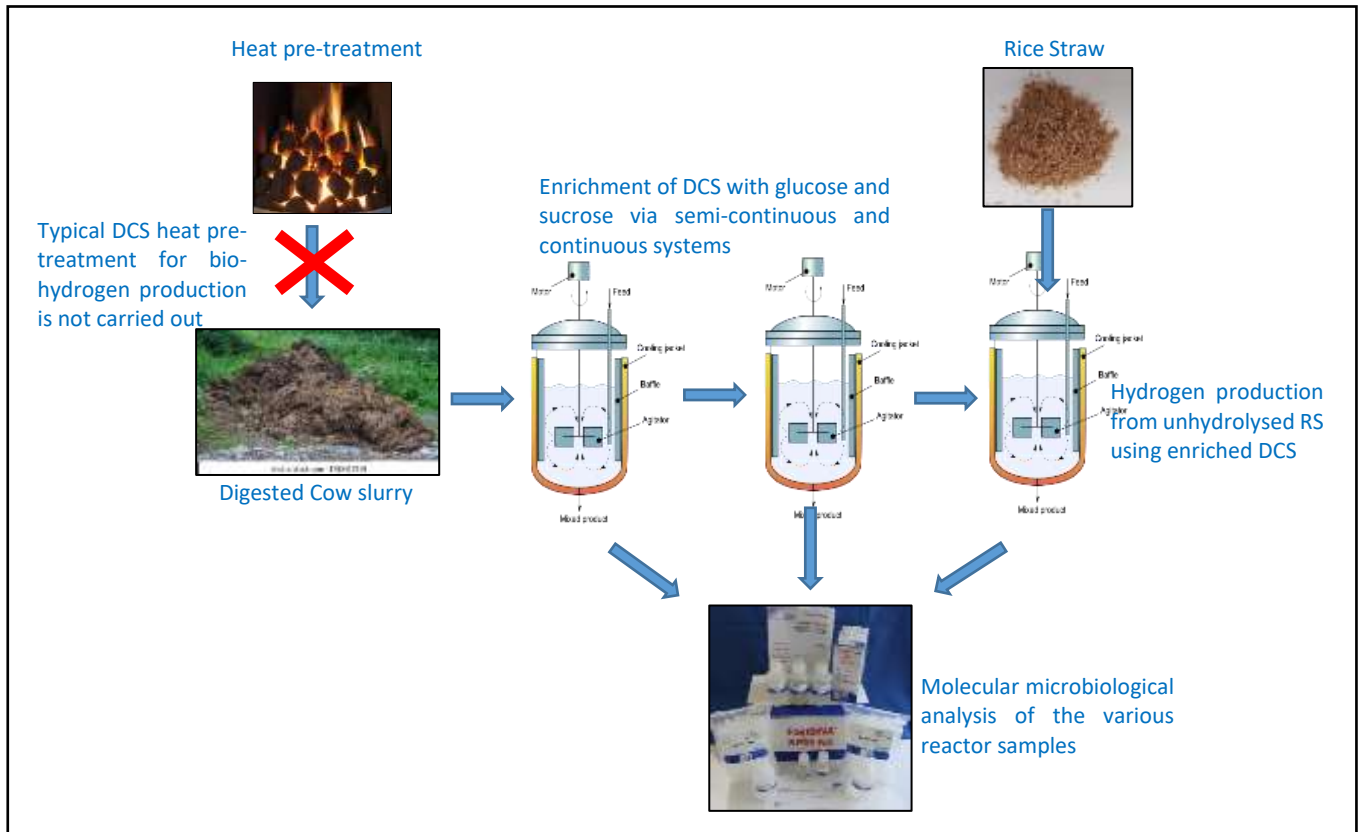


Fig 5-1: Biological hydrogen production from unhydrolysed raw rice straw co-digested with sugar-enriched digested cattle slurry

## 5.2 Materials and Methods

The digested cow slurry (DCS) and rice straw (RS) physicochemical attributes involved in the anaerobic digestion are characterised in Table 5-1.

Table 5-1: Analytical Assays of raw RS and DCS

Substrate	TS (g/mL)	TSS (g/mL)	VS (g/mL)	VSS (g/mL)	Ash (g/mL)	VS (%)	Ash (%)	C (%)	N (%)	NH <sub>4</sub> <sup>+</sup> -N (g/L)	Moisture Content (%)
RS	0.948	none	0.825	none	0.123	87	13	42.76	0.68	NA	3
DCS	0.093	0.067	0.071	0.052	0.022	76	24	38.54	3.00	0.28	95

ND: Not available, C is Carbon and N, Nitrogen

### 5.2.1 Experimental Procedures

#### 5.2.1.1 Batch and semi-continuous AD processes

Whereas the sludge enrichment was done using fed-batch mode as the initial reactor operation in which the substrate feeding was operated at 3 and 4 days for glucose and sucrose substrates respectively at 5 HRT, the batch system was used for acidogenic fermentation on unhydrolysed RS with sugar enriched DCS. The digestion was as outlined in Chapter 3, Section 3.8.1. The total biogas volumes produced by each borosilicate glass Duran bottle (BGDB) were measured daily, and the hydrogen concentration (%) was determined as described in Chapter 3, Section 3.9.

#### 5.2.1.2 Continuous anaerobic fermentation processes

Due to the anticipation of SCFA build-ups from sugar augmentation using the semi-continuous systems, even after the increased pH was regulated to 5.5 using 5M NaOH, the enrichment process was switched over to a continuous process in a CASBR using the same feedstock (glucose and sucrose) as mentioned previously. The CSABR set-up was defined in Chapter 3, Section 3.8.3 and the cultivation was done in duplicates under the same conditions as in the continuous process for hydrogen fermentation in Chapter 3 Section 3.8.3. Each reactor was seeded with the already enriched and

acclimatised DCS sludge from the preceding fed-batch systems, excluding the control reactors. After the reactivation of the inoculum inside the bioreactors, the continuous fermentation was operated for 10 days with the OLR of  $1.0\text{g VS L}^{-1}$  added  $\text{day}^{-1}$ . Under such single-phase HRT, a portion (10% of the digester working volume) of the fermentation supernatant was removed using germ-free syringes and replaced with the same amount of fresh medium consisting of the substrates ammonium nitrogen carbonate ( $10\text{g/L}$ ) and water. The fermentation augmentation with ammonium nitrogen carbonate was to maintain the depleting nitrogenous source. Afterwards, the reactors were purged with nitrogen for 5 min to provide oxygen-free conditions. Finally, each of the reactors was connected to 500 mL gas bags for biogas collections, and the total biogas volumes produced by each CSABR were measured daily, and the hydrogen content (%) was determined as described in Section 3.9.



## 5.3 Results and Discussion

### 5.3.1 Enrichment of Seeded Sludge from Different Feeding Systems

The question is, can hydrogen be produced biologically using an anaerobic fermentation process from untreated RS? Furthermore, can pretreated raw sludge be employed directly in the degradation of untreated RS? In answering this, the fed-batch mode of hydrogen production was done with communised RS (750  $\mu\text{m}$ ) co-digested with Heat-shocked but unenriched seed sludge under the stated fermentation conditions above. The daily hydrogen production from untreated RS using Heat-shocked DCS and biogas accumulation from untreated RS using Heat-shocked DCS is illustrated in Fig 5-2 and 5-3. The result showed that the hydrogen yield from untreated RS was 16 NmL H<sub>2</sub> g<sup>-1</sup> VS, while the biogas accumulation was 373 NmL g<sup>-1</sup> VS. In addition, the hydrogen content obtained ranges from 0.5 to 3% of the biogas. The result attained tallies with the findings of Alemahdi *et al.* (2015). They produced the highest bio-H<sub>2</sub> yield of 14.54 + 0.29 NmL H<sub>2</sub>/g VS at a concentration of 70.97% from their research work on enhanced mesophilic bio-hydrogen production of raw rice straw and activated sewage sludge by co-digestion.

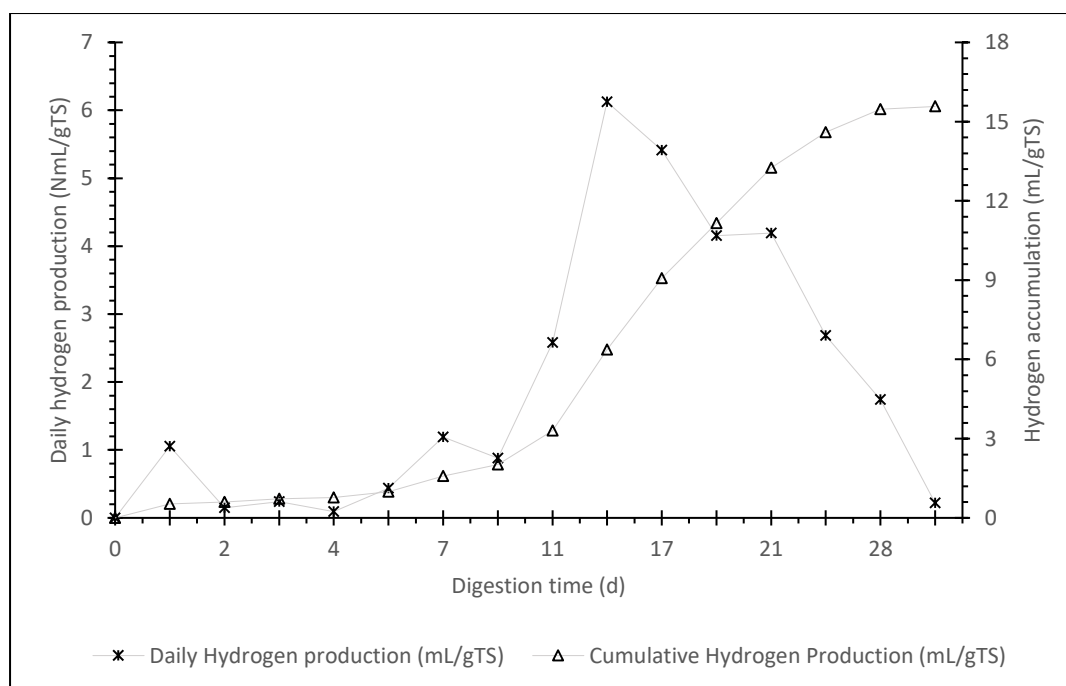


Fig 5-2: Daily hydrogen production from untreated RS using Heat-shocked DCS

On the other hand, the study outcomes slightly differ from the results obtained by Chen *et al.* (2012a) in their published article on thermophilic dark fermentation of untreated RS using mixed cultures. They achieved a hydrogen accumulation of 24.8 NmL H<sub>2</sub> g<sup>-1</sup> TS. Similarly, Kim *et al.* (2013), in their research work on hydrogen and methane production from untreated RS and raw sewage sludge under thermophilic anaerobic conditions using a two-stage system, obtained 21 NmL H<sub>2</sub> g<sup>-1</sup> VS as the peak hydrogen yield, while the hydrogen content was within the range of 58 and 61%. Although their reported hydrogen content differs from this study's findings, the variation is perhaps from the seeded sludge. Whereas the seeded sludge used in this study is from fresh Heat-shocked DCS, the seeded sludge cited is from fermenting hydrogen reactors, which means the composition of fermenting inoculum is essential for hydrogen production.

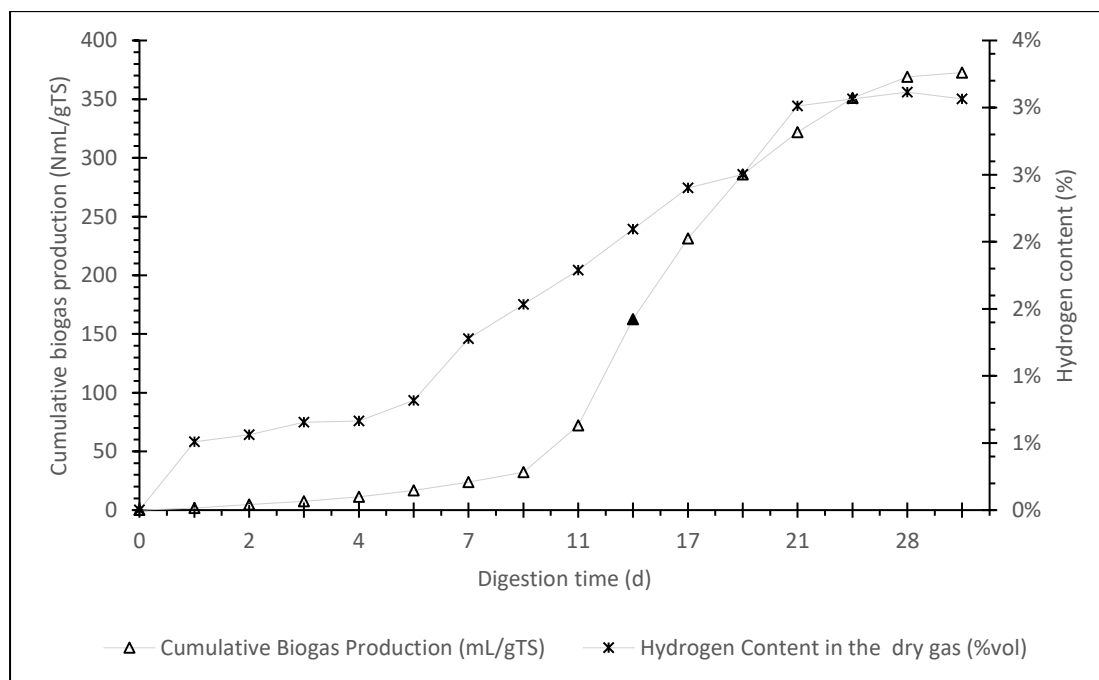


Fig 5-3: Biogas yield and hydrogen contents from untreated RS using Heat-shocked DCS

Furthermore, the low yield of hydrogen gas could be from the recalcitrant nature of RS and methanogens such as spore-formers and re-activation of non-spore-formers after heat-pre-treatment due to more extended lag phase involved in RS degradation (Fig 5-1 and 5-2); where inherent organic acids were consumed for growth and in methane production (Pendyala *et al.*, 2012). Recall that

hydrogen under normal circumstances is produced during the acidogenic stage in an AD process (Bundhoo *et al.*, 2015) from sugar consumption. Thus, hydrogen production is linked directly with the fermentation of sugar moieties. More so, the activation HCB soon dominates the HPB, which may become dormant under the lag phase as the sugar monomers are yet to be released for consumption.

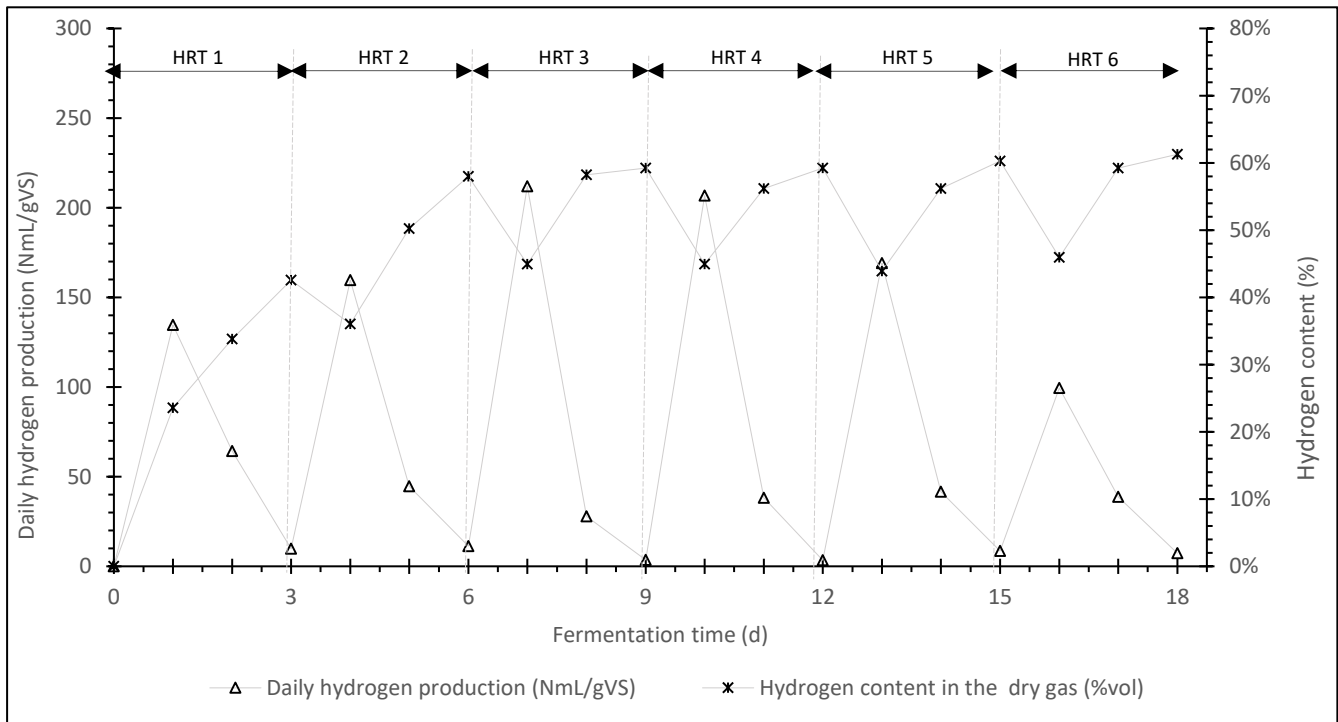


Fig 5-4: The enrichment of Heat-shocked DCS with glucose as the medium using fed-batch mode

### 5.3.2 Enrichment of Seeded Sludge for Hydrogen Producers Using Glucose and Sucrose

#### 5.3.2.1 Enrichment using a fed-batch system

Because of the low yield of hydrogen ( $16 \text{ NmL H}_2 \text{ g}^{-1} \text{ VS}$ ) obtained from untreated RS above, enrichment of seeded sludge after pre-treatments using sugars moieties (glucose and sucrose) before re-application on untreated RS is considered. It is believed that since hydrogen is produced during the acidogenesis, providing HPB with soluble substrates and repeated anaerobic fermentation will wash out the recalcitrant HCB and methanogens while increasing the growth of the HPB as most HCB have prolonged growth rates, especially the acetoclastic methanogens, which have a generation time of 3 to 10 days (Angelidaki *et al.*, 1999 and Gerardi, 2003). Therefore, as stated above, the enrichment

procedure was done with glucose and sucrose as substrates under fed-batch conditions. The semi-continuous mode was done 6 times, after which the enrichment was continued using the continuous system. The enrichment of Heat-shocked DCS using glucose and sucrose as media using semi-continuous systems is presented in Fig 5-4 and 5-5.

The result showed that hydrogen content (%) improved steadily (45 – 60%) from the 3<sup>rd</sup> to 6<sup>th</sup> feeding cycle using glucose and sucrose as the sole carbon sources. Additionally, the highest specific hydrogen yield (SHY) of 248 NmL H<sub>2</sub> g<sup>-1</sup> VS was obtained at the 4<sup>th</sup> feeding cycle even though the highest daily volumetric hydrogen production (VHP) of 211 NmL H<sub>2</sub> g<sup>-1</sup> VS was recorded at the 3<sup>rd</sup> feeding mode with glucose as the substrate (Fig 5-4). When sucrose was employed as the medium, the highest hydrogen accumulation of 421 NmL H<sub>2</sub> g<sup>-1</sup> VS and the highest daily VHP of 273 NmL H<sub>2</sub> g<sup>-1</sup> VS were obtained at the 3<sup>rd</sup> feeding mode (Fig 5-5). However, the daily VHP and the corresponding SHY declined from the 5<sup>th</sup> feeding cycle for glucose reactors (169 NmL H<sub>2</sub> g<sup>-1</sup> VS and 219 NmL H<sub>2</sub> g<sup>-1</sup> VS) and sucrose reactors (186 NmL H<sub>2</sub> g<sup>-1</sup> VS and 258 NmL H<sub>2</sub> g<sup>-1</sup> VS). There was also a significant reduction in both volumes for the daily VHP and SHY for glucose (99 and 145 NmL H<sub>2</sub> g<sup>-1</sup> VS) and sucrose (102 and 150 NmL H<sub>2</sub> g<sup>-1</sup> VS) reactors at the 6<sup>th</sup> feeding mode (Fig 5-4 and 5-5). The reduction of the daily VHP from the 5<sup>th</sup> feeding cycle despite the steady hydrogen content of 50 to 60% and no detectable methane could be a result of the accumulation of organic acids (Intanoo *et al.*, 2014), process inhibition, depletion of the nitrogenous source (Table 5-2) and hence, destabilisation of the nitrogen and carbon ratio. The accumulation of SCFA may have been the cause of the sweet sugary odour emanating from the reactors during the research experiment, particularly after the 6<sup>th</sup> feeding cycle. Some of these SCFA are precursors of many essential compounds required to maintain biomass (Wong *et al.*, 2014). However, the over-accumulation of these soluble organic acids (Table 5-2) may have inhibited the intracellular functions of the HPB. The inhibition of metabolic functions is perhaps due to two possible reasons a) inhibition due to rise in ionic strength and b) inhibition by un-dissociated acids (Ciranna *et al.*, 2014 and Srikanth and Mohan, 2014). Although the pH of the reactor was maintained at 5.6 to 5.8

using 5M NaOH, the un-dissociated acids at low extracellular pH less than the  $PK_a$  values of the associated organic acids (the  $PK_a$  values for acetate and butyrate are 4.75 and 4.8, respectively) may be able to penetrate microbial cell walls, where they will dissociate and release protons (cations) at higher intracellular pH (Ciranna *et al.*, 2014). This adversely affects microbial metabolism and growth by decreasing the intracellular pH while the accumulation of the anions ( $A^-$ ) increases the osmolarity of the cytoplasm and the cell turgor pressure (Elbeshbishy *et al.*, 2017).

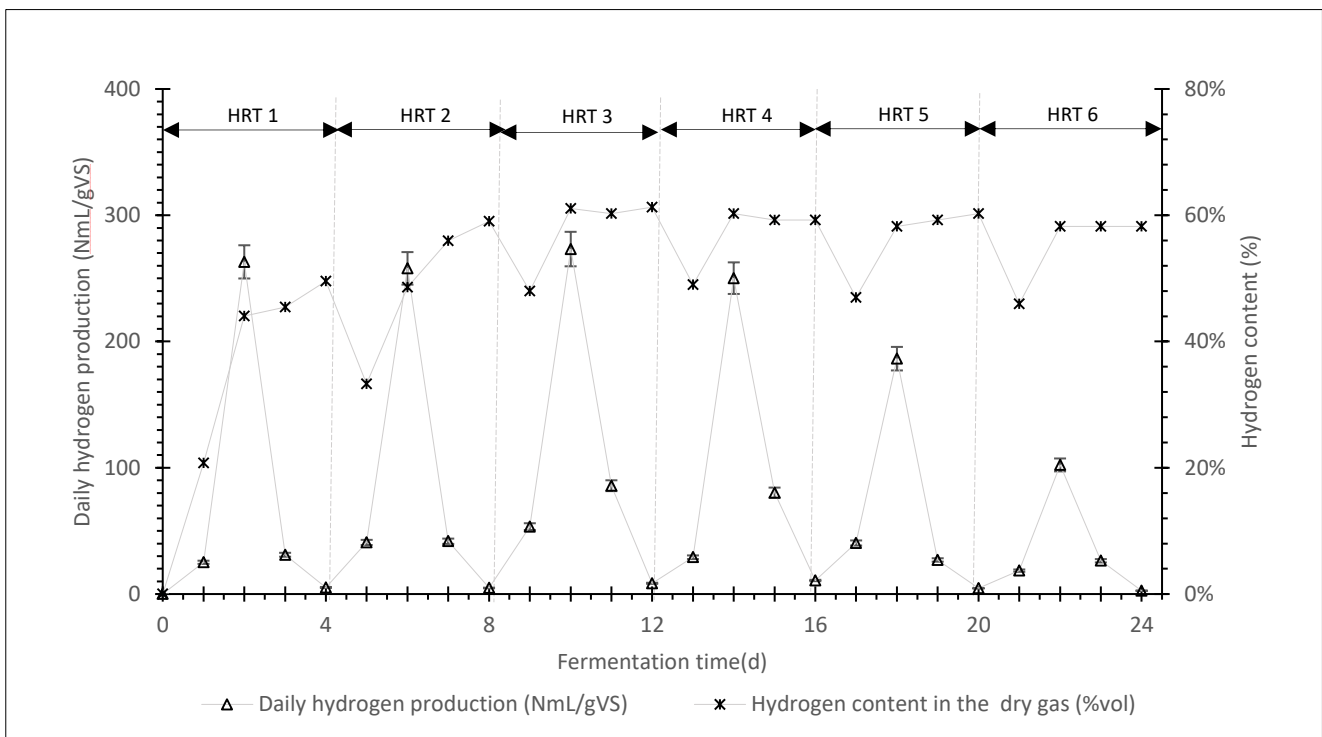


Fig 5.5: The enrichment of Heat-shocked DCS using sucrose as the medium using fed-batch mode

The decrease in intracellular pH may activate the hydrogen-consuming pathways for solvent production, depleting the intracellular ATP as more proton will be required to balance the intracellular pH, thereby reducing substrate utilisation and biomass growth (Khanal *et al.*, 2004).

Process inhibition is from repeated batch operations, resulting in a gradual decline in the hydrogen production yield over numerous runs due to substrate overloading in the digester. Process inhibition can also alter the hydrogen fermentation pathway, leading to solvent and lactic acid production

(Saady, 2013; Elbeshbishy *et al.*, 2017 and Neshat *et al.*, 2017). As mentioned before, hydrogen is produced during the acidogenic stage in an AD process (Bundhoo *et al.*, 2015) together with CO<sub>2</sub> and short-chain fatty acids (SCFA) made from either the pyruvate: formate lyase (PFL) route or the reduced ferredoxin (pyruvate: ferredoxin oxidoreductase (PFOR)) pathway (Holladay *et al.*, 2009). Therefore, alteration of this pathway may lead to a complete shutdown of the acidogenic process or diversion to other metabolic pathways.

Furthermore, nitrogen is an essential building precursor in microbial metabolism as it is required for critical cellular metabolic structures and enzymatic activities. Therefore, if this vital element is not adequate for microbial consumption, metabolic activities could be impeded due to deactivation/inhibition of essential enzymes and macromolecules necessary for microbial growth and activities (Bisaillon *et al.*, 2006). Ammonium concentration in ammoniacal nitrogen (NH<sub>4</sub><sup>+</sup> N) at a concentration below 50 mg L<sup>-1</sup> is reported to limit bacteria growth, leading to poor process performance (Poltronieri and D'urso, 2016). In addition to this, having the right balance of nitrogen to carbon ratio is also paramount for fermentative processes (Kim *et al.*, 2013), which apparently could have been significantly altered by the continuous addition of glucose or sucrose in the semi-continuous mode leading to more liberations of SCFA. The ammoniacal nitrogen may have been depleted from the continuous feeding leading to a decline in hydrogen fermentative activities from the 5<sup>th</sup> to the 6<sup>th</sup> feeding stage.

#### 5.3.2.2 Enrichment using continuous system

The continuous stirred anaerobic bioreactor (CASBR) systems were employed to enrich the HPB and resolve the challenges encountered from fed-batch systems, mainly the accumulation of organic acids and dwindling nitrogenous sources. In the continuous process, 79% of the enriched seeded sludge from the fed-batch were employed with the same conditions described under continuous fermentation. The remaining 21% were a mixture of 0.1M of ammonium hydrogen carbonate, mineral

medium and water. The steady-state conditions were achieved immediately after reactivation of the seeded sludge in the bioreactors. At this state, about 10% of the fermentation supernatant was removed daily using germ-free syringes and replaced with the same equal amount of fresh medium as detailed in the methods.

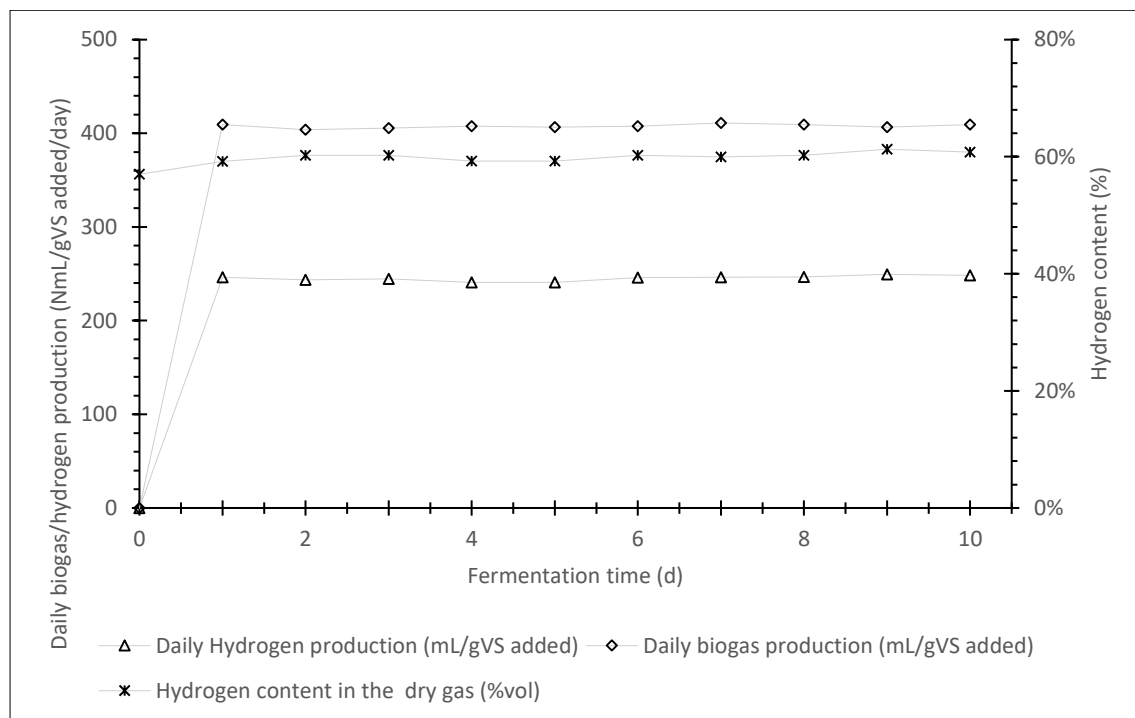


Fig 5-6: Enrichment of Heat-shocked DCS using glucose as substrates at steady-state

The result showed that the hydrogen content in both reactors remained steadily at 60 - 61%, with the mean daily VHP of 245 NmL H<sub>2</sub> g<sup>-1</sup> VS added d<sup>-1</sup> from glucose samples (Fig 5-6) and 439 NmL H<sub>2</sub> g<sup>-1</sup> VS added d<sup>-1</sup> from sucrose samples (Fig 5-7). The biogas yield was 408 NmL g<sup>-1</sup> VS added d<sup>-1</sup>, and 727 NmL g<sup>-1</sup> VS added d<sup>-1</sup> for glucose and sucrose substrates. There was no detectable methane in both reactors, indicating complete wash-out of HCB and methanogens (Angelidaki *et al.*, 1999 and Gerardi, 2003) and both TVFA and ammonical nitrogen were found to stabilised at controlled conditions (Table 4-2). The result was slightly close to Fang and Liu (2002) findings on the effect of pH on hydrogen production from glucose by mixed culture.

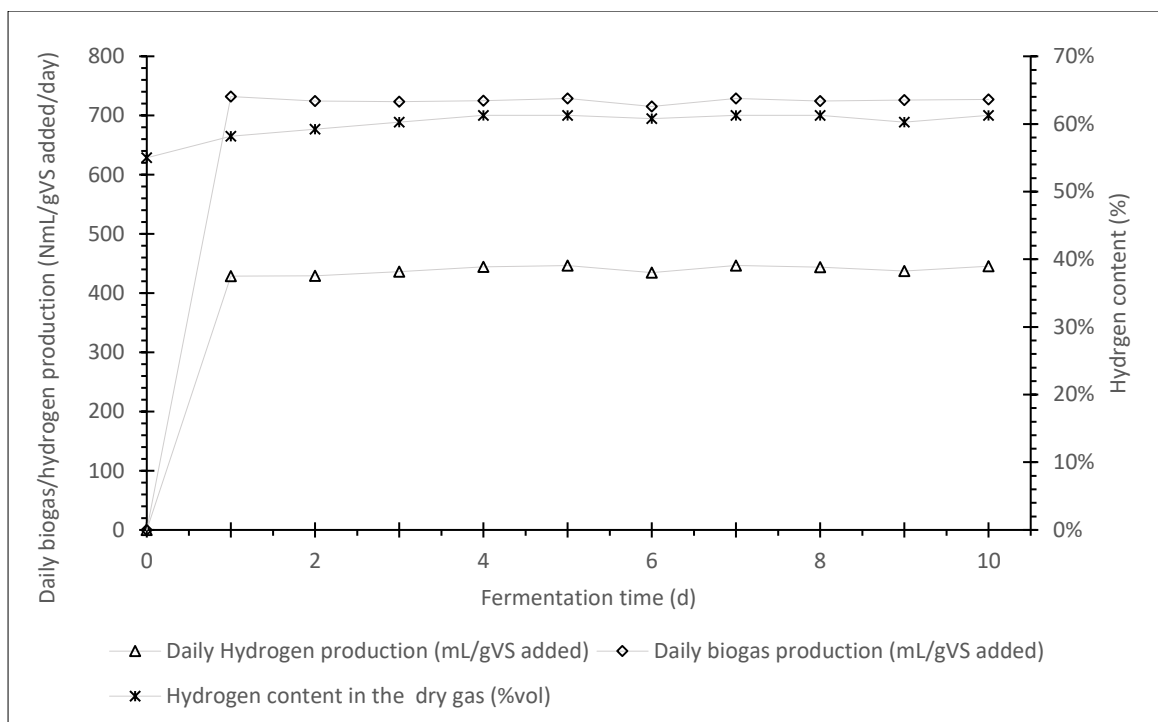


Fig 5-7: The enrichment of Heat-shocked DCS using sucrose as substrates at continuous mode

At the optimal pH of 5.5 and temperature of 36°C, the biogas produced comprised 64±2% hydrogen with a yield of  $2.1 \pm 0.1 \text{ mol-H}_2/\text{mol-glucose}$  and a specific production rate of  $4.6 \pm 0.4 \text{ l-H}_2/(\text{g-VSS day})$ .

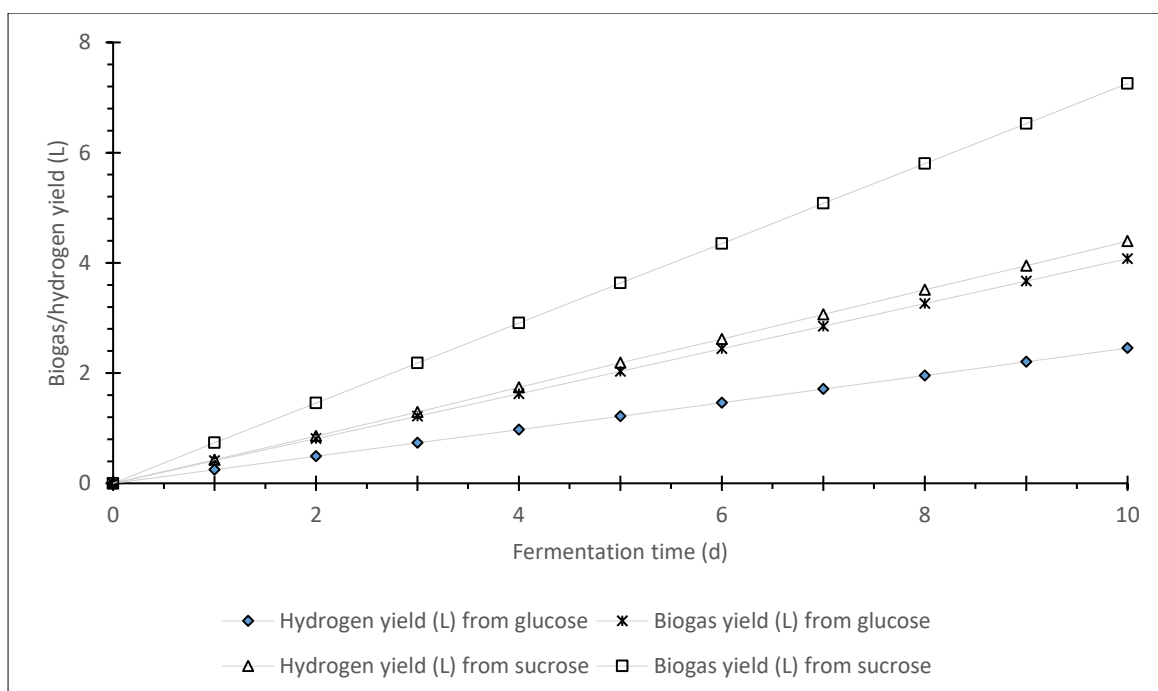


Fig 5-8: The biogas and hydrogen accumulation from the enriched Heat-shocked DCS using either glucose or sucrose as substrates



The progressive increase in the biogas and hydrogen yield (NL) from the enriched Heat-shocked DCS using the sugar medium (glucose or sucrose) showed the establishment of an active steady-state and effectiveness of the fermentation process (Fig 5-8). From the graph, it can be seen that after the 10 days fermentation process, the hydrogen and biogas accumulation were 2.45 and 4.08 NL, respectively, when glucose was added to the reactors. Similarly, when sucrose was employed as the digesters substrates, the hydrogen and biogas yield rose to 4.39 and 7.26 NL, respectively.

Table 5-2: Production of SCFA and consumption of ammoniacal nitrogen from various reactors

Sludge Enrichments	Acetic (mg/L)		Butyric (mg/L)		Formic (mg/L)		SCOD (mg/L)		NH <sub>4</sub> N <sup>+</sup> (mg/L)	
	Glucose	Sucrose	Glucose	Sucrose	Glucose	Sucrose	Glucose	Sucrose	Glucose	Sucrose
Feeding 1	535.05	729.09	859.68	1079.75	Na	na	1223.70	2307.23	250	260
Feeding 2	858.80	1165.60	1289.52	1619.63	Na	na	2223.32	3066.44	225	238
Feeding 3	1115.08	1420.55	1611.92	2159.00	2.45	3.50	2912.50	3867.05	180	208
Feeding 4	1320.06	1719.64	1977.26	2429.06	3.45	3.70	3411.01	4333.14	140	156
Feeding 5	1669.02	2203.86	2553.25	3157.99	4.35	4.70	4416.23	5654.63	90	100
Feeding 6	1983.66	2639.66	3071.64	3813.97	4.40	5.20	5224.13	6780.26	42	48
CASBR	1129.45	1479.55	1522.50	2117.05	3.00	3.00	2805.72	3715.20	235	342
Raw DCS	370.04		157.15		NA		600.54		280	
Unhydrolysed RS	1220.04		1740.05		NA		2904.3		262	

### 5.3.3 Hydrogen Production from Unhydrolysed RS Using Enriched Seeded Sludge

Improved VHP was investigated using the sugar-enriched DCS seeded sludge from CASBR systems on untreated RS residue with the conviction that the HCB and methanogens have been thoroughly washed out. After proper acclimatisation with untreated RS, the fermentation was done using batch fermentation systems and conditions recorded above. The fermentation mixture was augmented with 0.1M of ammonium hydrogen carbonate (10g/L). The hydrogen accumulation profile from untreated RS was modelled using the Gompertz equation. The SHY of 149 NmL H<sub>2</sub> g<sup>-1</sup> TS was produced, while the production rate of 55 mL H<sub>2</sub> g<sup>-1</sup> TS was obtained after 14 days lag period (Fig 5-9). The daily highest VHP of 66 NmL H<sub>2</sub> g<sup>-1</sup> TS was also achieved on day 14. The longer lag duration could be from the degree of the structural complexity of RS. The highest hydrogen content of 57% was also achieved.

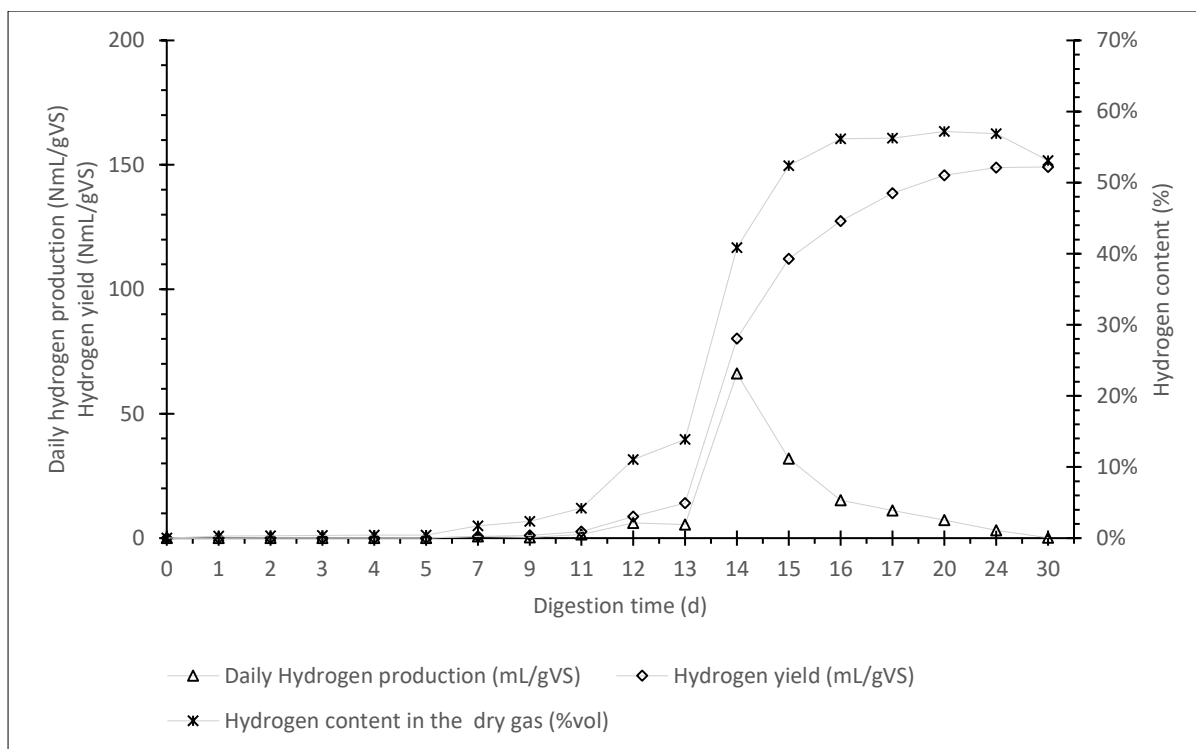


Fig 5-9: Daily hydrogen production and hydrogen accumulation from Untreated RS.

Although the result of the hydrogen yield produced differs considerably from the predicted theoretical hydrogen yield from RS using the AD system, which is  $301 \text{ Nml H}_2 \text{ g}^{-1} \text{ TVS}$  (Cheng *et al.*, 2011b), the value obtained is significantly (100%) higher than the previous hydrogen production from untreated RS co-digested without sugar-enriched DCS. Additionally, the SHY produced from untreated RS using sugar enriched DCS is much more increased than the findings of Chen *et al.* (2012a), Kim *et al.* (2013) and Alemahdi *et al.* (2015), even though the stable hydrogen content were almost the same (58 – 61%) except for the result of Alemahdi *et al.* (2015). There is no clear explanation for this improvement in hydrogen performance from untreated RS using sugar-enriched DCS. However, the enrichment procedures could have enhanced the growth of HPB and microbes capable of hydrolysing lignocellulose (Ward *et al.*, 2008), while many HPB and methanogens are supposedly washed out under such an enriching process. In addition, the removal of excess organic acids, which negatively affects acidogenesis during the continuous feeding mode, might have also played a factor (Oreopoulou and Russ, 2006; Ciranna *et al.*, 2014 and Srikanth and Mohan, 2014).

Nevertheless, subsequent hydrogen production studies proved futile from co-digestion of unhydrolysed RS with the sugar-enriched DCS using the same protocol and conditions. The results obtained showed increased biogas production after 8 to 15 days lag phase without detectable significant hydrogen content, but up to 30% increased methane content. Perhaps, the longer lag phase duration was sufficient for reactivation and doubling some HCB and methanogens (Angelidaki *et al.*, 2011 and Westerholm *et al.*, 2016). Thus, whilst it is evident that DCS sugar enrichment processes encourage and favour the growth of HPB and hydrolytic microorganisms (Fig 5-10) and therefore the daily VHP improvement, the procedure could also boost the growth of HCB and methanogens (Fig 5-10). Besides, there was evidence of a reduction in the SCFA concentration (Table 5-2) and increased alkalinity in the operational medium. There is no defined explanation for the above drawbacks. However, SCFA build-up, despite repeated withdrawals and increments in the TCOD concentration during the enriched DCS storage, may have mostly played a part (Oreopoulou and Russ, 2006). In addition, the inhibition or alteration of metabolic pathways due to the rise in ionic strength or inhibition by un-dissociated acids penetrating the microbial cell walls may have occurred, leading to the production of methane and solvents or even the death of HPB and other hydrolytic microbes (Ciranna *et al.*, 2014; Srikanth and Mohan, 2014 and Elbeshbishy *et al.*, 2017).

#### **5.3.4 Microbial Community Composition**

After the enrichment and subsequent fermentation process, the microbial composition was investigated with the bacteria community's relative abundance and taxonomic distribution in each sample analysed at the genus and phylum levels (Fig 5-10). However, a detailed discussion on the microbial composition would be given at the phylum level because of the large number of unidentified Taxa at the genus level. *Firmicutes* were the most dominant phylum accounting for ~60 to 85% in the Heat-shocked and sugar enriched samples compared to the control and unhydrolysed RS samples where *Proteobacteria* in the range of ~22 to 47% were the most principle phylum. From the control digestate, it can be seen that a total of 25 phyla were identified with *Proteobacteria* (~22) and

*Firmicutes* (~22) the most abundant, followed by *Bacteroidetes* (~13%) and *Euryarchaeota* (~15%). However, after the Heat-shocked procedure, the number of phyla were reduced to 7, with *Firmicutes* population increasing to about 85%, making it the most dominant phylum. *Actinobacteria* (~6%) also increased after Heat-shocked PT. Under the same pre-treatment condition, the population of *Proteobacteria* (~7%), *Bacteroidetes* (~2%), *Chloroflexi* (~1.5%), and *Euryarchaeota* (~2%) were reduced. The findings give credence to thermal pre-treatment of seeded sludge as a prerequisite before fermentation, where the HPB mainly represented by the *Firmicutes*, which can sporulate, can tolerate the harsh heat treatments (Liu *et al.*, 2020; Mockaitis *et al.*, 2020 and Yang *et al.*, 2020).

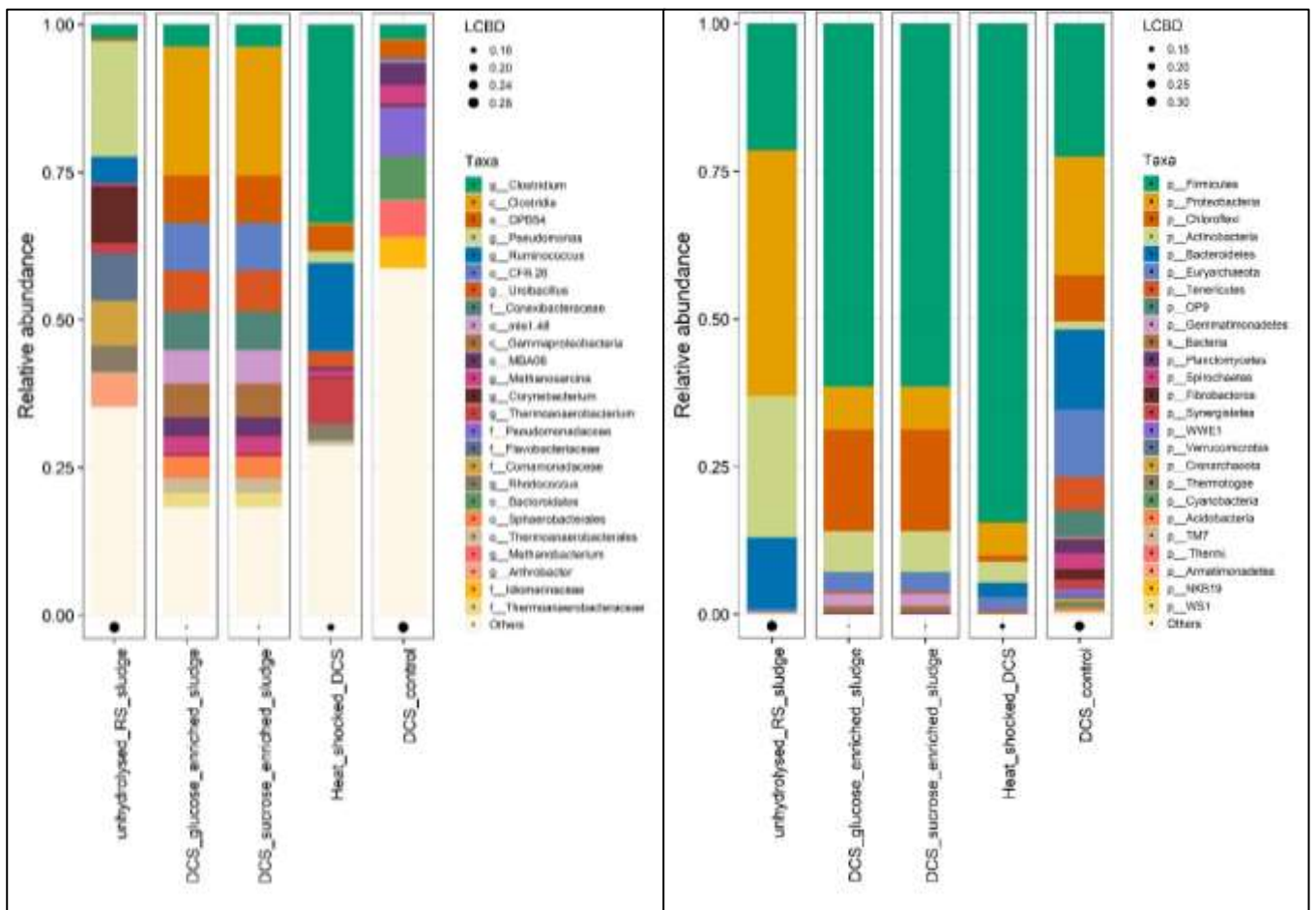


Figure 5-10: The relative abundance of the top 25 most abundant microbial communities at genus and phylum level of the various digestates. While the bars correspond to taxa that are most dominant within the sample, the black points whose diameter relate to the magnitude of the LCBD value of the digestates that is higher LCBD mean the sample has more unique species than others.

Even though the hydrogen content, hydrogen yield and daily hydrogen production were stable and there was no detectable methane from the sugar enriched digesters (Fig 5-4, 5, 6 and 7), there were

changes in the microbial community after sugar enrichments (Fig 5-10). Whereas the phyla *Proteobacteria* and *Euryarchaeota* were almost unaffected, it is observed from the graph that there was a reduction in the population of *Firmicutes* (~60%) and *Bacteroidetes* (~1%) compared to Heat-shocked DCS samples. Nonetheless, the microbial communities of *Chloroflexi* (~18%) and *Actinobacteria* (~9%) increased in population. In addition, there was also the appearance of a new phylum *Gemmatimonadetes* (~2%), which perhaps is believed to have existed but in few numbers but was able to utilise the soluble nutrients for growth. This view is because *Gemmatimonadetes*, a gram-negative bacteria (Takaichi *et al.*, 2010), are usually found in activated sludge or soils.

The sugar enriched reactors remained stable despite changes in microbial composition because the majority of the mentioned phyla are well-known hydrogen producers capable of utilising simple to complex substrates producing different fatty acids except for *Euryarchaeota* (which is insignificant in number) implicated in methane production processes and *Chloroflexi* known for degradation of organic matter especially ammonia (Suominen *et al.*, 2021).

The reduction in the population of *Firmicutes* and *Bacteroidetes* compared to Heat-shocked DCS samples could be from the dwindling amounts of degradable complex biomass presence in Heat-shocked DCS. Most *Firmicutes* are hydrolytic bacteria and may be washed away or inactivated in the absence or limited levels of degradable complex biomass.

After the sugar enrichment, the enriched DCS were subjected to fermentation using unhydrolysed RS as substrates. The microbial analysis showed a significant increase in *Proteobacteria* (~47%) population, followed by the phyla *Actinobacteria* (~28%), *Firmicutes* (~20) and *Bacteroidetes* (~13%) (Fig 5-10). The increased *Proteobacteria* could be from the more extended lag phase required for RS hydrolysis, which necessitated the growth of *Proteobacteria* and *Actinobacteria* or conversion of residual sugars by the identified organisms as a result of soluble substrates. Although these observations don't explain the increased methane content (30%) and no detectable hydrogen content from subsequent hydrogen production studies from co-digestion of unhydrolysed RS with the sugar

enriched DCS as discussed above, there were populations of *Euryarchaeota* (~0.5%) in the bar chart (Fig 5-10). Furthermore, even though these methane producers' presence was fewer in number, the LCBD was very high in magnitude (0.30). Thus, methane gas was produced by the *Euryarchaeota* utilizing the sugars released during RS hydrolysis or from residual sugar products (such as acetic acids).

At the genus level, the microbial community in the untreated DCS (control) samples were mainly not identified and were grouped as others. Among those identified, *Pseudomonadacea* (*Azotobacter*) *Bacteroidales*, *Methanobacterium* and *Clostridia* are the most abundant genera (Fig 5-10). Other notable genera were *Ureiacillus*, *Methanosarcina* and *Clostridium*. Whereas *Clostridium*, *Ruminococcus* and *Thermoanaerobacterium* were the principal genera among the identified genera following Heat-shocked PT, *Clostridia* was the most abundant genus in sugar enriched DCS. Finally, *Pseudomonas* was the most dominant genus in the unhydrolysed RS DCS sample. A detailed explanation of these genera has already been given for most identified bacteria in the preceding chapter. However, *Pseudomonas*, which belong to *Proteobacteria*, is also among the HPB that converts monomers of hydrolytic products such as unsaturated fatty acids, glycerol, monosaccharides and amino acids to short-chain fatty acids (SCFA), gases (hydrogen and carbon dioxide), acetic acids and alcohols (Yu *et al.*, 2010; Angelidaki *et al.*, 2011; Khan *et al.*, 2017b and An *et al.*, 2020b).

## 5.4 Conclusion

The feasibility of producing hydrogen biologically from untreated RS via dark fermentation using glucose or sucrose enriched seeded sludge is explored. The enrichment was carried out with the belief that since hydrogen is produced during the acidogenesis, providing HPB with soluble substrates and reducing the HRT will flush out the recalcitrant HCB while increasing the growth of the HPB as most HCB grow slowly, especially the acetoclastic methanogens, which have a generation time of 3 to 10 days.

The result obtained from the semi-continuous system showed that hydrogen content (%) improved steadily (45 – 60%) from the 3<sup>rd</sup> to 6<sup>th</sup> feeding cycle using glucose and sucrose as the sole carbon sources. Consequently, the highest SHY of 248 NmL H<sub>2</sub> g<sup>-1</sup> VS was obtained with glucose as the substrate at the 4<sup>th</sup> feeding cycle. When sucrose was used as a carbon source, the highest hydrogen accumulation of 421 NmL H<sub>2</sub> g<sup>-1</sup> VS was achieved at the 3<sup>rd</sup> feeding mode. Subsequently, with a significant reduction in the daily SHY and VHP for glucose (99 and 145 NmL H<sub>2</sub> g<sup>-1</sup> VS) and sucrose reactors (102 and 150 NmL H<sub>2</sub> g<sup>-1</sup> VS) respectively at the 6<sup>th</sup> feeding mode, the result obtained from CASBR mode showed that in both reactors, the hydrogen content remained steadily at 60- 61% with the mean daily VHP of 245 NmL H<sub>2</sub> g<sup>-1</sup> VS added d<sup>-1</sup> from glucose samples and 439 NmL H<sub>2</sub> g<sup>-1</sup> VS added d<sup>-1</sup> from sucrose samples. The SHY of 149 NmL H<sub>2</sub> g<sup>-1</sup> TS produced from untreated RS co-digested with sugar enriched DCS was significantly improved compared with hydrogen accumulation of 16 NmL H<sub>2</sub> g<sup>-1</sup> TS from untreated RS co-digested without sugar-enriched DCS.

Additionally, the hydrogen yield produced from untreated RS using sugar-enriched DCS is significantly higher than the literature findings. Nonetheless, subsequent replication of hydrogen production studies from co-digestion of untreated RS with sugar enriched DCS using the same protocol and conditions proved abortive without an unequivocal description. Finally, the microbial community analysis showed that the dominant phylum *Firmicutes* represented by the *Clostridium* and *Ruminococcus* were the most abundant bacteria in the sugar enriched reactors. In contrast,

*Pseudomonas*, which belong to the phylum *Proteobacteria* was the most dominant in the unhydrolysed RS digestates.



## **Chapter 6    A solution to Nigeria’s energy challenges with hydrogen and methane co-produced from agro-industrial pre-treated rice straw in three-stage anaerobic digestion processes**

### **6.1    Introduction**

Despite the benefits of the anaerobic digestion (AD) process for hydrogen and methane production, the rice straw (RS) AD process for biogas production is limited by the low digestibility of its fibre content (Wei *et al.*, 2014, Dong *et al.*, 2019 and 2020) and its high ash content of 15 – 20% (Menardo *et al.*, 2015). It has been said that without pre-treatment of lignocellulose biomass, only 20% hypothetical maximum sugar can be obtained from enzymatic hydrolysis (Dong *et al.*, 2019 and Zhang *et al.*, 2020). Thus, effective and efficient pre-treatments are required to break the complex and heterogeneous matrix, increase surface area and create micropores on the lignocellulose material to enhance enzyme accessibility and hydrolysis and cellulose degradation (Dong *et al.*, 2019 and 2020). There have been several works on RS pre-treatments for improving acidogenic and methanogenic processes by Lo *et al.* (2010), Chang *et al.* (2011), He *et al.* (2014), Liu *et al.* (2014), Mustafa *et al.* (2016), Dong *et al.* (2019) and (2020), Kainthola *et al.*, (2019), Kannah *et al.*, (2019) Balachandar *et al.*, (2020) and Srivastava *et al.* (2021). Nevertheless, pre-treatment of lignocellulose biomass invariably increases biogas production cost and presents environmental hazards. Therefore, ways and alternative means of pre-treatment lignocellulose that are environmentally friendly and cost-effective are being studied. Hence in this research study, some agro-industrial wastes – potash extract (PE), cassava-steep wastewater (CSSW) and corn-steep liquor (CSTL), as pre-treatment agents, were explored as substitutes for lignocellulose chemical pre-treatment. Whereas PE is alkaline and contains varying metallic cations and anions that may affect the physiology of lignin components of lignocellulose biomass (LCB) like base pre-treatment agents (Salakkam *et al.*, 2019), the steep wastewaters from CSWW and CSTL are acidic. Perhaps, the wastewaters produce the same effects as

HCl on LCB, which are the hydrolysis of both the cellulose and hemicellulose via breakage of the  $\beta$ , 1-4 glucosidic bonds and reduction of the OH groups of glucosidic bonds (Salakkam *et al.*, 2019).

Furthermore, a three-stage anaerobic digestion process that produces hydrogen and methane from RS co-digested with DCS is proposed to maximise RS's energy value. In this three-stage process (Fig 6-1), the acidogenic microorganism converts RS hydrolysates to hydrogen, carbon dioxide, and SCFA in a separate reactor under acidic pH while the hydrolysed RS residues are washed, dried and stored for future use in methane production. Whereas the hydrogen produced is collected from the reactor using a gas-bags, the SCFA enter the second stage, where they are further processed down to methane and carbon dioxide. The third and final stage involves methane production from the pre-treated RS residues. In this stage, as with the second stage, slow-growing methanogens are preferable under neutral pH at longer HRT (7 – 30 days).

The three-stage anaerobic digestion process is categorised based on reactants (feedstock) rather than the traditional products typical in two-stage AD processes. The main difference between the two-stage and three-stage hydrogen and methane production processes is that while hydrogen production processes are optimised in both processes, RS residues are further broken down to methane in the latter process. Therefore, energy is maximised and recovered from the RS substrates.

Although there are many documentations on individual hydrogen (Li *et al.*, 2007, Lo *et al.*, 2010, Chang *et al.*, 2011, Chen *et al.*, 2012a, Quéméneur *et al.*, 2012a, He *et al.*, 2014, Liu *et al.*, 2014, Patel *et al.*, 2014, Alemahdi *et al.*, 2015, Sattar *et al.*, 2016b; Kumar *et al.*, 2016, Dong *et al.*, 2019 and 2020, Kannah *et al.*, 2019, Balachandar *et al.*, (2020) and Srivastava *et al.* (2021).) and methane AD processes (Yu and Schanbacher *et al.*, 2010; Mustafa *et al.*, 2016 and Kainthola *et al.*, 2019) and few reports on the two-stage co-production processes (Parawira *et al.*, 2004; Ueno *et al.*, 2007; Zhu *et al.*, 2008; An *et al.*, 2020a and b and Yan *et al.*, 2020), to the best of the writer's knowledge, there are no documentations on three-stage *reactants* processes. In addition to this, there is no known research

on using agro-industrial wastes (PE, CSTL and CSWW) as chemical pre-treatment agents. Thus, this study aims to a) investigate hydrogen and methane co-production from agro-industrial pre-treated enzymatically-enhanced rice straw in a three-stage anaerobic digestion process; b) establish the mass balance of the RS digestion processes; c) calculate and compare the various energy (power, thermal and cooling fluid) values of the produced biogas from the three-stages using the CCHP strategy and finally d) investigate the microbial community composition of the fermentation and digestion processes.

### Graphical Introduction

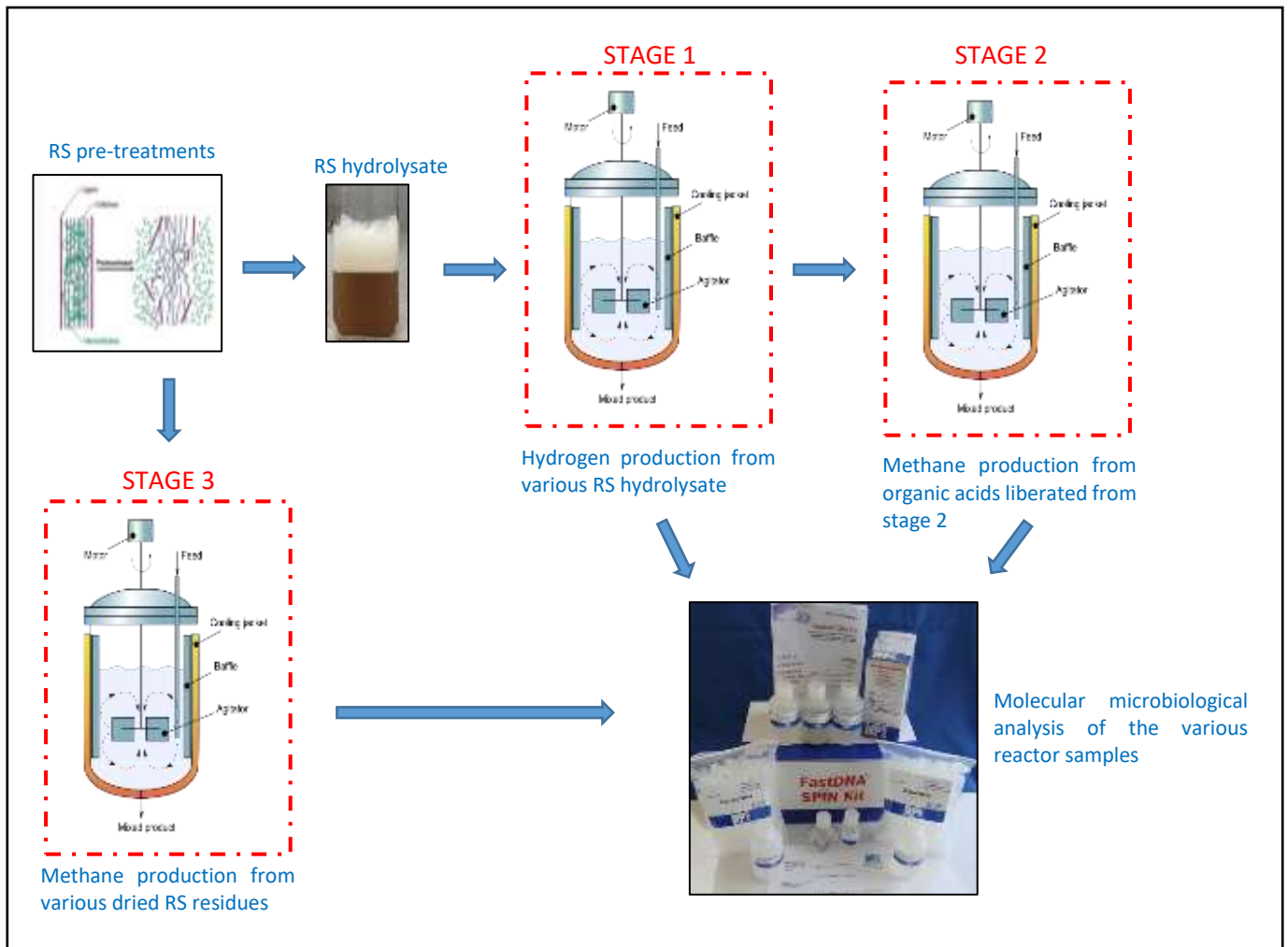


Fig 6-1: Hydrogen and methane co-production from agro-industrial pre-treated enzymatically-enhanced rice straw in a three-stage anaerobic digestion process

## 6.2 Materials and Methods

The seeded sludge and RS physicochemical attributes and solid analysis applied in the anaerobic digestion are characterised in Table 6-1, while the C/N ratio was kept at 25.

Table 6-1: Physicochemical properties of raw RS and seeded sludge

Analysis	RS	ADS	DCS
TS (g/mL)	0.938	0.016	0.095
TSS (g/mL)	ND	0.013	0.069
VS (g/mL)	0.815	0.009	0.073
VSS (g/mL)	ND	0.008	0.0052
Ash (g/mL)	0.123	0.007	0.0022
VS (%)	87	56	77
Ash (%)	13	44	23
Carbon (%)	42.76	34.22	38.54
Nitrogen (%)	0.68	2.92	2.98
Hydrogen (%)	6.3	3.77	3.99
C/N ratio	ND	11.7	12.9
NH <sub>4</sub> <sup>+</sup> -N (mg/L)	ND	0.23	0.27
Moisture Content (%)	3	97	95
Alkalinity (mg CaCO <sub>3</sub> L <sup>-1</sup> )	ND	5280	4010

ND: Not determined



Fig 6-2: Some of the chemical-PT RS samples before filtration and detoxification

## 6.2.1 Preparation of Rice Straw Hydrolysate

### 6.2.1.1 Acid pre-treatment of rice straw

Employing a modified method of Zhang and Cai (2008), 100g of milled RS was added to a conical flask containing 400ml of 1M of hydrochloric acid, CSWW processed at RT and CSTL to maintain the ratio of solid to liquid as 1:4. The mixtures were then heated at 100 °C for 1 hr. Subsequently, the RS mixtures (Fig 6-2) were filtered using 0.2µm filter paper, while the RS residues were washed thoroughly with distilled water until neutral pH was achieved. Later, the filtrates were diluted to 6.0 using 5M of NaOH, detoxified by lime treatment, and stored at -20°C until use. Finally, the RS residues were dried in the oven at 70°C for 24 h and kept at RT for subsequent use.

Alternatively, CSWW-PT at a cold temperature (4°C) was done using CSWW extracts at 4°C. In the pre-treatment procedure, milled RS (20g) was added to a beaker containing 400 mL of cold CSWW extract. After incubation for 3.0 days, the mixture (Fig 6-2) was diluted to 6.0 using 5M of NaOH and filtered using a 0.2µm filter paper. The filtrate was stored at a temperature of -20°C until use, while the RS residue was washed with de-ionised water to neutral pH, oven-dried at 70°C for 24 h and stored at RT until use.

### 6.2.1.2 Base pre-treatment of rice straw

Revised solid-state NaOH-PT as prescribed by He *et al.* (2008) was applied - First, 20 g of dry milled rice straw was placed into the 200ml beaker, and then a mixture of 1 g of NaOH and 20 g of distilled water was added to it to bring the moisture content to 80% on a dry basis. Later, the prepared beaker was covered with foil, closed with plaster, and was kept at room temperature for 3.0 weeks. After the incubation, the RS residue was washed extensively to remove adhered sodium ions with deionised water, and the pH was neutralized by soaking in 0.1M Tris-acid buffer. Afterwards, the pre-treated RS was oven-dried at 70°C for 24 h, placed in a clean container and stored at RT until used.

In the same vein, amended Zhang and Cai (2008) protocol, as employed in HCl pre-treatment, was applied. However, 2% NaOH was used, and the filtrate was diluted to 6.0 using 5M of HCl. The salts precipitates were filtered using 0.2µm filter paper and stored at -20°C until use. Afterwards, the RS residue was dried in the oven at 70°C for 24 h and kept at RT for subsequent use.

### 6.2.1.3 Potash extract pre-treatment of rice straw

The exact process for solid-states described above on-base pre-treatment was used for rice straw pre-treatment using potash extract. However, 20 ml of potash extract was used. Also, as stated above, improvised Zhang and Cai (2008) protocol was applied, but 400 ml of potash extract was employed in the pre-treatment process.

All the chemical pre-treatments were done in triplicates, and the mean values were presented, while the controls were also prepared without the respective PT agents following the same procedures

Table 6-2: Characterisation of some PT RS residues and untreated RS

PT-RS Samples	Calculated DM (TS) Content (%)	Calculated DM (VS) Content (%)	Ash (%)
HCl-PT RS	98	90	8
PE-PT RS	94	88	6
NaOH-PT RS	96	89	7
Solid PE-PT	92	84	8
Solid NaOH-PT	96	89	7
CSWW-PT	95	84	11
CSTL-PT	95	83	12
Untreated	95	82	13

### 6.2.2 Enzymatic Hydrolysis

The cellulase enzyme was assumed to be isolated and optimised from the soil using the protocol of Acharya *et al.* (2008) and (2012) and Kshirsagar *et al.* (2015). However, for this study, the dried PT RS residues from chemical pre-treatments were enzymatically hydrolysed after solids analysis (Table 6-

2) using cellulase (0.8U/mg) (SIGMA) in 0.05M sodium citrate buffer at 5% (w/v) PT RS concentration on a rotary shaker at 150rpm for 5.0 days. The incubation temperature was kept at 37 °C while the pH of the buffer was  $4.95 \pm 0.4$ . After the incubation period, the hydrolysis reaction was stopped by heating at 100°C for 20 mins. The cellulase enzyme was loaded at a different concentration to obtain the best enzymatic hydrolysis condition for sugar production, and samples were taken every 24 h for sugar concentration analysis. The enzymatic hydrolysis reaction was done in triplicate, and the average result was presented. The hydrolysates were stored at -20°C until used for analysis and hydrogen fermentation while the various RS enzymatic residues (HCl-PT RS, NaOH-PT RS and PE-PT RS) were washed extensively, dried and stored in a zip-lock back at RT until use. One unit of cellulase activity was defined as 1.0 µg reducing sugar equivalent released per min. Finally, the enzymatic conversion rate of the various PT RS residues was obtained as the percentage difference from the original sample before hydrolysis and after hydrolysis.

### **6.2.3 Lignin Determination Test**

Zhao et al. (2010) revised method was used in the de-lignification analysis. PT RS residue and untreated (500mg) powder forms (200µm) were placed in a 100 ml flask containing 35 ml of distilled water and then heated in a water bath at 80°C. After about 30 mins, a mixture of 0.5g of sodium chloride and 0.1 ml of acetic acid (100%) was added to the mix every hour thrice. The mixtures were filtered using the Buchner funnel, and then the residue was rinsed with distilled water. The RS residues were dried at 105°C for 24hr to determine their weight. The weight loss was considered as lignin content.

### **6.2.4 Detoxification of the Filtrate**

In HCl PT RS filtrate detoxification, Palmqvist and Hahn-Hagerdal (2000) protocol was used - The pH value of the original RS PT filtrate was adjusted to 10.0 by adding Ca (OH)<sub>2</sub> and was agitated for an hour. The pH value of this solution was then adjusted to 5.5 by adding H<sub>2</sub>SO<sub>4</sub> (1N). The precipitates

were removed, and activated carbon (1.5% w/v) was added to the supernatants. The mixture was stirred for an hour. Afterwards, the supernatant was collected and stored at -20°C for future use in hydrogen production.

## **6.2.5 Hydrogen Fermentation Process (Stage 1 Process)**

### **6.2.5.1 Batch fermentation process**

The acidogenesis setup was as outlined in Table 6-3 and discussed in Chapter 3, Section 3.8.1. The total biogas volumes produced by each BGDB were measured daily, and the hydrogen concentration (%) was determined as described in Chapter 3, Section 3.9. The bioreactors were identified throughout the study as HCl, PE and NaOH-PT RS, reflecting their respective PT RS substrates. The untreated RS was labelled as raw RS.

### **6.2.5.2 Continuous fermentation procedure**

After the batch hydrogen fermentation using the RS PT hydrolysates, the hydrogen production was switched over to a continuous process in a CSABR using RS PT hydrolysate as feedstock. The CSABR set-up was as defined in Table 6-3 and Chapter 3, Section 3.8.3. The cultivation was done in duplicates at the same conditions as the continuous hydrogen fermentation Chapter 3 Section 3.8.3. The CASBR was seeded with pre-treated and acclimatised DCS sludge to commence the digestion process. After the reactivation of the inoculum inside the bioreactors, the continuous fermentation was operated at OLR of 1.0 gCOD L<sup>-1</sup> added day<sup>-1</sup>. The fermentation lasted 40 days duration after steady-state conditions were achieved. The steady-state involves the daily draining of about 10% (of the reactor working volume) of the digestate using germ-free syringes and replacing it with the same equal amount of fresh medium consisting of the RS PT hydrolysate ammonium nitrogen carbonate (10g/L) and water. The reactors were purged with nitrogen for 5 min to provide oxygen-free conditions. Each of the reactors was connected to 500 mL gas bags for biogas collections, and the total biogas volumes



produced by each CSABR were measured daily, and the hydrogen content (%) was determined as described in Section 3.9.

Table 6-3: Operational parameters of hydrogen and methane fermentation processes

Operational Parameter	Hydrogen fermentation bioreactor (Stage 1)	
	Batch	CSABR
HRT	4 days	40days
Substrate Type	PT RS hydrolysates	PT RS hydrolysates
OLR	-	1.0 gCOD/sugar L <sup>-1</sup> added day <sup>-1</sup>
F/M	0.75	0.75
pH	5.5	5.5
Reactor size	500 mL	1 L
Temperature	55°C	55°C
	Methane fermentation bioreactor (Stage 2)	
	Fed-batch	CSABR
HRT	30 days (3 HRT)	40days
Substrate Type	VFA	VFA
OLR	1.0 gCOD L <sup>-1</sup>	1.0 gCOD L <sup>-1</sup> added day <sup>-1</sup>
F/M	0.40	0.40
pH	7.0	7.0
Reactor size	1 L	1 L
Temperature	37°C	37°C
	Methane fermentation bioreactor (Stage 3)	
	Batch	CSABR
HRT/SRT	30 days	60 days
Substrate Type	PT RS residues	PT RS residues
OLR	-	1.0 gTS L <sup>-1</sup> added day <sup>-1</sup>
F/M	0.40	0.40
pH	6.9	6.9
Reactor size	500 mL	5 L
Temperature	37°C	37°C

## 6.2.6 Methane Digestion Process (Stage 2 and 3 Processes)

### 6.2.6.1 Utilization of effluents (organic acids) and pretreated RS residues for methane production

The withdrawn effluents from the continuous reactor for hydrogen fermentation (stage 1 process) and the PT RS residue were used to produce methane. The seeded sludge employed was obtained from an active methane-producing sludge (the ADS) and acclimatised as stated in Chapter 3, Section 3.7.3. The methane digestion process was defined in two stages. a) In the stage 2 process, the fed-

batch mode was employed to produce methane using VFA as substrates, and feeding was done once every 10 days for three times with OLR of 1.0 gCOD L<sup>-1</sup> before switching the reactor to continuous mode via the CSABR system. In contrast, b) in the stage 3 process, batch mode and continuous systems (CSABR) were employed for methane production using the different RS PT residues as feedstock (Table 6-3).

The COD removal was calculated using Eqn 6-1, while a specific volume of the reactor supernatant was removed and replaced with the same amount of fresh effluent in the respective digesters from stage 1 continuous anaerobic fermentation process.

$$\text{COD removal (\%)} = \frac{\text{COD}_A \times \text{VOL}_{IN} - \text{COD}_B \times \text{VOL}_{OUT}}{\text{COD}_A \times \text{VOL}_{IN}} * 100 \quad \text{Eqn 6-1}$$

Where COD<sub>A</sub> is the COD of the effluent feeding, the VOL<sub>IN</sub> is the volume of effluent going in, COD<sub>B</sub> is the COD of the supernatant withdrawn from the methanogenic reactor, and VOL<sub>OUT</sub> is the volume of supernatant withdrawn from the methanogenic reactor.

Single-stage or process methane production was also conducted with raw RS using stage 3 defined conditions for comparison purposes. The cultivations were done in triplicates in the batch and fed-batch systems as defined in Chapter 3, Section 3.8.2. In addition to this, no pH adjustment of VFA effluents before addition to the reactor was required. On the other hand, the CSABR set-up and cultivation were as described in Chapter 3, Section 3.8.3 and 3.8.4, respectively. At pseudo-steady-state conditions, the reactors were fed with 1.0 gCOD L<sup>-1</sup> added d<sup>-1</sup> for 40days for VFA and 60 days for PT RS residues. In both states, a portion (10% of the reactor working volume) of the digestate was removed daily using sterile syringes and replaced with the same equal amount of fresh medium consisting of the substrates (SCOD or RS monitored daily. Each reactor was connected to a 1L Supel<sup>TM</sup>-Inert Multi-Layer Foil gas bag for daily gas sampling, while the total biogas volumes produced by each CSABR were measured daily, and the methane content (%) determined as described in Chapter 3, Section 3.9.

The alkalinity of the systems was sustained at FOS/TAC (*Fluchtige Organische Sauren* (mg HAc L<sup>-1</sup>)/ *Totales Anorganisches Carbonate* (mg L<sup>-1</sup> CaCO<sub>3</sub>) ratio 0.2 – 0.28, which was calculated by titrating the weekly effluents to pH 5.75 for partial alkalinity (PA) and pH 4.3 for the intermediate alkalinity (IA) (Lossie and Putz, 2008). The bicarbonate alkalinity (BA), the same as the PA, is corrected using Eqn 6-2.

$$BA = [TA - (0.85 \times 0.83 \times TVFA)] \quad \text{Eqn 6-2}$$

Where BA is the bicarbonate alkalinity in mg L<sup>-1</sup> CaCO<sub>3</sub>, TA is the total alkalinity measured in mg L<sup>-1</sup> CaCO<sub>3</sub>, and TVFA is the total volatile fatty acids in mg HAc L<sup>-1</sup>. Thus, the numbers of 0.85 and 0.83 are correction factors that consider 85% of ionization of the acids to the titration endpoint and acetic acid into alkalinity.

Finally, at the end of the experiment, the digestates from the various PT RS residue reactors were separated by centrifugation at 5000g for 15 min, dried at 80°C for 24 h and stored at RT for use in silica production, while the degree of degradation or percentage TS RS reduction calculated using Eqn 6-3.

$$TS_{red} = \frac{Q_{in} * TS_{in} - Q_r * TS_r}{Q_{in} * TS_{in}} * 100 \quad \text{Eqn 6-3}$$

Where Q<sub>in</sub> is the flow into the reactor, Q<sub>r</sub> is the flow out of the reactor, TS<sub>in</sub> is the TS content in the incoming substrates, and TS<sub>r</sub> is the TS content in the effluent.

### 6.2.7 Energy Value, Electricity, and Thermal Generation from Pretreated RS samples

The hydrogen and methane yield from the three stages in this study were used to calculate the corresponding lower calorific value (LCV) from different pre-treated RS for both the hydrolysates and the residues. The energy yields were estimated in kg and tonne of rice straw per weight for biogas and individual hydrogen and methane at 99% purity (Table 6-4). The biogas therein is considered a mixture of H<sub>2</sub> and CO<sub>2</sub> or CH<sub>4</sub> and CO<sub>2</sub>, while the energy value was presented in KJ/kg instead of KJ/m<sup>3</sup> using the densities of hydrogen and methane gas of 0.09 mg/ml and 0.716 mg/ml, respectively. From the

individual energy yield, the corresponding electricity and thermal yield were calculated using the conversion factors as listed in Table 6-2. Finally, the average values were used for the CCHP calculation.

Table 6-4: Data for calculation of energy equivalents, electricity and thermal yield

Reference	Unit	Value	Calorific value	% purity
1kWh	MJ	3.6		
1m <sup>3</sup> of methane (enriched)	kWh	9.97		99
1m <sup>3</sup> of methane (biogas)	kWh	6.94		70
1m <sup>3</sup> of methane	MJ	36	Lcv	99
1m <sup>3</sup> of biogas	MJ	25	Lcv	70
1m <sup>3</sup> of hydrogen	MJ	10.88	Lcv	99
1m <sup>3</sup> of hydrogen (biogas)	MJ	5.98	Lcv	55
CHP efficiency <sub>elect.</sub>	%	33-38		
CHP efficiency <sub>therm</sub>	%	45-50		

Data based on figures from (Poschl *et al.*, 2010) and Prager *et al.* (2019)

## 6.3 Results and Discussion

### 6.3.2 Preparation of Rice Straw Hydrolysate

#### 6.3.2.1 Pre-treatments of rice straw and de-lignification

The greatest challenge in using RS is the solubilisation of the carbon content. Since hydrogen is produced at the acidogenesis stage of the anaerobic fermentation, there is a need to break the complex structure of RS to liberate the sugar monomers for easy solubilisation. This difficulty in solubilisation is brought by the fermentable polysaccharide sugars (hexose and pentose) being masked by a non-fermentable lignin polymer (Kumar *et al.*, 2013 and 2015). Similarly, lignocellulose can resist degradation due to cell walls, which confers hydrolytic stability and structural robustness (Kratky and Jirout, 2011). The structural robustness is owing to the crosslinking of the polysaccharide's sugars (cellulose and hemicellulose) with the complex aromatic polymer (lignin) through ester and ether linkages (Kumar *et al.*, 2013). Hence, it is pertinent to detach the cellulose from the lignin first and realign the ultrastructural components to increase the surface area to a final particle size of 0.2 – 2mm (Kratky and Jirout, 2011) for effective hydrolysis through pre-treatments.

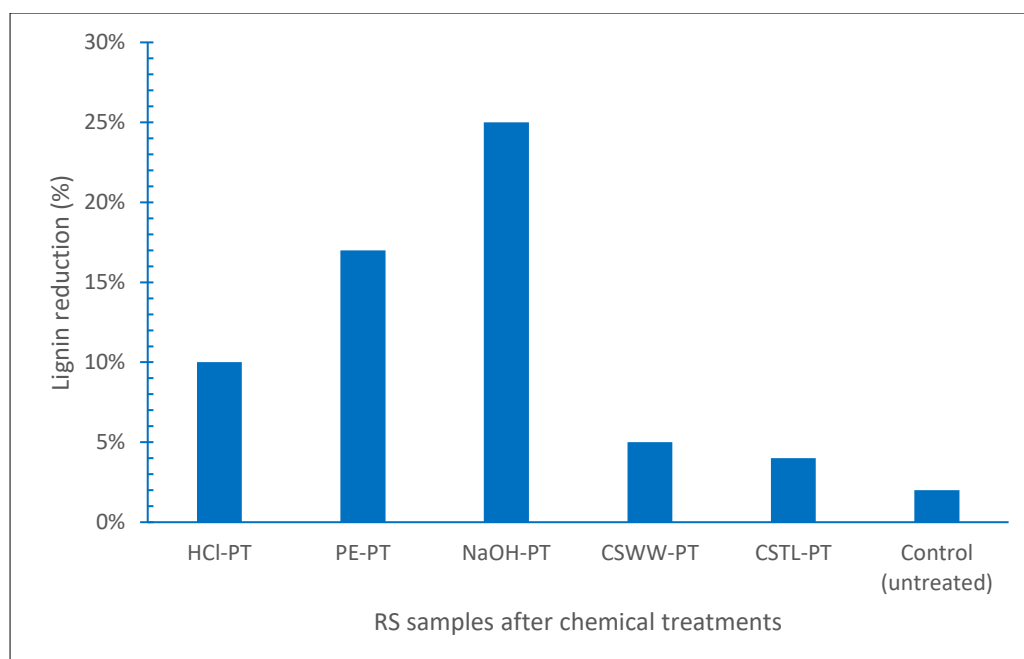


Fig 6-3: De-lignification of some chemical-PT RS samples represented as percentage lignin loss

In the study, pre-treatment of RS was done using 1M HCL, 2% NaOH and Solid NaOH. In addition, agro-industrial wastes (PE, CSTL and CSWW) were also employed in the pre-treatment. The effect of CSWW-PT at 4°C was insignificant on RS, and such CSWW-PT depicting CSWW at 121°C (hot CSWW PT) was used all through the discussion. Similarly, solid pre-treatment by amended He *et al.* (2008) was found to have effects close to the revised Zhang and Cai protocol, and as such, the latter was used and reported throughout the study. The de-lignification test was used as a good indicator of the hydrolysis rate, where the various PT RS residues were analysed for lignin reduction (Fig 6-3).

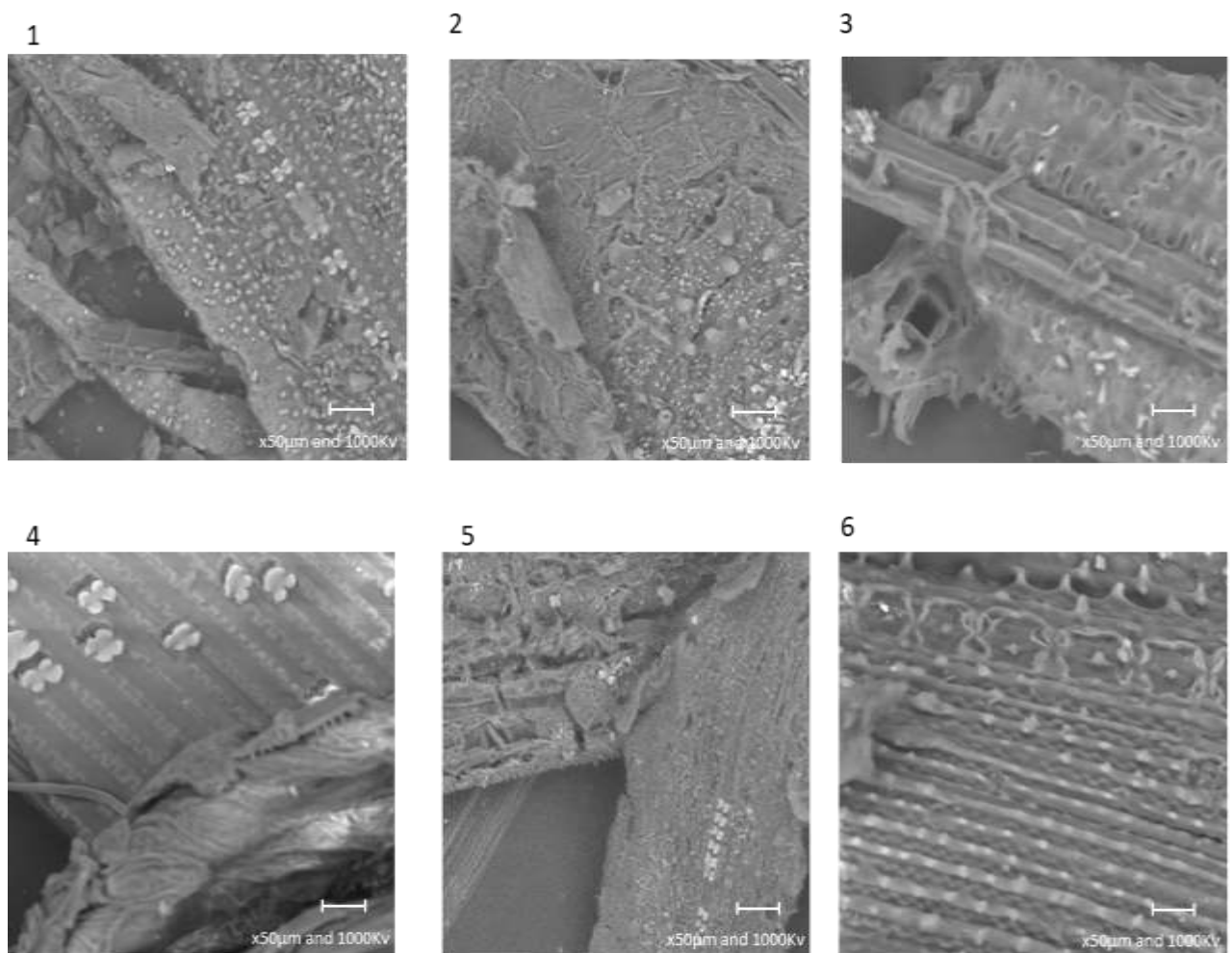


Fig 6-4: SEM micrographs of raw RS (1) and various PT RS (2: HCl, 3: PE, 4: NaOH, 5: CSTL and 6: CSWW) samples

The SEM micrographs of RS for untreated, HCl, NaOH, PE, CSWW and CSTL pre-treated RS are shown in Fig 6-4. The SEM results showed noticeable morphological and histological changes, more evident in NaOH and PE-PT RS residues. Similarly, the pictorial representation of the different pre-treated RS

residues is shown in Fig 6-5. As shown from the figure, there were morphological and physical changes that were brought about by physical and chemical pre-treatments as seen from “A and B” corresponding to 2mm sized RS and 750  $\mu\text{m}$  RS powder and from “C to G” analogous to different chemical PT RS residues (NaOH, HCl, CSWW, solid PE, and solid PE-PT RS).

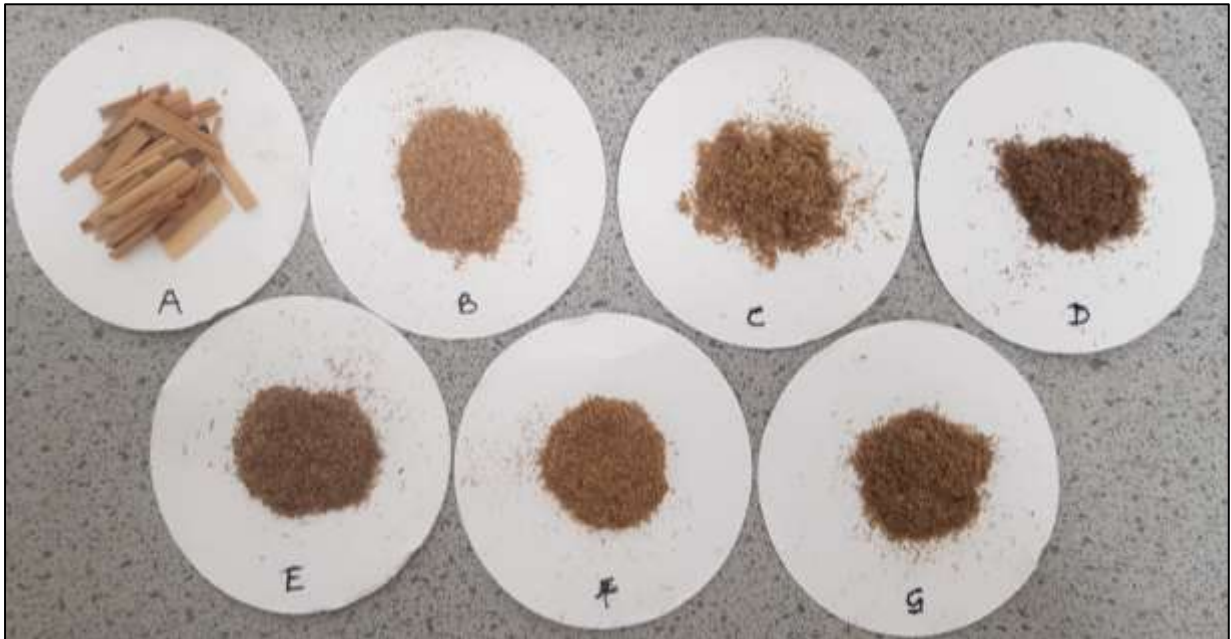


Fig 6-5: some PT RS samples (A: 2mm sized RS; B: Milled RS; C: NaOH-PT RS; D: HCl-PT RS; E: CSWW-PT RS; F: PE Solid PT; G: PE-PT RS samples)

The physical configuration of RS was the same as a result obtained by Zhang and Cai (2008), who recorded structural changes in their work on enzymatic hydrolysis of alkali pre-treated RS by *Trichoderma reesei* ZM4-F3. Morphologically, NaOH-PT RS had a woolly and curled appearance after pre-treatment, while PE-PT RS was wholly and had improved the particles' individuality after pre-treatment (Fig 6-5). The histological alterations in these residues were a result of the cleavage of the ester and ether bonds in lignin (Salakkam *et al.*, 2019), which created micro-pores and made the RS structure shrink giving rise to significant histological changes (Fig 6-4) (Cheng *et al.*, 2011b). The result was also in tandem with the findings from the de-lignification analysis where it was observed that lignin loss from the RS residues of NaOH and PE-PT RS residues were much more (25% and 17%, respectively) compared to other pre-treatments methods (Fig 6-3). The lignin removal is consistent

with the result obtained by Zhao *et al.* (2010), with lignin loss within the range of 7 – 17%. The de-lignification of RS from NaOH and PE-PT residues could also be from the dissolution of lignin components, which resulted in the rupturing of intermolecular bonds between lignin and hemicellulose, thereby improving the porosity of the RS biomass (Lo *et al.*, 2010; Cheng *et al.*, 2011b, Sattar *et al.*, 2016b and Salakkam *et al.*, 2019) and yield of cellulose (Zhu *et al.*, 2010). This dissolution is probably from the anionic and earth elements in PE (Table 3-1) and NaOH. As reported previously, PE is generally added as a softener during the cooking of hard and dry seeds or meats. This supplementation quickens the tenderness or shortens the time spent in meal preparation in Eastern Nigeria.

On the other hand, due to the low concentration of weak acids in CSWW and CSTL (Table 3-2), the effects of de-lignification were insignificant (Fig 6-3), which explains why the sugar content in the corresponding hydrolysates was low. This development also agrees with the result obtained with He *et al.* (2014). They recorded no significant change in lignin content after pre-treatment of RS using a hydrothermal treatment. More so, although there were minor tissue changes in acid PT RS samples, especially on the HCl PT RS sample (Fig 6-4), the lignin loss was better improved than raw RS residues (Fig 6-3 and 6-4). The changes in the morphology of acid PT RS samples were a result of hydrolysis of both the cellulose and hemicellulose via breakage of the  $\beta$ , 1-4 glucosidic bonds and reduction of the OH groups of glucosidic bonds, which made the fibrils collapse and look sparse (Salakkam *et al.*, 2019). Hence, more levels of reducing sugar in the HCl PT supernatant. In contrast, the raw RS (control) sample showed rigid and highly organised fibrils even after grinding (Fig 6-4 and 6-5). These results agreed with the outcomes obtained by Cheng *et al.* (2011b) on microwave-assisted alkali pre-treatment of rice straw and Pan *et al.* (2011) on dilute acid hydrolysis on cornstalks.



Table 6-5: Analysis of raw and various PT RS filtrates

Meaning	Reducing Sugar (g/L)	COD (g/L)	Total Carbon (g/L)	Inorganic carbon (g/L)	Total organic carbon (g/L)
HCL-PT RS	7.28	19.9	11.32	0	11.32
HCL-PT RS FILT	4.52	7.5	5.26	0	5.26
NaOH-PT RS	6.88	16.5	13.48	0.22776	13.25
NaOH-PT RS FILT	4.36	10.1	6.30	0	6.30
CSWW-PT RS @4	2.96	13.45	6.44	0	6.44
CSWW-PT RS @ 4 FILT	2.28	10.5	5.32	0	5.32
CSWW-PT RS @ 121°C	2.58	7.75	3.26	0	3.26
CSWW-PT RS @ 121°C FILT	2.38	4.45	2.57	0	2.57
PE-PT RS	6.64	17	11.52	1.3904	10.14
PE-PT RS FILT	4.4	8.1	6.64	0	6.64
CSTL-PT RS	2.68	10.9	5.55	0	5.55
CSTL-PT RS FILT	2.48	7.25	3.74	0	3.74
CONTROL	0.88	4.7	2.16	0	2.16
CONTROL FILT	0.54	2.9	1.47	0	1.47
CONTROL @ 4	3.1	1.05	1.05	0	1.05
CONTROL @ 4 FILT	1.65	0.92	0.92	0	0.92
SOLID PE-PT RS	ND	4.56	1.24	0	1.24
SOLID NaOH-PT RS	ND	7.16	2.57	0.4092	2.16
SOLID CONTROL	ND	6.76	2.63	0	2.63

The analysis of various raw and filtered PT RS extracts for reducing sugar (DNS), COD and TOC (ALPHA Standards)

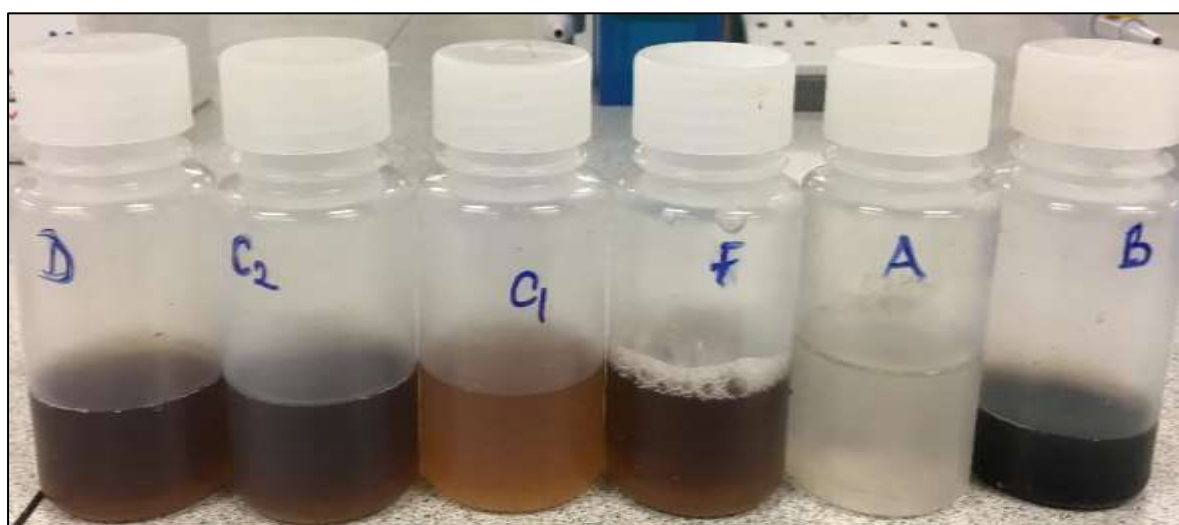


Fig 6-6: Detoxified or filtered samples of some PT RS hydrolysates A: HCl-PT; B: NaOH-PT; C<sub>1</sub>: Control, C<sub>2</sub>: PE-PT; D: CSWW-PT)

### 6.3.2.2 Rice straw hydrolysates detoxification

The RS filtrates were filtered to remove post-PT debris/inhibitors after pH neutralization, while the HCL-PT RS filtrates were detoxified before use for acidogenic fermentation. Then, the RS hydrolysates were stored in a sealed container (Fig 6-6) at -20°C after determining the reducing sugar concentration, COD, and total carbon content (Table 6-5). The reducing sugar concentrations (g/L) and the carbon contents (mg/L) of the filtered/detoxified RS hydrolysates were lower than the raw, unfiltered RS hydrolysates (Fig 6-2). The weight difference could be from some RS pre-treatments inhibitors, which may inhibit DF processes (Table 6-5) (Du *et al.*, 2010 and Monlau *et al.*, 2015). The reducing sugar (g/L) concentration was lower than the total organic carbon (mg/L). The reduced levels could also be from the removal of contaminants (furan derivatives (furaldehyde (furfural) and 5 – hydroxymethylfurfural (HMF))), phenolic compounds (vanillin and syringaldehyde) and salt complexes from the filtered samples. These RS PT contaminants have been found to inhibit fermentation processes by affecting glycolysis, damaging cell membrane and DNA and a total shift in fermentation pathway (Du *et al.*, 2010 and Bundhoo and Mohee, 2016). Therefore, it could be said that the lime–treatment and pH neutralisation before filtration removed some of these inhibitors (Fig 6-2 and 6-6) (Palmqvist and Hahn-Hagerdal, 2000 and Sambusiti *et al.*, 2013). Nevertheless, removing inhibitors also decreases the reducing sugar concentration and the filtrates sample's organic content (Table 6-5).

From the table, the reducing sugar (6.64 g/L) and the total organic carbon (11.52 g/L) of PE-PT RS filtrate were a bit closer to that of HCL-PT RS filtrates (reducing sugar (7.28 g/L) and the total organic carbon (11.32 g/L) and NaOH-PT RS filtrates (reducing sugar (6.88 g/L) and the total organic carbon (13.48 g/L), when compared to other pre-treatments alternatives – CSTL-PT RS (reducing sugar 2.68 g/L and total organic carbon 5.55 g/L) and CSWW-PT RS (reducing sugar 2.58 g/L and total organic carbon 3.26) and the control (reducing sugar 0.88 g/L and total organic carbon 2.16) (Table 6-5).

The use of weak acids as an alternative for lignocellulose PT has been widely documented due to disadvantages associated with strong chemicals, such as the formation of inhibitors, cost implications, and severe environmental concerns (Zhao *et al.*, 2010). Nonetheless, the lower yield of reducing sugar produced from CSTL-PT and CSWW-PT was probably because of the low concentration of weak acids (Table 3-2) < 1 mol. In contrast, the moderate COD concentration - CSTL-PT RS (7.75 g/L) and CSWW-PT RS (13.45) make both wastes a potential substrate for the AD process for methane and hydrogen production. This idea is exemplified by Zhao *et al.* (2010) on methane production from rice straw pretreated by a mixture of acetic-propionic acid. The RS hydrolysates produced are rich in acetic acid, propionic acid, glucose, and pentose sugars (arabinose and xylose) and were employed in methane production.

Chang *et al.* (2011) work on RS hydrolysis reported that about 99.3 g/L of hexose and 80.1 g/L of pentose could be obtained from 30g of RS in 100mL water, which are much higher than the results obtained from the research study. Therefore, the different pre-treatment methods, pre-treatment agents, and hydrolysis conditions such as temperature, duration of pre-treatment, and RS ratio volume could explain the reason behind the reduced sugar yield from the pre-treatment applied.

### 6.3.2.3 Enzymatic hydrolysis of rice straw samples

The dried PT RS residues (HCl-PT RS, NaOH-PT RS, and PE-PT RS) from chemical pre-treatments with significant delignification rate and raw RS were enzymatically hydrolysed by cellulase (0.8U/mg). However, before application on the various RS samples, the optimal hydrolysis conditions in terms of concentration of the cellulase enzyme (0.2 to 2.0g) per 1g RS sample and hydrolysis duration (0 to 5 days) were established following the method outlined in section 3.6 and using NaOH-PT RS as feedstock. The cellulase activity at various concentrations and durations is represented in Fig 6-7. From the figure, although there were steady increments of reducing sugars and total organic carbons (TOC) in all the different levels of cellulase employed from the first day, there were no significant

changes in the concentration of reducing sugars and TOC when cellulase concentration was increased to 1.0 and 2.0g from day 2 to 5. In contrast, reducing sugars and TOC levels were observed to increase from 24 to 48 h when the enzyme concentration of 500 mg was used. The concentrations of reducing sugars and TOCs also grew linearly until “day 5”, when the enzyme at 200mg amount was employed. In the control samples without cellulase, the reducing sugars and TOC levels were inconsequential.

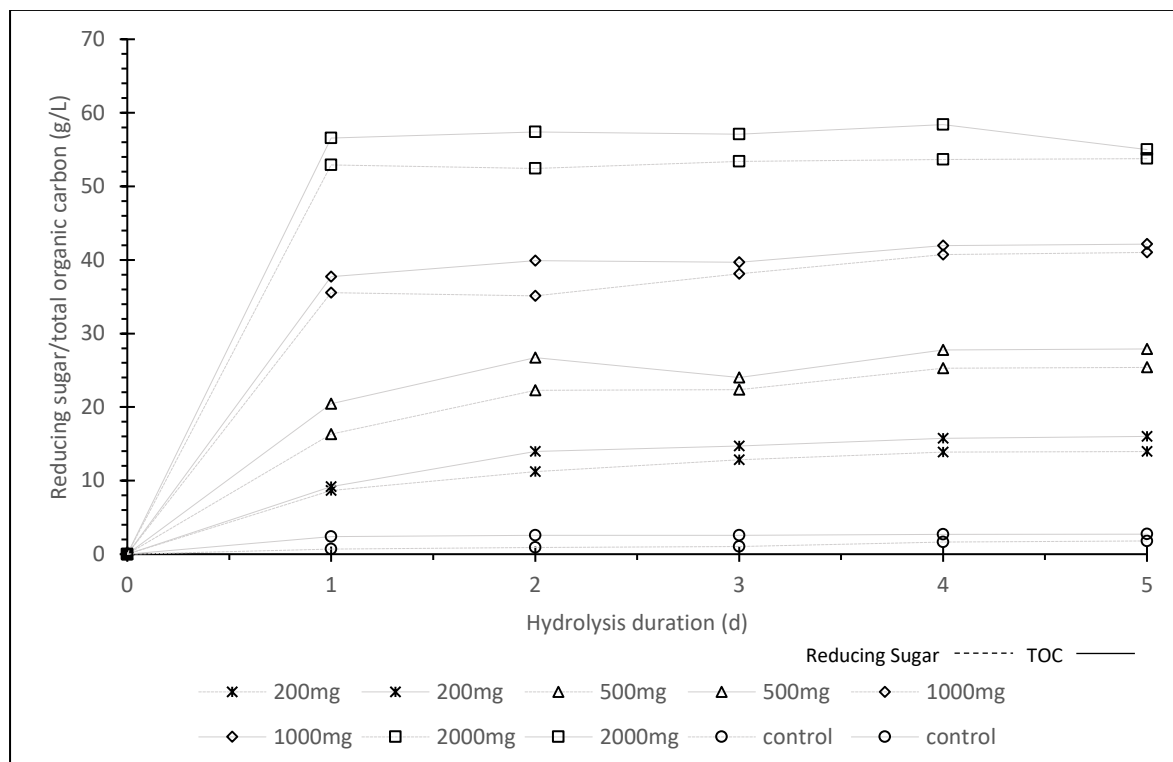


Fig 6-7: Cellulase activity at various concentrations and durations with cellulase enzyme at 500mg was used as the optimum concentration for 48 hrs on PT RS residues

Hence, the cellulase concentration at 500 mg and the duration of 48 hrs utilized in the RS hydrolysis were established and employed as the ideal concentration and time for the enzyme hydrolysis of the different PT RS residues. Even though the selected optimal conditions obtained vary from the results obtained from Zhang and Cai (2008), the result obtained is in line with the method employed by Pan *et al.*, 2011 on bio-augmented cellulosic hydrogen production from cornstalk. Furthermore, the established optimal standards tally closely with the findings by Gao *et al.* (2020) on their work on enhanced enzymatic hydrolysis of RS via PT with deep eutectic solvents-based micro-emulsions. The

established duration of 48 hrs employed in the hydrolysis was also within the range of 24 – 50 hrs used by Quéméneur *et al.* (2012a). The differences from the outcome of Zhang and Cai (2008) study could be from RS sample sizes, nature and purity of the enzyme materials and mode of enzymatic hydrolysis.



Fig 6-8: Representative of RS hydrolysate after enzyme hydrolysis

Table 6-6: Analysis of enzyme PT RS Hydrolysates

RS PT Residues	Enzyme Conversion (%)	Reducing Sugar (g/L)	Reducing Sugar (g/g TS RS)	TOC (g/L)	VFA (g/L)
HCl PT RS	17	26.5	0.49	30.2	0.02
PE PT RS	28	30.5	0.56	33.4	0.03
NaOH PT RS	36	34.0	0.62	37.3	0.04
Raw RS	8	8.5	0.16	10.5	0.012

After the ideal conditions were determined, the enzymatic hydrolysis of the various PT RS residues was carried out. Subsequently, after the enzyme solubilisation (Fig 6-8), the pH of the different PT RS hydrolysates was within the range of 6.0 to 6.5. The experimental result of the reducing sugars, TOC and enzymatic conversion rate from the various PT RS residues is summarised in Table 6-6. From the table, both NaOH and PE-PT RS residues had the highest enzyme conversion rate of 36% and 28%, respectively. Therefore, the reducing sugar (g/g TS RS) yield from the various RS PT residues is almost

close to the maximum predicted value of 0.56 obtained by Pan *et al.* (2011), even though the substrates employed are different.

In addition to this, the highest reducing sugars (34.0 and 30.5 g/L) and TOC (37.3 and 33.4 g/L) from NaOH-PT RS and PE-PT RS respectively show that the cellulase enzyme had more access to the RS hollo-cellulose components. The enzyme accessibility is a result of removal of lignin (Fig 6-3) and creation of micro-pores on the RS structure that was brought about by pre-treatment (Zhang and Cai, 2008 and Salakkam *et al.*, 2019) with either NaOH or PE when compared with raw RS which had the least enzyme conversion rate of 8% with resultant 8.5 g/L reducing sugar and TOC of 10.5 g/L. Although the enzyme conversion rate from HCl PT RS residue was 17%, the reducing sugar (26.5 g/L) and TOC (30.2 g/L) (Table 6-6) was found to be nearly as close as to those of NaOH and PE despite having reduced de-lignification activity (Fig 6-3). The good yield of sugars could be from the exposure of cellulase enzyme to cellulose brought about by the rupturing of  $\beta$  1, 4-glucosidic bonds and hence, some collapse of the cellulose polymers to sugars monomers. The result was also confirmed from the SEM images reported above (Fig 6-4). A small amount of VFA, mainly acetic acid in all the pre-treated samples, could not be explained (Table 6-6). Nonetheless, it is suggested they could have emanated from gradual degradation of reducing sugars during post hydrolysis processes and possibly during storage before application for hydrogen production.

### **6.3.3 Hydrogen Fermentation Process (Stage 1 Process)**

The hydrogen yield from chemically PT RS hydrolysates was within the range of 10 – 15 NmL H<sub>2</sub> g<sup>-1</sup> COD (figure not included), which is a result of low concentration of reducing sugars (Table 6-6) and the presence of inhibitors (such as phenolic compounds) which have inhibitory effects on hydrogenotrophic microorganisms (Quéméneur *et al.*, 2012b, Kumar *et al.*, 2015 and Monlau *et al.*, 2015). This argument asserts the results obtained by Chang *et al.* (2011) and reviews by Kapdan and Kargi (2006) on their assessment on bio-H<sub>2</sub> production from wastes, where it was shown that H<sub>2</sub> could

be produced in high quantities from sugar-containing wastes. Moreover, hydrogen is produced as a glucose consumption “product” during the acidogenic phase in an AD process (Eqn 2-9 and 2-10). Therefore, the amount of glucose in a solution or substrates correlates directly with the yield of hydrogen gas (Monlau *et al.*, 2012), while the evolution of H<sub>2</sub> responds inversely as reducing sugar depreciates. These arguments are affirmed with the yield of H<sub>2</sub> from enzymatically PT RS hydrolysates (Fig 6-9 and Fig 6-10).

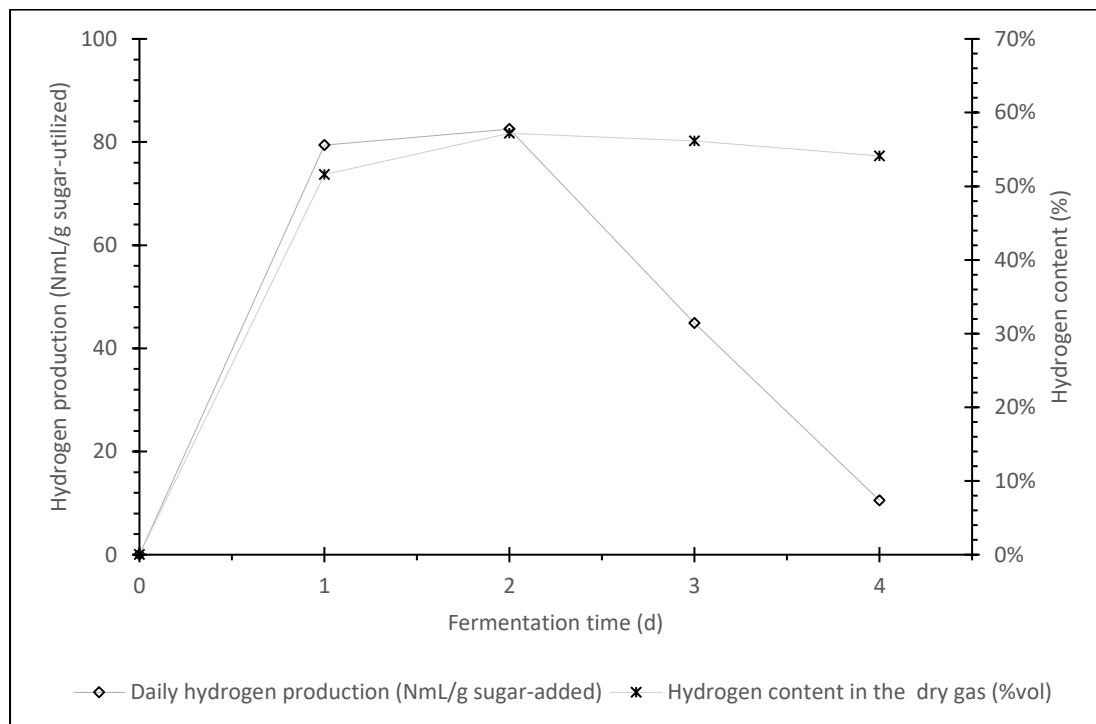


Fig 6-9: Daily hydrogen production (mL g<sup>-1</sup> sugar-utilized) and hydrogen content (%) from enzymatically PT RS residues via batch mode

The daily volumetric hydrogen production (NmL g<sup>-1</sup> sugar-utilized) and hydrogen content of enzymatically PT RS hydrolysates are shown in Fig 6-9 and Fig 6-10. After the enzyme hydrolysis of the various PT RS residues, the resultant hydrolysates (Fig 6-8) were pulled together and converted to H<sub>2</sub> gas via batch (Fig 6-9) and continuous process (Fig 6-10). The hydrogen production profile was simulated by reversed Gompertz equation, and it is observed from the batch result that while the biogas yield was 321 NmL g<sup>-1</sup> sugar-utilized, the cumulative hydrogen and the mean hydrogen content

were 221 NmL H<sub>2</sub> g<sup>-1</sup> sugar-utilized and 55%, respectively (Fig 6-9). Furthermore, the maximum hydrogen rate was 104 ± 2 NmL H<sub>2</sub> d<sup>-1</sup>, and the R-square value of 0.999 showed that the fermentation process was good. The production rate disagrees with those obtained by Lo *et al.* (2010) using xylanase on alkaline pre-treated RS and Kannah *et al.* (2019) bio-hydrogen production from RS pre-treated with dispersion thermochemical disintegration (DTCD). The disparities could be due to differences in the type and concentration of enzyme utilized, mode of alkaline pre-treatment and enzyme hydrolysis, and duration of H<sub>2</sub> production. Nonetheless, the hydrogen yield tallies with Dong *et al.* (2020) findings, where the maximum H<sub>2</sub> produced is 213.06 NmL H<sub>2</sub> g<sup>-1</sup> substrate after pre-treatment of RS with 3% NaOH and 6% urea for 15 days. The study also agrees closely with those obtained by Cheng *et al.* (2011b) on H<sub>2</sub> production from pre-treated RS. They achieved a maximum hydrogen yield of 155 NmL H<sub>2</sub> g<sup>-1</sup> TVS after RS was pre-treated with microwave-assisted alkali in addition to enzymatic hydrolysis. The research findings also agree with An *et al.* (2020a) and Zhang *et al.* (2020). They produced a VHY of 226 NmL g/ substrate and 222 NmL H<sub>2</sub> utilized-sugars.

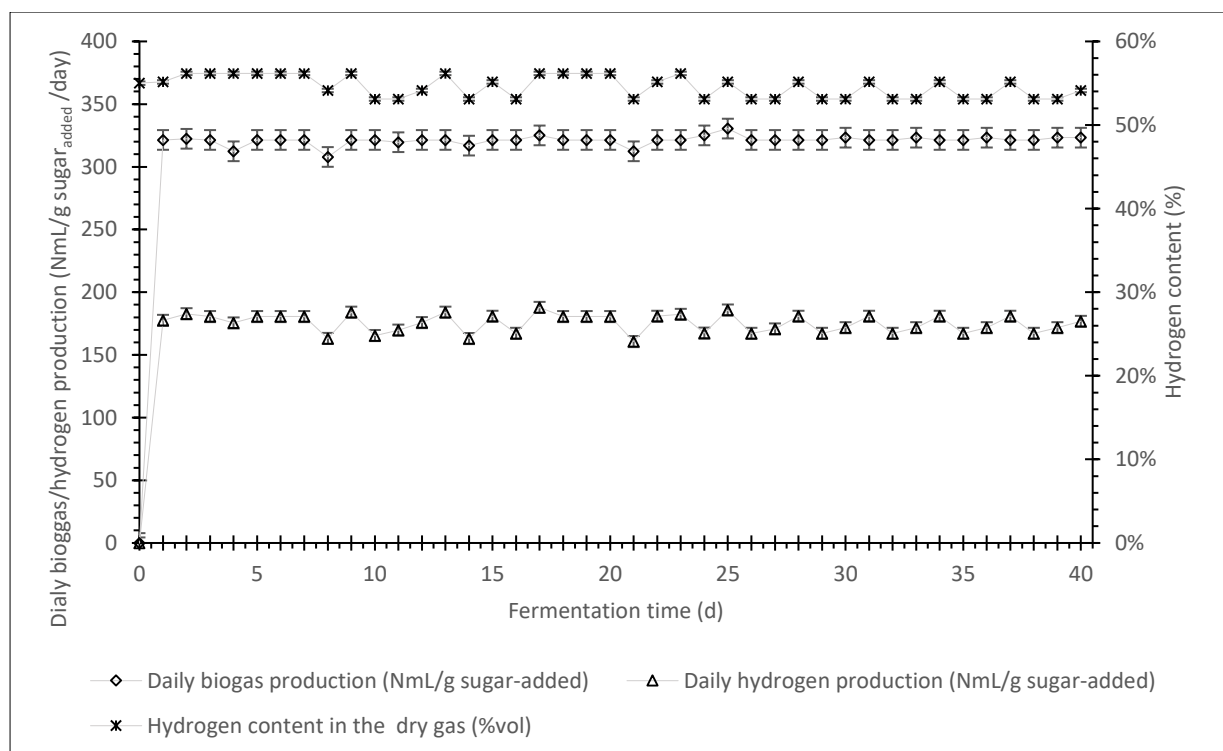


Fig 6-10: Daily hydrogen production (mL g<sup>-1</sup> sugar-utilized) and hydrogen content (%) from enzymatically PT RS residues via CSABR



Similarly, the result of CSABR indicated that the hydrogen content was within the range of 53 – 56%, and the minimum and maximum daily VHP of 163 and 185 NmL H<sub>2</sub> g<sup>-1</sup> sugar-utilized.d<sup>-1</sup> respectively were achieved (Fig 6-10). The mean specific biogas yield from the CSABR fermentation was 321 NmL g<sup>-1</sup> COD sugar-utilized d<sup>-1</sup>. The result obtained from the batch and continuous systems was validated using the theoretical yield of hydrogen from RS and was within the range. The theoretical hydrogen yield from RS using an AD system is 301 NmL H<sub>2</sub> g<sup>-1</sup> TVS (Cheng *et al.*, 2011b). Although the maximum SHY of 209.8 mL/g-TVS achieved by Pan *et al.* (2011) is slightly higher than the obtained values from this study, the key differences perhaps is from the feedstock and processes applied. In both the batch and CSABR hydrogen fermentation systems, the mixed H<sub>2</sub> gas was methane free.

Table 6-7: Hydrogen and biogas yield using hydrolysates from various PT RS residues

RS PT Hydrolysates	Reducing Sugars (g/g TS)	Batch Reactor		Continuous Reactor	
		Cumulative H <sub>2</sub> production (NmL g <sup>-1</sup> TS)	Cumulative biogas production (NmL g <sup>-1</sup> TS)	Daily H <sub>2</sub> production (NmL g <sup>-1</sup> TS d <sup>-1</sup> )	Daily biogas production (NmL g <sup>-1</sup> TS d <sup>-1</sup> )
HCl	0.49	109	159	91	159
PE	0.56	123	179	103	179
NaOH	0.62	137	198	114	199
Raw	0.16	35	51	30	51

Note: Result values were calculated from the data obtained from Fig 6-8, 6-9 and Table 6-6 with de-lignification percentage (Fig 6-2) also considered.

The specific hydrogen and biogas yield using hydrolysates from various PT RS residues is presented in Table 6-7 for batch and continuous systems. The cumulative and daily biogas production were almost in the same range for the reactor systems with NaOH and PE-PT RS hydrolysate having the highest value of 199 and 179 NmL g<sup>-1</sup> TS, respectively, when the continuous system was used (Table 6-7). The specific biogas yield for HCl-PT RS hydrolysate and raw RS was 159 and 51 NmL g<sup>-1</sup> TS, respectively, under CSABR mode. While the SHY from batch and the daily VHP from CSABR systems differed slightly, the highest values were from NaOH-PT hydrolysates (for batch (137 NmL H<sub>2</sub> g<sup>-1</sup> TS d<sup>-1</sup>) and CSABR (114 NmL H<sub>2</sub> g<sup>-1</sup> TS d<sup>-1</sup>) and PE-PT RS filtrates (for batch (123 NmL H<sub>2</sub> g<sup>-1</sup> TS d<sup>-1</sup>) and CSABR (103 NmL H<sub>2</sub> g<sup>-1</sup>

TS d<sup>-1</sup>) compared to enzymatically hydrolysed raw RS which gave cumulative H<sub>2</sub> production of 35 NmL H<sub>2</sub> g<sup>-1</sup> TS d<sup>-1</sup> from batch mode and VHP of 30 NmL H<sub>2</sub> g<sup>-1</sup> TS d<sup>-1</sup> from continuous mode (Table 6-7). Subsequently, the cumulative H<sub>2</sub> production of HCl PT RS samples was 109 NmL H<sub>2</sub> g<sup>-1</sup> TS d<sup>-1</sup> from the batch systems and VHP of 91 NmL H<sub>2</sub> g<sup>-1</sup> TS d<sup>-1</sup> from CSABR. These results show that chemical pre-treatment before enzymatic exposure of lignocellulose is essential to ensure maximum hydrolysis. This hypothesis is also confirmed from the SEM micrograph above (Fig 6-4).

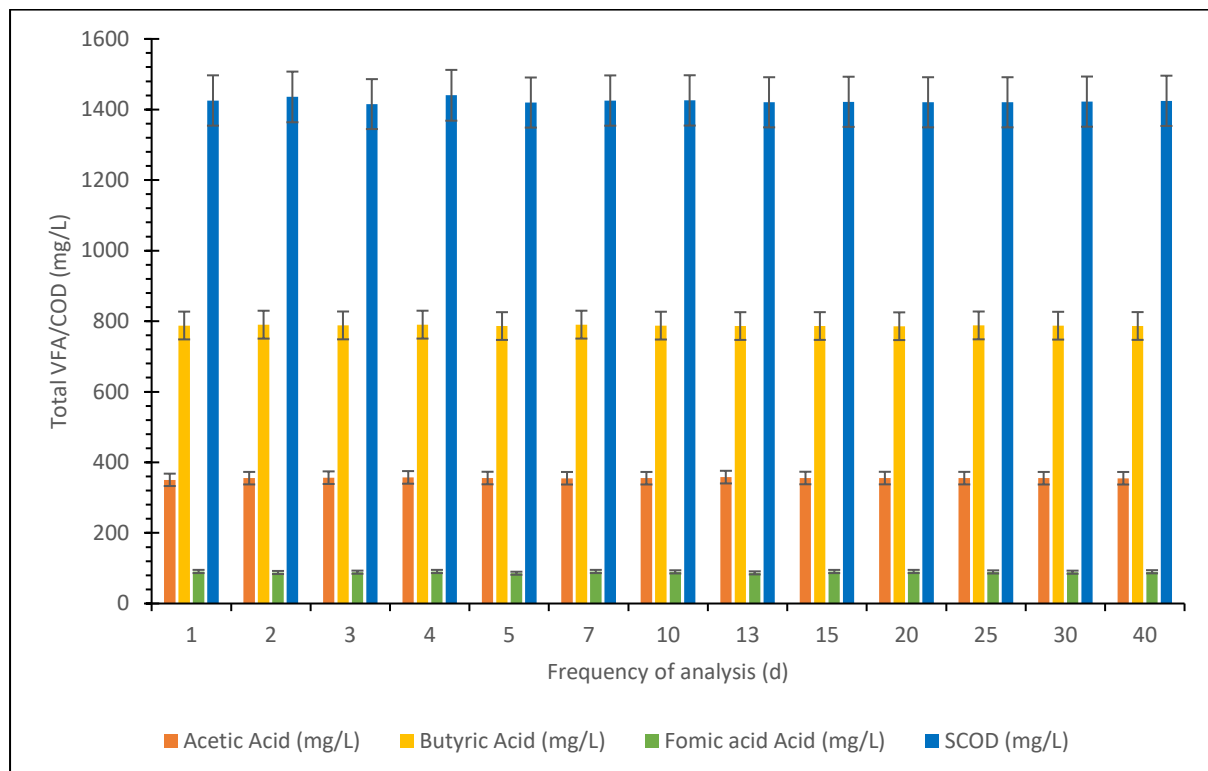


Fig 6-11: The associated VFA production after DF H<sub>2</sub> fermentation for continuous systems

### 6.3.4 Production of Short-chain Fatty Acids

The low levels of short-chain Fatty Acids (SCFA) in the hydrolysates (Table 6-6) after enzymatic pre-treatment did not inhibit hydrogen fermentation due to the high content of reducing sugars in the various hydrolysates favouring acidogenesis. Hence, the evolution of hydrogen and carbon dioxide gases with more volatile fatty acids. The most predominant volatile fatty acids (VFA) after the batch fermentation, which was acetic acid (HAc) (360.80 mg L<sup>-1</sup>), butyric acid (HBu) (792.8 mg L<sup>-1</sup>) and formic acid (Hfo) (78.9 mg L<sup>-1</sup>), agrees with the report of Ai *et al.* (2013) and Li *et al.* (2018). Figure 6-10 shows

the associated VFA production after DF H<sub>2</sub> fermentation for continuous systems. The pH after batch fermentation which was found to be 4.85 ± 0.5 (Table 6-10), indicated the presence of VFA (Eqn 2-9 and 2-10), and as such, the pH of the continuous system was maintained at 5.5 ± 0.2 using 5M NaOH. The production of various VFA also affirmed the hydrogen production rate from batch and continuous systems (Fig 6-11 and Table 6-8), and the results accomplished; H<sub>2</sub> was produced more than HAc and H<sub>2</sub>O, indicating that the fermentation pathway was mainly from the pyruvate: ferredoxin oxidoreductase (PFOR) (Holladay *et al.*, 2009).

There was an insignificant propionic acid concentration (200 µg L<sup>-1</sup>), signifying less solvent production tendencies. After the steady-state was established, the mean daily TVFA was 1232.5 mg L<sup>-1</sup>, comprising acetic acid, butyric acid, and formic acid as 355.4 mg L<sup>-1</sup>, 787.8 mg L<sup>-1</sup> 89.3 mg L<sup>-1</sup>, respectively (Fig 6-11). Similarly, the daily SCOD of the CSABR effluents were within the range of 1415.30 to 1435.60 mg L<sup>-1</sup>.

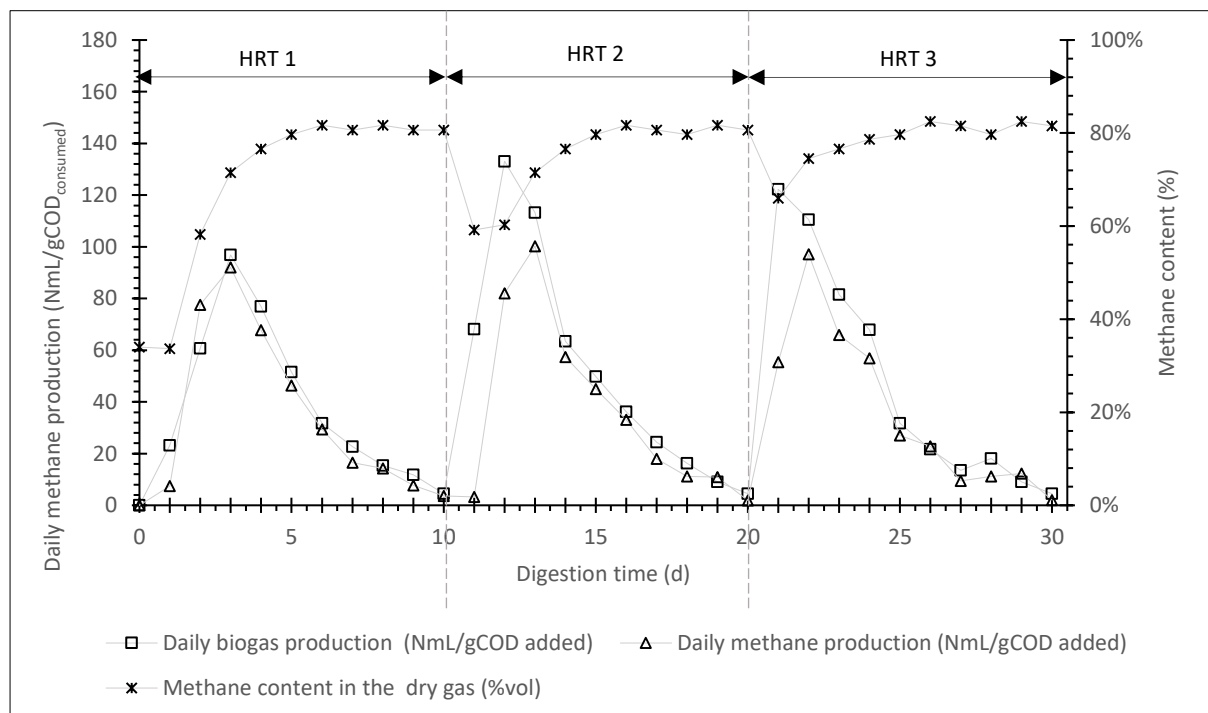
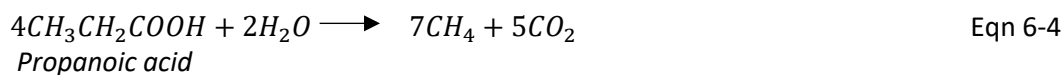


Fig 6-12: Fed-batch methane production from acidogenesis effluents (stage 2) after 3 HRTs.

Table 6-8: VFA, SCOD and Nitrogen content of reactor effluents and methane sludge

Sample Source	Acetic Acid (mg L <sup>-1</sup> )	Butyric Acid (mg L <sup>-1</sup> )	Formic Acid (mg L <sup>-1</sup> )	Soluble COD (mg L <sup>-1</sup> )	pH value	Ammonium Nitrogen (mg/L)
Heat-shocked DCS	407.25	270.00	107.80	920.45	8.62 ± 0.4	272.00
H <sub>2</sub> Batch Reactor	587.81	607.34	186.70	1640.43	4.85 ± 0.5	263.50
Initial H <sub>2</sub> CASBR	280.56	235.60	89.34	970.80	4.87 ± 0.3	230.52
ADS	780.24	220.78	NA	1210.65	8.50 ± 0.3	263.76
CH <sub>4</sub> Digesters	~400.00	~121.00	NA	~600.00	6.89 ± 0.3	~225..00
VFA methane batch digesters	25 - 30	NA	NA	NA	7.03 ± 0.2	NA



### 6.3.5 Production of Methane from Acidogenic Effluents (Stage 2 Process)

In the DF processes for hydrogen production from glucose, as previously stated, there is concomitant evolution of organic acids with acetate (Eqn 2-9) and butyrate (Eqn 2-10) as the most important soluble metabolites (Fig 6-11 and Table 6-8). These organic acids (including propanoic acid) were utilized in methane gas production (Eqn 2-17 and 6-4) to maximise the overall economic and energy value of the applied biomass (RS). The fermentation was done using a fed-batch process with feeding done once every 10 days thrice before switching the reactor to continuous mode via the CSABR system. Once the steady-state is established in the stage 2 process, the effluents from acidogenic continuous reactors were fed directly to the continuous stirred anaerobic bioreactor (CSABR) for methane production after debris removal. The methane production from the acidogenic effluents employing a fed-batch system is presented in Fig 6-12. It can be observed from the figure that methane was produced at a spontaneous rate within the first 4 days, which shows that acidogenic effluents are the ideal substrate for methane production. This idea was also shared by An *et al.* (2020b) and Qian *et al.* (2020). The acclimatisation of ADS before use in the AD process using effluents as substrates was also the reason for the high methane production rate. Although most methanogens grow slowly,

especially the acetoclastic methanogens (the generation time of *Methanosaeta* is 3.4 – 9 days) due to low energy yield from the methanogenesis pathway (Gerardi, 2003), the acclimatisation period ensures the complete growth of most acetoclastic methanogens.

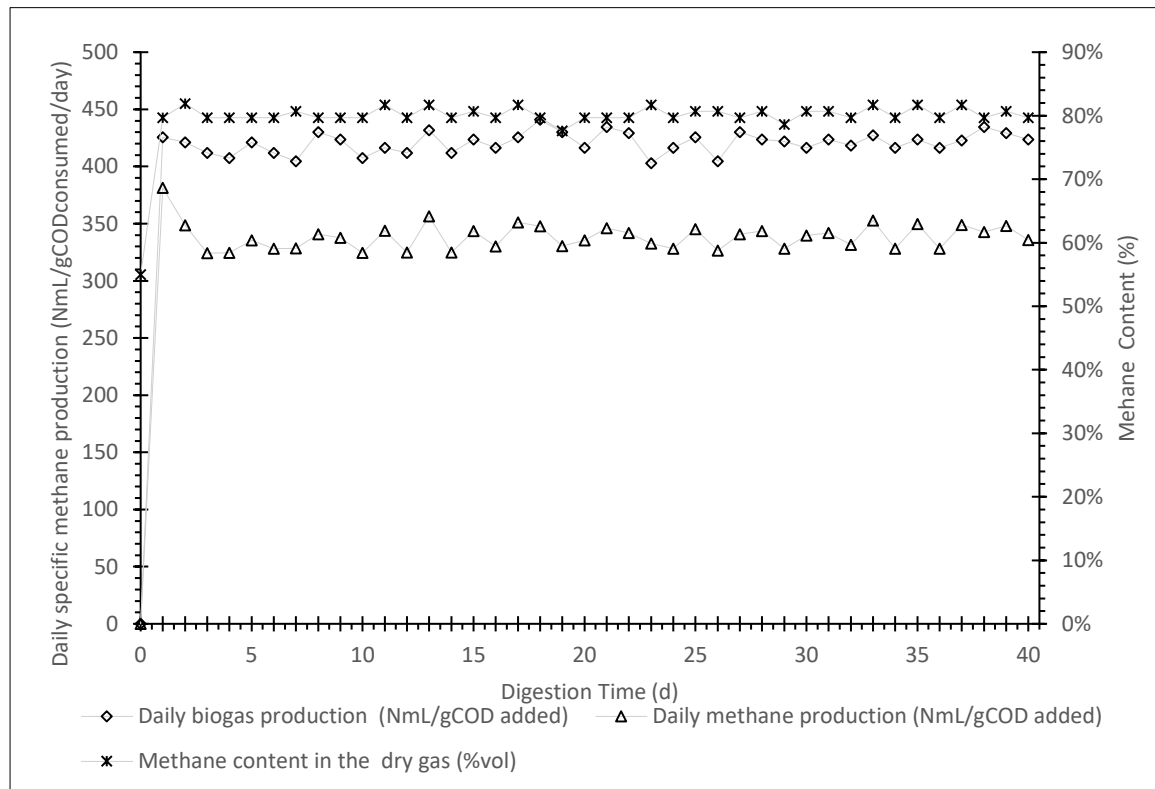


Fig 6-13: Continuous methane production from acidogenesis effluents (stage 2)

The mean SMY of  $362 \text{ NmL CH}_4 \text{ g}^{-1} \text{ COD}_{\text{consumed}}$  and the mean biogas yield of  $465 \text{ NmL g}^{-1} \text{ COD}_{\text{consumed}}$  were produced using the fed-batch systems after 3 HRTS (Fig 6-12). The reactors' highest and mean methane content of 80% and 75% were achieved using the fed-batch approach. Subsequently, the result of the continuous methane production from acidogenesis effluents is shown in Fig 6-13. The result obtained showed that using the continuous mode, the mean daily SMP was  $330 \text{ NmL CH}_4 \text{ g}^{-1} \text{ COD}_{\text{consumed}} \text{ d}^{-1}$ , and daily biogas yield was  $411 \text{ NmL g}^{-1} \text{ COD}_{\text{consumed}} \text{ d}^{-1}$ , while the average methane content is 80%. The theoretical methane yield at standard temperature and pressure for  $1.0\text{g CH}_3\text{COOH}$  and  $1.0\text{g CH}_3\text{CH}_2\text{COOH}$  is about 400 mL and 570 mL, respectively (Zhoa *et al.*, 2010); therefore, the findings are within the range of theoretical values. The results achieved were close to

the study outcome by Akobi *et al.* (2016) and An *et al.* (2020a and b). Methane production of 369, 341 and 376 NmL g<sup>-1</sup> COD<sub>consumed</sub> respectively were recorded from first stage acidogenic effluents. The consumption of VFA to methane was confirmed following an analytical test before and after the fermentation, where remaining VFA contents from the methane reactors were almost negligible (HAc 20 - 35 ± 0.2 mg/L (Table 6-8). The COD removal/ conversion rate of 81% for methane production at steady-state and 91% at batch system tallies with Akobi *et al.* (2016) study. The conversion rate was calculated by dividing the methane accumulation by theoretical methane yield of 400 mL/g COD<sub>consumed</sub> at 37<sup>o</sup>C (An *et al.*, 2020b).

Table 6-9: CH<sub>4</sub> and biogas yield using acidogenic effluents from various PT RS residues

RS PT Hydrolysates	TVFA (gCOD /gTS)	Batch Reactor		Continuous Reactor	
		SMY (NmL g <sup>-1</sup> TS)	Biogas yield (NmL g <sup>-1</sup> TS)	Daily SMP (NmL g <sup>-1</sup> TS d <sup>-1</sup> )	Daily biogas production (NmL g <sup>-1</sup> TS d <sup>-1</sup> )
HCl	0.30	110	142	100	125
PE	0.34	124	159	113	141
NaOH	0.38	138	177	126	156
Raw	0.10	36	46	33	41

The table above is calculated from acidogenic effluents with 1.0g reducing-sugar producing 615 mg L<sup>-1</sup> TVFA (comprising of acetic acid (HAc) (175.4 mg L<sup>-1</sup>), butyric acid (HBu) (317.5 mg L<sup>-1</sup>) and formic acid (Hfo) (89.3 mg L<sup>-1</sup>) and from Table 6-6.

The specific methane and biogas yield using acidogenic effluents from various PT RS residues is presented in Table 6-9 for batch and continuous systems. The table was calculated using Eqn 6-1, and the daily SCFA produced, which was 615 mg L<sup>-1</sup> g<sup>-1</sup> sugar-utilized. The daily SCFA value was obtained from the differences between the daily total SCFA (Fig 6-11) and the initial SCFA from the DCS (Table 6-8).

The SMY and biogas accumulation was significantly higher from PT RS residues than the raw for the two systems, with NaOH and PE-PT RS hydrolysate having the highest values. In batch mode, whereas NaOH PT reactors gave 138 NmL CH<sub>4</sub> g<sup>-1</sup> TS and 177 NmL g<sup>-1</sup> TS for SMY and biogas yield, PE-PT reactors

gave 124 NmL CH<sub>4</sub> g<sup>-1</sup> TS and 159 NmL g<sup>-1</sup> TS for SMY and biogas yield. A similar outcome was achieved for continuous systems where NaOH PT reactors gave 126 NmL CH<sub>4</sub> g<sup>-1</sup> TS and 156 NmL g<sup>-1</sup> TS for daily SMP and biogas production, respectively (Table 6-8). PE-PT reactors also gave 113 NmL CH<sub>4</sub> g<sup>-1</sup> TS and 141 NmL g<sup>-1</sup> TS for daily SMP and biogas production.

The increase in SMP, SMY, daily biogas production, and biogas yield from PT samples is because of improved production of TVFA during their respective acidogenesis in stage 1 of 0.30 to 0.38 g COD/ TS compared to raw RS that gave TVFA of 0.10 g COD/ TS.

### **6.3.6 Production of Methane from Pretreated RS Residues (Stage 3 Process)**

Like any lignocellulose biomass material, the utmost limitation in using rice straw for energy production, which needs to be resolved before rice straw can be hydrolysed and used for bio-hydrogen production, is de-lignification and deconstruction of its rigid structure (Wei *et al.*, 2014). Therefore, there is a need to detach the cellulose from the lignin first and realign the ultrastructural components to increase the surface area to a final particle size of 0.2 – 2mm (Kratky and Jirout, 2011) for effective solubilisation through pre-treatments. Having said this, the leftover residues from the various enzymatically PT RS were used for methane production via batch and continuous systems. Nevertheless, the control (raw/untreated RS) was used for practical comparison analysis. Fig 6-14 (a-d) shows the methane production from different PT RS residues using batch mode, while Table 6-10 is the Gompertz data for the methane production from the various PT RS residues. The highest SMY of 360 NmL CH<sub>4</sub> g<sup>-1</sup> TS and 335 NmL CH<sub>4</sub> g<sup>-1</sup> TS with volumetric methane production rate of 38.07 mL d<sup>-1</sup> and 33.85 mL d<sup>-1</sup> were obtained from NaOH and PE-PT RS residues, respectively compared to SMY of 303 NmL CH<sub>4</sub> g<sup>-1</sup> TS with a methane production rate of 23.17 mL d<sup>-1</sup> from HCl-PT RS residue and SMY of 267 NmL CH<sub>4</sub> g<sup>-1</sup> TS with a methane production rate of 22.22 mL<sup>-1</sup> d from raw RS (control) (Table 6-10). The result is consistent with the values obtained by Mustafa *et al.* (2016) on fungal pre-treatment of rice straw with *Pleurotus ostreatus* and *Trichoderma reesei* to enhance methane production under solid-state anaerobic digestion.

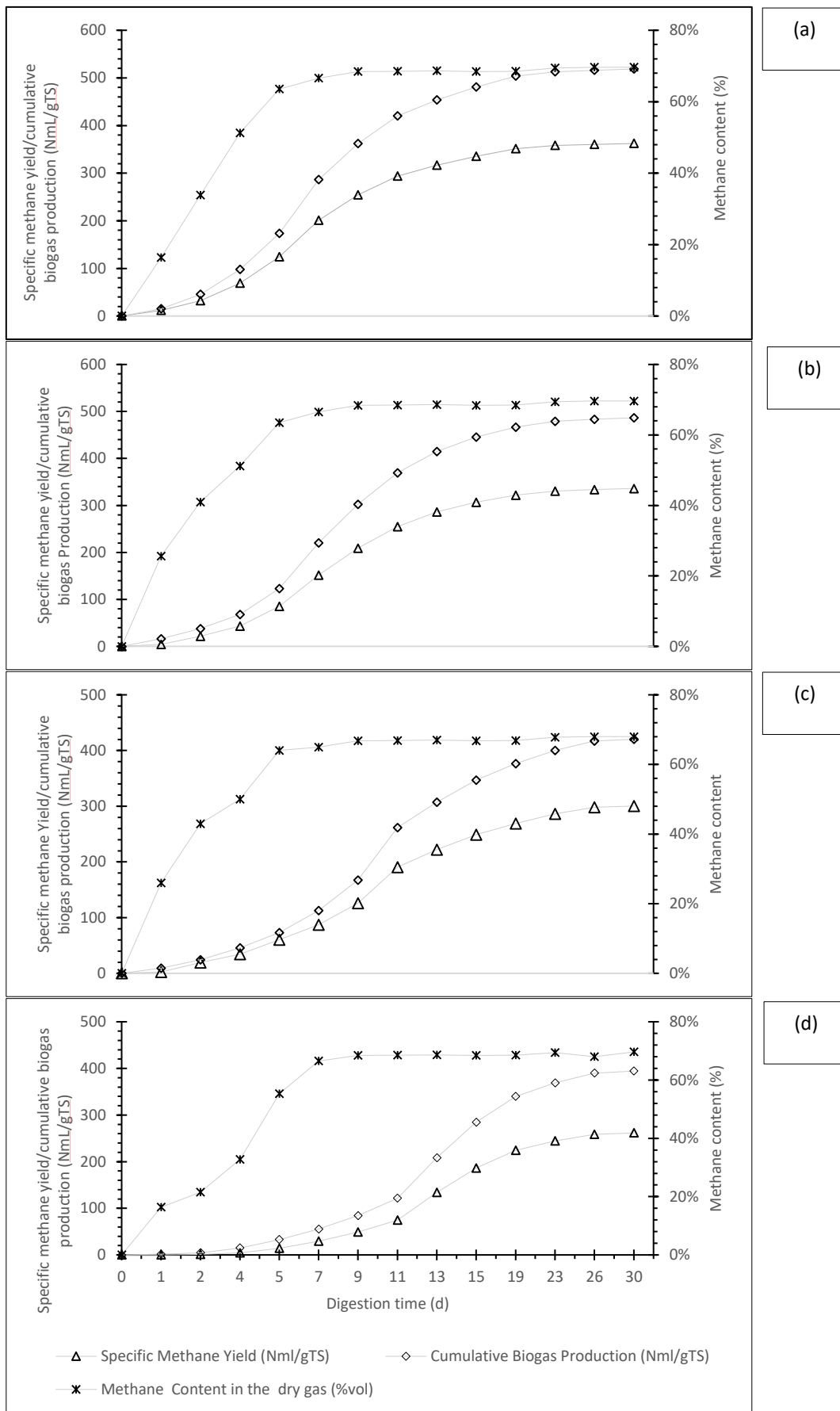


Fig 6-14: Specific methane yield and cumulative biogas production from different PT RS residues (“a” NaOH, “b” PE, “c” HCl and “d” Raw RS) using batch processes



Similarly, the result obtained is within the values obtained by Kainthola *et al.* (2019) on enhanced methane potential of RS with microwave-assisted pre-treatment. They reported methane production of 325 NmL CH<sub>4</sub> g<sup>-1</sup> VS for microwave pre-treated RS, while untreated RS was 231 NmL CH<sub>4</sub> g<sup>-1</sup> VS. Moreover, the methane yield value from the raw RS is within the values obtained by Lei *et al.* (2010). Nevertheless, the result differs from the values obtained by Zhao *et al.* (2010) on methane production from rice straw pretreated by a mixture of acetic-propionic acid. They reported that the final output of 280 NmL CH<sub>4</sub> g<sup>-1</sup> VS d<sup>-1</sup> was obtained from pre-treated RS while the raw RS gave 250 NmL CH<sub>4</sub> g<sup>-1</sup> VS d. The disparity could be from the agents applied in pre-treatment, and the employed PT RS was not exposed to biological (enzyme) hydrolysis.

Table 6-10: Gompertz data for the methane production from different PT RS residues

RS Residues	Gompertz Data			
	<i>P</i> (NmL CH <sub>4</sub> g <sup>-1</sup> TS)	$\lambda$ (d)	<i>R<sub>m</sub></i> (mL d <sup>-1</sup> )	R-Square
HCl-PT	303	2.9	23.17	0.9967
PE-PT	335	2.6	33.85	0.9992
NaOH-PT	360	1.9	38.07	0.9986
Raw (untreated)	267	6.9	22.22	0.9954

Applying the modified equation (Eqn 3-1) and Table 3-4, the chemical formula of the RS employed is C<sub>761</sub>H<sub>1336</sub>O<sub>595</sub>N<sub>10</sub>S, whilst the TBMP of the RS, calculated from Eqn 3-2, was 438 NmL CH<sub>4</sub> g<sup>-1</sup> TS. The TBMP of 438 NmL CH<sub>4</sub> g<sup>-1</sup> TS was also confirmed using the OBA<sup>TM</sup> BIOTRANSFORMERS TOOL (accessed on 8<sup>th</sup> August 2019). It can be seen from the TBMP that the values of methane from the PT residues and the control are within the expected range. However, the actual value obtained from the raw RS (control) was much reduced compared to the TBMP values, which could be from lack of pre-treatment before the AD process, while in TBMP and the OBA<sup>TM</sup> BIOTRANSFORMERS TOOL, it was assumed that the RS degradation was 100%.

The biogas yield from various PT RS residues showed that NaOH and PE-PT RS residues have the highest value of 519 NmL g<sup>-1</sup> TS and 487 NmL g<sup>-1</sup> TS (Fig 6-14). In contrast, the biogas yield of 394 NmL g<sup>-1</sup> TS obtained from raw RS was almost the exact value of the methane yield from NaOH-PT RS residue. The biogas accumulation value for HCl-PT RS was 420 NmL g<sup>-1</sup> TS. Although the SMY of 267 NmL CH<sub>4</sub> g<sup>-1</sup> TS and the cumulative biogas of 394 NmL g<sup>-1</sup> TS from raw RS were within the data reported by Swedish Gas Technology Centre Ltd (SGC) (2012) on biogas from straw, the low yield is due to the absence of both chemical and enzymatic pre-treatment which made the microstructure rigid and highly organised even after grinding (Fig 6-4)

Even though the mean methane content of the biogas from the various PT RS residues was 57% for raw RS, 60% for NaOH, 61% for PE, and 62% HCl-PT RS residues, the methane content of all the reactors stabilised to 67 – 70% after 5 days for NaOH, PE and HCl-PT reactors and 7 days for the raw RS reactor indicating that all the reactors were operating well (Fig 6-14). Nonetheless, the mean methane content of the biogas from the various PT RS residues ranged from 68% to 70% at steady states (Fig 6-15).

The daily specific methane production (a), daily biogas production (b) and specific methane yield (c) from different PT RS residues after 60days digestion time is shown in Fig 6-15. The daily specific methane yield and daily biogas production from the various PT RS residues were lower in continuous mode than when the batch system was applied under the same environmental conditions (Fig 6-14 and Fig 6-15). However, the result obtained tallied with the outcome of batch systems. The steady conditions were achieved from days 15 and 17, and the result presented therein is the mean values after the steady-state was achieved. The pictograph showed that NaOH and PE-PT RS residues gave the highest daily SMP (300 and 279 NmL CH<sub>4</sub> g<sup>-1</sup> TS added d<sup>-1</sup>) and daily biogas production (430 and 402 g<sup>-1</sup> TS added d<sup>-1</sup>) respectively compared with values obtained for raw RS which has daily SMP of (212 NmL CH<sub>4</sub> g<sup>-1</sup> TS added d<sup>-1</sup> and daily biogas production (279 NmL g<sup>-1</sup> TS added d<sup>-1</sup>. In the same vein,

HCl-PT RS residue gave daily SMP of 250 NmL CH<sub>4</sub> g<sup>-1</sup> TS added d<sup>-1</sup> and daily biogas production of 360 NmL g<sup>-1</sup> TS added d<sup>-1</sup>.

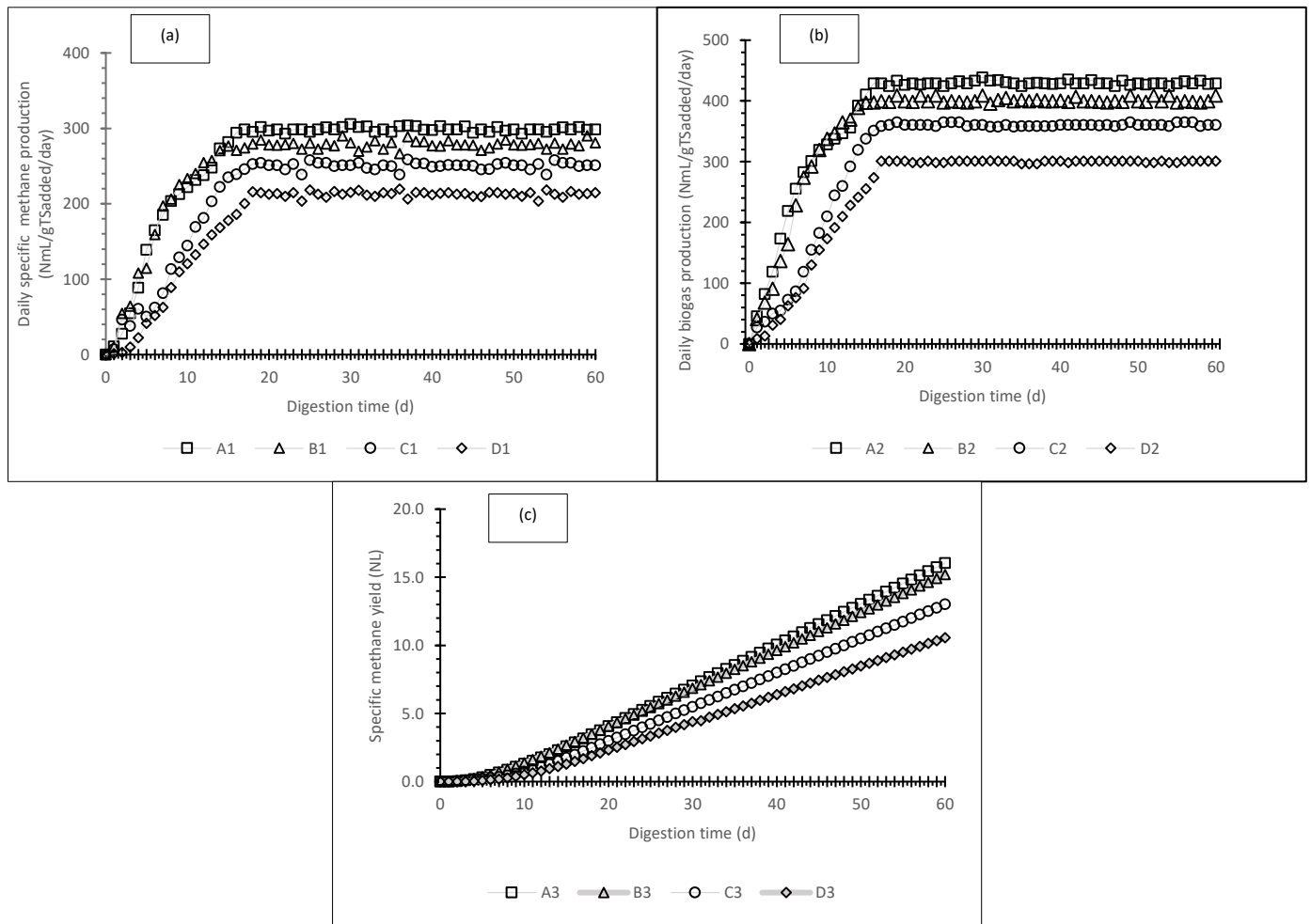


Fig 6-15: Daily specific methane production (NmL/gTS<sub>added</sub>/day) (a), daily biogas production (NmL/gTS<sub>added</sub>/day) (b) and specific methane yield (NL) (c) from different PT RS residues after 60days digestion time.

- A1: Daily SMP from NaOH-PT RS residues (NmL/gTS<sub>added</sub>/day)
- A2: Daily biogas production from NaOH-PT RS residues (NmL/gTS<sub>added</sub>/day)
- A3: SMY from NaOH-PT RS residues (NL)
- B1: Daily SMP from PE-PT RS residues (NmL/gTS<sub>added</sub>/day)
- B2: Daily biogas production from PE-PT RS residues (NmL/gTS<sub>added</sub>/day)
- B3: SMY from PE-PT RS residues (NL)
- C1: Daily SMP from HCl-PT RS residues (NmL/gTS<sub>added</sub>/day)
- C2: Daily biogas production from HCl-PT RS residues (NmL/gTS<sub>added</sub>/day)
- C3: SMY from HCl-PT RS residues (NL)
- D1: Daily specific methane production from raw RS (NmL/gTS<sub>added</sub>/day)
- D2: Daily biogas production from raw RS (NmL/gTS<sub>added</sub>/day)
- D3: SMY from raw RS (NL)

Chemical and biological pre-treatment of RS improved the daily SMP by 18%, 31.7% and 41.5% for HCL, PE and NaOH PT RS residues than raw RS at a steady state. The daily biogas production was also

improved following pre-treatments than raw RS with 53.9% for NaOH-PT RS, 43.9% for PE-PT RS, and 29% for HCl PT RS. Despite this, the result is varied slightly with the percentage increment obtained by Mustafa *et al.* (2016).

The much differences in the daily SMP and biogas from NaOH and PE-PT RS, when compared to the control (raw RS), could be from the dissolution of lignin components and collapse and shrinkage of the RS cellular structures brought about by breaking of both ester, ether and  $\beta$ , 1-4 glucosidic bonds (Lo *et al.*, 2010, Sattar *et al.*, 2016b and Salakkam *et al.*, 2019) by the chemical agents and the cellulosic enzyme. Therefore, the various pre-treatments exposed the RS to direct microbial attack, which ordinary may not be possible or even when possible will be time-consuming. This argument is also attested from the modified Gompertz model, where the methane production started approximately at day 2 when NaOH PT RS residue was employed as substrate and day 3 when PE and HCl-PT RS residues were used (Table 6-10). In contrast, though the methane production started approximately after 1 week of incubation (Table 6-10) when raw RS (control) was applied as feeders, the raw RS itself was pre-treated by reduction to 750  $\mu\text{m}$  size, improved the surface area to microbial attack. The highest methane yield was obtained from day 12, and this tallies with the study of Zhao *et al.* (2010).

Additionally, the graph showed that NaOH, PE, and HCl PT-RS reactors produced higher SMY values of 16.0, 15.2, 13.0 NL, respectively, after the 60days digestion process compared to the raw RS digesters that gave a SMY value of 10.6 NL (Fig 6-15c)

### **6.3.7 Material Balance of the Three-Stage Digestion Processes**

The mass balance of the three-stage digestion process is presented in Fig 6-16, while the corresponding purified and the biogas yield ( $\text{m}^3 \text{H}_2 \text{ tonne}^{-1} \text{TS added d}^{-1}$  and  $\text{m}^3 \text{CH}_4 \text{ tonne}^{-1} \text{TS added d}^{-1}$ ) of the different PT RS samples produced using CSABR mode is shown Table 6-11. Although the material mass balance started from 1000g (1kg) of raw RS from the material balance, the

corresponding gases were rounded to cubic metric per tonne per day (m<sup>3</sup>/tonne/d) to ease tabulation and calculations. The raw RS characterisation (Table 6-2) and lignocellulose composition (Fig 6-3) were used for subsequent calculation for both chemical and enzymatic pre-treatments (see Fig 6-16). However, for the stage 3 methane yield process, the analysis also included the characterisation of the individual PT RS (Table 6-2).

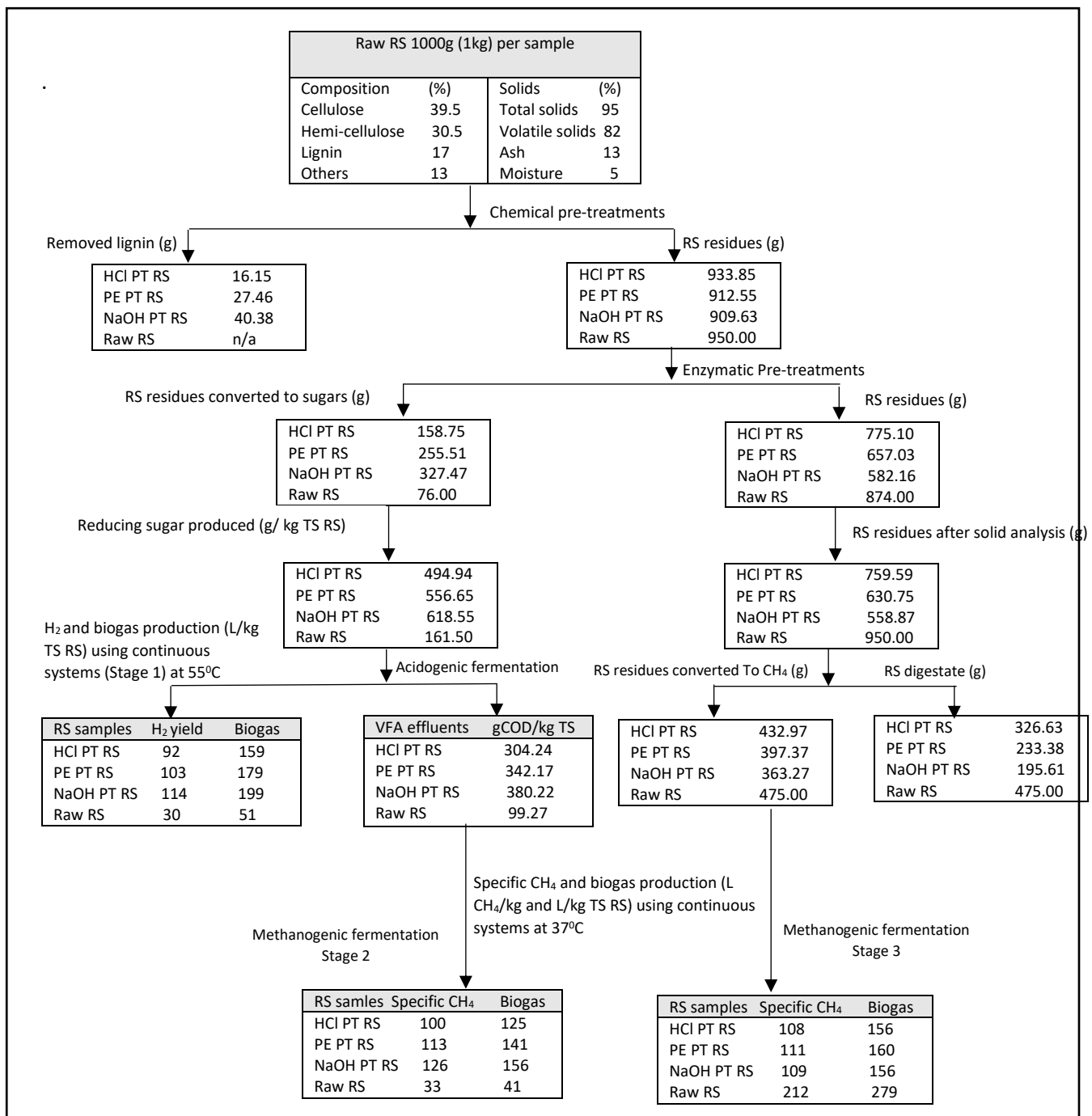


Fig 6-16: RS mass balance analysis of the three-stage fermentation process from different PT technologies.

The total solids (TS) analysis was applied to estimate the TS values of the PT RS residues. Whereas the various hydrolysates, PT RS residues, raw RS and VFA effluents are considered the inputs, the methane, hydrogen, carbon dioxide and digestates were measured as the outputs. The value of lignin removed was done based on the percentage of lignin loss (Fig 6-3), while the values of RS converted to sugars were done using the percentage of enzyme conversion (Table 6-6).

In the acidogenic process (stage 1), the daily hydrogen production ( $\text{L H}_2 \text{ kg}^{-1} \text{ TS RS}$ ) and biogas yield ( $\text{L kg}^{-1} \text{ TS RS}$ ) were produced from the PT RS hydrolysates, whereas the effluents VFA from the acidogenic reactors were utilised in the production of daily methane ( $\text{L CH}_4 \text{ kg}^{-1} \text{ TS RS}$ ) and biogas ( $\text{L kg}^{-1} \text{ TS RS}$ ) at stage 2. Finally, the remaining PT RS residues after enzymatic hydrolysis and raw RS (control) were used in the production of daily methane ( $\text{L CH}_4 \text{ kg}^{-1} \text{ TS RS}$ ) and respective biogas ( $\text{L kg}^{-1} \text{ TS RS}$ ) at the stage 3 process. It is pertinent to state that the laboratory methane values reported in stage 3 Section 6.3.6 were different from those in Fig 6-16, excluding the control (raw RS) value because the former was expressed in 1.0g TS, unlike the latter that were calculated and generated from the RS residues remainders after various pre-treatments and mass balancing.

The differences in materials in terms of substrates going in and out were determined using Eqn (6-1 and 3) via the batch system, whereas the gases ( $\text{CH}_4$ ,  $\text{H}_2$  and biogas) produced were calculated assuming that the fermentation system was in continuous (CSABR) mode.

In Stage 3 methane fermentation, unhydrolysed raw RS sample that was employed as the positive control was applied directly without pre-treatment, while the TS reduction/conversion to biogas used in the calculations were 57%, 63%, 65% and 50% for HCl, PE and NaOH-RS PT residues and raw RS respectively. Thus, even though the TS reduction of NaOH and PE-PT RS residues coincide with Lei *et al.* (2010) outcomes, there were differences in the duration of fermentation and method of pre-treatments. The higher TS reduction after pre-treatment from NaOH and PE-PT suggests that the pre-treatment probably improved the accessibility of fermentative microorganisms for better utilization and conversion of the lignocellulose into biogas. Although the conversion values are slightly higher

than those obtained by Monlau *et al.* (2015) and reported in the literature (Zieminski and Frac, 2012), the differences could be from the type of seeded sludge and the biomass and methods of pre-treatments employed. Finally, the total gases were calculated by adding all the gases produced for enriched (purified) and raw biogas in all the stages.

Table 6-11: The purified gas and biogas yield ( $\text{m}^3 \text{H}_2/\text{CH}_4 \text{ tonne}^{-1} \text{TS added d}^{-1}$  and  $\text{m}^3 \text{ tonne}^{-1} \text{TS added d}^{-1}$ ) from different PT RS samples produced via CSABR

RS Residues	Stage 1		Stage 2		Stage 3		Total gases produced	
	$(\text{m}^3 \text{H}_2 / \text{tonne TS/d})$		$(\text{m}^3 \text{CH}_4 / \text{tonne TS/d})$		$(\text{m}^3 \text{CH}_4 / \text{tonne TS/d})$		$(\text{m}^3 / \text{tonne TS/d})$	
	Enriched	Raw	Enriched	Raw	Enriched	Raw	Enriched	Raw
HCl-PT	92	159	100	125	108	156	300	440
PE-PT	103	179	113	141	111	160	327	479
NaOH-PT	114	199	126	156	109	156	349	511
Raw RS	NA	NA	NA	NA	212	279	212	279

Table 6-11 shows the purified gas and biogas yield ( $\text{m}^3 \text{H}_2/\text{CH}_4 \text{ tonne}^{-1} \text{TS added d}^{-1}$  and  $\text{m}^3 \text{ tonne}^{-1} \text{TS added d}^{-1}$ ) from different PT RS reactors. From the result, the pre-treated RS samples produced by far the highest yield of gases (purified and raw biogas) after the three-stage processes with both NaOH and PE-PT RS substrates having the highest output of 349 and 327  $\text{m}^3 \text{ tonne}^{-1} \text{TS added d}^{-1}$  for enriched and 511 and 480  $\text{m}^3 \text{ tonne}^{-1} \text{TS added d}^{-1}$  for raw biogas respectively than the raw RS which gave 212  $\text{m}^3 \text{ tonne}^{-1} \text{TS added d}^{-1}$  as purified biogas and 279  $\text{m}^3 \text{ tonne}^{-1} \text{TS added d}^{-1}$  as raw biogas assuming that only stage 3 process was applied. Similarly, the total gases produced from the HCl PT RS sample was 300  $\text{m}^3 \text{ tonne}^{-1} \text{TS added d}^{-1}$  as purified biogas and 440  $\text{m}^3 \text{ tonne}^{-1} \text{TS added d}^{-1}$  as raw biogas.

The methane production efficiency (MPE) was 80% for NaOH, 75% for PE, 68% for HCl RS PT feedstock, while the control (raw RS) was 48%. The MPE was calculated by dividing the total gases ( $\text{Nml CH}_4 \text{ g}^{-1} \text{TS}$ ) produced in all the stages, excluding the raw RS (control), by the TBMP value of RS, which is 438  $\text{Nml CH}_4 \text{ g}^{-1} \text{TS}$ . In this study, even  $\text{H}_2\text{S}$  is also presumed to be included in the calculation.

From the table, the purified biogas from stage 2 had almost similar methane yield to the enriched volumetric biogas from stage 3 in all the RS PT substrates except the raw RS. This development could

be from the methane content of the raw biogas, which is within 78 - 80% and requires the removal of small quantities of impurities (<20% CO<sub>2</sub>) (Fig 6-13). In contrast, the raw biogas from the acidogenic stage gave the highest volumetric yield in all the RS PT samples compared to their respective enriched biogas volume from the other stages (Table 6-11), which is a result of a high content of impurities (about 45% CO<sub>2</sub>) which made up the volume of the produced biogas.

Table 6-12: The energy value (GJ) of the produced gases (purified and raw biogas) in m<sup>3</sup> and kg biogas per tonne RS

RS Residues	Stage 1 process		Stage 2 process		Stage 3 process		Total energy	
	(GJ/m <sup>3</sup> biogas/tonne TS)		(GJ/m <sup>3</sup> biogas/tonne TS)		(GJ/m <sup>3</sup> biogas/tonne TS)		(GJ/m <sup>3</sup> biogas/tonne TS)	
	Enriched	Raw	Enriched	Raw	Enriched	Raw	Enriched	Raw
HCl-PT	1.00	0.95	3.61	3.13	3.9	3.9	8.51	7.98
PE-PT	1.12	1.07	4.07	3.52	4.0	4.0	9.19	8.59
NaOH-PT	1.24	1.19	4.52	3.91	3.9	3.9	9.66	9.00
Raw RS	NA	NA	NA	NA	7.6	7.0	7.6	7.0

RS Residues	Stage 1 process		Stage 2 process		Stage 3 process		Total energy	
	(GJ/kgbiogas/tonne TS)		(GJ/kgbiogas/tonne TS)		(GJ/kgbiogas/tonne TS)		(GJ/kgbiogas/tonne TS)	
	Enriched	Raw	Enriched	Raw	Enriched	Raw	Enriched	Raw
HCl-PT	11.07	10.56	5.05	4.37	5.45	5.45	21.57	20.38
PE-PT	12.45	11.87	5.68	4.91	5.58	5.58	23.71	22.36
NaOH-PT	13.83	13.19	6.31	5.46	5.48	5.45	25.62	24.10
Raw RS	NA	NA	NA	NA	10.66	9.75	10.66	9.75

NA Not available

### 6.3.8 Energy Value, Electricity and Thermal Generation from various RS Samples

The energy value of the produced gases (purified and raw) is shown in Table 6-12. The energy values were calculated using data from Table 6-4. The H<sub>2</sub> and CH<sub>4</sub> content were set as obtained from the literature to reflect the laboratory values, assuming that the CH<sub>4</sub> content in the raw biogas and purified gas is 70% and 99%, respectively. The H<sub>2</sub> content in raw biogas and purified gas is also expected to be 55% and 99%, respectively. The result of the energy value (GJ) of the produced gases (purified and raw biogas) in m<sup>3</sup> and kg per tonne is presented in Table 6-12, and it is shown that the cumulative



energy yield from the three-stage processes was much more improved from the pre-treated samples than the raw RS supposing that only stage 3 process was applied.

The highest cumulative energy value ( $\text{GJ}/\text{m}^3_{\text{biogas}}/\text{tonne TS RS}$ ) of 9.66 ( $25.62 \text{ GJ}/\text{kg}_{\text{biogas}}/\text{tonne TS RS}$ ) and 9.19 ( $23.71 \text{ GJ}/\text{kg}_{\text{biogas}}/\text{tonne TS RS}$ ) for purified gases and 9.00 ( $24.1 \text{ GJ}/\text{kg}_{\text{biogas}}/\text{tonne TS RS}$ ) and 8.59 ( $22.36 \text{ GJ}/\text{kg}_{\text{biogas}}/\text{tonne TS RS}$ ) for raw biogas were obtained after the three-stage process from NaOH and PE pre-treated samples respectively (Table 6-12). The raw RS (control) had an energy value of 7.60 and  $7.00 \text{ GJ}/\text{m}^3_{\text{biogas}}/\text{tonne TS RS}$  ( $10.66$  and  $9.75 \text{ GJ}/\text{kg}_{\text{biogas}}/\text{tonne TS RS}$ ) for purified and raw biogas, respectively, at stage 3 AD process. In the same vein, the cumulative energy value ( $\text{GJ}/\text{m}^3_{\text{biogas}}/\text{tonne TS RS}$ ) from HCl-PT sample was 8.51 ( $21.57 \text{ GJ}/\text{kg}_{\text{biogas}}/\text{tonne TS RS}$ ) for enriched and 7.98 ( $20.38 \text{ GJ}/\text{kg}_{\text{biogas}}/\text{tonne TS RS}$ ) for raw biogas.

The achieved values were within the range of gross calorific value (HHV), and the net energy value (LHV) of the raw RS sample, determined from the oxygen bomb calorimeter and calculated also using Eqn 3-3a and b and 3-4, which are  $15.9$  and  $14.13 \text{ MJ kg}^{-1}$ , respectively. The energy value of RS obtained from the bomb calorimeter was validated using Dulong Eqn 6-5. From Dulong, an HHV of  $15.5 \text{ MJ kg}^{-1}$  for RS was achieved. The obtained values were also within the LHV of RS from the literature, ranging from  $13.0$  and  $13.9 \text{ MJ kg}^{-1}$  (Nguyen *et al.*, 2016; Biswas *et al.*, 2017 and Maguyon-Detras *et al.*, 2020).

$$HHV = 337C + 1419 (H - 0.125 O) + 93S + 23N \quad \text{Eqn 6-5}$$

Where C, H, O, S, N are percentages of carbon, hydrogen, oxygen, sulphur and nitrogen in RS.

Furthermore, from Table 6-12, the highest energy values measured in  $\text{GJ}/\text{m}^3_{\text{biogas}}/\text{tonne TS RS}$  were obtained from purified biogas produced from the VFA methane process (stage 2 process) ranging from 4.07 ( $5.68 \text{ GJ}/\text{kg}_{\text{biogas}}/\text{tonne TS RS}$ ) to 4.52 ( $6.31 \text{ GJ}/\text{kg}_{\text{biogas}}/\text{tonne TS RS}$ ) for all the pre-treated digesters especially PE and NaOH PT RS reactors. On the other hand, the acidogenic stage (stage 1 process) had the highest calorific values when measured in  $\text{GJ}/\text{kg}_{\text{biogas}}/\text{tonne TS RS}$  for both purified and raw gases, particularly the hydrolysed samples (11.07 to 13.83). This high value in  $\text{GJ}/\text{kg}_{\text{biogas}}/\text{tonne TS RS}$  is

because hydrogen gas has a higher heating energy value of 142 MJ/kg compared to methane produced in other stages (2 and 3), which have high thermal energy of 56 MJ/Kg (Das and Verziroghu, 2001 and Bharathiraja, 2016). Therefore, the variations in calorific values between hydrogen and methane are critical parameters in the process comparison, as seen in Table 6.12, where the energy values measured in  $\text{GJ}/\text{m}^3_{\text{biogas}}/\text{tonne}$  of the raw RS is almost closer, especially with the energy values of HCl-PT RS. In contrast, the control sample's energy values ( $\text{GJ}/\text{kg}_{\text{biogas}}/\text{tonne TS RS}$ ) were approximately half of the energy values of pretreated RS samples. Therefore, the energy produced from PT RS samples will be more efficient, stable, and environmentally friendly than raw RS.

The electricity and thermal energy generation was done using CCHP and were determined using Table 6-13 and, on the postulation that data employed were from purified bio-hydrogen that is from the acidogenic stage (Stage 1) and raw biogas that is from the methanogenic stage (Stage 2 and 3). This idea is because the enriched biomethane from stage 2 and 3 processes were expected to be utilized as a natural gas substitute and in the gas grid. Also, it is generally believed that most CHP systems can accept small biogas impurities. The CHP mechanism is defined as mentioned above (section 2:13).

Table 6-13: The electricity ( $\text{KWh}_{\text{elect.}}$ ) and thermal energy ( $\text{KWh}_{\text{thermal}}$ ) generation produced from the corresponding energy values at the different stages of the process

RS Residues	Stage 1 process (KWh/ tonne TS)		Stage 2 process (KWh/ tonne TS)		Stage 3 process (KWh/ tonne TS)		Total energy (KWh/ tonne TS)	
	Electricity	Thermal	Electricity	Thermal	Electricity	Thermal	Electricity	Thermal
HCl-PT	98.61	131.94	308.65	412.99	384.58	514.58	791.85	1059.51
PE-PT	110.44	147.78	347.11	464.44	394.44	527.78	852.00	1140.00
NaOH-PT	122.28	163.61	385.57	515.90	384.58	514.58	892.43	1194.10
Raw RS	NA	NA	NA	NA	690.28	923.61	690.28	923.61

NA Not available

Table 6-13 shows the electricity and thermal energy generation produced from the corresponding energy values at the different conversion process stages. It is clear from the table that NaOH and PE-

PT RS residues gave the highest electricity and thermal values than HCl-PT RS and raw RS samples. The total output energy shows that both NaOH and PE-PT RS gave the most increased electricity (892.43 and 852.00 KWh<sub>elect.</sub> /tonne TS) and thermal (1194.10 and 1140.00 KWh<sub>therm.</sub> /tonne TS) values respectively from the three-stage processes. In contrast, the raw RS digester (control) yielded electricity and thermal values of 690.28 KWh<sub>elect.</sub> /tonne TS and 923.61 KWh<sub>therm.</sub>/tonne TS, respectively. Finally, the cumulative electricity and thermal yield from the HCl-PT RS source were 791.85 KWh<sub>elect.</sub> /tonne TS and 1059.51 KWh<sub>therm.</sub>/tonne TS.

Since Nigeria is in the tropics, most of the heat energy generated was employed in air conditioning, refrigeration, and process fluid cooling employing absorption chiller as described in the literature (Chapter 2 Section 2:14) using values from the US Department of Energy (2017) and Prager *et al.* (2019). Therefore, the various thermal energy values from Table 6-13 were converted to cooling fluid for refrigeration and air conditioning with an outlet temperature of 6.7°C. As a result, the cooling fluid in KWh<sub>cool</sub> produced per tonne of TS RS was 835.57, 798.00 and 741.66 for NaOH, PE and HCl PT RS samples assuming that the cooling coefficient of performance (COP) is 0.7 (US Department of Energy, 2017). Also, the cooling fluid (KWh<sub>cool</sub>/ tonne TS) value obtained for raw RS was 646.53. These cooling fluids can be employed in refrigeration and chilling processes in manufacturing industries, hospitals, large commercial office buildings, cold storage warehouses and research institutes.

### 6.3.9 Microbial Community Analysis

The microbial configuration was examined at the end of the acidogenic and methanogenic processes, with the relative abundance and taxonomic distribution of the bacteria community in each sample analysed at the genus and phylum levels (Fig 6-17). However, same as the preceding chapter, a detailed microbial composition was discussed at the phylum level because of many unidentified Taxa at the genus level. Firmicutes were the most dominant phylum for hydrogen digesters accounting for ~85%, followed by *Proteobacteria* and *Euryarchaeota*, which were about 5% and 4%, respectively. Others that accounts for ~6% of the total microbial composition were *Bacteroidetes* (~2.5%),

*Actinobacteria* (~2%) and *Synergistetes* (~1%). While most of the mentioned phyla are well-known hydrogen producers from simple to complex substrates producing varying fatty acids, *Euryarchaeota* is fastidious and strict anaerobes that produce methane using the WLP. The phylum *Synergistetes* were also identified by An *et al.* (2020b) on their work on performance and energy recovery of single and two-stage biogas production from paper sludge: *Clostridium thermocellum* augmentation and microbial community analysis, where it was also reported as the significant microbial population in AD processes.

The most principle phyla in the VFA digester (Stage 2) were the *Euryarchaeota* (~29%) and *Firmicutes* (~29%), followed by the *Chloroflexi* (~10%), *Bacteroidetes* (6%) and *Proteobacteria* (~3%). Other identified phyla (23%) contributed to the remaining microbial community (Fig 6-17). The increased microbial population of *Firmicutes* in the VFA digestion reactors despite stable methane production from the phylum *Euryarchaeota* could have been from introduction during feeding as discussed in Section 6.2.8 and 6.3.5.

In contrast, methane production from various PT RS residues has different microbial compositions. Whereas *Euryarchaeota* (~40%) was the most abundant phylum followed by *Proteobacteria* (~20%), *Firmicutes* (~20%) and *Synergistetes* (~9%) in NaOH and PE-PT RS digesters, *Proteobacteria* (~55%) was the dominant phylum followed by *Euryarchaeota* (~20%), *Firmicutes* (~8%) and *Synergistetes* (~3%) in HCl-PT RS digestates (Fig 6-17). The existence of *Firmicutes* and *Proteobacteria* with *Euryarchaeota* in PT RS digestates is justified as their liberated product “hydrogen” is utilised in the production of methane by hydrogenotrophic methanogens of *Euryarchaeota*. Thus, in the production of methane phyla *Firmicutes*, *Proteobacteria* and *Euryarchaeota* should exist mutually together. In addition, most *Firmicutes* are hydrolytic bacteria and are required in the solubilisation and digestion of rigid RS lignocellulose to soluble derivatives such as sugars, amino acids and fatty acids (Weiland, 2010; Angelidaki *et al.*, 2011 and Khan *et al.*, 2017b) essential for the growth of methanogens. However, even though *Euryarchaeota* was not the most abundant phylum in HCl-PT RS reactors, the magnitude

of the LCBD value of 0.25, which represented the highest value, ensured stability in the methane production process similar to the other pretreated RS samples (Fig 6-14 and 6-15). More so, it is anticipated that the methane production followed the hydrogenotrophic pathway, where methane is produced via the reduction of CO<sub>2</sub> by H<sub>2</sub> produced by the *Proteobacteria* (Aryal *et al.*, 2018).

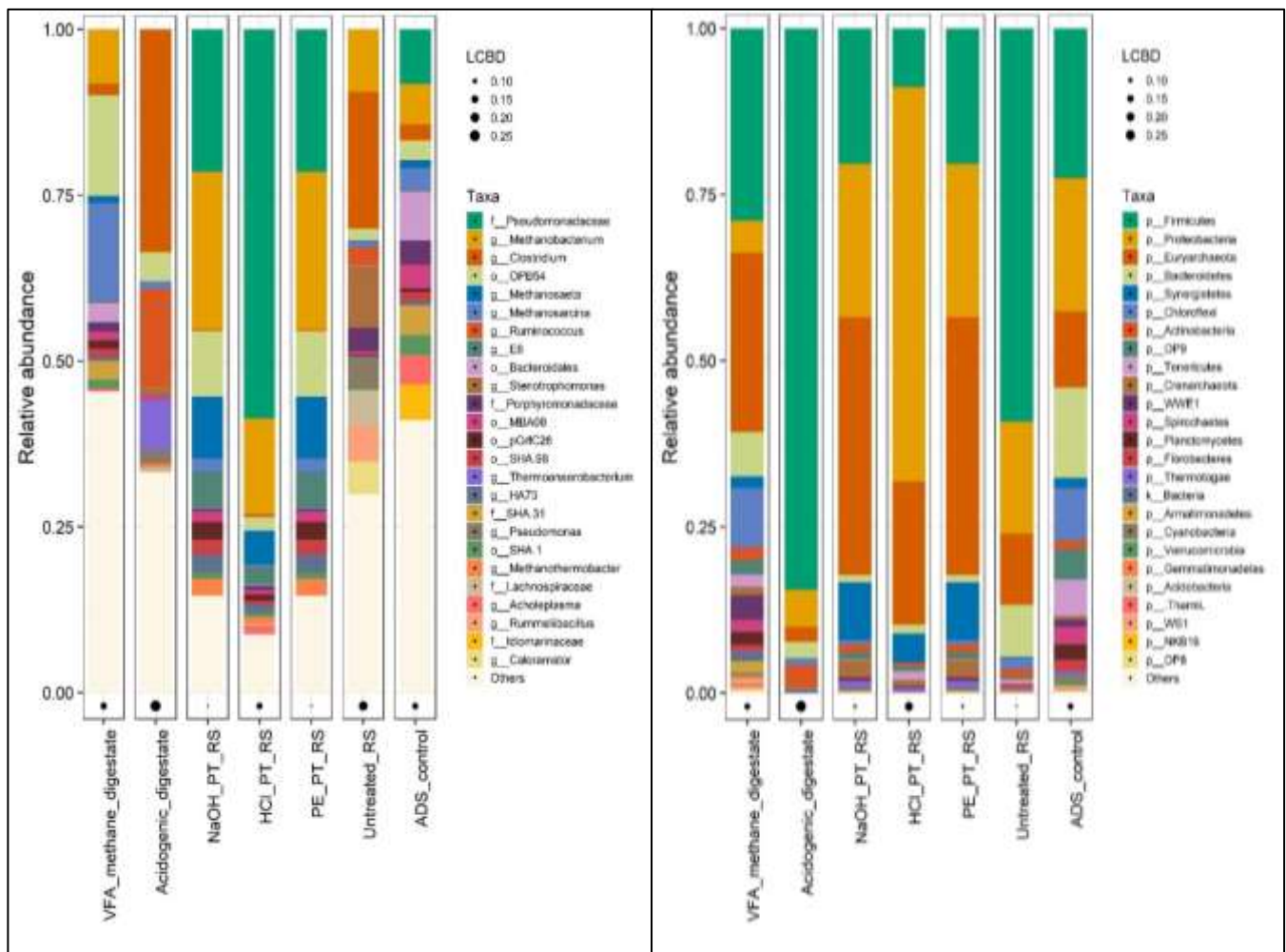


Figure 6-17: The relative abundance of top 25 most abundant microbial communities at genus and phylum levels from acidogenic and methanogenic reactors. While the bars correspond to taxa that are most dominant within the sample, the black points whose diameter relate to the magnitude of the LCBD value of the digestates that is higher LCBD mean the sample has more unique species than others.

Furthermore, while the raw (untreated) RS sample had *Firmicutes* (~55%) as the most principle phylum, followed by *Proteobacteria* (~15%), *Euryarchaeota* (~12%) and *Bacteroidetes* (9%), the ADS (control) has *Firmicutes* (~23%) as the most abundant phylum, followed by *Proteobacteria* (~18%), *Bacteroidetes* (15%), *Euryarchaeota* (~12%) *Chloroflexi* (~9%), *Synergistetes* (~4%) and others (19%).

At the genus level, it can be observed from the graph that *Clostridium*, *Ruminococcus* and *Thermoanaerobacterium* were the most dominant genera and constituted most of the *Firmicutes* (Fig 6-17) in the acidogenic digesters. These organisms have been discussed extensively in the previous Chapters. On the other hand, *Methanosarcina* and *Methanobacterium*, which constitute most of the *Euryarchaeota*, were the most abundant genera in VFA-digested reactors. While the high population of *Methanosarcina* is justified and expected as they are acetotrophic (acetoclastic) methanogens capable of utilizing acetate compound (VFA) for methane generation (Aryal *et al.*, 2018); the presence of *Methanobacterium* (though less populated compared to *Methanosarcina*) a known hydrogenotrophic methanogen is not entirely clear. However, the genus *Methanobacterium* might have been involved in methane production through the methylotrophic pathway using various C<sub>1</sub> compounds (Costa and Leigh, 2014 and Aryal *et al.*, 2018) contained in the VFA feedstock.

In the methane reactors from RS residues, *Methanobacterium* belonging to the phylum *Euryarchaeota*, and *Azotobacter* and *Pseudomonas* (*Pseudomonadaceae*), which belong to the phylum *Proteobacteria* were the most principle genera in NaOH and PE-PT RS digestates. This is followed by other methanogens such as *Methanosaeta*, *Methanosarcina* and *Methanothermobacter*. On the other hand, *Azotobacter* (*Pseudomonadaceae*) was the most genera in HCl-PT RS digesters, followed by *Methanobacterium* and *Methanosaeta*.

As explained before, *Methanobacterium* (and *Methanothermobacter*), a hydrogenotrophic methanogen, rely on the fermentation products (H<sub>2</sub> and CO<sub>2</sub>) of *Azotobacter* and *Pseudomonas* for methane production and thus explains the relative abundance in the microbial distribution mainly in the HCl-PT RS sample. However, *Methanosaeta* and *Methanosarcina* are acetotrophic (acetoclastic) methanogens. Since under normal circumstances, the final phase of an AD process proceeds to methanogenesis, which involves converting C<sub>1</sub> methylated compounds, primarily acetate, to methane

by acetotrophic methanogens (Gerardi, 2003 and Angelidaki *et al.*, 2011), they (*Methanosaeta* and *Methanosarcina*) would always be present in stable and efficient methane reactors.

Lastly, the raw (untreated) RS digester had *Clostridium*, a *Firmicutes*, as the most abundant genus, followed by *Methanobacterium* (*Euryarchaeota*), *Stenotrophomonas* and *Pseudomonas* (*Proteobacteria*). There were also few communities of *Methanosarcina*. The complex and structural robustness of raw RS compared to PT-RS might have led to the dominance of *Clostridium*, which is known to have hydrolytic abilities. Therefore, methane production by the methanogens is possible after RS degradation and liberation of fermentable products by *Firmicutes* and *Proteobacteria*.

## 6.4 Conclusion

This study investigated bio-H<sub>2</sub> and bio-CH<sub>4</sub> co-production from pretreated rice straw in a three-stage anaerobic digestion process with the produced biogas converted to power, heat, and cool using the CCHP strategy. Experimental results showed that at acidogenesis stage, hydrogen and biogas yield was insignificant when chemical and agro-industrial agents were employed alone. However, the daily VHP increased when the PT RS residues were biologically hydrolysed with NaOH (114 NmL H<sub>2</sub> g<sup>-1</sup> TS d<sup>-1</sup>) and PE-PT RS residues (103 NmL H<sub>2</sub> g<sup>-1</sup> TS d<sup>-1</sup>) having the highest values at steady states and raw RS producing the least (30 NmL H<sub>2</sub> g<sup>-1</sup> TS d<sup>-1</sup>). The daily VHP for HCl-PT RS was 91 NmL H<sub>2</sub> g<sup>-1</sup> TS d<sup>-1</sup>. The result obtained is further confirmed from the SEM images showing the histological effects of chemicals on RS structure. The same pattern was observed from the daily SMP from the acidogenic effluents, where NaOH, PE, HCl-PT and raw RS samples gave 126, 113, 100 and 32 NmL CH<sub>4</sub> g<sup>-1</sup> TS d<sup>-1</sup> at continuous mode. Mechanical and chemical pre-treatment followed by biological hydrolysis of RS improved the daily SMY by 18%, 31.7% and 41.5% for HCL, PE and NaOH-PT RS residues compared with the raw RS (control) sample. In the same vein, the PT RS residues produced much improved total gases (purified and raw biogas) after the three-stage processes. The MPE was 80% for NaOH, 75% for PE, 68% for HCl RS PT samples, while the control (raw RS) was 48%. In terms of energy values, the highest cumulative energy value (GJ/m<sup>3</sup> biogas/tonne TS RS) of 9.66 and 9.19 for purified gases and 9.00 and 8.59 for raw biogas were obtained after the three-stage process from NaOH and PE-PT samples, respectively compared to the raw RS, which had an energy value of 7.6 and 7.0 GJ/ m<sup>3</sup> biogas/tonne TS RS for purified and raw biogas respectively.

In addition, the total output energy expressed in electricity and thermal production using CCHP from the three stages was calculated and from the result obtained, NaOH and PE-PT RS residues also gave the highest electricity (892.43 and 852.00 kWh<sub>elect.</sub> / tonne TS) and thermal (1194.10 and 1140 kWh<sub>therm.</sub> / tonne TS) yield respectively. On the other hand, the HCl-PT RS residues gave electricity (791.85 kWh<sub>elect.</sub> / tonne TS) and thermal (1059.51 kWh<sub>therm.</sub> / tonne TS) yield. In contrast, the energy



produced from raw RS has a corresponding electricity value of 690.28 KWh<sub>elect.</sub> / tonne TS and a thermal value of 923.61 KWh<sub>therm.</sub> /tonne TS.

Meanwhile, most of the heat generated was employed in air conditioning, refrigeration and process fluid cooling using an absorption chiller since Nigeria is in the warmer climatic region. Thus, the cooling fluid in KWh<sub>cool</sub> produced per tonne of TS RS was 835.57, 798.00 and 741.66 for NaOH, PE and HCl PT RS samples but, the control RS sample produced 646.53 KWh<sub>cool</sub> /tonne TS RS.

Finally, whereas the *Clostridium*, *Ruminococcus* and *Thermoanaerobacterium*, which belong to the *Firmicutes*, were the dominant genera in acidogenic digestates, *Methanosarcina* and *Methanobacterium* belonging to the phylum *Euryarchaeota* were the most abundant genera in VFA-digested reactors. In NaOH and PE-PT RS digestates, *Methanobacterium* belongs to the phylum *Euryarchaeota* and *Azotobacter* and *Pseudomonas* (*Pseudomonadaceae*) belonging to the phylum *Proteobacteria* were the most primary genera. On the other hand, *Azotobacter* (*Pseudomonadaceae*) was the principal genera in HCl-PT RS digesters, followed by *Methanobacterium* and *Methanosaeta*. The raw (untreated) RS digester also has *Clostridium*, a *Firmicutes* as the most abundant genus, followed by *Methanobacterium* (*Euryarchaeota*), *Stenotrophomonas* and *Pseudomonas* (*Proteobacteria*).



## Chapter 7 The production of nano-silica precursors from agro-industrial wastes leached and anaerobically digested rice straws

### 7.1 Introduction

Rice straw is a natural source for silica production (Khosand *et al.*, 2012; Permatasari *et al.*, 2016 and Mirmohamadsadeghi and Karimi, 2018). RS, which is the vegetative stem of the rice plant that is removed during rice harvest, can be used for silica fabrication as its inorganic component, known as rice straw ash (RSA), is about 10 -15% by weight (Agbagla-Dohnani *et al.*, 2001; Sangnark and Noomhorm, 2004 and Bakar and Carey, 2020). These inorganic constituents are rich in silica, silicon compounds, alkali, and alkaline earth metals (Agbagla-Dohnani *et al.*, 2001 and Guzman *et al.*, 2015). Nigeria currently produces around 14 to 15 million tonnes of rice straw (RS) per year (FAOSTAT, 2017 and 2018), which are among the biomass wastes that constitute 76% of Nigeria's total primary energy supply, especially from cooking (International energy agency, 2016). Hence, the over-reliance on RS biomass as the primary energy source has contributed to greenhouse gases, notably anthropogenic CH<sub>4</sub>, CO<sub>2</sub>, CO, and NO<sub>x</sub> and volatile organic acids, a precursor of ozone (IEA, 2020). Moreover, the rice straw ash (RSA) produced from such combustion method has high impurities, reduced reactivity, and can produce crystalline silica, which can cause silicosis (Della *et al.* 2002). Therefore, utilizing this large biomass waste for socioeconomic growth should be considered while preserving the silica content. In RS biogas plants, apart from heat and electricity generation via conversion of the biofuels, the digestate produced can be used for silica production, which is so because the impurities usually present in RS and decreased reactivity of silica must have been leached and consumed by the digesting microbes.

Even though there is limited research on silica production from anaerobically digested biomasses to the best of the writer's knowledge, Wattanasiriwech *et al.* (2010) carried out a study on the production of amorphous silica nanoparticles from rice straw with microbial hydrolysis pre-treatment. After RS

microbial hydrolysis and subsequent thermal decomposition, amorphous silica with a particle size range of 50 and 80 nm was produced. Although Wattanasiriwech and colleagues' work is slightly similar to the study hypothesis, applying pure microbial cultures is expensive. Also, the RS hydrolysis 72 h duration may not be sufficient for complete leaching of impurities as seen from the relatively high levels of manganese and phosphate. On the other hand, Mirmohamadsadeghi and Karimi (2018) studied the energy recovery and amorphous nano-silica production from RS via dry anaerobic digestion. They concluded that high-quality nano-silica could be obtained from anaerobic digestion. Although Mirmohamadsadeghi and Karimi research is similar to the author's objectives, the RS residue recovery was 75.2% after the AD process, with 24.8% digested and transformed to gas, indicating a flawed digestion process attributed to a lack of pre-treatment before digestion. Thus in the present study, a) the feasibility of producing amorphous silica biologically from pre-treated RS digestates from acidogenic (Chapter 5) and methane-producing reactors (Chapter 6) was examined (Fig 7-1). Also, b) the possibility of removing or leaching out impurities from RS using agro-industrial wastes – cassava-steep wastewater (CSSW) and corn-steep liquor (CSTL) before silica production by thermal extraction was investigated. The agro-industrial wastes are considered a green and cleaner alternative to leaching instead of applying a strong acid that can be expensive and have environmental issues (Umeda and Kondoh, 2008 and 2010 and Permatasari *et al.*, 2016). In contrast, the agro-industrial wastes are weak acids due to the concentration of SCFA and can be utilised as a leaching alternative as proposed by Umeda and Kondoh (2008 and 2010).

## Graphical Introduction

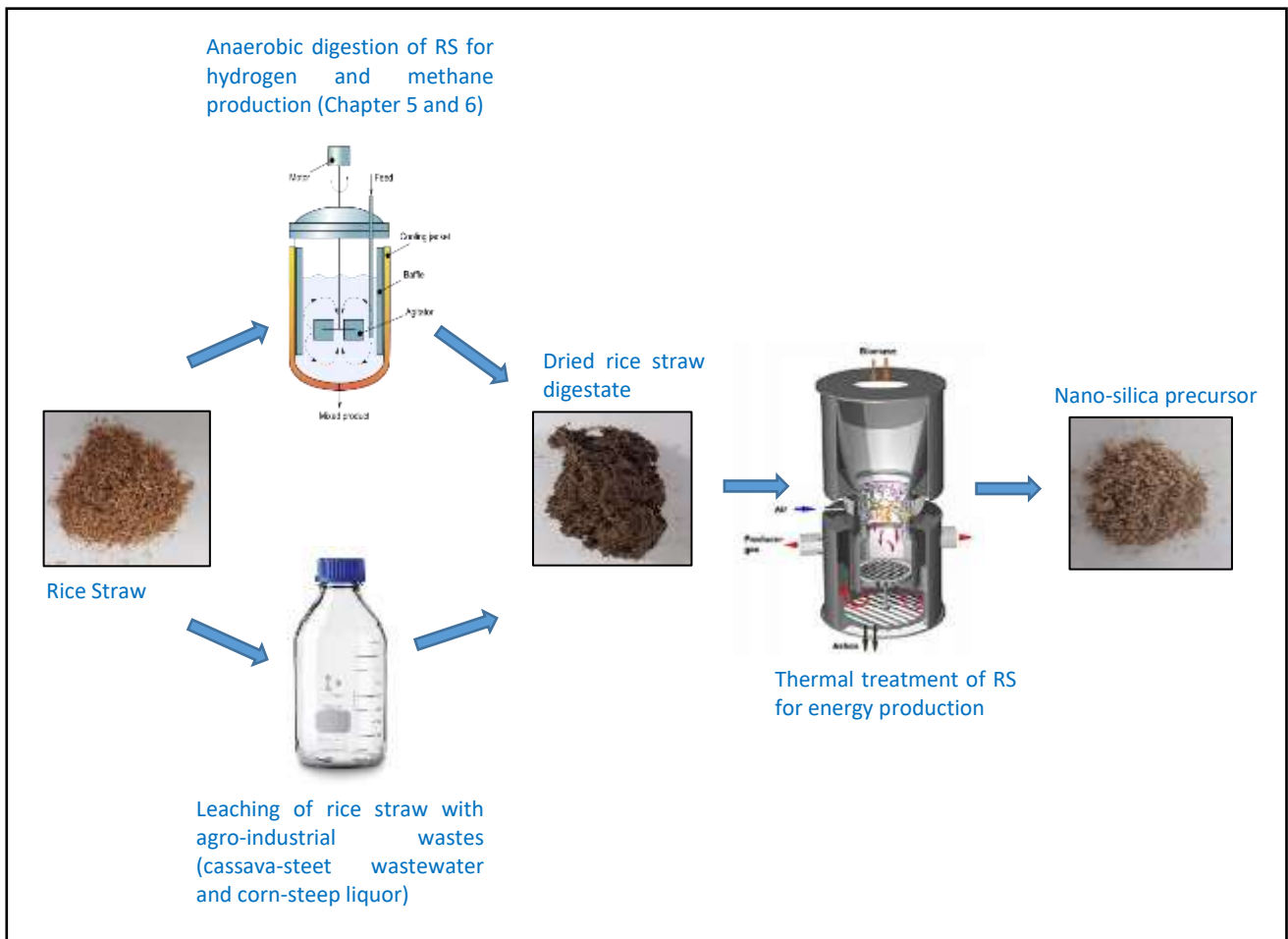


Fig 7-1: Production of amorphous silica from pre-treated RS digestates from AD reactors and from agro-industrial wastes leached RS

## **7.2 Materials and Methods**

### **7.2.1 Digestate Preparation from Acidogenic and Methanogenic Reactors**

After the various anaerobic digestion processes for hydrogen and methane production from different chemically (NaOH, HCl, and PE) pre-treated RS reactors have been completed (see chapter 5 and 6), the RS digestate typically employed for manure substitute (Tambone *et al.*, 2009) for agricultural purposes is used for silica production. First, the RS digestates were collected from their reactors, separated from the reactor liquor, and thoroughly washed with tap water on a 250 µm sieve to remove the sludge. Later, the digestate RS residues were dried at 80°C for 24 h and stored at RT until use (Fig 7-1).

### **7.2.2 Preparation of Leached Rice Straw Using Agro-Industrial Wastes**

Already communised RS was placed in 500 mL grade 3.3 borosilicate glass Duran bottles (BGDB) (VWR 215-1594) containing either CSWW or CSTL solution in the ratio of 1:4. The mixtures were incubated for 30 days in an automated stirred incubator system at 100 rpm. The reaction setup was done in triplicates. At the end of the incubation, the leached RS digestates were filtered, washed with tap water, and dried at 80°C for 24 h. Later, the dried leached RS digestates were stored at RT until use (Fig 7-2). Finally, RS incubated with water following the same procedure was used as the control.

### **7.2.3 Silica Preparation from Various Digestates and Leached Rice Straw Residues**

The silica was prepared using the modified method prescribed by Chen *et al.* (2010) and Wattanasiriwech *et al.* (2010). About 10g of the various dried digestates and leached RS residues were placed in a well-labelled porcelain crucible and calcined in an electric furnace at 550°C for 6 h with a constant heating rate of 10 °C/min. Raw RS was also prepared using the same method as the control. After cooling down in an air-tight desiccator, the rice straw ash (RSA) samples were weighed and immediately stored for further analysis.

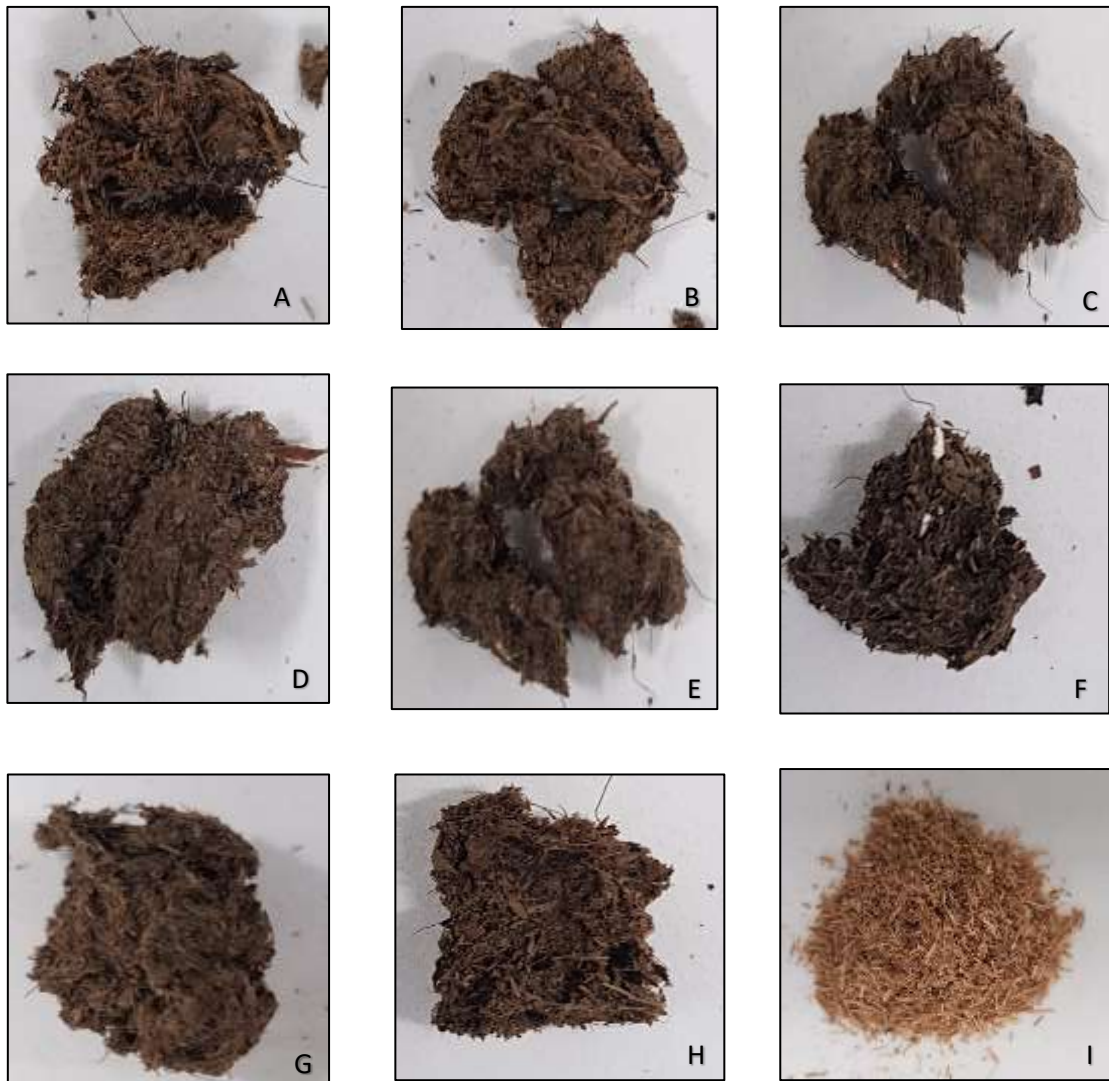


Fig 7-2: Various dried digestates (A: CSWW-L RS; B: CSTL-L RS; C: Water-L RS; D: HCl-PT RS; E: PE-PT RS; F: NaOH-PT RS; G: Untreated-PT RS; H: Digestate from hydrogen reactor and I: Raw RS)

#### 7.2.4 Analyses of Raw Rice Straw and Rice Straw Ash

The various RS samples were analysed using an energy-dispersive X-ray fluorescence spectrometer (EDX) (Quantex 70) operated at 15 kV from the SEM HITACHI NEXUS to determine the chemical contents of the rice straw ash (RSA). At the same time, the phase analysis was examined using an X-ray powder diffractometer using the PANalytical X'pert pro Multipurpose Diffractometer (MPD).

## 7.3 Results and Discussion

### 7.3.1 Characterisation of Agro-industrial Wastes

The chemical characteristics of CSWW and CSTL are shown in Table 7-1. In both samples, the pH was within 3.0 and 4.0, which confers acidity resulting from the organic acids. The predominant VFA were acetic and butyric acid. These were employed in the leaching of raw RS for 30days.

Table 7-1: Characterisation of CSWWs and CSTL

Sample	Acetic Acid (mg/L)	Butyric Acid (mg/L)	Formic Acid (mg/L)	Lactic Acid (mg/L)	Total COD (mg/L)	Soluble COD (mg/L)	pH
CSWW	2502.08	2435.79	25	ND	13640.00	5337.67	3.70
CSTL	1745.72	1159.33	30	Nd	7520.00	3450.20	3.40

### 7.3.2 Characterisation and Thermal Analysis of Rice Straw Samples

The already prepared leached RS residues, together with the digested RS samples from methane reactors and hydrogen reactors, were analysed to determine their solid content and proximate characteristics as prescribed in ALPHA standards (Table 7-2). The same was done for the raw RS sample. As a result, the pH of RS samples from acidogenic reactors was within 5.4 and 5.6, while that from methanogenic digesters was 7.05 before tap-washing.

From Table 7-2, it was observed that the rate of VS degradation, also known as the energy conversion efficiency (%), was between 67 to 87%, with the raw RS (control) having the highest percentage of 87 and the methanogenic digestates producing the lowest of 67%. Although this outcome is slightly higher than the reported values by Maguyon-Detras *et al.* (2020), the variation could be from the mode of energy conversion technology. The result showed that there were high levels of ash content (29.91 to 33.67%) from the methanogenic reactors (reactors A to D), which perhaps is explained by the removal of the digestible organic part of the RS during AD operations for methane (Table 7-2). However, the low ash content of 19.62% from acidogenic reactor E compared with the methane-producing digesters might be from a low yield of hydrogen gas from the acidogenic samples (see



Chapter 4). Therefore, even though there was an evolution of gases (biogas) from the hydrogen fermenters, the poor performance of hydrogen reactors when RS was employed as substrates is from reduced RS biomass degradation as acidogenic conditions persist.

Table 7-2: The solid/thermogravimetric analysis of leached RS, various PT Digestates and raw RS samples

Substrates	TS (g)	VS (g)	Ash (g)	VS (%)	Ash (%)
Raw RS	0.937	0.815	0.122	86.980	13.020
CSSW-L RS	0.994	0.895	0.099	90.040	9.960
CSTL-L RS	0.992	0.899	0.093	90.625	9.375
Water-L RS	0.987	0.898	0.089	90.983	9.017
Reactor A	0.989	0.725	0.264	73.306	26.694
Reactor B	0.987	0.712	0.275	72.138	27.862
Reactor C	0.985	0.715	0.27	72.589	27.411
Reactor D	0.983	0.779	0.204	79.247	20.753
Reactor E	0.989	0.815	0.174	82.406	17.594

Reactor A: Digestate from NaOH-PT RS methane reactor

Reactor B: Digestate from PE-PT RS methane reactor

Reactor C: Digestate from HCl-PT RS methane reactor

Reactor D: Digestate from untreated RS methane reactor

Reactor E: Digestate from hydrogen reactor

“L” in the above table denotes “leached.”

There were not many variations in terms of ash content among the various leached samples (9.017 to 9.960%) with the raw RS (13.020%), which agrees with the values reported in the literature (Agbagla-Dohnani *et al.*, 2001 and Sangnark and Noomhorm, 2004). Nonetheless, the reduced ash content in leached samples compared with the raw RS could be from the leaching of inorganic and metallic impurities of the RS residue during the incubation period (Vaibhav *et al.*, 2015 and Kongmanklang and Rangsiwatananon, 2015). Although these findings are a bit different from Chen *et al.* (2010) report on the preparation of nano-silica materials: the concept from wheat, the disparity could be from the type of biomass and approach employed. They achieved a 93% weight loss, while 8% represents the silica and metallic impurities. Nevertheless, the result is close to Wattanasiriwech *et al.* (2010)

outcome on the production of amorphous silica nanoparticles from RS with microbial hydrolysis pre-treatment. They reported 10%, 12%, and 23% ash content from untreated RS, LDD1, and TR-hydrolysed RS.



Fig 7-3: RSA (silica) preparation from (A: CSWW-L RS; B: CSTL-L RS; C: Water-L RS; D: Untreated-PT RS; E: HCl-PT RS; F: PE-PT RS; G: Raw RS; H: NaOH-PT RS and I: Digestate from hydrogen reactor)

### 7.3.3 Rice Straw Ash (silica) Characterisation

As stated previously, although the digestate from the AD processes has been commonly employed as manure for agricultural purposes, they constitute an environmental hazard and can even affect the

normal flora of soil if not efficiently used. Therefore, in an economic sense, the application of digestate from RS degradation for silica production could be more beneficial than organic fertiliser.

#### 7.3.3.1 Morphological and physical appearance of silica materials

Figure 7-3 shows the various nano-silica preparation from the different samples. From the figure, the ash obtained from the leached samples (Fig 7-3a, b, and c), methanogenic samples (Fig 7-3, e, f and h), and acidogenic sample (Fig 7-3i) were much better in quality, consistency, and colour which was indicative of relatively pure silica as compared to the raw RS ash. In terms of colour, the leached and digested samples were grey-white, while the raw RS ash was black. Even though there is no clear explanation for the colour differences, it can be said that the colour variations compared to the control could be from the residual carbon materials requiring higher temperature or a longer combustion time (Wattanasiriwech *et al.*, 2010 and Askaruly *et al.*, 2020) and the presence, and absence of metallic impurities in raw RS and leached/digested samples respectively. These impurities are believed to have been leached during the incubation period/the digestion period, giving the samples a white colour (Umeda and Kondoh, 2008 and 2010; Vaibhav *et al.*, 2015; Kongmanklang and Rangsiwatananon, 2015 and Bakar *et al.* 2016). This postulation is supported by the findings of Bakar *et al.* (2016) on the production of high purity amorphous silica from rice husk. They suggested that high purity silica can be produced by controlled combustion after acid treatments. In furtherance, they observed that acid treatments could eliminate metallic purities such as iron, manganese, calcium, sodium, potassium, and magnesium that influence silica colour and purity before combustion. Similar findings were obtained by Rafiee *et al.* (2012), where 1M of HCl was used to produce silica from rice husk and achieved silica with a good surface area. In contrast, the raw RS contained inorganic compounds and metallic ions that will constitute reduced quality if used directly for silica production and give a dark colour to nano-silica impurities (Agbagla-Dohnani *et al.*, 2001 and Guzman *et al.*, 2015). The same result was obtained by Wattanasiriwech *et al.* (2010) and Mirmohamadsadeghi and Karimi (2018). Furthermore, the ash sample from the untreated RS looks edgy and brittle on touch and lacks

consistency, which could be from the formation of a crystalline form of silica such as potassium silicate and calcite compared to the leached and digested samples, which feel soft and tender on touch and have increased surface areas that can be likened to cement (Fig 7-3).

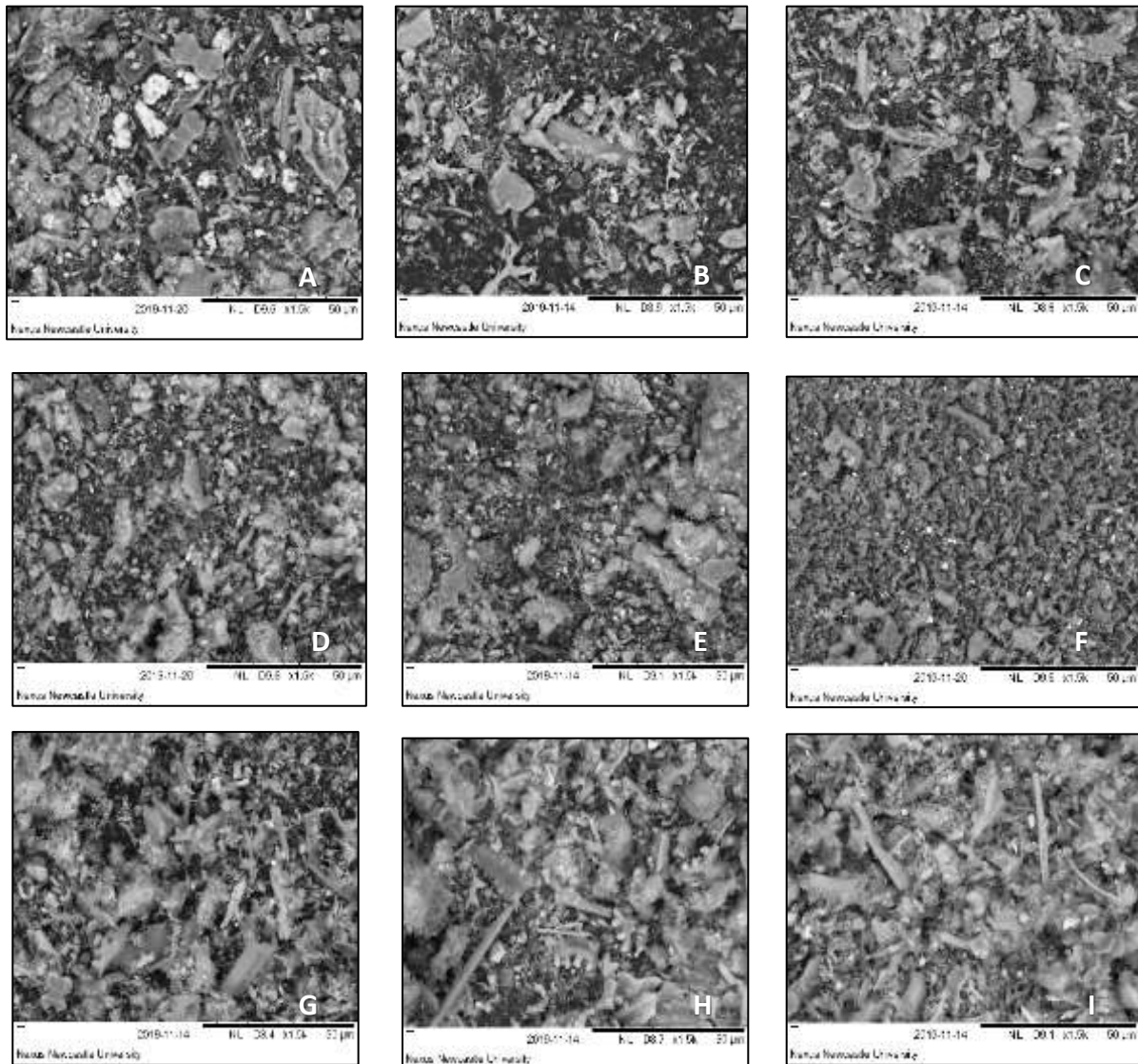


Fig 7-4: SEM micrograph of the different RSA samples (A: Untreated-PT RS; B: CSTL-L RS; C: CSWW-L RS; D: HCl-PT RS; E: NaOH-PT RS; F: PE-PT RS; G: Water-L RS; H: Digestate from hydrogen reactor and I: Raw RS)

### 7.3.3.2 Scanning electron images of silica precursors

The SEM micrographs of the RS ash samples are shown in Fig 7-4. Although the SEM images cannot be clearly defined, from the micrograph, the nano-silica was observed in an amorphous form from the methanogenic PT digestates (Fig 7-4d, e and f).

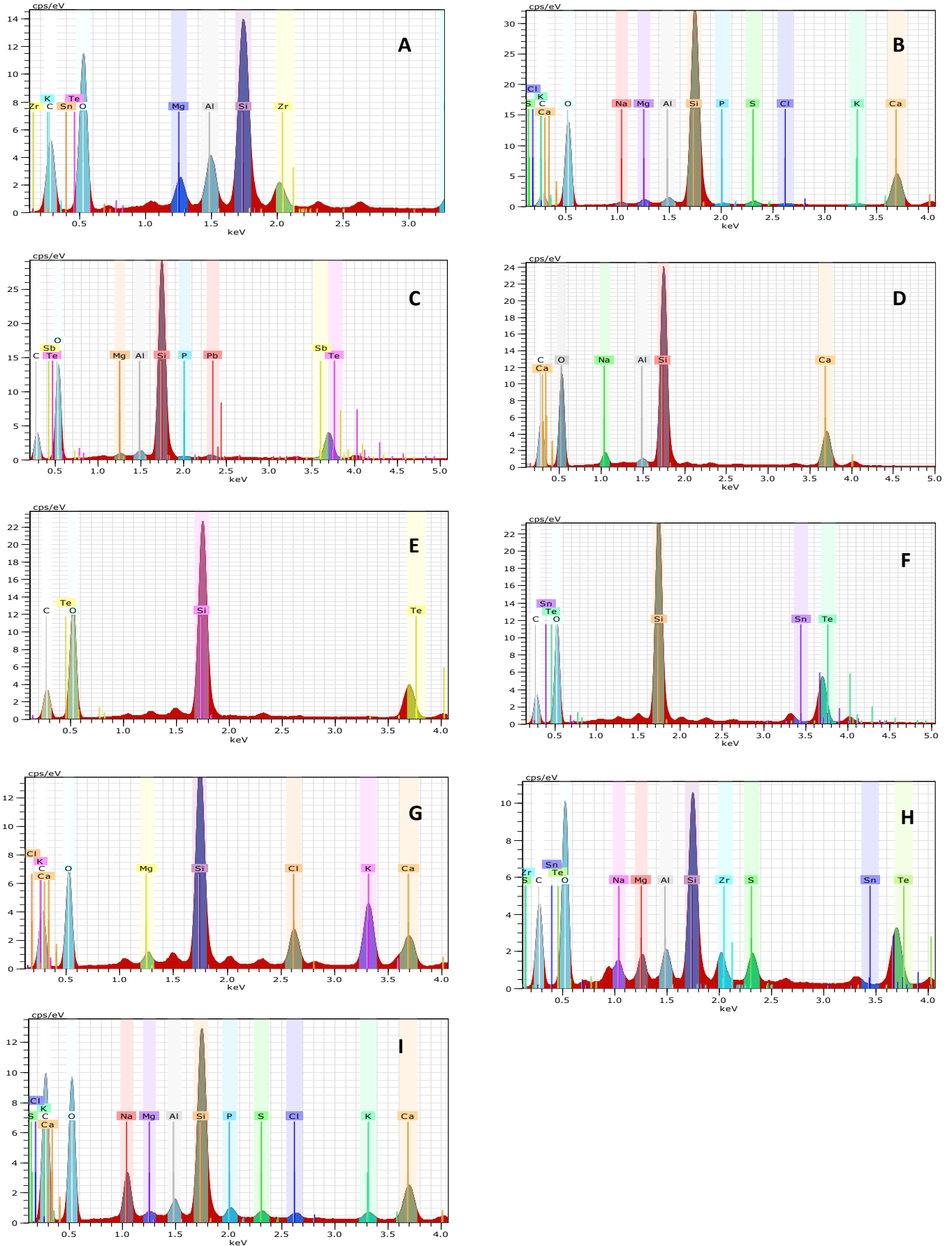


Fig 7-5: The elemental composition of silica samples (A: Untreated-PT RS; B: CSTL-L RS; C: CSWW-L RS; D: HCl-PT RS; E: NaOH-PT RS; F: PE-PT RS; G: Water-L RS; H: Digestate from hydrogen reactor and I: Raw RS)

The leached samples (Fig 7-4 and c) and digested untreated RS digestates (Fig 7-4a) also showed a bit of amorphousness under scanning microscopy. In contrast, the SEM images from raw RS, water-leached RS, and acidogenic RS samples presented the silica in crystalline forms (Fig 7-4i, g, and h), which might be from metallic impurities from the samples. Incomplete combustion of RS samples could also be another reasonable cause—the results tally with Mirmohamadsadeghi and Karimi (2018) and Askaruly *et al.* (2020) findings.

#### **7.3.4 Chemical Analysis of Rice Straw Ash (Silica Materials)**

The elemental composition of silica samples is shown in Fig 7-5. It is seen from the graphs that silica was the principal element with the highest peaks, followed by oxygen from the XRF analysis, which affirms silica ( $\text{SiO}_2$ ) as the chief element in the sample. This result is consistent with Chen *et al.* (2010) and Vaibhav *et al.* (2015) report on applying agricultural waste as a source from the production of silica nanoparticles. The findings also agree with Askaruly *et al.* (2020) and Imoisili *et al.* (2020) study outcomes. A similar effect was also obtained from the elemental spread of RSA digestates, where silica was also the dominant element (Fig 7-6), which confirms that RS is an excellent raw material for silica production (Wattanasiriwech *et al.*, 2010; Khorsand *et al.*, 2012; Lu and Hsieh, 2012, Permatasari *et al.*, 2016 and Mirmohamadsadeghi and Karimi, 2018). Nevertheless, there were peaks of other elements, notably potassium, sodium, calcium, chloride, magnesium, manganese, iron, aluminium, and lead. Others that were insignificant quantities include tellurium, chromium, antimony, and zirconium. These inorganic compounds in oxidised forms were reported by Wattanasiriwech *et al.* (2010), Vaibhav *et al.* (2015) and Mirmohamadsadeghi and Karimi (2018). Imoisili *et al.* (2020) also obtained inorganic impurities such as sodium and potassium from the substrate used for the SEM/EDX analysis. The carbon element found in all the graphs was from the mounting adhesives made from carbon. These elements have been reported to contribute to the impurities associated with biological silica production (Kongmanklang and Rangsriwatananon, 2015). Of particular importance is the compound potassium ions, which causes the melting of nano-silica at relatively low temperatures

during combustion due to the eutectic phenomenon with SiO<sub>2</sub> (Mirmohamadsadeghi and Karimi, 2018).

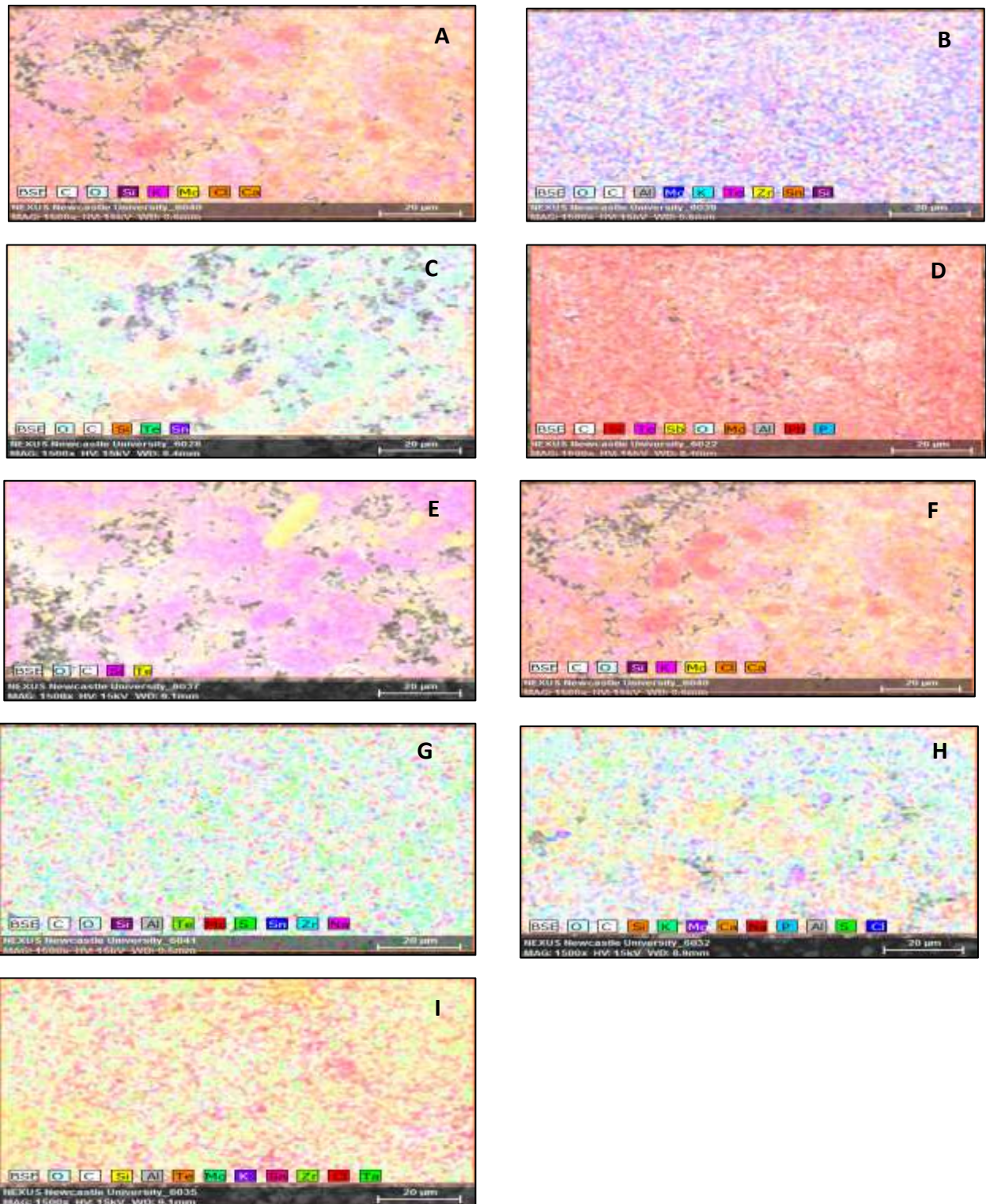


Fig 7-6: The elemental spread of RSA samples (A: Untreated-PT RS; B: CSTL-L RS; C: CSWW-L RS; D: HCl-PT RS; E: NaOH-PT RS; F: PE-PT RS; G: Water-L RS; H: Digestate from hydrogen reactor and I: Raw RS) with silica ion having the most concentration

Therefore acid leaching is essential before silica extraction (Bakar *et al.*, 2016). This leaching activity could explain the reason the methanogenic RS ashes were more amorphousness (7-4d, e, and f) than the raw (untreated) RSA (7-4i) as the inorganic impurities were negligible in methanogenic RS samples (7-5d, e, and f) compared to the raw RSA (7-3g and 7-4i), which has varying significant of the inorganic elements. It is believed that these impurities are converted to their respective individual ions after acid treatment (Vaibhav *et al.*, 2015). Even though the leached samples (Fig 7-4b and c) and digested untreated RSA (reactor control) (Fig 7-4a) also showed a bit of amorphousness under SEM, they still had some amount of impurities (Fig 7-5a, b and c) which could be from the type of weak acid employed in the leaching process for the samples. There is no clear explanation for inorganic impurities in the digested untreated RSA compared with other methanogenic RS samples. However, it could have been from the basal media employed, the seeded sludge and exogenous salt applied for pH stability and nutrient supplementation. The same inorganic elements were achieved by Wattanasiriwech *et al.* (2010), Vaibhav *et al.* (2015) and Mirmohamadsadeghi and Karimi (2018) in their respective works on silica production from agricultural wastes.

The numerous peaks of inorganic elements recorded in the water-leached, acidogenic RSA and raw RS samples (Fig 7-5g, h and i) explain the crystal forms of nano-silica and, thus, reduced specific surface area reported under SEM images (Fig 7-4g, h and i). The impurities further reaffirm the need for leaching of RS biomass before combustion.

As mentioned above, the increased amount of inorganic elements could also be from the basal media used, and the exogenous addition of salt compounds (NaOH and HCl) required to maintain the pH during the hydrogen production process (see chapter 4). Also, insufficient quantity of organic acids from incomplete digestion of RS biomass in hydrogen fermenters as the RS biomass is highly recalcitrant, and digested cow slurry may not solubilise it for hydrogen production but will instead produce methane rather than hydrogen. Therefore, the seeded culture employed for the RS samples

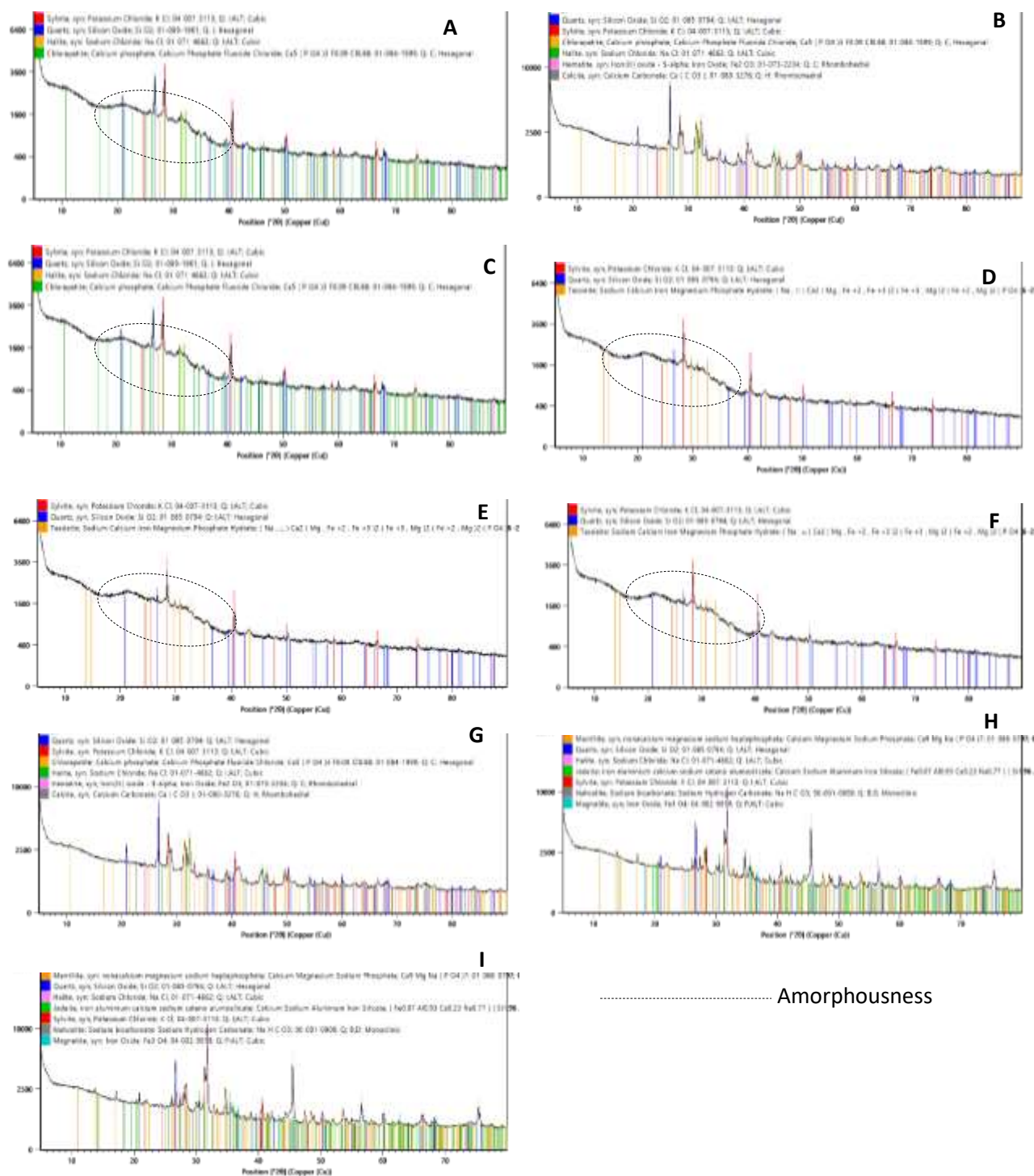


were highly enriched with sucrose and hence more alkali was added to balance the pH leading to more  $\text{Na}^{2+}$  concentration in the reactor medium (see Chapter 5).

Furthermore, the acidogenic digestates used was from one digestion cycle (hydraulic retention time (HRT 1)), and hence, some inherent metallic ions (Guzman *et al.*, 2015) have not been wholly eliminated away before use in silica production. These reasons were affirmed by the work of Wattanasiriwech *et al.* (2010) on their experiment on the production of amorphous silica nanoparticles from rice straw with microbial hydrolysis pre-treatment. They reported the elevated potassium ions on the elemental composition from external potassium addition employed to enhance cellulase activity. Conversely, no leaching activity was observed for water-leached RS, and raw RS samples (Figure 7-5 and 7-6) as water is a neutral compound with no leaching activity.

### **7.3.5 X-ray Powder Diffractometer Pattern Analysis**

The X-ray powder diffractometer (XRD) patterns showed that the RSA from methanogenic reactors contained amorphous silica (Fig 7-7) as seen from the broad peak observed at  $2\theta$  ranging from  $16^\circ$  to  $28^\circ$ , which confirmed the presence of amorphous silica (Fig 7-7d, e and f). Similar peaks were reported Mirmohamadsadeghi and Karimi (2018). The peaks were also consistent with the findings by Chen *et al.*, 2010, Shim *et al.* (2015), Askaruly *et al.* (2020) and Imoisili *et al.* (2020) in their nano-silica production from agricultural wastes. However, their peaks were much more defined and broader due to further silica purification approaches employed. Although there were minor contaminants at the  $29^\circ$  and  $40^\circ$  representing sylvite (potassium chloride), which could have been gotten from exogenous addition during the AD process, the absence of significant peaks indicates the lack of crystals on the nano-silica material (Fig 7-7d, e and f). The formation of these phases by the contaminants was also reported by Vaibhav *et al.* (2015). These findings further validate the SEM report on the production of the amorphous silica from methanogenic digested RSA samples (Fig 7-4). In contrast, the broad peak was not seen in the XRD spectra for water-leached, acidogenic and raw RSA samples, demonstrating the lack of amorphousness in the nano-silica material (Fig 7-7g, h and i).



..... Amorphousness

Fig 7-7: The XRD spectra of RSA samples (A: Untreated-PT RS; B: CSTL-L RS; C: CSWW-L RS; D: HCl-PT RS; E: NaOH-PT RS; F: PE-PT RS; G: Water-L RS; H: Digestate from hydrogen reactor and I: Raw RS

Instead, the samples have sharp and several peaks, mainly quartz (silicon oxide), sylvite (potassium chloride), chlorapatite (calcium phosphate) and Halite (Iron (III) oxide), which shows the crystalline nature of the nano-silica in the various RSA samples. This result also confirms the SEM findings above. Even though the digested untreated RSA and the CSWW-leached RSA samples contained sharp peaks similar to water-leached, acidogenic and raw RSA samples, they have a slight broad peak at the  $2\theta$  ranging from  $16^\circ$  to  $25^\circ$  (Fig 7-7a and c), which shows some degree of amorphousness. The findings also tally with the SEM report where the leached samples (Fig 7-4c) and digested untreated RSA (Fig 7-4a) showed a bit of amorphousness under scanning electron microscopy. Thus, the sharp peaks could have been from incomplete leaching activity from the weak acids employed in CSWW and exogenous salts used during the AD process for untreated RSA samples. Nonetheless, there was no explanation for the lack of broad peaks at the  $2\theta$  from about  $30^\circ$  in the CSTL-leached RSA sample (Fig 7-7b), which indicates the absence of amorphousness in the nano-silica compound. This result contradicts the SEM interpretation reported earlier, but the reason could also be from incomplete leaching activity from the weak acids employed in CSTL agro-industrial waste.

#### 7.4 Conclusion

The purpose of this study was to evaluate the feasibility of producing nano-silica from RS that has been hydrolysed and digested for hydrogen and methane productions. Also considered for nano-silica precursors was RS leached with agro-industrial wastes such as CSTL and CSWW. The study findings showed that pre-treated and digested methanogenic RSA samples contain amorphous silica materials confirmed by the SEM, EDX and XRD results. The EDX results showed the high presence of silica with a negligible amount of inorganic elements, while the XRD patterns showed that the RSA from methanogenic reactors contained amorphous silica as seen from the broad peak observed at  $2\theta$  ranging from  $16^\circ$  to  $28^\circ$ . In contrast, the result of pre-treated and digested acidogenic RSA samples appeared in crystalline forms seen from the XRD patterns and SEM, even though they still contain a high concentration of silica compounds with a considerable amount of other elements from the EDX graphs. The agro-industrial wastes (CSTL and CSWW) are good but probably weak leaching agents as the RSA were slightly amorphous. The leaching attributes of agro-industrial wastes and their subsequent RSA amorphousness were confirmed from the SEM and EDX values. However, the XRD result shows that CSWW-leached RSA offers more potency as a leaching agent than CSTL-leached RSA. CSWW-leached RSA samples have a slight broad peak at the  $2\theta$  ranging from  $16^\circ$  to  $25^\circ$ , which shows some degree of amorphousness, while CSTL-leached RSA shows the absence of broad peaks at the  $2\theta$  from about  $30^\circ$ . Thus, nano-silica can be produced from RS digestates from methanogenic reactors and RS leached with CSWW.



## **Chapter 8 The energy assessment of the digestion and post digestion processes in the integrated system**

### **8.1 Background of Study**

The analyses considered the energy balances of the AD processes (defined in Chapter 6) using various PT RS as feedstock co-digested with DCS and other processes in the energy integrated unit. The combined energy system comprises biogas plants, dryer, gasifier, combined cooling, heating and power (CCHP), and biogas upgrading unit (Fig 1-1). As mentioned before, RS, the stem/vegetative part of the rice plant removed during rice harvest, is among other lignocellulose materials biomass that can be used for biogas and hydrogen production. Rice straw is more than twice the rice paddy yield (Yuan, 2002), implying that Nigeria produces around 14.1 million tonnes of RS per year. Almost all the states in Nigeria produce rice depending on quantity and environmental conditions, with the following states Kebbi, Ebonyi, Kaduna, Kano, Cross River, Niger, Benue, Taraba and Borno, producing the most yield. In addition to this, Nigeria has about 20 to 21 million cattle (FAOSTAT, 2017) and generate about 0.59 million tonnes of cattle slurry daily and approximately about 215 million tonnes of cattle slurry annually.

The benefits of biogas, especially bio-hydrogen, has been covered exclusively in the Introduction Chapter 1 of this thesis. However, it should be noted that biogas is arguably a more flexible renewable energy source due to its determinate energy value and ease of storage (Poschl *et al.*, 2010). Also, the direct application for heating, cooling and electricity generation and vehicular fuels is another advantage of biogas (Krich *et al.*, 2005 and Su *et al.*, 2018). Furthermore, the AD product-digestate can be utilised as a fertilizer substitute, reducing dependence on energy-intensive mineral fertilizers (Tambone *et al.*, 2009). Therefore, GHG emissions associated with these mineral fertilizers are mitigated (Poschl *et al.*, 2010). These biogas advantages notwithstanding, the commercial application of biogas has been limited due to insufficient data in the analysis of energy balance and efficiencies in

the life-cycle of integrated biogas energy systems. However, there have been studies on integrated energy systems by Bruno *et al.* (2009), El-Emam and Dincer (2018), Su *et al.* (2018), Koirala *et al.* (2021). Similarly, there are several publications on the advantages of CCHP systems for performance improvement and GHG reduction (Keshavarzzadeh *et al.*, 2019)

There is no known information on the number of biogas plants in Nigeria. However, small-scale biogas systems (with an installed capacity of <500 kW<sub>el</sub>) and large scale biogas plants (>500 kW<sub>el</sub> installed capacity) are being proposed to handle the sizeable agricultural waste produced and the plants was sited at other rice-producing communities across the country. These systems are designated to handle rice straw waste (14.1 million tonnes per year) and cow slurry (about 215 million tonnes of cow-dung). The energy produced from these systems is also proposed to be utilised locally, within the community, but with an option for the excess electricity to be fed into the national grid. The small scale biogas plants have a feedstock handling capacity of 10 000 tonnes per annum, while the large scale biogas systems, which is considered to produce more than 1.8 million m<sup>3</sup> of biogas per annum, have a feedstock handling capacity of 20 000 tonnes per annum (Nilsson *et al.*, 2001 and Poschl *et al.*, 2010).

The energy analysis will ensure the sustainability of an AD process as an efficient alternative to fossil energy. Therefore, the purpose of this energy assessment as it relates to this study is to a) determine the total energy-demand of the integrated energy study, b) investigate the total energy produced from the biogas and other post AD products through CHP, gasification and absorption chillers and finally c) analyse the energy ratio between energy input and output to determine the efficiency of the system.

## 8.2 Methods and Expectations

Firstly, all the energy flows in the biogas-energy systems, the input and operational power, were identified and detailed from a life-cycle perspective and compared with biogas output. The biogas-energy scheme comprises the different biological processes and the energy conversion steps (Hijazi *et al.*, 2016). The length of the life cycle as it relates to this study and for analysis consists of a) feedstock supply that entails the collection and handling of the agricultural wastes (RS and DCS) and the transportation of these wastes to biogas plant; b) bio-energy production, which includes methane and hydrogen gases; c) digestate utilisation, which is the conversion of produced digestate to silica and d) biogas application that is the utilisation of the fuel for electricity generation and its end-use in vehicles. These processes are summarised in Fig 8-1.

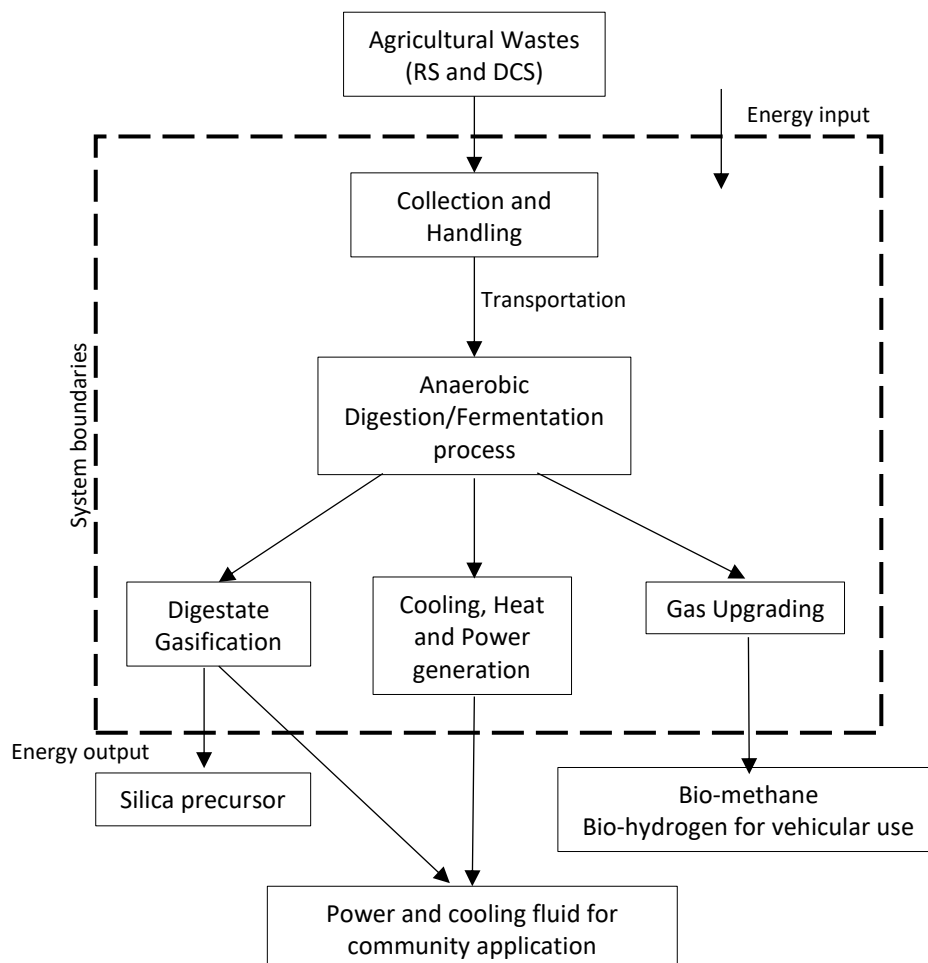


Fig 8-1: Summary of the life cycle of the integrated unit studied. The arrows indicate the flow of the energy and mass material in the unit



The arrow indicates the energy and mass material flow in the integrated energy system studied, while the dotted line specifies the system boundary. First, whereas the biogas (hydrogen and methane) production, in terms of daily continuous yield and silica were values obtained from the research study, the biogas and energy value calculations were based on the literature (Berglund and Borjesson, 2003, Poschl *et al.*, 2010, and Prager *et al.* 2019). Secondly, to evaluate the energy balance of the integrated energy system, the energy demands of all operations required to run the system were determined, also based on review data. Nonetheless, no energy demand associated with the production of rice straw is included since RS and DCS are considered waste. However, the energy inputs are included for collecting, transportation, and pre-treatment of cow dung and rice straw feedstock.

The third assumption determined the energy balance as the primary energy input to output ratio (PEIO). Consequently, all energy inputs statistics are based on primary energy inputs. Primary energy inputs are all energy flows that are unconverted and untransformed natural resources (Berglund and Borjesson, 2006). Therefore, primary energy inputs include all energy calculations required to produce energy carriers, vehicles and machines together with the energy contained in these products (Berglund and Borjesson, 2006). For example, in the production and distribution of diesel, the estimated energy inputs correspond to 10% of the energy content of the fuel (Berglund and Borjesson, 2006). Thus, the energy value required to manufacture and maintain trucks used to transport raw materials and digestate corresponds to 8% and 20% respectively of energy content in diesel fuel (Nilsson, 1997). To elaborate, if 1L diesel is used for transportation by either truck or tractor, which has an energy value of 42.6MJ, the energy input was 46 and 50 MJ, respectively (Berglund and Borjesson, 2006).

Similarly, the energy input required in producing 1 MJ of electricity, assuming natural gas is used as the fuel source with 50% conversion efficiency, is 2.2 MJ of primary energy (Berglund and Borjesson, 2006). The conversion efficiency of 50% considers distribution losses in the electricity grid and energy demands in the production and distribution of natural gas. The biogas produced in the biogas systems

supplies the heating requirement in the biogas plants, assuming 1.3MJ primary energy is required to produce 1MJ of biogas (Berglund and Borjesson, 2006).

Finally, the energy output was evaluated as the total sum of potential energy conversion from the biogas yield from RS and cow slurry. The integrated energy system is deemed efficient if the PEIO value is low and poor if the PEIO value is high or exceeds unity (Poschl *et al.*, 2010). Hence, the energy output includes assumed energy values from biogas conversion to potential electricity and heat generation and energy values from bio-hydrogen/bio-methane and digestates. It was also presumed that the energy embodied in the biogas plants are insignificant and therefore not considered in the study.

### 8.3 Description of Scenarios

An integrated energy system (Fig 1-1) was designed to evaluate and analyse the energy efficiency in the entire life cycle based on different scenarios. The scenarios are calculated based on the results from the laboratory studies and data obtained from the literature presented as base estimates and assumptions (Berglund and Borjesson, 2006, Holm-Nielsen *et al.*, 2009 and Poschl *et al.*, 2010).

Table 8-1: Characterisation of some PT RS residues and untreated RS

PT-RS Samples	Calculated DM (TS) Content (%)	Calculated DM (VS) Content (%)	Ash (%)
HCl-PT RS	98	90	8
PE-PT RS	94	88	6
NaOH-PT RS	96	89	7
Untreated RS	95	82	13

#### 8.3.1 Feedstock Scenarios

The base scenario of the study is the acidogenic process for producing hydrogen from different RS hydrolysates and the AD process for methane production from VFA effluents and pre-treated RS residues co-digested with cow slurry (Table 8-1). In addition, utilising the digestates from the reactors

for more energy yield and silica production was explored. Biogas upgrading as fuel for vehicles and substitute for natural gas was also considered.

The transport distance between the biogas plant and feedstock origin was assumed for 10 km for both RS and cow slurry. The AD digestion process was done for small scale biogas plants, which have a feedstock handling capacity of 10 000 tonnes per annum and large scale biogas systems with a feedstock handling capacity of 20 000 tonnes per annum. The reactor digestate was dewatered, dried and pelletised on-site to reduce energy demand for transportation.

Table 8-2: Technical data of medium-scale wood gasification plant HKA 45

Characteristics	Data
Wood fuel consumption	0.9 kg/kWh <sub>el</sub>
Outlet temperature	85°C
Return temperature	65°C
Energy output	See result data
Electrical power	45 kWh <sub>el</sub> , efficiency 23.3%
Heat power	102.2 kWh <sub>th</sub> , efficiency 52.92%

Facts are based on figures from medium-scale wood gasifiers from Spanner Re<sup>2</sup> HKA 45 and Prager *et al.* (2019). Though the data is for natural wood, it is assumed that pelletised digestate will give similar results.

### 8.3.2 Energy Conversion Scenarios

The biogas conversion scenarios are from decentralised CHP generating units that handle the immediate community energy (power) needs with the option of feed-in the excess energy capacity to the national grid (Poschl *et al.*, 2010). The digestates from the AD reactors also provided additional energy from gasification technology. Even though the gasification process was not carried out in this research thesis, it is believed that the gasification of the reactors digestate will lead to more energy products. Hence, the inclusion of the gasification process in the integrated energy unit (Fig 1-1). Also, it would be easier to calculate the RS energy flow in a gasifier than in a thermal furnace applied in Chapter 7. The energy from the digestate is calculated based on the specific wood fuel consumption

data of a reference biomass CHP system (HKA 45, Spanner Re<sup>2</sup> GmbH, Neufahrn, Germany, fixed-bedwood gasifier with combined heat and power plant), Table 8-2.

Since Nigeria is in a tropical climate, most of the heat generated from the CHP plants was utilised via sorption chillers (Absorption Chillers for CHP Systems, US Department of Energy (2017) to provide air conditioning, refrigeration, and process-fluid cooling to enhance the integrated system efficiency.

Table 8-3: The primary energy for collection and transport of feedstock from sources

Feedstock	DM content (%)	Energy Input (MJ/tonne)
Rice straw <sup>a</sup> (recovery/baling)	82 – 95	300
Cow slurry <sup>b</sup> (Collection and transportation)	15-20	280

Trucks<sup>a</sup> and Tractors<sup>b</sup> were used as feedstock transporter.

The RS biomass is predicted to be produced at 2 tonnes per hectare and year (Nilson, 1997)

Data is calculated based on figures from Berglund and Borjesson (2006) and Poschl *et al.* (2010)

## 8.4 Statistics of Primary Energy Flow

### 8.4.1 Energy demand in the collection and transportation of feedstock

The energy inputs in the collection and transportation of RS and cow slurry were determined from the literature (Table 8-3). This energy calculation includes the energy utilised in the recovery (baling the straws) and collecting cow slurries. The transport distance between the biogas plant and the origin of feedstock was assumed to be 10 km for RS and cow slurry, which is because it is believed that the integrated energy system is installed within the RS farm community (Table 8-4). The gasifier plant and the CCHP were also believed to be situated 10 km from the biogas plant. It is presumed that the collection route and traffic situation do not significantly impact the energy input in normal circumstances.

In the design of the energy unit, there is no assumption of return transport as the digestate produced is transported to the gasifier and not returned to the farms as manure. The energy demand is calculated based on diesel fuel consumption per tonne per kilometre transported (tkm). The values are from the literature.

Table 8-4: The energy demand for the transport of feedstock and digestate from/to the biogas plant

Feedstock	Energy Input (MJ/tonne-km)	Energy Input (MJ/tonne)
Rice straw <sup>a</sup>	6.5 (6.9)	65 (69)
Cow slurry <sup>b</sup>	2.5 (2.8)	25 (28)
Solid digestate (pellets) <sup>b</sup>	8.0	80

<sup>a</sup> Trucks and <sup>b</sup> Tractors were used as feedstock transporter, and “km” denotes the distances

Data is adjusted based on Poschl *et al.* (2010), and those in parenthesis are original values reported in the literature.

The high energy input per tonne of straw is because of its low density (Sonesson, 1996).

It is assumed that the liquid digestate is dewatered, dried and pelletised on-site to solid digestate, and as such, transportation for solid digestate will have high energy input and higher density.

#### 8.4.2 Energy input in pre-treatment of feedstock

Table 8-5 shows the energy demands required for the pre-treatment of RS for sugar extraction and cow slurry to inhibit hydrogen-consuming bacteria used in the DF process for hydrogen production. The data used were adjusted from the data obtained from the literature for municipal solid waste (MSW), slaughterhouse waste and food residues (Poschl *et al.*, 2010) and validated with laboratory results. The enzyme hydrolysis was done at 37°C, and hence, the thermal energy required was assumed to be negligible.

Table 8-5: The primary inputs for the pre-treatment and sterilisation of feedstock

Feedstock	Pre-treatment Processes	Electricity (MJ t <sup>-1</sup> )	Heat (MJ t <sup>-1</sup> )
Rice straw	Pre-treatment with agents, e.g. NaOH, PE and HCl (100°C, 1 hr)	72	
Digested cattle slurry	Sterilization (100°C, 1 hr)		37.8

Data is adjusted based on figures from Poschl *et al.* (2010)

It was assumed that the DCS sterilisation was for the stage 1 process (acidogenic), and thus the values represented are one-third of the reported values by Poschl *et al.* (2010).

### 8.4.3 Energy demand in biogas plant operation

Even though the energy demand in biogas plant operation is determined by various factors such as feedstock type, insulation, deployed digestion technology, and other AD processes utilised such as a stirring requirement for maintaining slurry homogeneity, pump rating for liquid feedstock and conveyor for solid feedstock (Poschl *et al.*, 2010), the electricity and heating requirement were determined for the operation of large scale, and farm-scale biogas plants (Table 8-6) based on studies from the literature but were validated using laboratory research data. The figures represent conditions for batch, fed-batch and continuous systems for processes for hydrogen and methane productions operating at mesophilic temperature (37°C). It was assumed that extra energy demand for thermophilic conditions (55°C) used in acidogenesis process was negligible.

Table 8-6: Energy input in biogas plant operation

Biogas plant	Heat (MJ/tonne)	Electricity (MJ/tonne)
Farm scale biogas	250	33
Large scale biogas	110	66

Information is based on figures from Berglund and Borjesson (2006).

The small scale biogas plants have a feedstock handling capacity of 10 000 tonnes per annum, while the large scale biogas systems, which typically produce more than 1.8 million m<sup>3</sup> of biogas per annum, have a feedstock handling capacity of 20 000 tonnes per annum (Poschl *et al.*, 2010).

From the study of Berglund and Borjesson (2006) and Poschl *et al.* (2010), the energy demand is expressed as MJ per tonne added to the fermentation digester surmising that “tonne” refers to a mixture of substrates having a 10% digested (dry) matter (DM). The 10% DM mixture, a wet digestion process, was employed in the laboratory research study. Furthermore, the required DM content is achieved using freshwater or mixing raw materials with different DM contents. In the latter scenario, the energy input for the various raw materials added is calculated with the excess water from the wet raw materials allocated to the drier feedstock. Therefore, when computing the energy demand, 1 tonne of cow slurry with 15% DM is assumed to have 1.5 tonnes of a mixture, generating 1.5 tonnes of digestate mixture. At the same time, 1 tonne of RS with 90% DM is considered to have 9.0 tonnes

of a mix, which will generate 9.0 tonnes of digestate mixture. The energy input can also be expressed as a per cent of either electricity or biogas produced. However, for this study, the energy demand is in a unit of MJ per tonne (Table 8-6). It is generally believed that the energy demand for farm-scale biogas plants is higher per tonne of feedstock than the large scale biogas due to the poor heat insulations and heat exchanges from small scale biogas plants (Poschl *et al.*, 2010). More so, the energy demand for hydrogen production plants may be lower than methane plants due to liquid substrate (RS hydrolysate) used as feedstock in bio-hydrogen plants and less efficient lagging of digester.

Table 8-7: Energy input in dewatering, drying and pelletisation of digestate

Process	Activity	Electricity Demand (MJ tonne <sup>-1</sup> TS RS)	Heat Demand (MJ tonne <sup>-1</sup> TS RS)
Separation	Decanter	74.3	
	Screw-press	4.3	
Solid digestate	Loading	3.78	Exhaust gas (CHP) <sup>a</sup>
	Drying	140	

Numbers is modified from Becker *et al.* (2007); Lootsma and Raussen (2008) and Awiszus *et al.* (2018)

The “a” represent digestate drying method as described by Maurer and Muller (2019) and reported by Hengeveld *et al.* (2020)

#### 8.4.4 Energy Demand in Post Anaerobic Digestion Processes

##### 8.4.4.1 Energy input in the silica production process

Instead of utilising the digestate from the biogas plants as a fertiliser substitute for the spread on agricultural lands, the digestate was explored in silica production. Hence, the liquid digestate was dewatered, dried to a maximum water content of <13% and pelletised for use in a gasifier for more energy production (Awiszus *et al.*, 2018). The weight of the dewatered digestate is reduced after drying, and thus, the storage and transportation value of the material increases. The convection drying technique is assumed to be employed, where heat is transferred from exhaust gas to the digestate (Awiszus *et al.*, 2018) or heat from the CHP plants (Hengeveld *et al.*, 2020). The dried digestate is also pelletised to minimise bulk density and maximise energy density (Fig 8-2). The energy inputs for

dewatering and drying is outlined in Table 8-7, while the energy input used for pelletisation was surmised to be 3% of the primary energy of the dried digestate, assuming the densification factor is 0.588. During the sunny/drying season, drying is presumed to be done by controlled sun-drying safely and hygienically. This is because Nigeria is situated in a tropical climate, and as such, no energy requirement is expended on both processes. The energy input (electricity) required for gasification of the pelletised solid digestate was put at 5% of the total energy output obtained from data of medium-scale wood gasifier from Spanner Re<sup>2</sup> HKA 45 (Table 8-2).



Fig 8-2: A typical pellets sample for use in a gasifier (Maguyon-Detras *et al.*, 2020)

#### 8.4.4.2 Energy demand from biogas utilisation

As discussed hitherto, the biogas was utilised in decentralised CCHP generating units to produce power for the immediate community energy needs with the option of feed-in the excess energy capacity to the national grid. In the same way, most of the heat generated from the CHP plants was utilised via sorption chillers to provide air conditioning, refrigeration and process fluid cooling using Absorption Chillers for CHP Systems (US Department of Energy, 2017). The absorption chiller utilises water, and lithium bromide serves as refrigerant and absorbent, respectively. The detailed summary of the process is recorded in Chapter 2, Section 2.14. The Cooling coefficient of performance (COP)



was assumed to be 0.70. The conversion from thermal to cooling fluid maximises the energy efficiency of the integrated system as Nigeria is situated in the tropical climate zone and has no need for district heating. Therefore, energy demands are paramount in achieving the above biogas conversion route. Although Table 8-8 shows the efficiencies of CHP units and their energy inputs, for ease of calculation, the CHP efficiencies as recorded in Table 6-4 (Chapter 6 Section 6.2.7) was used.

Table 8-8: Efficiency and corresponding energy demand for CHP generation

Biogas plants	Efficiency and corresponding energy demand for CHP generation		
	CHP efficiency <sub>elect.</sub>	CHP efficiency <sub>therm.</sub>	Energy demand (electricity) for operating CHP (%)
Small scale plants (%)	33	50	3
Large scale plants (%)	40	48	4.5

Information based on figures from Walla and Schneeberger (2008) and Poschl *et al.*, 2010).

Typically, thermal efficiency is always higher than the electrical efficiency in all CHP plants. However, in large-scale CHP plants, the thermal efficiency is lower, and about 40% electrical efficiency has been reported for CHP plants (>0.7 MW<sub>elect.</sub>) electrical output (Becker *et al.*, 2007 and Poschl *et al.*, 2010).

Furthermore, heat transmission losses for heat utilisation processes are presented in Table 8-9, which depend mainly on thermal volume flow rate and transmission distance (Daniel *et al.*, 2008). However, the sorption chiller is assumed to be 0.5km away from the large scale CHP plants in this present study.

Table 8-9: Estimated heat losses in transmitting the heat to absorption chillers

Biogas plants	Estimated Loss values by distance	
	0.5km	2km
Small scale plants (%)	3.5	13.5
Large scale Plants (%)	1.0	4.0

Records are based on figures from (Becker *et al.*, 2007 and Poschl *et al.*, 2010).

Part of the heat generated from CHP is utilised for other processes such as electricity generation via Sterling engines and provision of refrigeration and process fluid cooling from sorption chillers.

It is imperative to mention that about 25 to 30% of the total heat generated from the CHP plants is utilized in the AD process for temperature maintenance and sterilisation of cow slurry to inhibit hydrogen-consuming bacteria during the DF process for hydrogen production.

#### 8.4.4.3 Energy input from biogas enrichment

Even though there is currently no regulation and outright permission for injecting bio-methane into the natural gas grid and as vehicular fuel in Nigeria, biogas can be enriched to bio-methane or pure hydrogen for more efficient application and to increase the energy value (Kapdi *et al.*, 2005). Biogas upgrading is a multi-complex process ranging from removing unwanted impurities (CO<sub>2</sub>, H<sub>2</sub>S, water vapour) to compression and storage, and these processes are energy demanding. The procedures employed in biogas upgrading is described extensively in Chapter 2 Section 2.9. Table 8-10 shows the assumed energy inputs for biogas upgrade to bio-methane, while both the biogas lost and the energy input per m<sup>3</sup> for cylinder transportation was expected to be negligible (Poschl *et al.*, 2010)

Table 8-10: Energy input in biogas enrichment

Process	Energy demand (MJ/m <sup>3</sup> <sub>biogas</sub> )	Energy demand (MJ/t km)
Electricity input	1.1	
Heat input	0.36	
Compression to 1.6 MPa <sup>a</sup>	0.18	
Transmission of gas		0.2
Compression to 20 Mpa <sup>b</sup>	0.47	

Data is based on figures from Daniel *et al.* (2008)

Pressures are required for some biogas upgrade technology, for introducing into natural grid<sup>a</sup> and for use as a vehicular fuel<sup>b</sup> (Becker *et al.*, 2007; Borjesson and Matiasson, 2008).

About 0.5 km transmission distance to the natural gas grid was assumed (Poschl *et al.*, 2010).

## 8.5 Energy Output

### 8.5.1 Energy yield from biogas production

The AD process was done as outlined in chapter 6, where a three-stage anaerobic digestion process producing both hydrogen and methane from RS co-digested with digested cattle slurry (DCS) was employed. In this three-stage process, the acidogenic microorganism converted the pre-treated RS hydrolysates to hydrogen and other products in the first stage, while the pre-treated RS residues were used in methane production in the third stage. Whereas the hydrogen produced is collected from the reactor using a gas-bags, the SCFA enters the second stage, where they are further processed down

to methane and carbon dioxide. The main reason for the three-stage hydrogen and methane production processes is process and energy optimisation from the RS substrates.

The energy values of the acidogenic (stage 1) and methanogenic (stage 2 and 3) processes using RS as substrates under continuous state were obtained from Chapter 6 Section 6.3.8 (Table 6-12 and 13).

### 8.5.2 Energy output from gasification of silica

The RS digestates were as detailed in preceding Chapter 6. Even though the biological silica production from RS is described in chapter 7, the energy liberated from digestate during the process is calculated (Table 8-11) based on the specific wood fuel consumption data of a reference biomass CHP system (HKA 45, Spanner Re<sup>2</sup> GmbH, Neufahrn, Germany, fixed-bedwood gasifier with combined heat and power plant, Table 8-2 using a pelletisation factor of 0.588 (Sikkema *et al.*, 2010).

Table 8-11: Energy from different PT RS digestates obtained during silica production

RS Digestates	RS digestate (tonne <sup>-1</sup> RS) <sup>a</sup>	Digestate pellets (tonne <sup>-1</sup> RS) <sup>b</sup>	Gasification rate (%) <sup>c</sup>	Converted pellets (tonne <sup>-1</sup> RS) <sup>d</sup>	Silica precursor (tonne <sup>-1</sup> RS) <sup>e</sup>	D <sub>electricity</sub> (kWh tonne <sup>-1</sup> RS) <sup>f</sup>	D <sub>thermal</sub> (kWh tonne <sup>-1</sup> RS) <sup>g</sup>
HCl-PT	326625.24	192055.64	73%	139432.40	52623.2	154.92	351.87
PE_PT	233377.91	137226.21	72%	98802.87	38423.3	109.78	249.34
NaOH-PT	195605.76	115016.19	73%	83961.82	31054.4	93.29	211.89
Raw RS	475000.00	278300.00	86%	240198.00	39102.0	266.89	606.16

<sup>a</sup> The various RS digestates from AD processes as described in Chapter 6.

<sup>b</sup> The gasifier requires larger particle sizes than typically dried RS digestates for optimum energy conversion. Therefore, the dried RS digestate was converted to RS digestate pellets using a pelletisation factor of 0.588 (Sikkema *et al.*, 2010), as depicted in Fig 8-2.

<sup>c</sup> The gasification rate is the amount of volatile solids (VS) (tonne RS)<sup>d</sup> in the RS digestate converted to energy (electricity and thermal). The rate was calculated from Table 7-2.

<sup>e</sup> The nano-silica (RSA) produced from the various RS PT digestates after gasification was calculated from Chapter 7 Section 7.3.2 (Table 7-2).

The digestate electricity in (kWh) and thermal energy (kWh) are produced using Table 8-2 with a total efficiency kept at 76.22% with electricity at 23.30% and heating at 52.92%.

## 8.6 Results and Discussion

### 8.6.1 Energy Input for Anaerobic Digestion Processes

Having outlined and stated the assumptions for energy demands for each process in the AD processes, the total energy inputs calculated per tonne TS RS of all the processes involved in hydrogen and methane production are summarised in Fig 8-3 and Fig 8-4. It is seen from the picture that the total energy input required to operate the AD process was about 3635 MJ tonne<sup>-1</sup> TS RS for small scale operations and 2672 MJ tonne<sup>-1</sup> TS RS for large scale operations. The variations from the two plants operations could be from the management of the energy efficiencies of the systems. From the total energy inputs of all the processes, the most energy-demanding process was in operating and maintaining the biogas plants, with small scale biogas plant utilising about 70% energy which is equivalent to 2547 MJ tonne<sup>-1</sup> TS RS and large scale biogas plant consuming 59% energy inputs (2672 MJ tonne<sup>-1</sup> TS RS) (Fig 8-3 and 8-4). Similar findings were obtained by Berglund and Borjesson (2006) and Poschl *et al.* (2010), where operation of the biogas plant was generally the most energy-consuming process in the AD system, which corresponds to 50-80% of the energy input.

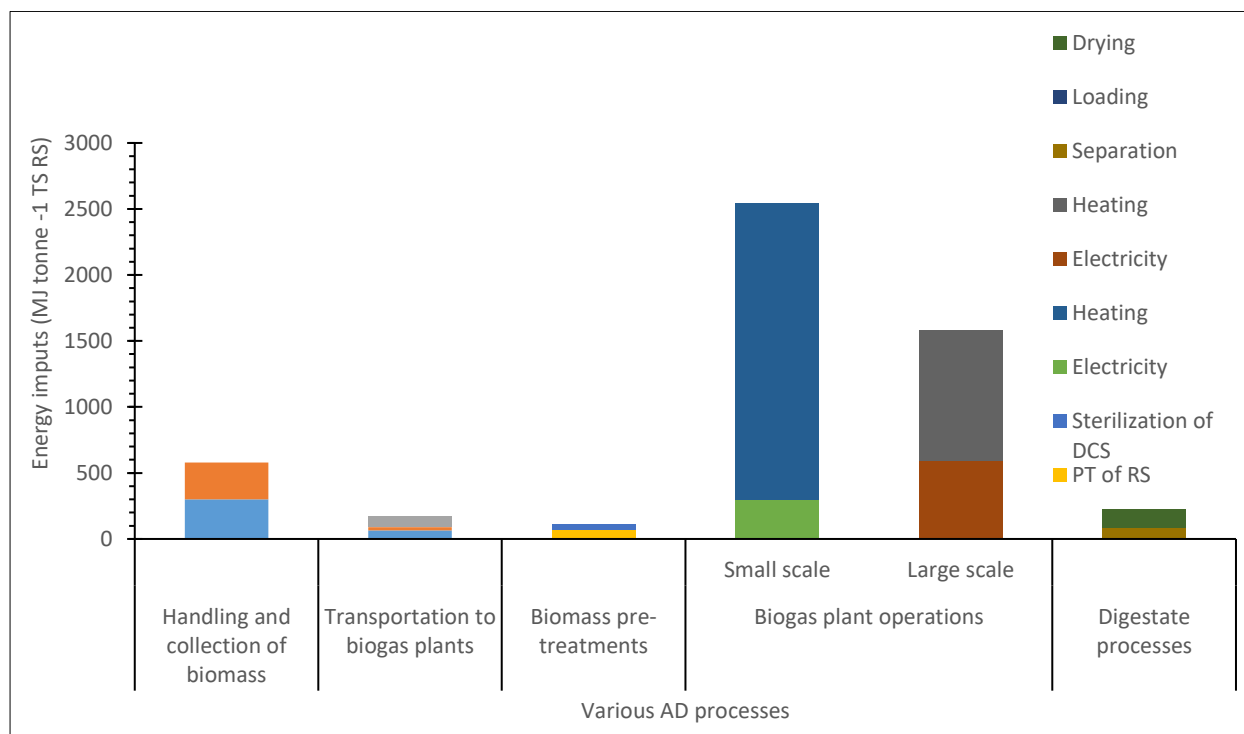


Fig 8-3: Total energy inputs of all the processes involved in hydrogen and methane production

The differences in energy consumption from the two biogas plants, as stated before, is from the management of the energy efficiencies of the systems as it is believed that large scale processes are automated. The high energy demand in biogas plant operation is because energy is required to maintain the temperature of the digestion process, in stirring to maintain the slurry homogeneity, in pumping-in or conveying of feedstock in ease of biogas liberation (Poschl *et al.*, 2010). However, the high energy demand value recorded under biogas operation is because the AD process was performed using wet digestion processes where the feedstock DM content was 10%. The 10% wet digestion process means that 1 tonne of RS with 90% DM is assumed to have 9.0 tonne of a mixture, generating 9.0 tonne of DM. As the energy demand is expressed as MJ per tonne, the fermentation digester surmises that “tonne” refers to a mixture of substrates having a 10% DM.

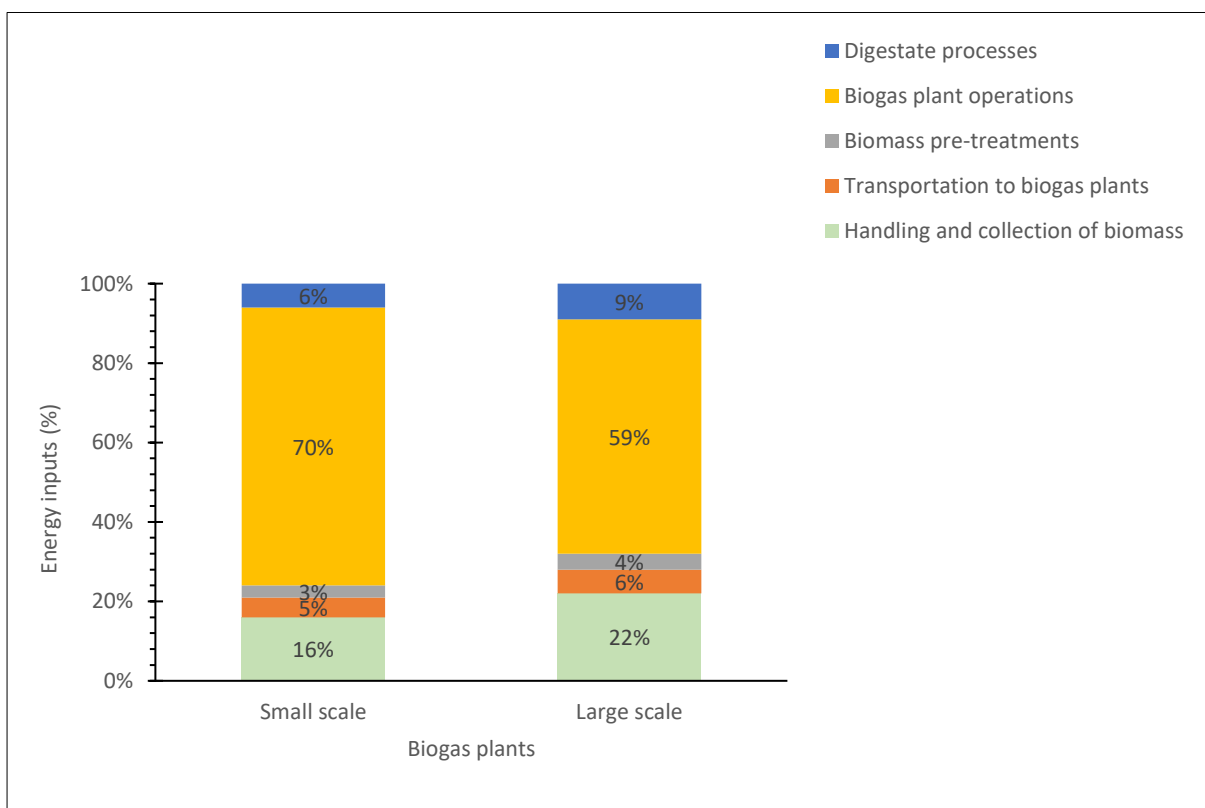


Fig 8-4: The percentages of the energy inputs of all the processes involved in hydrogen and methane production

In contrast, biomass pre-treatments and sludge sterilisations for acidogenic processes had the least energy input of 110 MJ tonne<sup>-1</sup> TS RS, corresponding to 3% for small scale and 4% for large scale

processes (Fig 8-3 and 8-4). The second most energy-demanding process was the handling and collecting DCS and RS at 580 MJ tonne<sup>-1</sup> TS RS corresponding to 16 and 22% for small and large scale processes, respectively (Fig 8-2 and 8-3). This is followed by digestate processes that include separation, loading and drying mechanisms and an energy consumption value of 228 MJ tonne<sup>-1</sup> TS RS (Fig 8-3). However, under the drying processes, it is expected in this study that the heat comes from either the CHP or controlled sun drying as Nigeria is in the tropical climate, and as such, the energy demand in drying is reduced. This argument explains why the energy input in digestate processing and management in this study is different from some recorded values in the literature. For example, Poschl *et al.* (2010) reported a heat demand of 623.5 MJ tonne<sup>-1</sup> for drying digestate.

Finally, the second least energy-demanding process was the transportation of collected biomass to the biogas, which stood at 170 MJ tonne<sup>-1</sup> TS RS (Fig 8-3 and 8-4). The transportation processes contributed 5% and 6% of the total energy input for small and large scale operations.

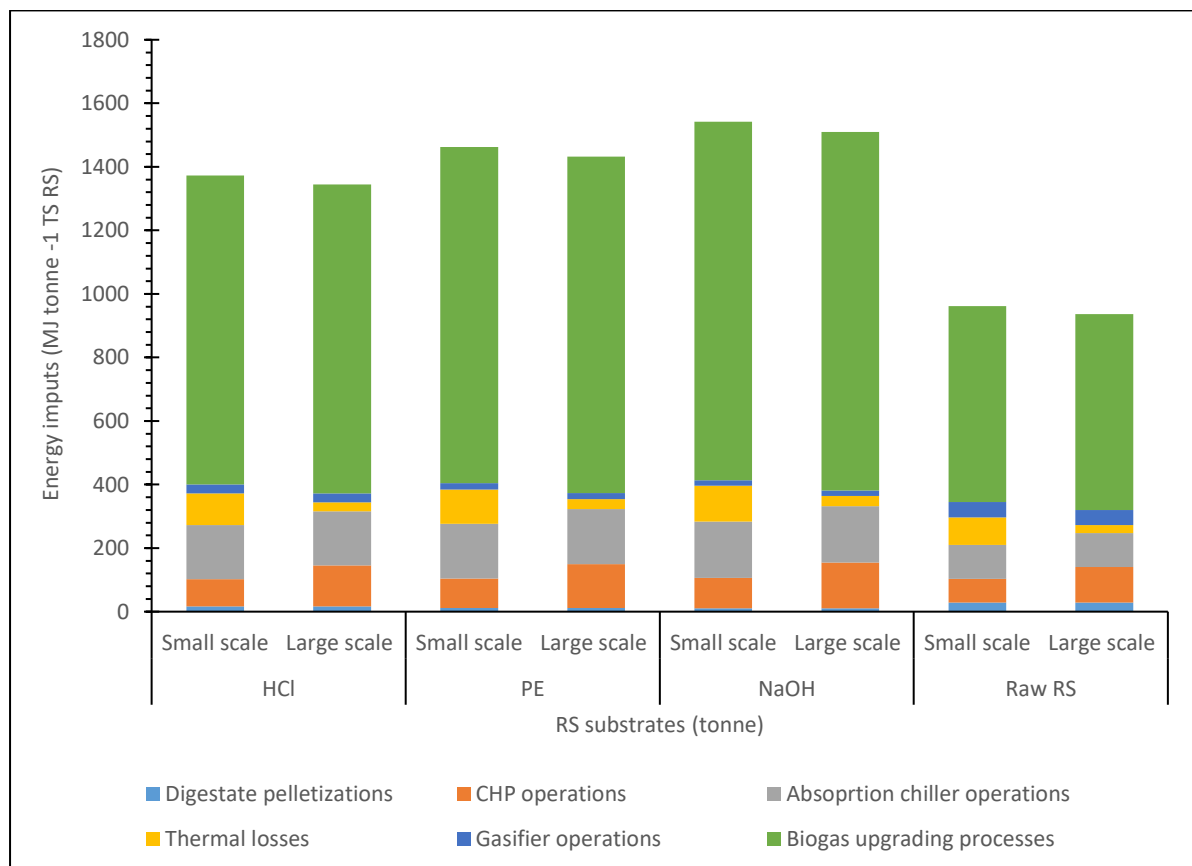


Fig 8-5: Total energy inputs of post AD processes from various PT RS samples

### 8.6.2 Energy Demand for Post Anaerobic Digestion Processes

The post AD procedures involve converting biogas and energy products produced in the AD processes to more useable energy forms such as enriched biogas (bio-methane), solid digestate and silica, and electricity and thermal, which means that the energy demand for post AD processes depends on the useable products. Thus, energy consumptions for post AD processes are typically represented by the proportions of valuable energy products. This research article estimates the energy input for post AD procedures from Chapter 6 Section 6.3.8 (Table 6-12 and 13) and Table 8-11 for the various PT RS samples.

The total energy inputs of post AD processes from various PT RS samples are represented in Figures 8-5, while the percentages of the energy inputs required in post AD processes from different PT RS substrates are shown in Graph 8-6. It can be seen from Figure 8-5 that PT samples consumed more energy ranging from 1344 MJ tonne<sup>-1</sup> TS RS to 1542 MJ tonne<sup>-1</sup> TS RS in processing produced energy products such as biogas than raw RS, which utilised 937 to 962 MJ tonne<sup>-1</sup> TS RS. This high energy consumption is from the energy demand required in purifying the high amount of biogas produced during the AD process, which is adduced from pre-treatment procedures., unlike raw RS that is not pre-treated and, as such, has reduced biogas yield and hence lower energy input for post AD procedures, especially in biogas upgrading.

Furthermore, small scale operations were more energy demanding than large scale operations among all the processes considered. Therefore, the variations from the two operations can be explained as differences in the energy efficiencies of the two systems (Fig 8-5). Not only this, the NaOH-PT RS sample consumed more energy 1510 to 1542 in the conversion of the free AD products to useable forms than the others. This energy consumption is followed by the PE-PT RS sample with an energy input of 1432 to 1463 MJ tonne<sup>-1</sup> TS RS and HCl-PT RS sample, which require an energy value of 1344 to 1373 MJ tonne<sup>-1</sup> TS RS (Fig 8-6).

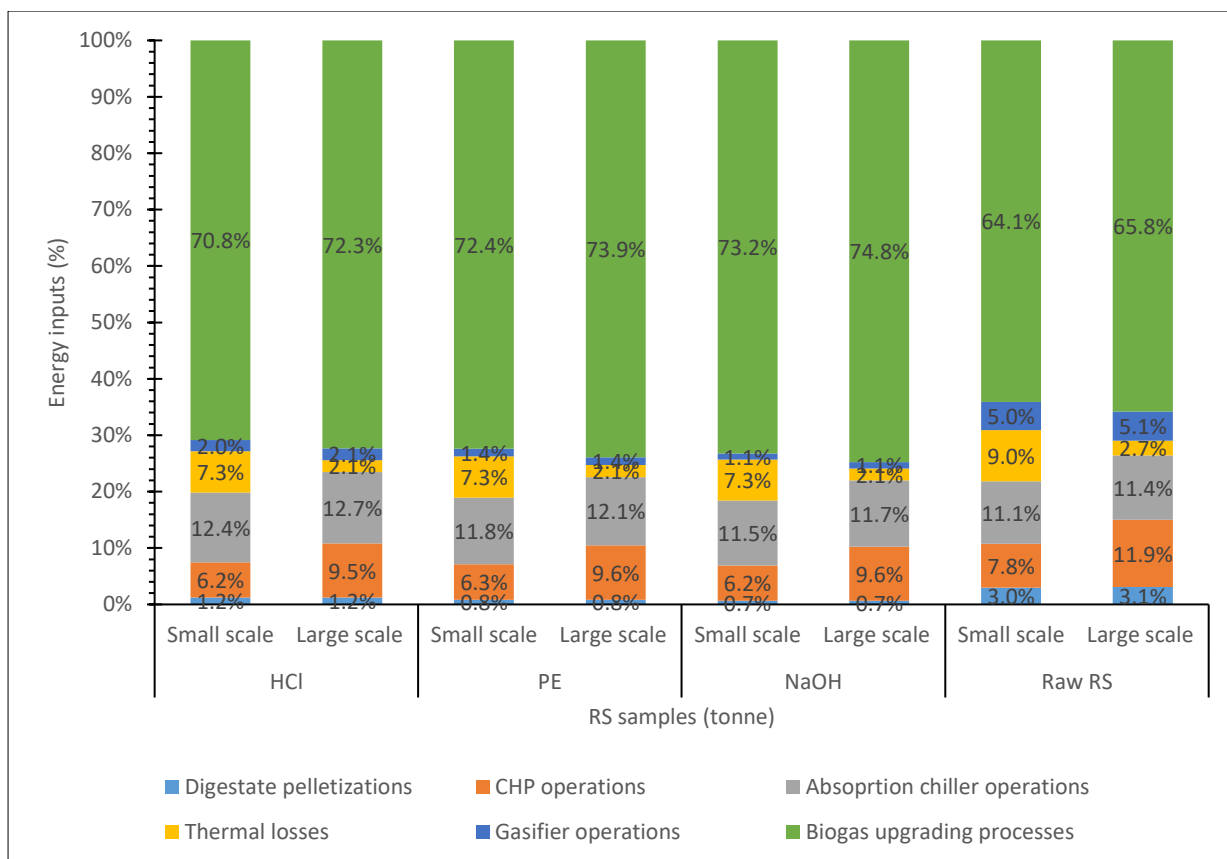


Fig 8-6: The percentages of the energy inputs required in post AD processes from different PT RS samples

Biogas upgrading processes was the most energy demanding at 64 to 75% of all the post AD processes, while digestate pelletisation was the most minimal energy-consuming process for the PT RS residues at 0.7 to 1.2% and raw RS at 3.0% under small scale operations (Fig 8-6). Although digestate pelletisation had almost the same percentage of energy demand for raw RS on small and large scale processes, the thermal losses were the least energy-consuming at 2.7% in large scale operations. In contrast, thermal losses from PT RS substrates varied between the two scales of operation with 7.3% under small scale and 2.1% under large scale (Fig 8-6). The thermal losses were also different for raw RS substrates which account for the third-most energy-demanding operation when the small scale is used (9.0%). The digitisation and modernisation of most large scale machines and plants can explain this variation in thermal losses compared to small scale.

The absorption chiller operations, which uses up to 11 to 13% of all the energy demand in post AD processes, was the second most energy-demanding process (Fig 8-6) except for raw RS under large



scale that have CHP operation (11.9%) as the second most energy-consuming process. The CHP operations followed the second most energy-demanding process, which required about 6.2 to 9.6% energy demand of all the post AD processes but for raw RS samples. Whereas gasifier operations were the second least energy-consuming process at 1.1 to 2.0% of all the post AD processes for all the RS PT, the percentage of the energy demand of the gasifier operation was higher at 5.0 to 5.1% for raw RS, which has more digestate pellets for gasification.

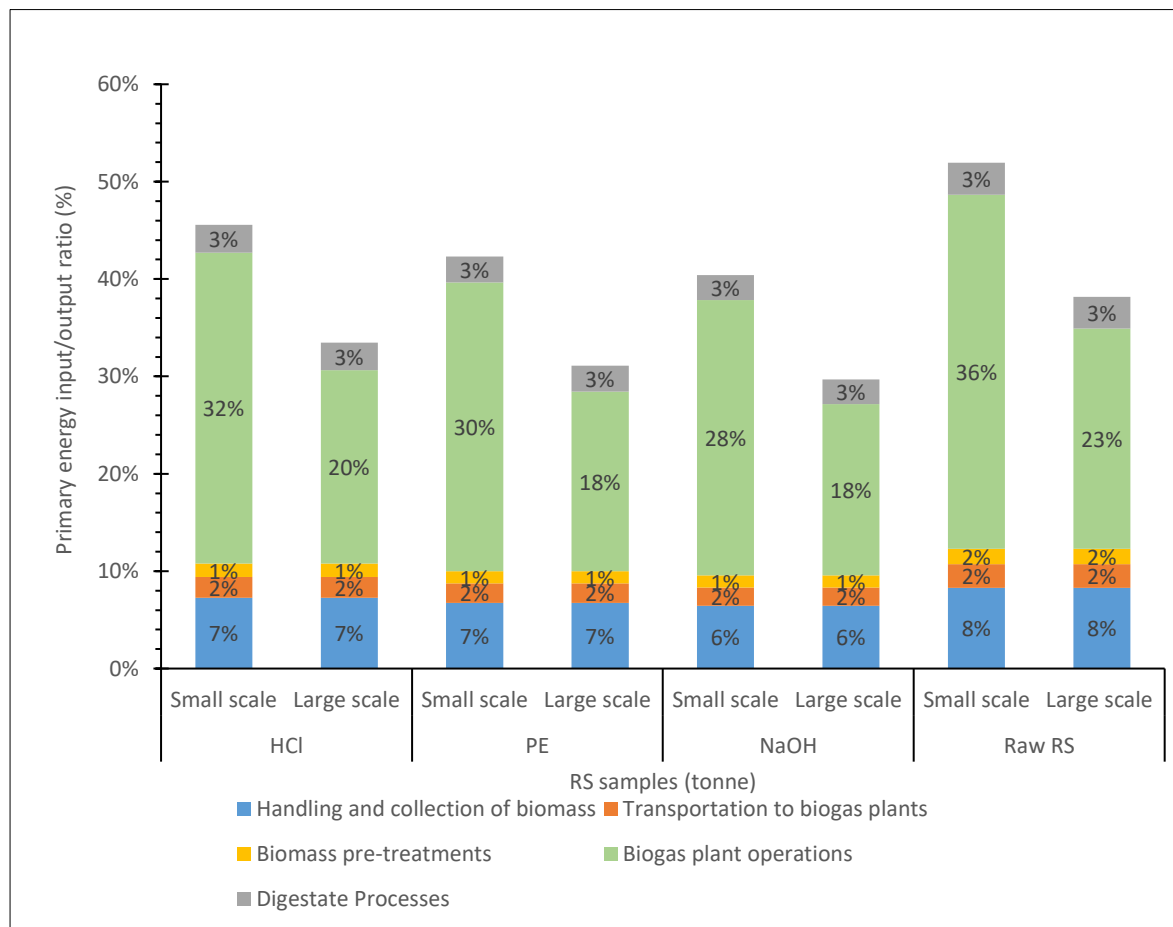


Fig 8-7: The percentages of the PEIO of the AD processes for the various PT RS samples

### 8.6.3 Energy Balance of the Anaerobic Digestion Processes

The energy balance or the energy efficiency of the integrated energy set-up was determined by calculating the PEIO ratio, the ratio of primary energy input to output. Here, the energy demands of the AD processes (Fig 8-3) was considered as the primary energy input while the energy output was the total energy equivalent ( $\text{MJ tonne}^{-1}$  TS RS) of the various RS samples biogas yield ( $\text{m}^3 \text{tonne}^{-1}$  TS

RS) (Table 6-13). The more reduced the PEIO value is, the higher the energy efficiency of the integrated system, and the energy efficiency cum the energy output is said to be negative or inefficient for  $PEIO \geq 1$ . The graphical representation of the percentages of the PEIO of the AD processes for the various PT RS samples is shown in Fig 8-7. It can be seen from the graph that the PEIO ratio was below 50% for all the RS samples but for raw RS under small scale, which had a PEIO value of 52%. In all the samples, large scale operations gave a better PEIO ratio of 30 to 38% than small scale processes (40 to 52%), which is also explained as differences in the energy efficiencies of the two systems in terms of automation and heat regulation and usage. Although Berglund and Borjesson (2006) achieved a PEIO value of about 35% for straw substrates, the straw type and biomass pre-treatment were not specified.

In addition, PT RS samples had a much better PEIO quotient in terms of the corresponding scale of operations than raw RS, with NaOH-PT RS samples having the most positive PEIO ratio of 30% under large scale and 40% under small scale processes, followed by PE-PT RS feedstock having PEIO ratio of 31% under large scale and 42% under small scale practise. The HCl-PT RS samples gave a PEIO ratio of 33% under large scale and 45% under small scale processes (Fig 8-7). In contrast, the raw RS samples produced the least positive PEIO ratio of 38% under large scale and 52% under small scale procedures. Moreover, among all the AD processes in the RS samples, biogas plant operations contributed the highest energy input to the PEIO ratio of 18 to 36% than others (Fig 8-7).

On the other hand, the minimum contributors to the PEIO value were biomass pre-treatments (1 to 2%), including the energy expended in sludge sterilisations and transportation of collected biomass to the biogas plant (2%). Although the raw RS samples are presumed not to be pre-treated, energy was still utilised in grinding to fine form to increase surface area and enhance the ease of accessibility to microbial degradation during the digestion process. Other processes contributing to the increased PEIO ratio were handling and collecting biomass from farm sources at 6 to 8% and digestate processing at a PEIO ratio of 3% (Fig 8-7).

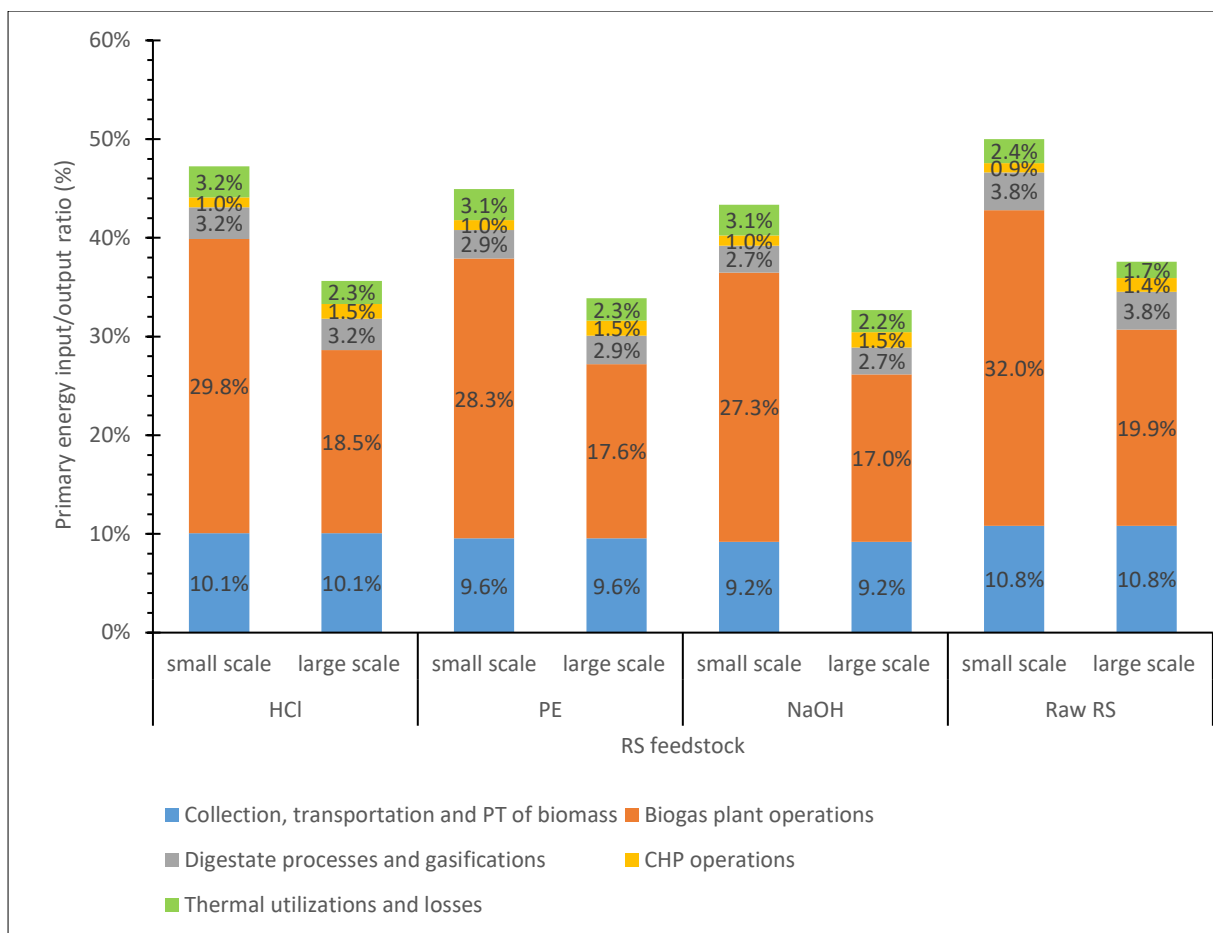


Fig 8-8: The proportions of the energy balances of the integrated system

#### 8.6.4 Energy Balance of the Integrated Energy System

The energy balance of the integrated energy system is defined as the PEIO ratio of the energy demand of all the AD processes (Fig 8-3) and post AD processes (8-5) of the various RS samples with either the total energy equivalent (MJ tonne<sup>-1</sup> TS RS) of the different RS samples biogas yield (m<sup>3</sup> tonne<sup>-1</sup> TS RS) (Table 6-12) and the energy yield from RS digestate gasification (Table 8-11) or the total energy equivalent (MJ tonne<sup>-1</sup> TS RS) of the enriched and upgraded biogas of the various RS feedstock (m<sup>3</sup> tonne<sup>-1</sup> TS RS). The proportions of the energy balances of the integrated unit are illustrated in Fig 8-8, while the percentages of the energy balances of the integrated system when bio-methane is the end-use product is presented in Fig 8-9. From the graphs that have a bit similar interpretation to Fig 8-7, it can be seen that the PEIO ratio was below 50% for all the RS samples. Also, in all the samples, large scale operations had a better PEIO ratio of 33 to 38% than small scale processes (43 to 50%) (Fig 8-8).

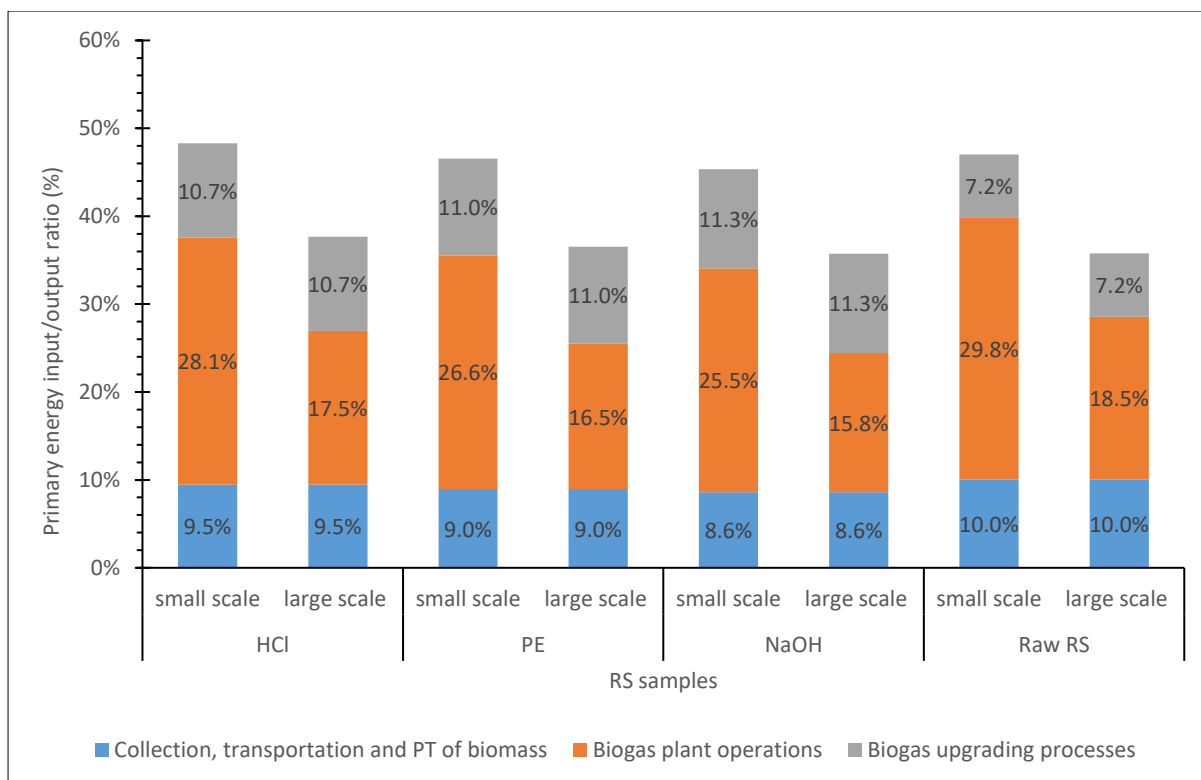


Fig 8-9: The proportions of the energy balances of the integrated system when bio-methane is the end-use product

More so, the PT RS samples gave a much better PEIO ratio under the individual scale of practices than raw RS, with NaOH-PT RS samples having the least PEIO ratio of 33% under large scale and 43% under small scale processes, followed by PE-PT RS feedstock having PEIO ratio of 34% under large scale and 45% under small scale processes, followed by HCl-PT RS samples had a PEIO ratio of 36% under large scale and 47% under small scale processes (Fig 8-8). Nonetheless, the raw RS samples produced the highest PEIO ratio of 38% under large scale and 50% under small scale procedures. These outcomes tally closely with the findings by Poschl *et al.* (2010) and Wang *et al.* (2015) on the energy efficiencies of integrated energy systems.

A similar interpretation was observed for the percentages of the energy balances of the integrated system when bio-methane is the end-use product (Fig 8-9), where the large scale operations had good PEIO ratio of 36 to 38% than small scale processes (45 to 48%) in all the feedstock (Fig 8-9). However, there was much deviation from the preceding graph (Fig 8-8), that is, the proportions of the energy balances for the integrated system, where the least PEIO ratios of 36% were recorded on the raw RS

and NaOH-PT RS samples under large scale practices. In contrast, the PEIO ratios of 37% and 38% were obtained for PE and HCl-PT RS residues, respectively. This unconventionality from the previous results (graphs) is due to the high volumetric yield of biogas produced in PT RS samples, specifically NaOH and PE-PT RS (Chapter 6), requiring increased energy in biogas upgrading compared to raw (untreated) RS that had a reduced biogas yield and hence, low energy input in biogas enrichment. Nonetheless, when small scale operations were employed, the PEIO values were almost the same for all the RS substrates, with NaOH-PT RS having a PEIO ratio of 45%, raw RS and PE-PT feedstock having a PEIO value of 47% and finally, HCl-PT having a PEIO ratio of 48% (Fig 8-9).

Among the integrated system processes for energy generation, biogas plant operations again had the highest energy consumption to the PEIO ratio of 17 to 32% than others (Fig 8-8). However, the CHP operations were the minimum contributors to the PEIO value of 0.9% to 1.5%. This is followed by thermal utilisation and losses together with digestate processes and gasification, which had a PEIO share of 1.7% to 3.2% and 2.7 to 3.8% in that order. It is pertinent to mention that biomass pre-treatments which gave the minimum PEIO ratio of 1 to 2% in the percentages of the PEIO of the AD processes for the PT RS samples, followed by transportation of collected biomass to the biogas plant (2%) (Fig 8-7), were subsumed into the collection, transportation and PT of biomass (Fig 8-8 and 8-9) for ease of tabulation and calculation. Therefore, adding these processes to a single process increased the corresponding proportion of the PEIO value from 9.2 to 10.8% in Figure 8-8 and 8.6 to 10.0% in Figure 8-9.

Finally, whereas the biogas plant processes remained the highest contributor to the PEIO ratio of 16.0 to 28.0% in all the RS substrates, the collection, transportation and PT of biomass had the smallest PEIO ratio of 8.6 to 9.5% for RS PT samples (Fig 8-9). In contrast, the most negligible PEIO value of 7.2% was recorded on biogas upgrading for raw RS. Therefore, the contradictions explanation has been given in the immediate paragraph: the difference in the volumetric yield of biogas produced for PT RS

substrates requiring more energy in biogas upgrading with a PEIO share of approximately 11% approximately than raw RS samples consumed lesser energy in gas purification.

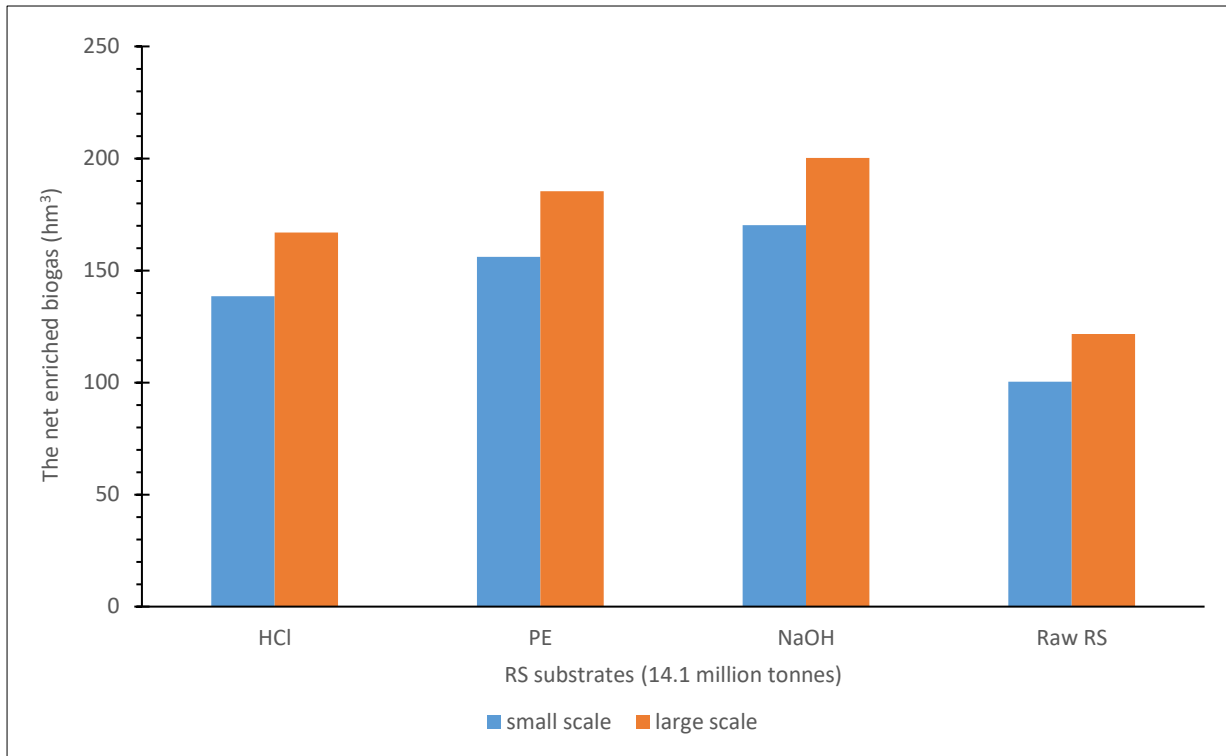


Fig 8-10: Predicted net bio-methane production (million cubic meters) at 1.6mpa from Nigeria’s annual RS yield (14.1 million tonnes) of the various RS feedstock

### 8.6.5 Net Energy Production from Rice Straw Annual yield in Nigeria

This thesis has already cited that Nigeria produces about 14.1 million tonnes of RS yearly. Therefore, using the above information on PEIO, the net energy (bio-methane, electricity, thermal and cooling) of Nigeria’s RS annual yield was estimated. The graph in Fig 8-10 is the predicted net bio-methane production (million cubic meters) from Nigeria’s annual RS yield (14.1 million tonnes) of the various RS feedstock. It is seen from the figure that the net bio-methane at 1.6mpa ranged from 100 to 170 hm<sup>3</sup> if small scale processes are applied and 122 to 200 hm<sup>3</sup> when large scale operations are used. In both scale operations, PT RS samples gave much more bio-methane gas with NaOH and PE-PT producing the highest at 170 and 156 million cubic meters under small scale and 200 and 185 million cubic meters under large scale respectively compared to raw RS that had 100 hm<sup>3</sup> for small scale

operation and 122 hm<sup>3</sup> for large scale processes. HCl-PT feedstock generated 139 and 167 million cubic meters of bio-methane gas at small and large scale operations, respectively. The bio-methane produced from the RS, which is environmentally friendly, can supplement and augment natural gas or be utilised wholly instead in gas stations, power plants, and for domestic use (Ahern *et al.*, 2015).

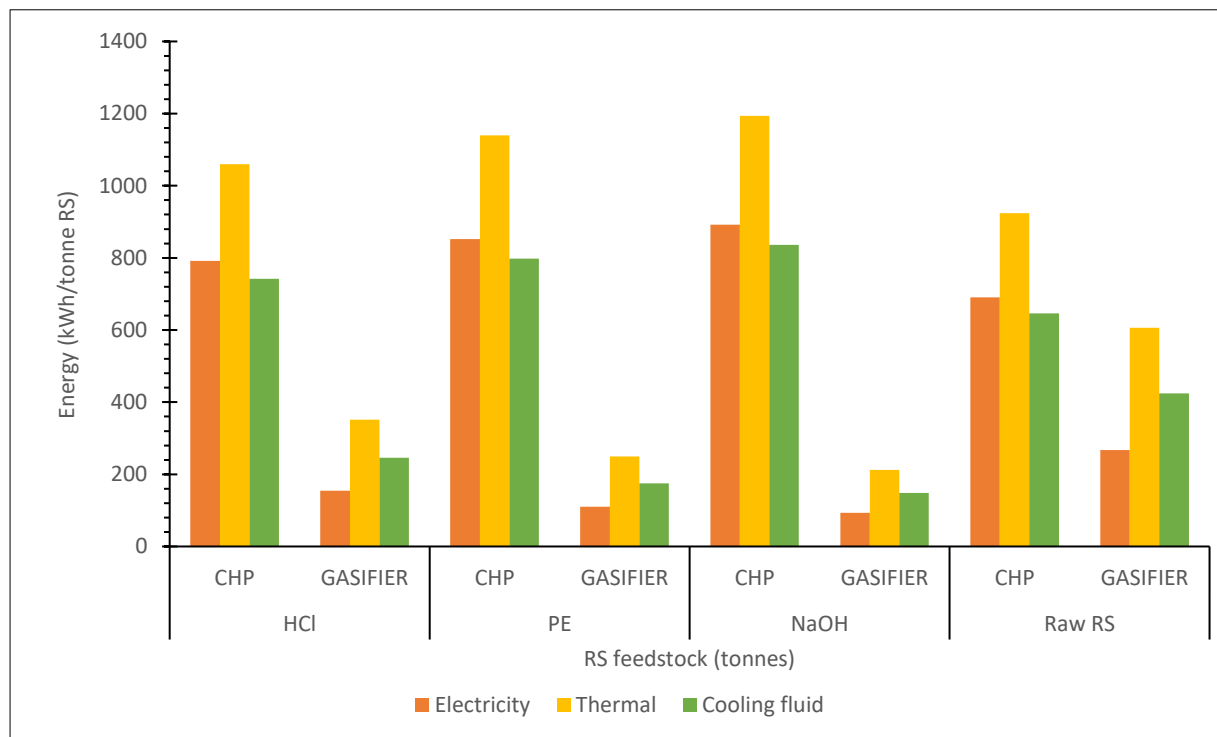


Fig 8-11: The total useful energy products from the various RS feedstock

Similarly, using the PEIO data from above, the estimated net electricity, thermal and cooling fluid using CHP and gasifier of the various RS samples from Nigeria annual RS yield of 14.1 million tonnes assuming large scale operations were employed is summarised in Figure 8-12a, which was calculated from Fig 8-11 (the total useful energy products from the various RS feedstock). From the graph (Figure 8-12a), while it was observed that CHP gave the highest energy output than gasifier, PT RS samples produced higher energy output using CHP technology than raw RS. However, the untreated RS samples had a higher energy yield using gasifiers than others, which is expected due to the undigested RS residue obtained after digestion. In contrast, PT RS substrates had about 80% RS degradation in the AD process, and thus, have little residue for gasification processes.

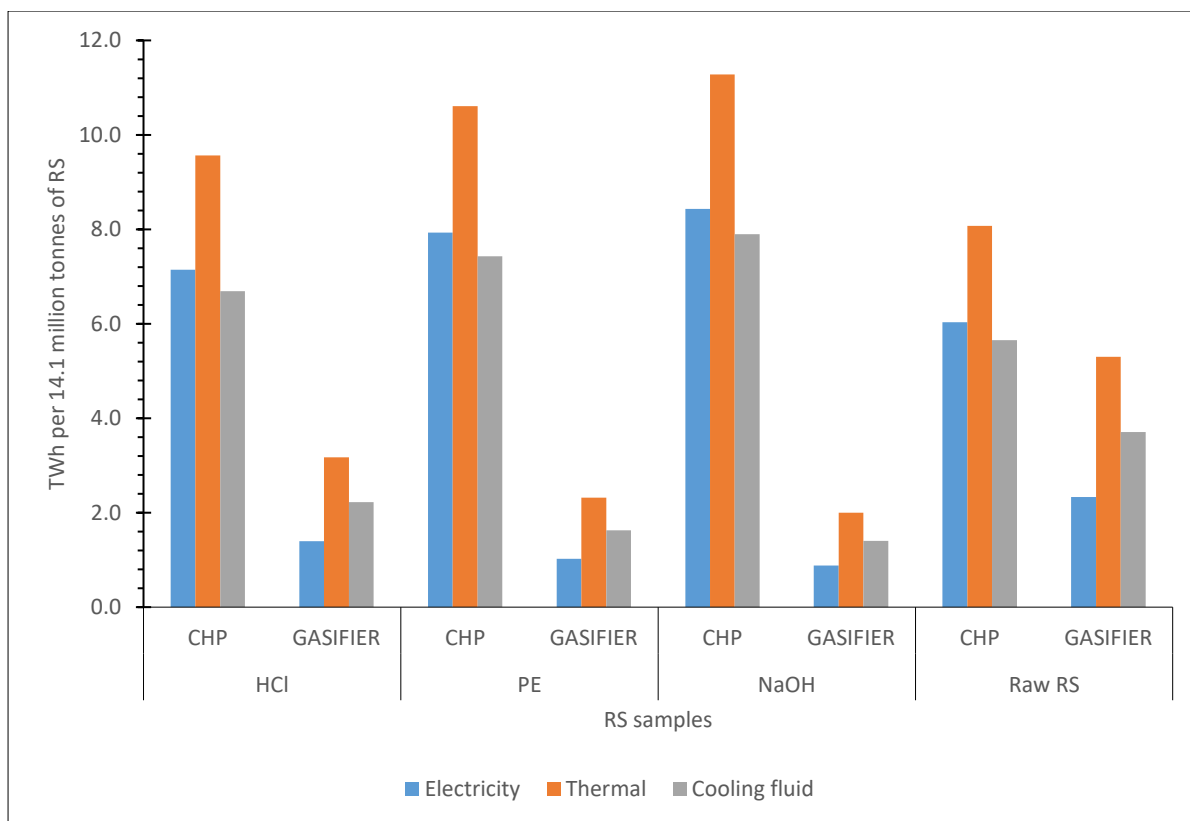


Fig 8-12a: The estimated net electricity, thermal and cooling fluid using CHP and gasifier of the various RS samples from Nigeria annual RS yield of 14.1 million tonnes

Similarly, the graph in Fig 8-12b shows that the net electricity produced in TWh available for use was within the range of 8.4 to 9.3 from combining the two electricity-generating technologies, CHP and gasifier. Although the net electricity value differed from reported European electricity production of 14.6 TWh from biogas in 2005 (Bruno *et al.*, 2009), it did not say whether the electricity produced was net value. In addition, the net thermal energy available for use was between 12.7 to 13.4 TWh, which was also obtained from the addition of the two technologies. However, most thermal energy is converted to cooling fluid as Nigeria is situated in the tropics. Therefore, the net cooling fluid produced and available for consumption ranged from 8.9 to 9.4 TWh (Fig 8-12b).

From the above findings, it is observed that Nigeria can produce about 8.4 to 9.3 TWh of electricity from biogas produced from RS, which can complement the total electricity consumption of Nigeria, which grew from 10.77 TWh in 1990 to 26.26 TWh (Fig 2-4). In addition, Nigeria's electricity



consumption per capita is relatively constant from 1990 (110 kWh) to 2016 (140 kWh) (IEA, 2016). At 140 kWh per capita in 2016, Nigeria trail significantly behind other developing nations in electricity per capita (IEA, 2016). For example, Ghana’s electricity per capita consumption is 403 kWh, about three times Nigeria, while South Africa stands at 4.36 MWh (Oyedepo *et al.*, 2018), about 31 times Nigeria’s electricity per capita. Going by the global minimum average electricity consumption per capita for emerging economies put at 500 kWh, Nigeria would require 180 GW of electricity for full power. Although the estimated demand is significantly miles away from the current electricity production (Usman and Abbasoglu, 2015 and Oyedepo *et al.*, 2018), energy from agricultural biomass primarily from RS could be used as seen from this research study to complement and supplement energy shortages in Nigeria. This energy complementation from biomass is evident from Germany, the UK, and Italy, where biogas energy stood at 92TWh, 27TWh and 22TWh in 2015 (Amaral *et al.*, 2020).

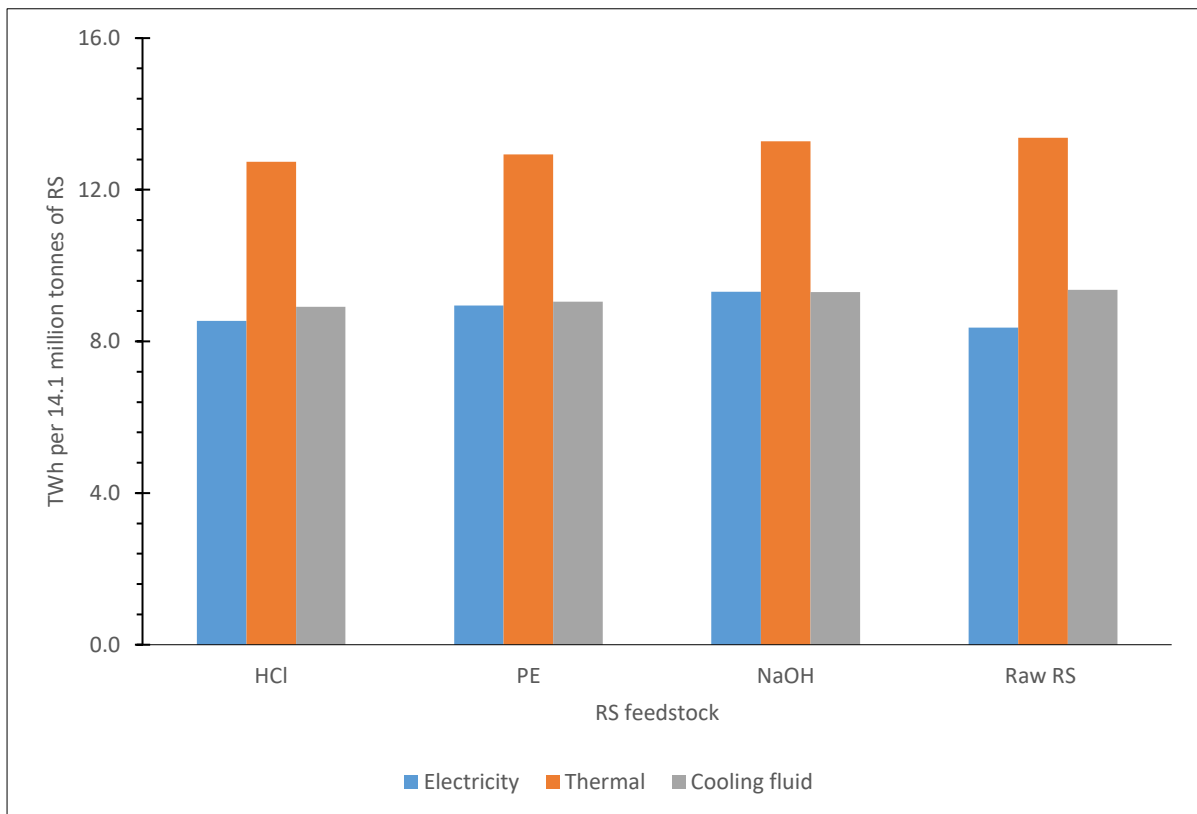


Fig 8-12b: Combined net electricity, thermal and cooling fluid of the various RS samples from Nigeria annual RS yield of 14.1 million tonnes.

## 8.7 Conclusion

The analyses considered the energy values of the two primary feedstock materials of rice straw (RS) and cow dung slurry employed in an energy integrated unit. The integrated system comprises biogas plants, dryer, gasifier, CCHP unit and biogas upgrading unit used to produce biogases (hydrogen and methane) and silica precursor's generation of power and heat. The energy balances of the integrated unit were calculated using data from laboratory studies and the literature. The result obtained showed that the PEIO ratio was below 50% for the various RS feedstock. In all the samples, large scale operations had a better PEIO ratio of 33 to 38% than small scale processes (40 to 52%). In addition, the PT RS substrates gave a much better PEIO ratio under both scales of practices than raw RS. Among the integrated system processes for energy generation, biogas plant operations produced the highest energy consumption to the PEIO ratio of 17 to 32% than others, while the most minimum contributors to the PEIO value of 0.9% to 1.5% was the CHP operations.

A similar interpretation was observed for the percentages of the energy balances for the integrated system when bio-methane is the end-use product, where the large scale operations had an excellent PEIO ratio of 36 to 38% than small scale processes (45 to 48%) in all the samples. However, there was much deviation from the proportions of the energy balances for the integrated system, where the least PEIO ratio of 36% was recorded on the raw RS and NaOH-PT RS samples under large scale practices. In contrast, the PEIO ratios of 37% and 38% were obtained for PE and HCl-PT RS residues, respectively. Whereas the biogas plant processes remain the highest contributor to the PEIO ratio of 16.0 to 28.0% in all the RS substrates, the collection, transportation, and PT of biomass produced the minimum PEIO ratio of 8.6 to 9.5% for RS PT feedstock (Fig 8-9). Biogas upgrading for raw RS recorded the most negligible PEIO value of 7.2%.

Finally, using the PEIO data, the net energy (bio-methane, electricity, thermal and cooling) from Nigeria's RS annual yield was estimated. It was found that the net bio-methane at 1.6mpa ranged from

100 to 170 hm<sup>3</sup> if small scale processes were applied and 122 to 200 hm<sup>3</sup> when large scale operations were used. In the same vein, the predicted electricity produced in TWh available for use was within the range of 8.4 to 9.3. In addition, the net thermal energy available for use was between 12.7 to 13.4 TWh. However, most thermal energy is converted to cooling fluid as Nigeria is situated in the tropics. Therefore, the net cooling fluid produced and available for consumption ranged from 8.9 to 9.4 TWh.



## Chapter 9 Final remarks and recommendations for further research work

### 9.1 Final Remarks

Sustainable and cost-effective energy is critical to any nation's social and economic development, which perhaps explains why Nigeria has not fully progressed despite its numerous human and natural resources. This PhD study provides a solution to the energy situations currently experienced in the country through AD technology. Most importantly, except for the gasification procedure, processes from the AD processes and its energy products are environmentally friendly and indirectly contribute to eradicating GHG emissions and carbon reduction in the atmosphere. Another gain of the research study is the effective utilization of agricultural wastes (rice straw (RS) and digested cow slurry (DCS)) that ordinarily would have constituted environmental pollution in producing bio-hydrogen and bio-methane, versatile renewable energy sources.

This research thesis provides energy and power to the local communities by designing an integrated energy system comprising biogas plants, gasifiers, CHP plants, and absorption chillers. Although methane gas was also studied in this research work, hydrogen gas which is the future energy, was the major biofuel of interest. Many investigators have carried out an extensive study on the production of H<sub>2</sub> from biomass and other feedstock. However, bio-hydrogen production is affected, among others, mainly by the quality of seeded sludge in the DF process and RS's complex, recalcitrant, and lignified nature. These factors affecting biological hydrogen were studied in the research work, and the findings were promising. In the same vein, agro-industrial waste such as PE, CSWW, and CSTL, which constitute environmental pollution from agricultural wastes, were investigated as seeded sludge enrichment, RS pre-treatment and RS leaching agent. Although the result was positive, PE presented a more realistic and promising agent than others. Furthermore, the amorphous silica-precursors that have more economical and nanostructural value produced from the various RS digestates, indicated the success of this thesis. Finally, life-cycle and energy assessment of the biogas systems showed an excellent PIEO ratio for both small scale and large scale operations.

## 9.2 Summary of Research Outcomes

- ✚ In the first experimental chapter, the effectiveness of applying agro-industrial waste materials as alternative materials that can enrich the level of HPB and inhibits the population of HCB in DCS was investigated. Based on the result obtained, it is concluded that agro-industrial waste materials can enrich HBP in DCS. Although Heat-shock DCS produced the highest daily VHP of 135 NmL H<sub>2</sub> g<sup>-1</sup> VS on the second day when compared to other PT DCS using glucose as substrates, it is followed by PE-PT DCS, which gave the highest daily VHP of 115 NmL H<sub>2</sub> g<sup>-1</sup> VS but at a shorter time (24 h). The other PT DCS - CSWW-PT DCS and CSTL-PT DCS produced lower daily VHP of 92 and 82 NmL H<sub>2</sub> g<sup>-1</sup> VS, in that order, while the untreated DCS had 37 NmL H<sub>2</sub> g<sup>-1</sup> VS as its highest daily VHP.
- ✚ The second experimental chapter studies the feasibility of producing hydrogen biologically from untreated RS via DF using glucose or sucrose enriched seeded sludge. The research findings showed that SHY of 149 NmL H<sub>2</sub> g<sup>-1</sup> TS produced from untreated RS co-digested with sugar-enriched DCS was significantly higher than the hydrogen accumulation of 16 NmL H<sub>2</sub> g<sup>-1</sup> TS from untreated RS co-digested without sugar-enriched DCS. Nonetheless, subsequent hydrogen production studies from co-digestion of untreated RS with sugar-enriched DCS using the same protocol and conditions proved abortive without an unequivocal elucidation.
- ✚ This study examined bio-H<sub>2</sub> and bio-CH<sub>4</sub> co-production from pretreated rice straw in a three-stage anaerobic digestion process with the produced biogas converted to power, heat, and cool using the CCHP strategy. Experimental results showed that at acidogenesis stage, hydrogen and biogas yield was insignificant when chemical and agro-industrial agents were employed alone. However, the daily VHP increased when the PT RS residues were biologically hydrolysed with NaOH (114 NmL H<sub>2</sub> g<sup>-1</sup> TS d<sup>-1</sup>) and PE-PT RS residues (103 NmL H<sub>2</sub> g<sup>-1</sup> TS d<sup>-1</sup>) having the highest values at steady states and raw RS producing the least (30 NmL H<sub>2</sub> g<sup>-1</sup> TS d<sup>-1</sup>). Furthermore, mechanical and chemical pre-treatment followed by biological hydrolysis also improved the daily SMY by 18%, 31.7% and 41.5% for HCL, PE and NaOH-PT RS residues

compared with the raw RS (control) sample. The total output energy expressed in electricity and thermal production using CCHP from the three stages was calculated and from the result obtained, NaOH and PE-PT RS residues also gave the highest electricity (892.43 and 852.00  $\text{KWh}_{\text{elect.}} / \text{tonne TS}$ ) and thermal (1194.10 and 1140  $\text{KWh}_{\text{therm.}} / \text{tonne TS}$ ) yield respectively. On the other hand, the HCl-PT RS residues gave electricity (791.85  $\text{KWh}_{\text{elect.}} / \text{tonne TS}$ ) and thermal (1059.51  $\text{KWh}_{\text{therm.}} / \text{tonne TS}$ ) yield. In contrast, the energy produced from raw RS has a corresponding electricity value of 690.28  $\text{KWh}_{\text{elect.}} / \text{tonne TS}$  and a thermal value of 923.61  $\text{KWh}_{\text{therm.}} / \text{tonne TS}$ . In the meantime, most of the heat generated was employed in air conditioning, refrigeration and process fluid cooling using an absorption chiller since Nigeria is in the warmer climatic region. Thus, the cooling fluid in  $\text{KWh}_{\text{cool}}$  produced per tonne of TS RS was 835.57, 798.00 and 741.66 for NaOH, PE and HCl PT RS samples but, the control RS sample produced 646.53  $\text{KWh}_{\text{cool}} / \text{tonne TS RS}$ .

✚ Whereas the *Clostridium*, *Ruminococcus* and *Thermoanaerobacterium*, which belong to the *Firmicutes*, were the dominant genera in acidogenic digesters, *Methanosarcina*, *Methanobacterium*, and *Methanosaeta* belonging to the phylum *Euryarchaeota* were the most abundant genera in methane-producing reactors.

✚ In Chapter 7, which also is experimental chapter 4, the purpose of the study was to evaluate the feasibility of producing nano-silica from RS that has been hydrolysed and digested for hydrogen and methane productions. Also considered for nano-silica precursors was RS leached with agro-industrial wastes such as CSTL and CSWW. The study findings showed that pre-treated and digested methanogenic RSA samples contained amorphous silica materials confirmed by the SEM, EDX and XRD results. The agro-industrial wastes (CSTL and CSWW) are good but probably weak leaching agents as the RSA were slightly amorphous. The leaching attributes of agro-industrial wastes and their subsequent RSA amorphousness were confirmed from the SEM and EDX values. However, the XRD result shows that CSWW-leached RSA offers more potency as a leaching agent than CSTL-leached RSA.

✚ The last experimental chapter analysed the life cycle and energy assessment of the digestion and post digestion processes in the integrated system, and the result obtained showed that the PEIO ratio was below 50% for the various RS feedstock. In all the samples, large scale operations had a better PEIO ratio of 33 to 38% than small scale processes (40 to 52%). In addition, the PT RS substrates produced a much better PEIO ratio than raw RS. Among the integrated system processes for energy generation, biogas plant operations gave the highest energy consumption to the PEIO ratio of 17 to 32% than others, while the most minimum contributors to the PEIO value of 0.9% to 1.5% was the CHP operations. Using the PEIO data, the net energy (bio-methane, electricity, thermal and cooling) from Nigeria's RS annual yield was estimated. It was found that the net bio-methane at 1.6mpa ranged from 100 to 170 hm<sup>3</sup> if small scale processes were applied and 122 to 200 hm<sup>3</sup> when large scale operations were used. In the same vein, the predicted electricity produced in TWh available for use was within the range of 8.4 to 9.3. In addition, the net thermal energy available for use was between 12.7 to 13.4 TWh. However, most thermal energy is converted to cooling fluid as Nigeria is situated in the tropics. Therefore, the net cooling fluid produced and available for consumption ranged from 8.9 to 9.4 TWh

### **9.3 Recommendations and Observations**

Although the stipulated objectives and hypothesis of the PhD study mainly were fulfilled, there were limitations in the research resources, which perhaps impacted the scale of laboratory work regarding protocols and various laboratory analyses employed in the experimental Chapters. Therefore, further research study should be carried on primarily on the following areas and topics:

1. First of all, although the result of hydrogen production from unhydrolysed raw rice straw co-digested with sugar enriched DCS was successful as reported in the thesis, subsequent hydrogen production from co-digestion of untreated RS with sugar enriched DCS using the same protocol and conditions proved futile. Failure to replicate results has been discussed



extensively in the thesis. However, sugar enrichment of DCS in a unique reactor where seeded sludge is suspended as a biofilm should be considered in future studies. This development will significantly reduce HPB washed out and the impact of SCFA on hydrogen pathways, especially during the steady-state processes. In addition, genetic modification of bacteria that can both degrade lignocellulose biomass and convert sugar monomers directly to hydrogen gas can also be explored. The gene alteration can be either be achieved by blocking the end-stage methanogenesis or improving the genes required for hydrolysis and acidogenesis.

2. Secondly, other agro-industrial wastes such as Brewers' effluents should be explored for DCS enrichment and delignification capabilities for lignocellulose biomass. Starchy-containing agro-industrial wastes such as CSWW and CSTL should also be investigated for their suitability for methane production.
3. The elemental composition analysis obtained from this study (Chapter 3, Table 3-1) shows that PE could be used as buffers in an AD process, especially for methane production. Thus, the novel idea can be studied and investigated to the best of the author's knowledge. In addition, potassium ion has been known to counter the effects of high nitrogen concentration; therefore, PE as buffers in methane production balances ammonification.
4. Perhaps to improve the enzymes accessibility and, thus, the sugar yield for hydrogen production in Chapter 6, the concentration of chemical agents and PE should be slightly increased from the concentrations employed in the research study. The explanation is that the sugar hydrolysates used for hydrogen production are mainly from biological hydrolysis, and results from chemical pre-treatments hydrolysates were discarded. Therefore, processes that favour sugar yields from biological processes should be encouraged to increase VHY.
5. The writer suggested that to improve better the silica amorphousness from RS digestates, RS substrates to be used as silica should have an AD residency duration of at least 80 days (that is, the RS feedstock should stay 80 days in the digester) to ensure the complete removal and leaching of impurities.

6. Finally, although not covered in this report, applying PE in chemical absorption processes similar to scrubbing with alkali described in Section 2.9.3.2.1 is very promising for removing CO<sub>2</sub> from biogas. The author intends to complete this research investigation. Still, on biogas purification, work on biogas purification using *in-situ* chemoautotrophic biogas technology is also in progress. In this trial study, H<sub>2</sub> and CO<sub>2</sub> liberated during acidogenesis enter a scrubbing chamber containing PE, where most CO<sub>2</sub> is absorbed. Then, the H<sub>2</sub> enters an active methanogenic reactor containing mostly hydrogenotrophic methanogens. In the methane digester, the CO<sub>2</sub> produced is converted from non-energy yielding to CH<sub>4</sub> by these methanogens under mild experimental conditions that contribute significantly to biogas' general value. Thus, the eventual biogas will contain high H<sub>2</sub> and CH<sub>4</sub> contents and a minimal or no amount of CO<sub>2</sub>.



# Appendices

## Appendices for Chapter Six

Appendix 1 Analysis of rice straw mass balance, purified gas and biogas yield of the three-stage fermentation process from different pre-treatment technologies.

This screenshot shows an Excel spreadsheet with multiple data tables. The top table, titled 'Working Gas Production per 100 kg DM', lists parameters like 'Working Gas', 'Biogas', and 'Purified Gas' with values for 'kg DM' and 'kg DM/kg DM'. Below it, there are sections for 'Substrate' and 'Product' with detailed mass flow data. The bottom part of the spreadsheet contains summary statistics and additional process parameters.

This screenshot displays another view of the Excel spreadsheet, focusing on different data sections. It includes tables for 'Substrate' and 'Product' with mass flow data. There are also sections for 'Biogas' and 'Purified Gas' production, showing yields and costs. The spreadsheet uses various colors to highlight different data points and includes several formulas.

This screenshot shows a third view of the Excel spreadsheet, detailing the mass balance and biogas yield. It features tables for 'Substrate' and 'Product' with mass flow data. The spreadsheet also includes sections for 'Biogas' and 'Purified Gas' production, showing yields and costs. The data is organized into clear sections with headers and sub-headers.

This screenshot shows a detailed Excel spreadsheet with multiple columns and rows. The data is organized into sections for 'Raw Biogas Production' and 'Purified Biogas Production'. Each section includes sub-sections for 'Methane Production' and 'CO<sub>2</sub> Production'. The columns represent various parameters such as 'Methane (m<sup>3</sup>)', 'CO<sub>2</sub> (m<sup>3</sup>)', 'Methane (kg)', and 'CO<sub>2</sub> (kg)'. The rows represent different stages or components of the production process. The spreadsheet uses color-coding (green and yellow) to highlight specific data points.

This screenshot shows a section of the Excel spreadsheet focusing on 'Methane Production' and 'CO<sub>2</sub> Production'. It contains several tables with columns for 'Methane (m<sup>3</sup>)', 'CO<sub>2</sub> (m<sup>3</sup>)', 'Methane (kg)', and 'CO<sub>2</sub> (kg)'. The data is presented in a structured format with multiple rows and columns, likely representing different stages or components of the production process. The spreadsheet uses color-coding (green and yellow) to highlight specific data points.

Appendix 2 Calculation of the energy value of the produced gases (purified and raw biogas) in m<sup>3</sup> and kg biogas per tonne RS for the various rice straw pretreated samples

This screenshot shows another section of the Excel spreadsheet, similar to the previous one, focusing on 'Methane Production' and 'CO<sub>2</sub> Production'. It contains several tables with columns for 'Methane (m<sup>3</sup>)', 'CO<sub>2</sub> (m<sup>3</sup>)', 'Methane (kg)', and 'CO<sub>2</sub> (kg)'. The data is presented in a structured format with multiple rows and columns, likely representing different stages or components of the production process. The spreadsheet uses color-coding (green and yellow) to highlight specific data points.

2022-2023

Category	Revenue	Expenses	Profit
Revenue	1000		1000
Expenses		500	500
Profit			500

2023-2024

Category	Revenue	Expenses	Profit
Revenue	1200		1200
Expenses		600	600
Profit			600

2022-2023

Category	Revenue	Expenses	Profit
Revenue	1000		1000
Expenses		500	500
Profit			500

2023-2024

Category	Revenue	Expenses	Profit
Revenue	1200		1200
Expenses		600	600
Profit			600

2022-2023

Category	Revenue	Expenses	Profit
Revenue	1000		1000
Expenses		500	500
Profit			500

2023-2024

Category	Revenue	Expenses	Profit
Revenue	1200		1200
Expenses		600	600
Profit			600

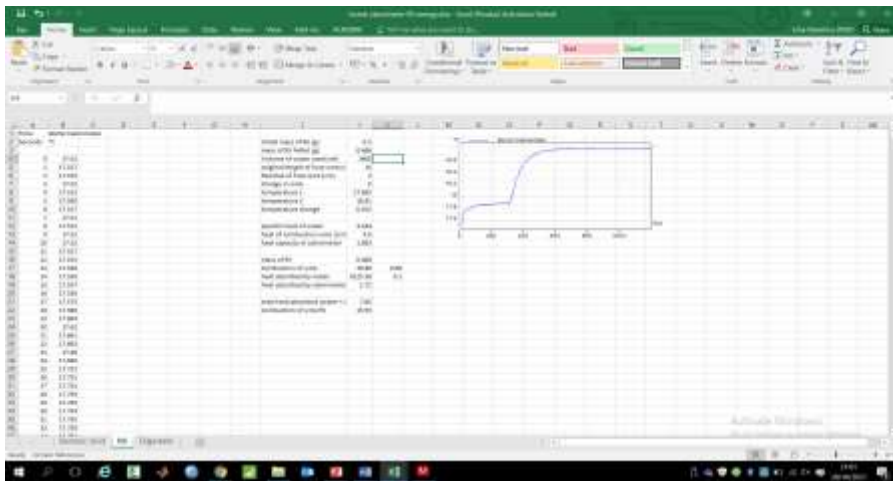
2022-2023

Category	Revenue	Expenses	Profit
Revenue	1000		1000
Expenses		500	500
Profit			500

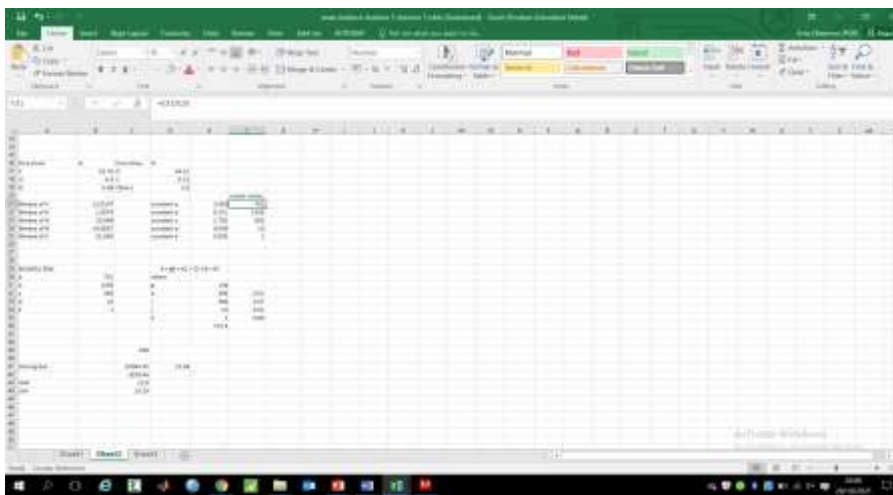
2023-2024

Category	Revenue	Expenses	Profit
Revenue	1200		1200
Expenses		600	600
Profit			600

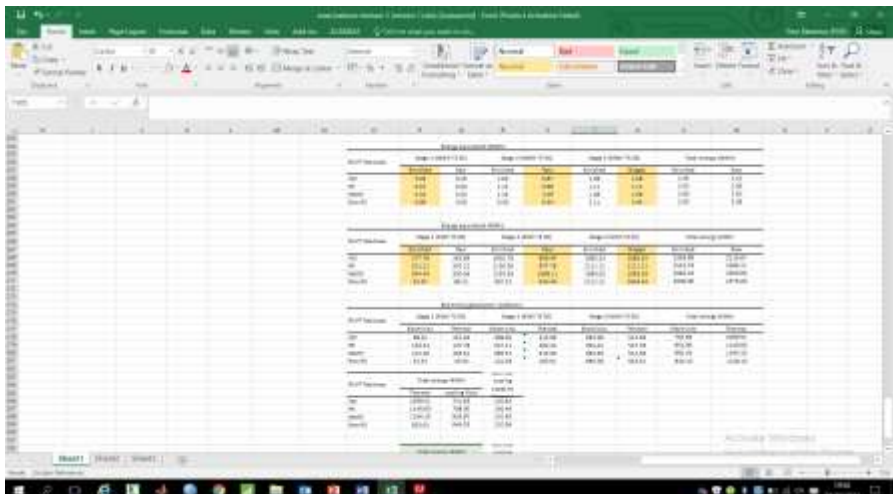
Appendix 3 Assessment of RS energy value using bomb calorimeter and from Eqn 3-3b



Appendix 4 Calculation of Buswell for TBMP and Dulong Equations.

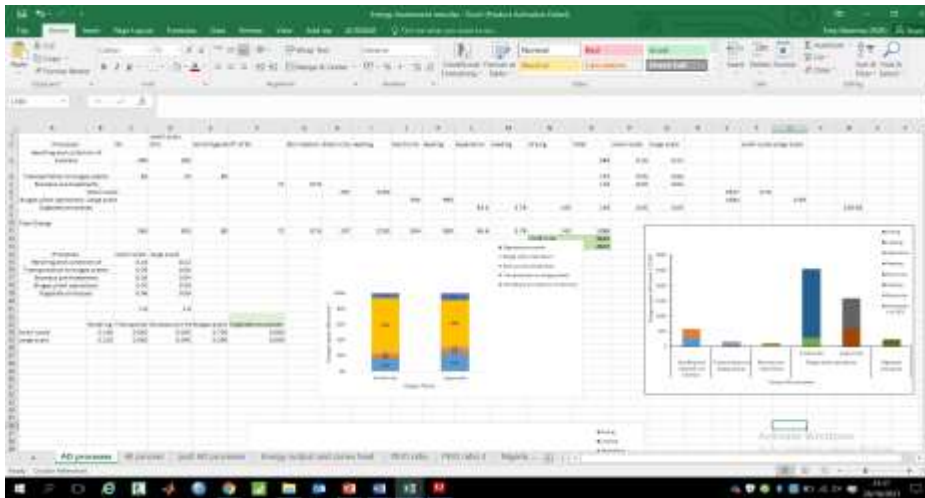


Appendix 5 Estimation of the the electricity (KWh<sub>elect.</sub>) and thermal energy (KWh<sub>thermal</sub>) generation produced from the corresponding energy values of the different PT RS at the different stages of the process.

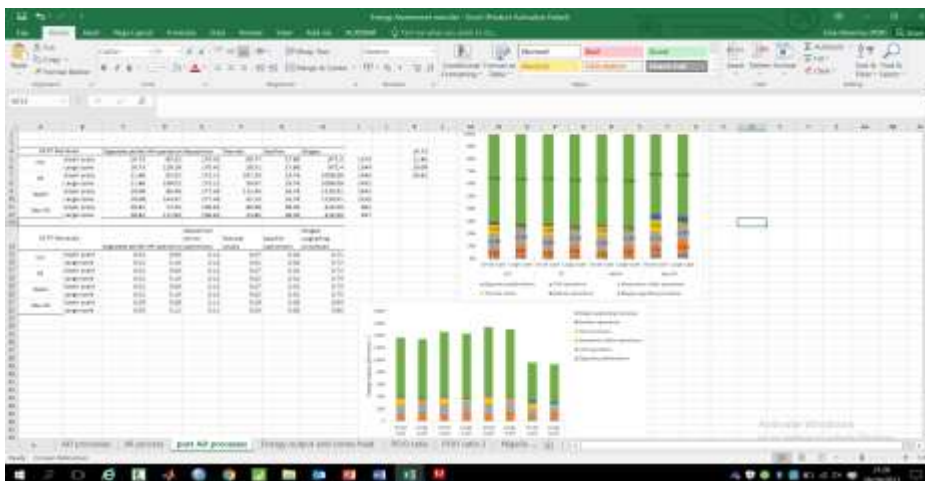


## Appendices for Chapter 8

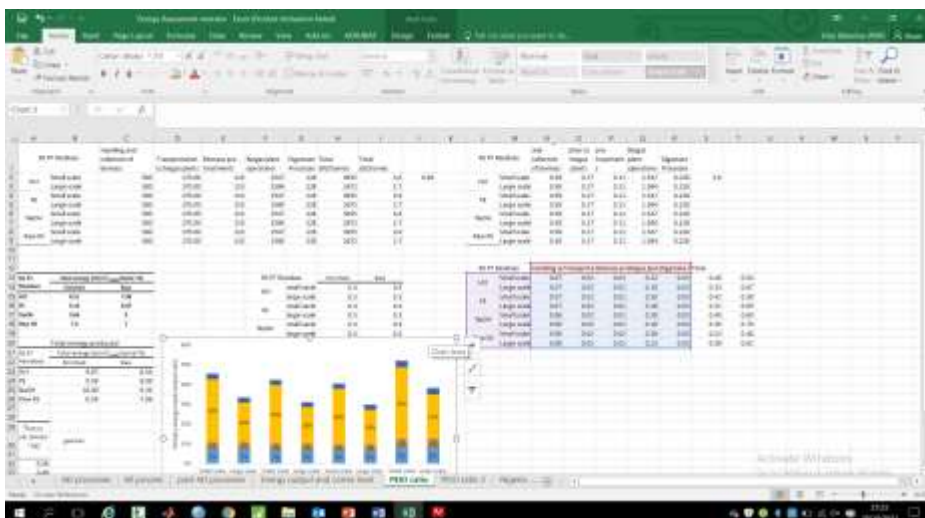
Appendix 1 Calculation of total energy inputs of all the processes involved in hydrogen and methane production.



Appendix 2 Estimation of total energy inputs of post AD processes from various PT RS samples.

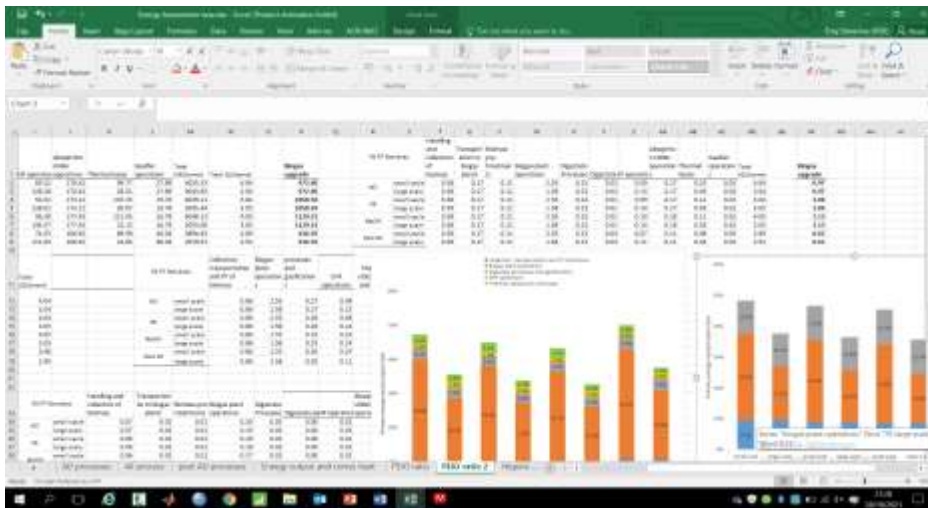


Appendix 3 Analysis of the percentages of the PEIO of the AD processes for the various PT RS samples

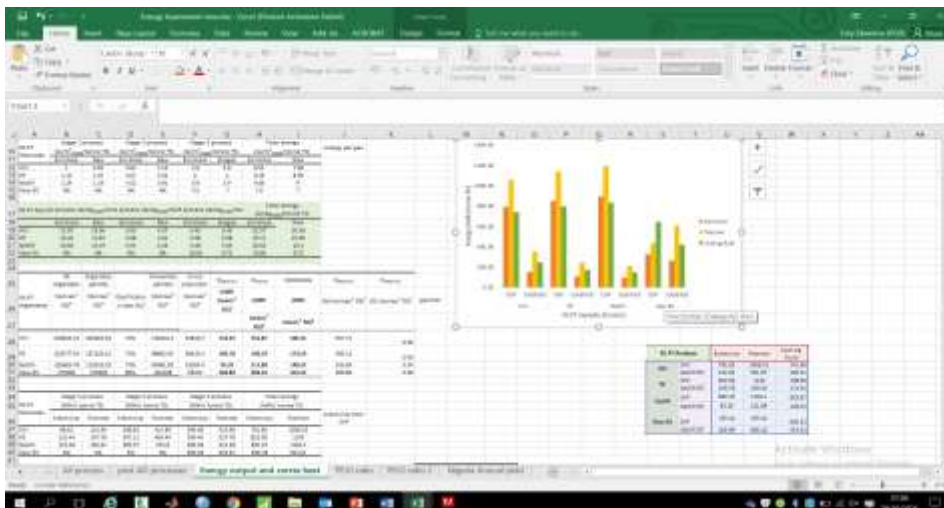




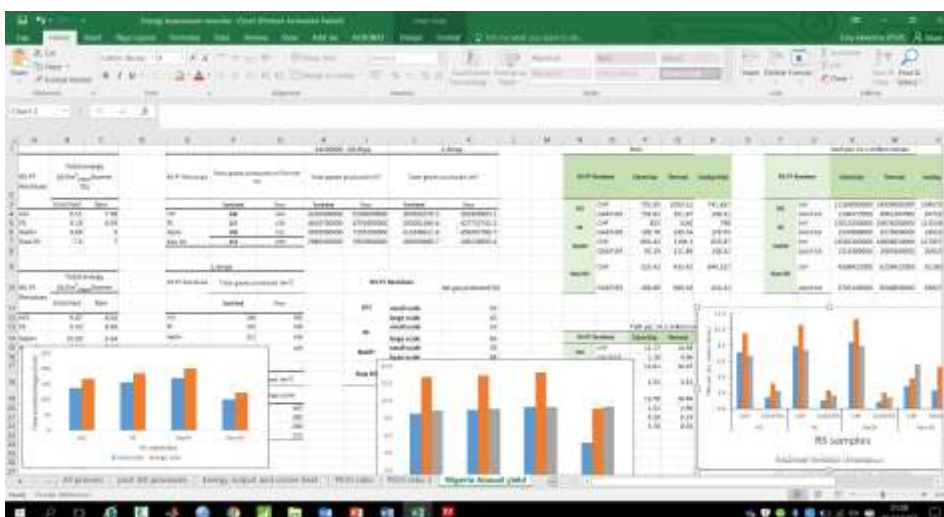
Appendix 4 Assessment of the energy balances (%) of the integrated system



Appendix 5 Estimation of post AD processes' total useful energy products from the various RS feedstock.



Appendix 6 The bio-methane, electricity, thermal and cooling fluid estimation using CHP and gasifier of the various RS samples from Nigeria annual RS yield of 14.1 million tonnes.



## References

- Abasi, S. A. and Abasi, T. (2011). Renewable hydrogen: prospect and challenges. *Renewable and Sustainable Energy Reviews* 15: 3034 – 3040.
- Abatzoglou, N. and Boivin, S. (2009). A review of biogas purification processes. *Biofuels, Bioproducts and Biorefining*, 3(1), 42-71.
- Acharya, P. B., Acharya, D. K. and Modi, H. A. (2008). Optimisation for cellulase production by *Aspergillus niger* using sawdust as substrate. *African Journal of Biotechnology*, 7(22).
- Acharya, A., Joshi, D. R., Shrestha, K. and Bhatta, D. R. (2012). Isolation and screening of thermophilic cellulolytic bacteria from compost piles. *Scientific world*, 10(10), 43-46.
- Achinas, S. and Euverink, G. J. W. (2016). Theoretical analysis of biogas potential prediction from agricultural waste. *Resource-Efficient Technologies*, 2(3), 143-147.
- Adam, F., Ahmed, A. E. and Min, S. L. (2008). Silver modified porous silica from rice husk and its catalytic potential. *Journal of Porous Materials*, 15 (4), 433-444.
- Adebisi, J. A., Agunsoye, J. O., Ahmed, I. I., Bello, S. A., Haris, M., Ramakokovhu, M. M. and Hassan, S. B. (2020). Production of silicon nano-particles from selected agricultural wastes. *Materials Today: Proceedings*.
- Adekunle, K. F. and Okolie, J. A. (2015). A review of the biochemical process of anaerobic digestion. *Adv. Biosci. Biotechnol.* 06: 205 - 212.
- Adney W. S, Rivard, C. J., Ming, S. A., *et al.* (1991). Anaerobic digestion of lignocellulosic biomass and wastes. Cellulases and related enzymes. *Appl Biochem Biotechnol* 30:165–183.
- Affandi, S., Setyawan, H., Winardi, S., Purwanto, A. and Balgis, R. (2009). A facile method for production of high-purity silica xerogels from bagasse ash. *Advanced Powder Technology*, 20(5), 468-472.
- Agbagla-Dohnani, A., Nozière, P., Clément, G. and Doreau, M. (2001). In sacco degradability, chemical and morphological composition of 15 varieties of European rice straw. *Animal feed science and technology*, 94(1-2), 15-27.
- Agneessens, L. M., Ottosen, L. D. M., Voigt, N. V., Nielsen, J. L., de Jonge, N., Fischer, C. H. and Kofoed, M. V. W. (2017). In-situ biogas upgrading with pulse H<sub>2</sub> additions: the relevance of methanogen adaption and inorganic carbon level. *Bioresource technology*, 233, 256-263.

Ahmad-Alyosef, H., Schneider, D., Wassersleben, S., Roggendorf, H., Weiß, M., Eilert, A., ... and Enke, D. (2015). Meso/macroporous silica from miscanthus, cereal remnant pellets, and wheat straw. *ACS Sustainable Chemistry & Engineering*, 3(9), 2012-2021.

Ahmadi, P., Dincer, I. and Rosen, M. A. (2013). Environmental impact assessments of integrated multigeneration energy systems. In *Causes, Impacts and Solutions to Global Warming* (pp. 751-777). Springer, New York, NY.

Ahern, E. P., Deane, P., Persson, T., Gallachóir, B. Ó. and Murphy, J. D. (2015). A perspective on the potential role of renewable gas in a smart energy island system. *Renewable Energy*, 78, 648-656.

Ai, B., Li, J., Song, J., Chi, X., Meng, J., Zhang, L. and Ban, Q. (2013). Butyric acid fermentation from rice straw with undefined mixed culture: enrichment and selection of the cellulolytic butyrate-producing microbial community. *International Journal of Agriculture and Biology*, 15(6).

Ajmi, A. N., Hammoudeh, S., Nguyen, D. K., & Sato, J. R. (2015). On the relationships between CO<sub>2</sub> emissions, energy consumption and income: the importance of time variation. *Energy Economics*, 49, 629-638.

Akobi, Chinaza, Hyeongu Yeo, Hisham Hafez, and George Nakhla. "Single-stage and two-stage anaerobic digestion of extruded lignocellulosic biomass." *Applied energy* 184 (2016): 548-559.

Alalayah, W. M., Kalil, M. S., Kadhum, A. A. H., Jahim, J. M. and Alauj, N. M. (2009). Effect of environmental parameters on hydrogen production using *Clostridium saccharoperbutylacetonicum* N1-4 (ATCC 13564). *American Journal of Environmental Sciences* 5(1): 80-86.

Alemahdi, N., Man, H. C., Nasirian, N. and Yang, Y. (2015). Enhanced mesophilic bio-hydrogen production of raw rice straw and activated sewage sludge by co-digestion. *International Journal of Hydrogen Energy*, 40 (46), 16033-16044.

Alshiyab, H., Kalil, M. S., Hamid, A. A. and Yusoff, W. M. W. (2008). Trace metal effect on hydrogen production using *C. acetobutylicum*. *OnLine Journal of Biological Sciences* 8(1): 1-9.

Amaral, A. F., Previtali, D., Bassani, A., Italiano, C., Palella, A., Pino, L., ... and Manenti, F. (2020). Biogas beyond CHP: The HPC (heat, power & chemicals) process. *Energy*, 203, 117820.

An, Q., Bu, J., Cheng, J. R., Hu, B. B., Wang, Y. T. and Zhu, M. J. (2020a). Biological saccharification by *Clostridium thermocellum* and two-stage hydrogen and methane production from hydrogen peroxide-acetic acid pretreated sugarcane bagasse. *International Journal of Hydrogen Energy*, 45(55), 30211-30221.

An, Q., Cheng, J. R., Wang, Y. T. and Zhu, M. J. (2020b). Performance and energy recovery of single and two-stage biogas production from paper sludge: *Clostridium thermocellum* augmentation and microbial community analysis. *Renewable Energy*, 148, 214-222.

An, Q., Wang, J. L., Wang, Y. T., Lin, Z. L. and Zhu, M. J. (2018). Investigation on hydrogen production from paper sludge without inoculation and its enhancement by *Clostridium thermocellum*. *Bioresource technology*, 263, 120-127.

Andreoli, C. V., Von Sperling, M., Fernandes, F. and Ronteltap, M. (2007). Sludge treatment and disposal. IWA publishing.

Andric, P., Meyer, A. S., Jensen, P. A. and Dam-Johansen, K. (2010). Effect and modelling of glucose inhibition and in situ glucose removal during enzymatic hydrolysis of pretreated wheat straw. *Appl Biochem Biotech* 160: 280 – 297.

Angelidaki, I., Ellegaard, L. and Ahring, B. K. (1999) A comprehensive model of anaerobic bioconversion of complex substrates to biogas. *Biotechnology and Bioengineering*, 63(3): 363-372.

Angelidaki, I., Karakashev, D., Batstone, D. J., Plugge, C. M. and Stams, A. J. M. (2011) Biomethanation and Its Potential. *Methods in Enzymology*, 494: 327-351

Angelidaki, I., Treu, L., Tsapekos, P., Luo, G., Campanaro, S., Wenzel, H. and Kougias, P. G. (2018). Biogas upgrading and utilisation: Current status and perspectives. *Biotechnology advances*, 36(2), 452-466.

Antonopoulou, G., Gavala, H. N., Skiadas, I. V. and Lyberatos, G. (2010). Influence of pH on fermentative hydrogen production from sweet sorghum extract. *International Journal of Hydrogen Energy* 35(5): 1921 - 1928.

APHA Standard (2005). Methods for the Examination of Water and Wastewater. 21st ed. Washington, DC, USA: American Public Health Association, American Water Works Association, Water Environment.

Appels, L., Lauwers, J., Degrève, J., Helsen, L., Lievens, B., Willems, K., Impe, J. and Dewil, R. (2011) Anaerobic digestion in global bio-energy production: potential and research challenges. *Renewable and Sustainable Energy Reviews*, 15(9), pp. 4295-4301.

Argun, H., Gokfiliz, P. and karapinar, I. (2017). Biohydrogen Production Potential of Different Biomass Sources. *Biohydrogen Production: Sustainability of Current Technology and Future Perspective* 10 (2): 11 – 48.

Argun, H., Kargi, F., Kapdan, I. K. and Oztekin, R. (2008). Biohydrogen production by dark fermentation of wheat powder solution: effects of C/N and C/P ratio on hydrogen yield and formation rate. *International Journal of hydrogen energy*, 33(7): 1813-1819.

Armor, J. N. (1999). The multiple roles for catalysis in the production of H<sub>2</sub>. *Appl Catal A: Gen*, 176: 159-176

Artkla, S., Kim, W., Choi, W. and Wittayakun, J. (2009). Highly enhanced photocatalytic degradation of tetramethylammonium on the hybrid catalyst of titania and MCM-41 obtained from rice husk silica. *Applied Catalysis B: Environmental*, 91(1-2), 157-164.

Aryal, N., Kvist, T., Ammam, F., Pant, D. and Ottosen, L. D. (2018). An overview of microbial biogas enrichment. *Bioresource technology*, 264, 359-369.

Askaruly, K., Azat, S., Sartova, Z., Yeleuov, M., Kerimkulova, A., & Bekseitova, K. (2020). Obtaining and characterisation of amorphous silica from rice husk. *Journal of Chemical Technology & Metallurgy*, 55(1).

Athinarayanan, J., Periasamy, V. S., Alhazmi, M., Alatah, K. A., and Alshatwi, A. A. (2015). Synthesis of biogenic silica nano-particles from rice husks for biomedical applications. *Ceramics International*, 41(1), 275-281.

Atulegwu P.U, and Egwuonwu N, "quality Assessment of the mill effluent polluted Eutric- tropoflurent soil".Research. *Journal of Environmental Science*. 5:342-353, 2011.

Augelletti, R., Conti, M., & Annesini, M. C. (2017). Pressure swing adsorption for biogas upgrading. A new process configuration for the separation of biomethane and carbon dioxide. *Journal of Cleaner Production*, 140, 1390-1398.

Awiszus, S., Meissner, K., Reyer, S. and Müller, J. (2018). Ammonia and methane emissions during drying of dewatered biogas digestate in a two-belt conveyor dryer. *Bioresource technology*, 247, 419-425.

Azizi, S. N. and Yousefpour, M. (2010). Synthesis of zeolites NaA and analcime using rice husk ash as silica source without using an organic template. *Journal of Materials Science*, 45 (20), 5692-5697.

Bajracharya, T. R., Dhungana, A., Thapaliya, N. and Hamal, G. (2009). Purification and compression of biogas: A research experience. *Journal of the Institute of Engineering*, 7(1), 90-98.

Bakar, A. H. A. and Carey, C. J. N. (2020). Extraction of Silica from Rice Straw Using Alkaline Hydrolysis Pretreatment. In *IOP Conference Series: Materials Science and Engineering* (Vol. 778, No. 1, p. 012158). IOP Publishing.

Bakar, R. A., Yahya, R., & Gan, S. N. (2016). Production of high purity amorphous silica from rice husk. *Procedia Chemistry*, 19, 189-195.

Baker, R. W. (2012). *Membrane technology and applications*. John Wiley & Sons.

Balachandar, G., Varanasi, J. L., Singh, V., Singh, H. and Das, D. (2020). Biological hydrogen production via dark fermentation: A holistic approach from lab-scale to pilot-scale. *International Journal of Hydrogen Energy*, 45(8), 5202-5215.

- Banu, J. R., Sharmila, V. G., Kannah, R. Y., Kanimozhi, R., Elfasakhany, A., Gunasekaran, M., ...and Kumar, G. (2022). Impact of novel deflocculant ZnO/Chitosan nanocomposite film in disperser pretreatment enhancing energy efficient anaerobic digestion: Parameter assessment and cost exploration. *Chemosphere*, 286, 131835.
- Bao, M. D., Su, H. J. and Tan, T. W. (2013). Dark fermentative bio-hydrogen production: Effects of substrate pre-treatment and addition of metal ions or L-cysteine. *Fuel*, 112, 38-44.
- Barbosa, M. J., Rocha, J. M. S., Tramper, J. and Wijffels. R. H. (2001). Acetate as a carbon source for hydrogen production by photosynthetic bacteria. *J Biotechnol*, 85: 25 – 33.
- Barik, T. K., Sahu, B. and Swain, V. (2008). Nano-silica – from medicine to pest control. *Parasitology Research* 103 (2): 253 – 258.
- Barton, L. L., & Fauque, G. D. (2009). Biochemistry, physiology and biotechnology of sulfate-reducing bacteria. *Advances in applied microbiology*, 68, 41-98.
- Bassam, N. E. (2010). Handbook of Bioenergy Crops: A Complete Reference to Species, Development and Applications: Earthscan from Routledge.
- Bassani, I., Kougiyas, P. G., Treu, L. and Angelidaki, I. (2015). Biogas upgrading via hydrogenotrophic methanogenesis in two-stage continuous stirred tank reactors at mesophilic and thermophilic conditions. *Environmental science & technology*, 49(20), 12585-12593.
- Bastidas-Oyanedej, J. R., Mohd-Zaki, Z., Zeng, R. J., Bernet, N., Pratt, S., Steyer, J. P. et al. (2012). Gas controlled hydrogen fermentation. *Bioresour Technol* 110: 503 – 509.
- Batstone, D. J., Keller, J., Angelidaki, I., Kalyuzhnyi, S. V., Pavlostathis, S. G., Rozzi, A., ... and Vavilin, V. A. (2002). The IWA anaerobic digestion model no 1 (ADM1). *Water Science and Technology*, 45(10), 65-73.
- Bauer, F., Persson, T., Hulteberg, C and Tamm, D. (2013). Biogas upgrading–technology overview, comparison and perspectives for the future. *Biofuels, Bioproducts and Biorefining*, 7(5), 499-511.
- Becker, C., Döhler, H., Eckel, H., Fröba, N., Georgieva, T., & Grube, J. (2007). Empirical values for biogas.
- Beckers, L., Masset, J., Hamilton, C., Delvigne, F., Toyé, D., Crine, M., ... and Hilgsmann, S. (2015). Investigation of the links between mass transfer conditions, dissolved hydrogen concentration and biohydrogen production by the pure strain *Clostridium butyricum* CWBI1009. *Biochemical engineering journal*, 98, 18-28.
- Beg, Q. K., Kapoor, M., Mahajan, L. and Hoondal, G. S. (2001). Microbial xylanases and their industrial applications: a review. *Appl Microbiol Biotechnol* 56: 326 – 338.

Berglund, M and Börjesson, P. (2003). Energianalys av biogassystem (In Swedish: Energy systems analysis of biogas systems). Report No. 44, Environmental and Energy Systems Studies, Lund University, Sweden.

Berglund, M. and Börjesson, P. (2006). Assessment of energy performance in the life-cycle of biogas production. *Biomass and Bioenergy*, 30(3), 254-266.

Bharathiraja, B., Sudharsana, T., Bharghav, A., Jayamuthunagai, J. and Praveenkumar, R. (2016). Biohydrogen and Biogas – An overview of feedstocks and enhancement Process. *Fuel* 185: 810 - 828.

Bharathiraja, B., Sudharsana, T., Jayamuthunagai, J., Praveenkumar, R., Chozhavendhan, S. and Iyyappan, J. (2018). Biogas production—A review on composition, fuel properties, feed stock and principles of anaerobic digestion. *Renewable and Sustainable Energy Reviews*, 90(April), 570-582.

Biddle, A., Stewart, L., Blanchard, J. and Leschine, S. (2013). Untangling the genetic basis of fibrolytic specialisation by Lachnospiraceae and Ruminococcaceae in diverse gut communities. *Diversity*, 5(3), 627-640.

Bisaillon, A., Turcot, J. and Hallenbeck, P. C. (2006). The effect of nutrient limitation on hydrogen production by batch cultures of *Escherichia coli*. *International Journal of Hydrogen Energy*: 31(11), 1504-1508.

Biswarup, S., Yen-Ping, C., Shu-Yii, W. and Chun-Min, L. (2016). Pre-treatment conditions of rice straw for simultaneous hydrogen and ethanol fermentation by mixed culture. *International journal of hydrogen energy* 41: 4421 – 4428.

Biswas, B., Pandey, N., Bisht, Y., Singh, R., Kumar, J. and Bhaskar, T. (2017). Pyrolysis of agricultural biomass residues: Comparative study of corn cob, wheat straw, rice straw and rice husk. *Bioresource technology*, 237, 57-63.

Bocher, B. T., Agler, M. T., Garcia, M. L., Beers, A. R. and Angenent, L. T. (2008) Anaerobic digestion of secondary residuals from an anaerobic bioreactor at a brewery to enhance bioenergy generation. *Journal of Industrial Microbiology & Biotechnology*, 35(5), pp. 321- 329.

Borrel, G., Adam, P. S. and Gribaldo, S. (2016) Methanogenesis and the Wood–Ljungdahl Pathway: An Ancient, Versatile, and Fragile Association. *Genome Biology and Evolution*, 8(6), pp. 1706-1711.

Brenner, K., You, L. and Arnold, F. H. (2008). Applied metagenomics for biofuel development and environmental sustainability. *Trends Biotechnol.* 26(9): 483 – 489.

Bruno, J. C., Ortega-López, V. and Coronas, A. (2009). Integration of absorption cooling systems into micro gas turbine trigeneration systems using biogas: case study of a sewage treatment plant. *Applied energy*, 86(6), 837-847.

Budzianowski, W. M., Wylock, C. E. and Marciniak, P. A. (2017). Power requirements of biogas upgrading by water scrubbing and biomethane compression: a comparative analysis of various plant configurations. *Energy conversion and management*, 141, 2-19.

Bundhoo, M. Z. and Mohee, R. (2016). Inhibition of dark fermentative bio-hydrogen production: a review. *International Journal of Hydrogen Energy* 41(16): 6713-6733.

Bundhoo, M. Z., Mohee, R. and Hassan, M. A. (2015). Effects of pre-treatment technologies on dark fermentative biohydrogen production: a review. *Journal of environmental management* 157: 20-48.

Cai, M., Liu, J. and Wei, Y. (2004). Enhanced bio-hydrogen production from sewage sludge with alkaline pre-treatment. *Environmental science & technology*, 38(11), 3195-3202.

Callahan, B. J., McMurdie, P. J., Rosen, M. J., Han, A. W., Johnson, A. J. A and Holmes, S. P. (2016a). DADA2: high-resolution sample inference from Illumina amplicon data. *Nature methods*, 13(7), 581-583.

Callahan, B. J., Sankaran, K., Fukuyama, J. A., McMurdie, P. J. and Holmes, S. P. (2016b). Bioconductor workflow for microbiome data analysis: from raw reads to community analyses. *F1000Research*, 5.

Campanaro, S., Treu, L., Kougias, P. G., De Francisci, D., Valle, G. and Angelidaki, I. (2016) Metagenomic analysis and functional characterisation of the biogas microbiome using high throughput shotgun sequencing and a novel binning strategy. *Biotechnology for Biofuels*, 9(1).

Cao, X., and Zhao, Y. (2009). The influence of sodium on biohydrogen production from food waste by anaerobic fermentation. *Journal of material cycles and waste management* 11(3): 244-250.

Caporaso, J. G., Kuczynski, J., Stombaugh, J., Bittinger, K., Bushman, F. D., Costello, E. K., .. and Knight, R. (2010). QIIME allows the analysis of high-throughput community sequencing data. *Nature methods*, 7(5), 335-336.

Chandrasekhar, S., Satyanarayana, K. G., Pramade, P. N., Raghavan, P. and Gupta, T. N. (2003). Review processing, properties and applications of reactive silica from rice husk – an overview. *Journal of Materials Science* 38 (15): 3159 – 3168.

Chang, A. C., Tu, Y. H., Huang, M. H., Lay, C. H. and Lin, C. Y. (2011). Hydrogen production by the anaerobic fermentation from acid hydrolysed rice straw hydrolysate. *International journal of hydrogen energy* 36(21): 14280-14288.

Chang, F. Y. and Lin, C. Y. (2006). Calcium effect on fermentative hydrogen production in an anaerobic up-flow sludge blanket system. *Water science and technology* 54(9): 105.

Chang, S. H. (2014). An overview of empty fruit bunch from oil palm as feedstock for bio-oil production. *Biomass and Bioenergy* 62: 174 – 181



Chen, C. C. and Lin, C. Y. (2001). Start-up of anaerobic hydrogen-producing reactors seeded with sewage sludge. *Acta Biotechnol.* 21(4):371 – 379.

Chen, C. C., Chuang, Y. S., Lin, C. Y., Lay, C. H. and Sen, B. (2012a). Thermophilic dark fermentation of untreated rice straw using mixed cultures for hydrogen production. *International Journal of Hydrogen Energy*, 37(20), 15540-15546

Chen, H., Chen, B., Su, Z., Wang, K., Wang, B., Wang, Y., ... and Qin, P. (2020). Efficient lactic acid production from cassava bagasse by mixed culture of *Bacillus coagulans* and *Lactobacillus rhamnosus* using stepwise pH-controlled simultaneous saccharification and co-fermentation: *Industrial Crops and Products*, 146, 112175.

Chen, H., Liu, J., Chang, X., Chen, D., Xue, Y., Liu, P., Lin, H. and Han, S. (2017) A review on the pretreatment of lignocellulose for high-value chemicals. *Fuel Processing Technology*, 160: 196-206.

Chen, H., Wang, W., Martin, J. C., Oliphant, A. J., Doerr, P. A., Xu, J. F., .. and Sun, L. (2013). Extraction of lignocellulose and synthesis of porous silica nano-particles from rice husks: a comprehensive utilisation of rice husk biomass. *ACS Sustainable Chemistry & Engineering*, 1(2), 254-259.

Chen, H., Wang, F., Zhang, C., Shi, Y., Jin, G. and Yuan, S. (2010). Preparation of nano-silica materials: The concept from wheat straw. *Journal of Non-Crystalline Solids*, 356(50-51), 2781-2785.

Chen, J. L., Ortiz, R., Steele, T. W. J. and Stuckey, D. C. (2014). Toxicants inhibiting anaerobic digestion: A review. *Biotechnology Advances*, 32(8), 1523-1534.

Chen, L., Jian, S., Bi, J., Li, Y., Chang, Z., He, J. and Ye, X. (2016). Anaerobic digestion in mesophilic and room temperature conditions: Digestion performance and soil-borne pathogen survival. *J Environ Sci* 43, 224-233.

Chen, W. H., Pen, B. L., Yu, C. T. and Hwang, W. S. (2011) Pretreatment efficiency and structural characterisation of rice straw by an integrated process of dilute-acid and steam explosion for bioethanol production. *Bioresource Technology* 102: 2916 - 2924.

Chen, Y., Cheng, J. J. and Creamer, K. S. (2008). Inhibition of anaerobic digestion process: a review. *Bioresource Technology* 99(10): 4044-4064.

Chen, Y. R, Sarkanen S and Wang, Y. Y. (2012b) Lignin-degrading enzyme activities. *Methods Mol Biol* 908: 251 –2 68.

Cheng, C. L., Lo, Y. C., Lee, K. S., Lee, D. J., Lin, C. Y. and Chang, J. S. (2011a). Biohydrogen production from lignocellulose feedstock. *Bioresource Technology* 102: 8514 – 8523.

Cheng, J., Su, H., Zhou, J., Song, W. and Cen, K. (2011b). Microwave-assisted alkali pre-treatment of rice straw to promote enzymatic hydrolysis and hydrogen production in dark-and photo-fermentation. *International journal of hydrogen energy*, 36(3), 2093-2101.

Cheng, S., Xing, D., Call, D. F. and Logan, B. E. (2009). Direct biological conversion of electrical current into methane by electromethanogenesis. *Environmental science & technology*, 43(10), 3953-3958.

Chin, H. L., Chen, Z. S. and Chou, C. P. (2003). Fed-batch operation using *Clostridium acetobutylicum* suspension culture as biocatalyst for enhancing hydrogen production. *Biotechnology Progress* 19(2): 383-388.

Chong, M., Sabaratnam, V., Shiirai, Y., Ali, M. and Hassan, M. A. (2009). Biohydrogen production from biomass and industrial wastes by dark fermentation. *International Journal of Hydrogen Energy* 34: 3277 -3287.

Chouari, R., Dardouri, W., Sallami, F., Rais, M. B., Le Paslier, D. and Sghir, A. (2015). Microbial analysis and efficiency of biofiltration packing systems for hydrogen sulfide removal from wastewater off Gas. *Environmental Engineering Science* 32(2): 121-128.

Ciranna, A., Ferrari, R., Santala, V. and Karp, M. (2014). Inhibitory effects of substrate and soluble end products on bio-hydrogen production of the alkali thermophile *Caloramator celer*: kinetic, metabolic and transcription analyses. *International Journal of Hydrogen Energy*, 39(12): 6391-6401.

Coelho, L. F., Bolner de Lima, C. J., Bernardo, M. P., Alvarez, G. M. and Contiero, J. (2010). Improvement of L (+) -lactic acid production from cassava wastewater by *Lactobacillus rhamnosus* B 103. *Journal of the Science of Food and Agriculture*, 90(11), 1944-1950.

Collet, C., Adler, N., Schwitzguébel, J. P. and Péringier, P. (2004). Hydrogen production by *Clostridium thermolacticum* during continuous fermentation of lactose. *Int J Hydrogen Energy*, 29 (2004), pp. 1479-1485

Costa, K. C. and Leigh, J. A. (2014). Metabolic versatility in methanogens. *Current opinion in biotechnology*, 29, 70-75.

Cushion, E., Whiteman, A. and Dieterle, G. (2009). Bioenergy Development: Issues and Impacts for Poverty and Natural Resource Management: *World Bank Publications*.

Dabrock, B., Bahl, H. and Gottschalk, G. (1992). Parameters affecting solvent production by *Clostridium pasteurianum*. *Applied and Environmental Microbiology* 58(4): 1233-1239.

Dahlquist, E. E. (2013). Technologies for converting biomass to useful energy: combustion, gasification, pyrolysis, torrefaction and fermentation. CRC Press.

Dalimin, M.N. (1995). Renewable energy update: Malaysia. *Renew Energy*, 6(4):435 – 439.

Daniel, J., Scholwin, F. and Vogt, R. (2008). Biogas utilisation. In: Federal Ministry for the Environment, Nature Conservation (BMU). Optimisation for a sustainable expansion of biogas production and utilisation in Germany. Berlin (Germany): Cooperative project funded by BMU.

Das, D. and Veziroğlu, T.N. (2001). Hydrogen production by biological processes: a survey of the literature. *Int. J. Hydrogen Energy* 26: 13–28.

Das, D. and Veziroglu, T. N. (2008). Advances in biological hydrogen production processes. *International journal of hydrogen energy*, 33(21), 6046-6057.

De Bok, F. A. M., Harmsen, H. J. M., Plugge, C. M., de Vries, M. C., Akkermans, A. D. L., de Vos, W. M. and Stams, A. J. M. (2005) The first true obligately syntrophic propionate oxidising bacterium, *Pelotomaculum schinkii* sp. nov., co-cultured with *Methanospirillum hungatei*, and emended description of the genus *Pelotomaculum*. *International Journal of Systematic and Evolutionary Microbiology*, 55(4), pp. 1697-1703

De Gioannis, G., Friargiu, M., Massi, E., Muntoni, A., Poletti, A., Pomi, R. and Spiga, D. (2014). Biohydrogen production from dark fermentation of cheese whey: Influence of pH. *International Journal of Hydrogen Energy* 39(36): 20930-20941.

De Lemos Chernicharo, C. A. (2007). *Anaerobic Reactors*: IWA Publishing.

Della, V. P., Kühn, I. and Hotza, D. (2002). Rice husk ash as an alternate source for active silica production. *Mater. Lett.* 57: 818.

De Paepe, M., D’Herdt, P. and Mertens, D. (2006). Micro-CHP systems for residential applications. *Energy conversion and management*, 47(18-19), 3435-3446.

Department of Energy (2017). Energy Efficiency and Renewable Energy Hydrogen Storage. [www.hydrogenandfuelcells.energy.gov](http://www.hydrogenandfuelcells.energy.gov).

Dhar, B. R., Elbeshbishy, E., and Nakhla, G. (2012). Influence of iron on sulfide inhibition in dark biohydrogen fermentation. *Bioresource technology* 126,123-130.

Dong, L., Cao, G., Wu, J., Liu, B., Xing, D., Zhao, L., ... and Ren, N. (2019). High-solid pre-treatment of rice straw at cold temperature using NaOH/Urea for enhanced enzymatic conversion and hydrogen production. *Bioresource technology*, 287, 121399.

Dong, L., Liu, H. and Riffat, S. (2009). Development of small-scale and micro-scale biomass-fuelled CHP systems—A literature review. *Applied thermal engineering*, 29(11-12), 2119-2126.

Dong, L., Wu, J., Zhou, C., Xu, C. J., Liu, B., Xing, D., ... and Ren, N. (2020). Low concentration of NaOH/Urea pre-treated rice straw at low temperature for enhanced hydrogen production. *International Journal of Hydrogen Energy*, 45(3), 1578-1587.

Drosg, B. (2013). *Process monitoring in biogas plants*. Paris: IEA Bioenergy.

Du, B., Sharma, L. N., Becker, C., Chen, S. F., Mowery, R. A., van Walsum, G. P. and Chambliss, C. K. (2010). Effect of varying feedstock–pre-treatment chemistry combinations on the formation and

accumulation of potentially inhibitory degradation products in biomass hydrolysates. *Biotechnology and bioengineering*, 107(3), 430-440.

Duffield, C. (2010). Nigeria: 'World oil pollution capital. BBC News, Niger Delta.

Edwards, R. L., Font-Palma, C. and Howe, J. (2021). The status of hydrogen technologies in the UK: A multi-disciplinary review. *Sustainable Energy Technologies and Assessments*, 43, 100901.

El-Emam, R. S. and Dincer, I. (2018). Investigation and assessment of a novel solar-driven integrated energy system. *Energy Conversion and Management*, 158, 246-255.

Elbeshbishy, E., Dhar, B. R., Nakhla, G. and Lee, H. S. (2017). A critical review on the inhibition of dark biohydrogen fermentation. *Renewable and Sustainable Energy Reviews*, 79, 656-668.

Elsayed, Y., Refaat, J., Abdelmohsen, U. R. and Fouad, M. A. (2017). The Genus *Rhodococcus* as a source of novel bioactive substances: A review. *J. Pharmacogn. Phytochem*, 6(3), 83-92.

Emodi, N. V. and Boo, K. J. (2015). Sustainable energy development in Nigeria: Current status and policy options. *Renewable and Sustainable Energy Reviews*, 51, 356-381.

Esteves, M., Vargas, S., Castano, V. M. and Rodriguez, R. (2009). Silica nano-particles produced by worms through a bio-digestion process of rice husk. *Journal of Non-crystalline Solids* 355(14): 844 – 850.

Escaramboni, B., Núñez, E. G. F., Carvalho, A. F. A. and de Oliva Neto, P. (2018). Ethanol biosynthesis by fast hydrolysis of cassava bagasse using fungal amylases produced in optimised conditions. *Industrial Crops and Products*, 112, 368-377.

Fadhilulloh, M. A., Rahman, T., Nandiyanto, A. B. D. and Mudzakir, A. (2014). Review tentang sintesis SiO<sub>2</sub> nanopartikel. *Jurnal intergrasi proses*, 5 (1): 30 – 45.

Fan, Y., Li, C., Lay, J. J., Hou, H. and Zhang, G. (2004). Optimisation of the initial substrate and pH levels for germination of sporing hydrogen-producing anaerobes in cattle dung compost. *Bioresour Technol* 91: 189 – 193.

Fang, H. H., Li, C. and Zhang, T. (2006). Acidophilic biohydrogen production from rice slurry. *Int. J. Hydrogen Energy* 31(6): 683 – 692.

Fang H. H. P. and Liu, H. (2002). Effect of pH on hydrogen production from glucose by mixed culture. *Bioresour Technol* 82: 87–93.

FAOSTAT, <http://faostat.fao.org/>, (2017 and 2018) (accessed 6<sup>th</sup> May 2017 and 28<sup>th</sup> July 2018)

Federal Ministry of Agriculture and Natural Resources Nigeria (2006). Cassava Development in Nigeria. *FAO Document Repository*

Federal Ministry of Power (FMP). (2015). Federal Ministry of Power: National Renewable Energy and Energy Efficiency Policy (NREEEP) for the Electricity Sector, Abuja, Nigeria.

Federation, W. E. (2007). Operation of Municipal Wastewater Treatment Plants: Manual of Practice 11: New York: McGraw-Hill Professional.

Food and Agricultural Organisation (2017). Information update. *FAOSTAT* (accessed 5<sup>th</sup> September 2018)

Food and Agricultural Organisation (2018). Rice Market Monitor, Volume XXI - Issue No. 1 <http://www.fao.org/economic/est/publications/rice-publications/rice-market-monitor-rmm/en/> (accessed April, 22<sup>nd</sup> 2019).

Foglia, D., Wukovits, W., Friedl, A., De-Vrije, T. and Pieternel, A. M. (2006). Fermentative hydrogen production: influence of the application of mesophilic and thermophilic bacteria on mass and energy balances. *Chem Eng Trans 2*: 815 –820.

Fox, P. and Pohland, F. G. (1994). Anaerobic treatment applications and fundamentals: substrate specificity during phase separation. *Water Environment Research 66*(5): 716-724.

Gai, y. P., Zhang, W. T., Mu, Z. M. and Ji, X. L. (2014). Involvement of lignolytic enzymes in the degradation of wheat straw by *trametes trogii*. *Journal of Applied Microbiology 117*: 85 – 95.

Gao, J., Chen, C., Lin, Y., Zhang, L., Ji, H. and Liu, S. (2020). Enhanced enzymatic hydrolysis of rice straw via pretreatment with deep eutectic solvents-based microemulsions. *Bioresource Technology Reports, 10*, 100404.

Garba, N. A. and Zangina, U. (2015). Rice straw and husk as potential sources for mini-grid rural electricity in Nigeria. *Int. Journal of Applied Sciences and Engineering Research 4* (4).

Gerardi, M. H. (2003). The microbiology of anaerobic digesters: John Wiley & Sons.

Ghimire, A., Frunzo, L., Pirozzi, F., Trably, E., Escudie, R., Lens, P. N. L. and Esposito, G. (2015). A review on dark fermentative biohydrogen production from organic biomass: Process parameters and use of by-products. *Applied Energy 144*: 73 – 95.

Ghirardi, M., Zhang, L. L., Lee, J. W., Flynn, T., Seibert, M., Greenbaum, E. *et al.* (2000). Microalgae: a green source of renewable H<sub>2</sub>. *Tibtech 18*: 506-511

Ghorbani, F., Younesi, H., Mehraban, Z., Celik, M. Z., Ghoreyshi, A. A and Anbia, M. (2013). *Journal of the Taiwan Institute of Chemical Engineers 44* (5): 821-828

Ghosh, S. K. (2017). Utilisation and Management of Bioresources: Proceedings of 6th IconSWM 2016: Springer Singapore.

Gomes, B. C., Rosa, P. R. F., Etchebehere, C., Silva, E. L. and AmâncioVaresche, M. B. (2015). Role of homo-and heterofermentative lactic acid bacteria on hydrogen-producing reactors operated with cheese whey wastewater. *International Journal of Hydrogen Energy* 40(28): 8650-8660.

Gorris, L. G and van der Drift, C. (1994). Cofactor contents of methanogenic bacteria reviewed. *Biofactors* 4:139–145.

Guo, L., Li, X. M., Bo, X., Yang, Q., Zeng, G. M., Liao, D. X. and Liu, J. J. (2008). Impacts of sterilisation, microwave and ultrasonication pretreatment on hydrogen-producing using waste sludge. *Bioresource Technology*, 99(9): 3651-3658.

Guo, W., Liu, C., Zou, S. and Zhang, M. (2006). Progress in research and application of homoacetogen. *Chin J Appl Environ Biol* 12: 874-877.

Guo, X. M., Trably, E., Latrille, E., Carre're, H. and Steyer, J. P. (2010). Hydrogen production from agricultural waste by dark fermentation: A review. *International Journal of Hydrogen Energy* 35: 10660 – 10673

Guzmán, A. A., Delvasto, A. S. and Sánchez. V. E. (2015). Valorization of rice straw waste: an alternative ceramic raw material. *Ceramica* 61: 126 – 136.

Hadrami, A. E., Ojala, S., Chatir, E. M., Assaoui, J. and Bbrahmi, R. (2020). A comprehensive utilisation of rice husk biomass. *Moroccan Journal of Chemistry* 8 (3): 8-3.

Hagen, M., Polman, E., Myken, A., Jensen, J., Jönsson, O., Biomil, A. B. and Dahl, A. (2001). Adding gas from biomass to the gas grid. Final report, contract no: XVII/4.1030/Z/99-412. July 1999 – February 2001.

Hahn, S. K. (2006). An Overview of traditional processing and utilisation of cassava in Africa. *FAO Document Repository*.

Hallenbeck, P. C. (2009). Fermentative hydrogen production: principles, progress, and prognosis. *International Journal of Hydrogen Energy* 34(17): 7379-7389.

Hallenbeck, P. C., Abo-Hashesh, M. and Ghosh, D. (2012). Strategies for improving biological hydrogen production. *Bioresource Technology* 110: 1 – 9.

Hallenbeck, P. C. and Benemann, J. R. (2002). Biological hydrogen production; fundamentals and limiting processes. *International Journal of Hydrogen Energy* 27(11-12): 1185-1193.

Hallenbeck, P. C. and Ghosh, D. (2009). Advances in fermentative bio-hydrogen production: the way forward?. *Trends in Biotechnology*, 27(5), 287-297.

Hao, L., Gong, X., Xuan, S., Zhang, H., Gong, X., Jiang, W., and Chen, Z. (2006). Controllable fabrication and characterisation of biocompatible core-shell particles and hollow capsules as drug carriers. *Applied surface science*, 252 (24), 8724-8733.

Hassan, S. S., Williams, G. A. and Jaiswal, A. K. (2018). Emerging technologies for the pretreatment of lignocellulosic biomass. *Bioresource Technology* 262:310-318.

Hawkes, F. R., Dinsdale, R., Hawkes, D. L. and Hussy, I. (2002). Sustainable fermentative hydrogen production: challenges for process optimisation. *Int. J. Hydrogen Energy*, 27: 1339-1342.

He, D., Bultel, Y., Magnin, J. P., Roux, C. and Willison, J. C. (2005). Hydrogen photosynthesis by *Rhodobacter capsulatus* and its coupling to PEM fuel cell. *J Power Sources*, 141: 19 - 23

He, L., Huang, H., Lei, Z., Liu, C. and Zhang, Z. (2014). Enhanced hydrogen production from anaerobic fermentation of rice straw pretreated by hydrothermal technology. *Bioresource technology*, 171, 145-151.

He, Y., Pang, Y., Liu, Y., Li, X. and Wang, K. (2008). Physicochemical characterisation of rice straw 22: 2775 – 2781.

He, Z. W., Liu, W. Z., Gao, Q., Tang, C. C., Wang, L., Guo, Z. C., ...and Wang, A. J. (2018). Potassium ferrate addition as an alternative pre-treatment to enhance short-chain fatty acids production from waste activated sludge. *Bioresource technology*, 247, 174-181

Henderson, G., Naylor, G. E., Leahy, S. C. and Janssen, P. H. (2010). Presence of novel, potentially homoacetogenic bacteria in the rumen as determined by analysis of formyltetrahydrofolate synthetase sequences from ruminants. *Applied and Environmental Microbiology* 76(7): 2058-2066.

Hendriks, A. and Zeeman, G. (2009) Pretreatments to enhance the digestibility of lignocellulosic biomass. *Bioresource Technology*, 100(1): 10-18.

Hengeveld, E. J., Bekkering, J., Van Dael, M., van Gemert, W. J. T. and Broekhuis, A. A. (2020). Potential advantages in heat and power production when biogas are collected from several digesters using dedicated pipelines- a case study in the "Province of West-Flanders" (Belgium). *Renewable Energy*, 149, 549-564.

Hijazi, O., Munro, S., Zerhusen, B. and Effenberger, M. (2016). Review of life cycle assessment for biogas production in Europe. *Renewable and Sustainable Energy Reviews*, 54, 1291-1300.

Hiziroglu, S., Jarusombuti, S., Bauchongkol, P. and Fueangvivat, V. (2008). Overlaying properties of fiberboard manufactured from bamboo and rice straw. *Ind. Crops Prod.* 28: 107-111

Holladay, J. D., Hu, J., King, D. L. and Wang, Y. (2009). An overview of hydrogen production technologies. *Catalysis today* 139(4): 244-260.

Holm-Nielsen, J. B., Al Seadi, T. and Oleskowicz-Popiel, P. (2009). The future of anaerobic digestion and biogas utilisation. *Bioresource Technology*, 100(22), 5478-5484.

Hosseini, S. E., Wahid, M. A., Jamil, M. M., Anis, A. A. M. and Misbah, M. F. (2015). A review on biomass-based hydrogen production for renewable energy supply. *International Journal of Energy Research* 10: 1002 – 3381.

Howeler, R. (2020). Cassava in Asia: trends in cassava production, processing and marketing. In *Workshop on "Partnership in modern science to develop a strong cassava commercial sector in Africa and appropriate varieties by* (pp. 2-6).

Hull, S. R., Yang, B. Y., Venzke, D., Kulhavy, K. and Montgomery, R. (1996). Composition of Corn Steep Water during Steeping. *J. Agric. Food Chem.* 44: 1857 – 1863

Imoisili, P. E., Ukoba, K. O. and Jen, T. C. (2020). Synthesis and characterization of amorphous mesoporous silica from palm kernel shell ash. *Boletín de la Sociedad Española de Cerámica y Vidrio*, 59(4), 159-164.

Infield, D. and Freris, L. (2020). *Renewable energy in power systems*. John Wiley & Sons.

Intanoo, P., Rangsavigit, P., Malakul, P. and Chavadej, S. (2014). Optimisation of separate hydrogen and methane production from cassava wastewater using a two-stage up-flow anaerobic sludge blanket reactor (UASB) system under thermophilic operation. *Bioresource Technology* 173, 256-265.

International Energy Agency, 2016 <https://www.iea.org/countries/nigeria> (accessed 6th June, 2016).

International Energy Agency, 2020 <https://www.iea.org/countries/nigeria> (accessed 16th July, 2020).

Jaruwongwittaya, T. and Chen, G. (2010). A review: renewable energy with absorption chillers in Thailand. *Renewable and Sustainable Energy Reviews*, 14(5), 1437-1444.

Jeonsson, L. J. and Martín, C. (2016). Pretreatment of lignocellulose: formation of inhibitory by-products and strategies for minimising their effects. *Bioresour. Technol.* 199: 103 - 112.

Jiang, H., Quin, Y., Gadow, S. I., Ohnishi, A., Fujimoto, N. and Li, Y. Y. (2018). Bio-hythane production from cassava residue by two stages fermentative process with recirculation. *Bioresource Technology* 247: 769 – 775.

Jiang, X., Sommer, S. G. and Christensen, K. V. (2011) A review of the biogas industry in China. *Energy Policy* 39: 6073 – 6081.

Jimenez-Llanos, J., Ramirez-Carmona, M., Rendon-Castrillon, L. and Ocampo-Lopez, C. (2020). Sustainable biohydrogen production by *Chlorella* sp. microalgae: A review. *International Journal of Hydrogen Energy*, 45(15), 8310-8328.



Jin, X., Zhang, Y., Li, X., Zhao, N. and Angelidaki, I. (2017). Microbial electrolytic capture, separation and regeneration of CO<sub>2</sub> for biogas upgrading. *Environmental science & technology*, 51(16), 9371-9378.

Jørgensen, H., Kristensen, J. B. and Felby, C. (2007) Enzymatic conversion of lignocellulose into fermentable sugars: Challenges and opportunities. *Biofuels, Bioproducts and Biorefining*, 1(2), pp. 119-134.

Jung, K. W., Kim, D. H., Kim, S. H. and Shin, S. H. (2011). Bioreactor design for continuous dark fermentative hydrogen production. *Bioresource Technology* 102: 8612 – 8620.

Juturu, V. and Wu, J. C. (2014) Microbial cellulases: engineering, production and applications. *Renew Sust Energ Rev* 33: 188 – 203.

Kainthola, J., Shariq, M., Kalamdhad, A. S. and Goud, V. V. (2019). Enhanced methane potential of rice straw with microwave-assisted pre-treatment and its kinetic analysis. *Journal of environmental management*, 232, 188-196.

Kalapathy, U., Proctor, A. and Shultz, J. (2000). Production of silica from rice hull ash. *Bioresour. Technol.* 73: 2572.

Kalapathy, U., Proctor, A. and Shultz, J. (2002). An improved method for the production of silica from rice hull ash. *Bioresour. Technol.* 85: 285 – 289.

Kalil, M. S., Alshiyab, H. S. and Yusoff, W. M. W. (2008). Effect of nitrogen source and carbon to nitrogen ratio on hydrogen production using *C. acetobutylicum*. *American Journal of Biochemistry and Biotechnology* 4(4): 393-401.

Kampmann, K., Ratering, S., Baumann, R., Schmidt, M., Zerr, W. and Schnell, S. (2012). Hydrogenotrophic methanogens dominate in biogas reactors fed with defined substrates. *Systematic and applied microbiology* 35(6): 404-413.

Kannah, R. Y., Kavitha, S., Sivashanmugham, P., Kumar, G., Nguyen, D. D., Chang, S. W. and Banu, J. R. (2019). Biohydrogen production from rice straw: Effect of combinative pre-treatment, modelling assessment and energy balance consideration. *International Journal of Hydrogen Energy*, 44(4), 2203-2215.

Kapdan, I., K. and Kargi, F. (2006). Biohydrogen production from waste. *Enzyme and Microbial Technology* 38: 569 – 582.

Kapdi, S. S., Vijay, V. K., Rajesh, S. K. and Prasad, R. (2005). Biogas scrubbing, compression and storage: perspective and prospectus in the Indian context. *Renewable energy*, 30(8), 1195-1202.

Karlsson, A., Einarsson, P., Schnurer, A., Sundberg, C., Ejlertsson, J. and Svensson, B. H. (2012) Impact of trace element addition on degradation efficiency of volatile fatty acids, oleic acid and phenylacetate

and on microbial populations in a biogas digester. *Journal of Bioscience and Bioengineering*, 114(4), pp. 446-52.

Kasana, R. C and Gulati, A. (2011). Cellulases from psychrophilic microorganisms: a review. *Journal of Basic Microbiology* 51 (6): 572 – 579.

Kaye, G. W. C. and Laby, T. H. (1986). Tables of physical and chemical constants. 15<sup>th</sup> ed., Longman, NY 219.

Kayhanian, M. (1999). Ammonia inhibition in high-solids bio gasification: an overview and practical solutions. *Environmental Technology*, 20(4): 355-365.

Kelly-Yong, T. L., Lee, K. T., Mohamed, A. R. and Bhatia, S. (2007). The potential of hydrogen from oil palm biomass as a source of renewable energy worldwide. *Energy Policy* 35: 5692–5701.

Keshavarzzadeh, A. H., Ahmadi, P. and Safaei, M. R. (2019). Assessment and optimization of an integrated energy system with electrolysis and fuel cells for electricity, cooling and hydrogen production using various optimization techniques. *International Journal of Hydrogen Energy*, 44(39), 21379-21396.

Khan, I. U., Othman, M. H. D., Hashim, H., Matsuura, T., Ismail, A. F., Rezaei-DashtArzhandi, M., and Azelee, I. W. (2017a). Biogas as a renewable energy fuel—A review of biogas upgrading, utilisation and storage. *Energy Conversion and Management*, 150, 277-294.

Khan, M. A., Ngo, H. H., Guo, W., Liu, Y., Zhang, X., Guo, J., Chang, S. W., Nguyen, D. D. and Wang, J. (2017b). Biohydrogen production from anaerobic digestion and its potential as renewable energy *Renewable Energy* 30: 1 – 15.

Khanal, S., Chen, W. H., Li, L. and Sung, S. (2003). Biological hydrogen production: effects of pH and intermediate products. *Int J Hydrogen Energy* 29: 1123 – 131.

Khanal, S. K. (2008). Overview of anaerobic biotechnology. *Anaerobic biotechnology for bioenergy production: Principles and applications* 1-27.

Khanal, S. K. (2011). *Anaerobic biotechnology for bioenergy production: principles and applications*. John Wiley & Sons. Willey.

Khanal, S. K., Chen, W. H., Li, L. and Sung, S. (2004). Biological hydrogen production: effects of pH and intermediate products. *Int J Hydrogen Energy*, 29: 1123-1131.

Khorsand, H., kiayee, N. and Masoomparast, A. H. (2012). Rice straw ash – a novel of silica nano-particles. *Journal of Mechanical Research and Application* 4(3): 1 -9.

Kim, D. H., Han, S. K., Kim, S. H., and Shin, H. S. (2006). Effect of gas sparging on continuous fermentative hydrogen production. *Int. J. Hydrogen Energy*, 31: 2158 – 2169.

Kim, D. H., Kim, S. H. and Shin, H. S. (2009). Sodium inhibition of fermentative hydrogen production. *International Journal of Hydrogen Energy* 34(8): 3295-3304.

Kim, M., Liu, C. Noh, J. W., Yang, Y., Oh, S., Shimizu, K., Lee, D. Y. and Zhang, Z. (2013). Hydrogen and methane production from untreated rice straw and raw sewage sludge under thermophilic anaerobic conditions. *Int J Hydrogen Energy*, 38: 8648 – 8656.

Kim, M., Yang, Y., Morikawa-Sakura, M. S., Wang, Q., Lee, M. V., Lee, D. Y., Feng, C., Zhou, Y. and Zhang, Z. (2012). Hydrogen production by anaerobic co-digestion of rice straw and sewage sludge. *International Journal of Hydrogen Energy* 37 (4): 3142 – 3149.

Kim, S. H. and Shin, H. S. (2008). Effects of base-pre-treatment on continuous enriched culture for hydrogen production from food waste. *International Journal of Hydrogen Energy*, 33(19), 5266-5274.

Kim, S. H., Han, S. K. and Shin, H. S. (2004). Feasibility of biohydrogen production by anaerobic co-digestion of food waste and sewage sludge. *Int J Hydrogen Energy* 29: 1607 – 1616.

Koch, K., Lubken, M., Gehring, T., Wichern, M. and Horn, H. (2010) Biogas from grass silage. Measurements and modeling with ADM1. *Bioresource Technology*, 101(21), pp. 8158-65

Kohl, A. and Nielsen, R. (1997). *Gas Purification*, 5th edition, Gulf Professional Publishing, Houston, Texas.

Koirala, B., Hers, S., Morales-España, G., Özdemir, Ö., Sijm, J. and Weeda, M. (2021). Integrated electricity, hydrogen and methane system modelling framework: Application to the Dutch Infrastructure Outlook 2050. *Applied Energy*, 289, 116713.

Kongmanklang, C. and Rangsiwatananon, K. (2015). Hydrothermal synthesis of high crystalline silicate from risk husk ash. *Journal of Spectroscopy* 1 – 5.

Kosemani, B. S. and Bamgboye, A. I. (2020). Energy input-output analysis of rice production in Nigeria. *Energy*, 118258.

Kotay, S. M, and Das, D. (2008). Biohydrogen as a renewable energy resource – prospects and potentials. *Int J Hydrogen Energy* 33:258–63

Kothari, R., Buddhi, D. and Sawhney, R. L. (2008). Comparison of environmental and economic aspects of various hydrogen production methods. *Renewable and Sustainable Energy Reviews* 12: 553b– 563.

Kothari, R., Singh, D. P., Tyagi, V. V., Tyagi, S. K. (2012). Fermentative hydrogen production – an alternative clean energy source. *Renew Sustain Energy Rev* 16:2337–46.

Kougiyas, P. G., Treu, L., Benavente, D. P., Boe, K., Campanaro, S. and Angelidaki, I. (2017). Ex-situ biogas upgrading and enhancement in different reactor systems. *Bioresource technology*, 225, 429-437.

Kozich, J., Schloss, P., Baxter, N., Jenior, M. and Koumpouras, C. (2003) 16S rRNA Sequencing with the Illumina MiSeq: Library Generation, QC, & Sequencing Version 5.0. Available at: [https://github.com/SchlossLab/MiSeq\\_WetLab\\_SOP/blob/master/MiSeq\\_WetLab\\_SOP\\_v4](https://github.com/SchlossLab/MiSeq_WetLab_SOP/blob/master/MiSeq_WetLab_SOP_v4). md (Accessed: 15/12/16).

Kratky, L. and Jirout, T. (2011). Biomass size reduction machines for enhancing biogas production. *Chem. Eng. Technol.* 34: 391 – 399.

Krich, K., Augenstein, D., Batmale, J. P., Benemann, J., Rutledge, B. and Salour, D. (2005). Biomethane from dairy waste. *A Sourcebook for the Production and Use of Renewable Natural Gas in California*, 147-162.

Kshirsagar, S. D., Waghmare, P. R., Loni, P. C., Patil, S. A. and Govindwar, S. P. (2015). Dilute acid pretreatment of rice straw, structural characterisation and optimisation of enzymatic hydrolysis conditions by response surface methodology. *RSC Advances*, 5(58), 46525-46533.

Kuhad, R. C., Deswal, D., Sharma, S., Bhattacharya, A., Jain, K. K., Kaur, A., Pletschke, B. I., Singh, A. and Karp, M. (2016) Revisiting cellulase production and redefining current strategies based on major challenges. *Renew Sust Energ Rev* 55: 249 – 272.

Kuhad R. C., Kuhar, S., Sharma, K. K. and Shrivastava, B. (2013) Microorganisms and enzymes involved in lignin degradation vis-à-vis production of nutritionally rich animal feed: an overview. *Biotechnol Environ Manage Resource Recov* 3–44.

Kumagai, S. and Sasaki, J. (2009). Carbon/silica composite fabricated from rice husk by means of binderless hot-pressing. *Bioresource Technology*, 100(13), 3308-3315.

Kumar, G., Bakonyi, P., Periyasamy, S., Kim, S. H., Nemestóthy, N. and Bélafi-Bakó, K. (2015). Lignocellulose biohydrogen: practical challenges and recent progress. *Renewable Sustainable Energy Rev.* 44: 728–737.

Kumar, G., Sen, B. and Lin, C.Y. (2013). Pretreatment and hydrolysis methods for recovery of fermentable sugars from de-oiled *Jatropha* waste. *Bioresource Technology* 145 (1): 275 – 279

Kumar, G., Sivagurunathan, P., Biswarup, S., Mudhoo, A., Davila-Vazquez, G, Wang, G. and Kim, S. H (2016). Research and development perspectives of lignocellulose-based biohydrogen production *International Biodeterioration & Biodegradation* 30: 1 – 14.

Kumar, P., Barrett, D. M., Delwiche, M. J. and Stroeve, P. (2009). Methods for pretreatment of lignocellulosic biomass for efficient hydrolysis and biofuel production. *Industrial & engineering chemistry research*, 48(8), 3713-3729.

Lai, C. Y., Zhou, L., Yuan, Z. and Guo, J. (2021). Hydrogen-Driven Microbial Biogas Upgrading: Advances, Challenges and Solutions. *Water Research*, 117120.

- Lantz, M. (2012). The economic performance of combined heat and power from biogas produced from manure in Sweden—A comparison of different CHP technologies. *Applied Energy*, 98, 502-511.
- Le, D. T. H. and Nitorisavut, R. (2015). Modified hydrotalcites for enhancement of biohydrogen production. *International Journal of Hydrogen Energy* 40(36): 12169-12176.
- Lee, D. Y., Ebie, Y., Xu, K. Q., Li, Y. Y. and Inamori, Y. (2010). Continuous H<sub>2</sub> and CH<sub>4</sub> production from high-solid food waste in the two-stage thermophilic fermentation process with the recirculation of digester sludge. *Bioresource Technology* 101 (1): 42 - 47.
- Lee, H. S., Krajmalinik-Brown, R., Zhang, H. and Rittmann, B. E. (2009). An electron-flow model can predict complex redox reactions in mixed-culture fermentative BioH<sub>2</sub>: Microbial ecology evidence. *Biotechnology and bioengineering* 104(4): 687-697.
- Lee, H. V., Hamid, S. B. A. and Zain, S. K (2014). Conversion of lignocellulose biomass to nano-cellulose: Structure and chemical process<sup>1</sup>, *Scientific World Journal*, 631013, 20
- Lee, J. S., Chung, M. J. and Seo, J. G. (2013). In vitro evaluation of the antimicrobial activity of lactic acid bacteria against *Clostridium difficile*. *Toxicological research* 29(2): 99.
- Lee, K. S., Wu, J. F., Lo, Y. S., Lo, Y. C., Lin, P. J. and Chang, J. S. (2004). Anaerobic hydrogen production with an efficient carrier-induced granular sludge bed bioreactor. *Biotechnology and Bioengineering* 87(5): 648-657.
- Lee, M. J., Kim, T. H., Min, B. and Hwang, S. J. (2012). Sodium (Na<sup>+</sup>) concentration affects metabolic pathway and estimation of ATP use in dark fermentation hydrogen production through stoichiometric analysis. *Journal of environmental management*, 108: 22-26.
- Lee, Y. J., Miyahara, T. and Noike, T. (2001). Effect of iron concentration on hydrogen fermentation. *Bioresource Technology* 80(3): 227-231.
- Lei, Z., Chen, J., Zhang, Z. and Sugiura, N. (2010). Methane production from rice straw with acclimated anaerobic sludge: effect of phosphate supplementation. *Bioresource Technology*, 101(12), 4343-4348.
- Lemire, J. A., Harrison, J. J. and Turner, R. J. (2013). Antimicrobial activity of metals: mechanisms, molecular targets and applications. *Nature Reviews Microbiology* 11(6): 371.
- Lens, P. N. L., Dijkema, C. and Stams, A. J. M. (1998). <sup>13</sup>C-NMR Study of propionate metabolism by sludges from bioreactors treating sulfate and sulfide-rich wastewater. *Biodegradation*, 9(3-4): 179-186.
- Lever, M. A. (2016). A new era of methanogenesis research. *Trends in microbiology*, 24(2), 84-86.
- Levin, D. B., Pitt, L. and Love, M. (2004). Biohydrogen production: prospects and limitations to practical application. *Int J Hydrogen Energy* 29: 173 - 185

- Li, C. and Fang, H. P. P. (2007). Fermentative hydrogen production from wastewater and solid wastes by mixed cultures. *Crit Rev Environ Sci Technol* 37: 1 – 39.
- Li, D. (2009). Hydrogen production characteristics of the organic fraction of municipal solid wastes by anaerobic mixed culture fermentation. *Int J Hydrogen Energy* 34(2): 812 - 820.
- Li, J., Chi, X., Zhang, Y. and Wang, X. (2018). Enhanced coproduction of hydrogen and butanol from rice straw by a novel two-stage fermentation process. *International Biodeterioration & Biodegradation*, 127, 62-68.
- Li, J., Li, B., Zhu, G., Ren, N., Bo, L. and He, J. (2007). Hydrogen production from diluted molasses by anaerobic hydrogen-producing bacteria in an anaerobic baffled reactor (ABR). *International Journal of Hydrogen Energy*, 32(15), 3274-3283.
- Li, S., Li, F., Zhu, X., Liao, Q., Chang, J. S. and Ho, S. H. (2022). Biohydrogen production from microalgae for environmental sustainability. *Chemosphere*, 291, 132717.
- Li, Y. and Khanal, S. K. (2016). *Bioenergy: principles and applications*. John Wiley & Sons.
- Liczbiński, P. and Borowski, S. (2021). Effect of hyperthermophilic pretreatment on methane and hydrogen production from garden waste under mesophilic and thermophilic conditions. *Bioresource Technology*, 335, 125264.
- Limongi, A. R., Viviano, E., Luca, M. D., Radice, R. P., Bianco, G. and Martelli, G. (2021). Biohydrogen from Microalgae: Production and Applications. *Applied Sciences*, 11(4), 1616.
- Lin, C. Y. and Lay, C. H. (2004). Carbon/nitrogen-ratio effect on fermentative hydrogen production by mixed microflora. *International Journal of Hydrogen Energy*, 29(1): 41-45.
- Lin, L., Wan, C., Liu, X., Lei, Z., Lee, D.-J., Zhang, Y., Tay, J. H. and Zhang, Z. (2013) Anaerobic digestion of swine manure under natural zeolite addition: VFA evolution, cation variation, and related microbial diversity. *Applied Microbiology and Biotechnology*, 97(24), pp. 10575- 10583
- Liou, T. H., and Yang, C. C. (2011). Synthesis and surface characteristics of nano silica produced from alkali-extracted rice husk ash. *Materials science and engineering B*, 176(7), 521-529.
- Liu, C. M., Chu, C. Y., Lee, W. Y., Li, Y. C., Wu, S. Y. and Chou, Y. P. (2013). Biohydrogen production evaluation from rice straw hydrolysate by concentrated acid pre-treatment in both batch and continuous systems. *International journal of hydrogen energy* 38: 15823 – 15829.
- Liu, C. M., Wu, S. Y., Chu, C.Y. and Chou, Y.P. (2014). Biohydrogen production from rice straw hydrolysate in a continuously external circulating bioreactor. *Int. J. Hydrogen Energy* 39: 19317 – 19322.

- Liu, D., Zeng, R. J. and Angelidaki, I. (2008). Effects of pH and hydraulic retention time on hydrogen production versus methanogenesis during anaerobic fermentation of organic household solid waste under extreme- thermophilic temperature (70 degrees C). *Biotechnol Bioeng* 100: 1108 – 1114.
- Liu, G., and Shen, J. (2004). Effects of culture medium and medium conditions on hydrogen production from starch using anaerobic bacteria. *J Biosci Bioeng*, 98: 251 – 256.
- Liu, L., Sun, J., Li, M., Wang, S., Pei, H. and Zhang, J. (2009). Enhanced enzymatic hydrolysis and structural features of corn stover by FeCl<sub>3</sub> pretreatment. *Bioresour Technol* 100: 5853 – 5858.
- Liu, X., He, D., Wu, Y., Xu, Q., Wang, D., Yang, Q., ... and Li, X. (2020). Freezing in the presence of nitrite pre-treatment enhances hydrogen production from dark fermentation of waste activated sludge— *Journal of Cleaner Production*, 248, 119305.
- Lo, Y. C., Lu, W. C., Chen, C. Y., Chang and J. S. (2010). Dark fermentative hydrogen production from enzymatic hydrolysate of xylan and pretreated rice straw by *Clostridium butyricum* CGS5. *Bioresour. Technol.* 101, 5885–5891
- Londeree, D. J. (2002). *Silica-titania* composites for water treatment (Doctoral dissertation, University Florida).
- Lootsma, A. and Raussen, T. (2008). Current practise for pre-treatment and utilization of digestate, 20 Kasseler Abfall-und Bioenergieforum 2008. *Germany: Witzenhausen*.
- Lopez-Linares, J. C., Romero, I., Moya, M., Cara, C., Ruiz, E. and Castro, E. (2009). Pretreatment of olive tree biomass with FeCl<sub>3</sub> prior enzymatic hydrolysis. *Bioresour Technol* 128: 180 - 187.
- Lossie, U. and Pütz, P. (2008). Targeted control of biogas plants with the help of FOS/TAC. Practice Report Hach-Lange.
- Love, M. I., Huber, W. and Anders, S. (2014). Moderated estimation of fold change and dispersion for RNA-seq data with DESeq2. *Genome Biology*, 15(12), 1-21.
- Lu, L. and Ren, Z. J. (2016). Microbial electrolysis cells for waste biorefinery: A state of the art review. *Bioresource technology*, 215, 254-264.
- Lu, L., Ren, N., Zhao, X., Wang, H., Wu, D. and Xing, D. (2011). Hydrogen production, methanogen inhibition and microbial community structures in psychrophilic single-chamber microbial electrolysis cells. *Energy Environmental Science* 4 (4): 1329 – 1336.
- Lu, P., and Hsieh, Y. L. (2012). Highly pure amorphous silica nano-disks from rice straw. *Powder Technology*, 225, 149-155.
- Luo, G., Karakashev, D., Xie, L., Zhou, Q. and Angelidaki, I. (2011) Long-term effect of inoculum pretreatment on fermentative hydrogen production by repeated batch cultivations:

homoacetogenesis and methanogenesis as competitors to hydrogen production. *Biotechnol Bioeng* 108: 1816 – 1827.

Lusk, B. G., Colin, A., Parameswaran, P., Rittmann, B. E. and Torres, C. I. (2018). Simultaneous fermentation of cellulose and current production with an enriched mixed culture of thermophilic bacteria in a microbial electrolysis cell. *Microbial biotechnology*, 11(1), 63-73.

Lynd, L. R., Van Zyl, W. H., McBride, J. E. and Laser, M. (2005). Consolidated bioprocessing of cellulosic biomass: an update. *Current opinion in biotechnology*, 16(5), 577-583.

Ma, Y., Ma, Y., Wang, Q., Schweidler, S., Botros, M., Fu, T., ... and Breitung, B. (2021). High-entropy energy materials: challenges and new opportunities. *Energy & Environmental Science*.

Maeda, I., Miyasaka, K., Umeda, F., Kawase, M. and Yagi, K. (2003). Maximisation of hydrogen production ability in high-density suspension of *Rhodovulum sulfidophilum* cells using intracellular poly (3-hydroxybutyrate) as sole substrate. *Biotechnol Bioeng*, 81: 474-481.

Maghanki, M. M., Ghobadian, B., Najafi, G. and Galogah, R. J. (2013). Micro combined heat and power (MCHP) technologies and applications. *Renewable and Sustainable Energy Reviews*, 28, 510-524.

Maguyon-Detras, M. C., Migo, M. V. P., Van Hung, N. and Gummert, M. (2020). Thermochemical Conversion of Rice Straw. In *Sustainable Rice Straw Management* (pp. 43-64). Springer, Cham.

Mason, P. M. and Stuckey, D. C. (2016) Biofilms, bubbles and boundary layers – A new approach to understanding cellulolysis in anaerobic and ruminant digestion. *Water Research*, 104: 93-100.

Mata-Alvarez, J., Dosta, J., Romero-Güiza, M. S., Fonoll, X., Peces, M. and Astals, S. (2014) A critical review on anaerobic co-digestion achievements between 2010 and 2013. *Renewable and Sustainable Energy Reviews*, 36: 412-427.

Maurer, C. and Müller, J. (2019). Drying characteristics of biogas digestate in a hybrid waste-heat/solar dryer. *Energies*, 12(7), 1294.

McMurdie, P. J. and Holmes, S. (2013). phyloseq: an R package for reproducible interactive analysis and graphics of microbiome census data. *PloS one*, 8(4), e61217.

Menardo, S., Cacciatore, V. and Balsari, P. (2015). Batch and continuous biogas production arising from feed varying in rice straw volumes following pre-treatment with extrusion. *Bioresource technology*, 180, 154-161.

Milieudefensie (2011). Oil spills in the Niger Delta in Nigeria. <https://en.milieudefensie.nl/news/oilspills-in-nigeria-english.pdf>

Mirmohamadsadeghi, S. and Karimi, K. (2018). Energy recovery together with amorphous nano-silica production from rice straw via dry anaerobic digestion. *BioResources*, 13 (1), 1872-1884.



Mockaitis, G., Bruant, G., Guiot, S. R., Peixoto, G., Foresti, E. and Zaiat, M. (2020). Acidic and thermal pre-treatments for anaerobic digestion inoculum to improve hydrogen and volatile fatty acid production using xylose as the substrate. *Renewable Energy*, 145, 1388-1398.

Mohammed, M. A. A., Salmiaton, A. Wan-Azlina, W. A. K. G. and Mohamad –Amran. M. S. (2012). Gasification of oil palm empty fruit bunches: A characterisation and kinetic study. *Bioresource Technology* 110: 628–636

Mohapatra, S., Mishra, C., Behera, S. S. and Thatoi, H. (2017) Application of pretreatment, fermentation and molecular techniques for enhancing bioethanol production from grass biomass – A review. *Renewable and Sustainable Energy Reviews*, 78: 1007-1032.

Momirlan, M. and Veziroglu, T. N. (2002). Current status of hydrogen energy. *Renew Sustain Energy Rev* 6: 141 –179.

Monlau, F., Kaparaju, P., Trably, E., Steyer, J. P. and Carrere, H. (2015). Alkaline pre-treatment to enhance one-stage CH<sub>4</sub> and two-stage H<sub>2</sub>/CH<sub>4</sub> production from sunflower stalks: mass, energy and economic balances. *Chemical Engineering Journal*, 260, 377-385.

Monlau, F., Sambusiti, C., Barakat, A., Guo, X. M., Latrille, E., Trably, E., ...and Carrere, H. (2012). Predictive models of biohydrogen and biomethane production based on the compositional and structural features of lignocellulosic materials. *Environmental science & technology*, 46(21), 12217-12225.

Morgan, J. W., Evison, L. M. and Forster, C. F. (1991). Changes to the microbial ecology in anaerobic digesters treating ice cream wastewater during start-up. *Water Research* 25(6): 639-653.

Mosier, N., Wyman, C., Dale, B., Elander, R., Lee, Y. Y., Holtzapple, M. and Ladisch, M. (2005). Features of promising technologies for pretreatment of lignocellulosic biomass. *Bioresource Technology*, 96(6), 673-686.

Mu, Y., Yu, H. Q. and Wang, G. (2007). Evaluation of three methods for enriching H<sub>2</sub>-producing cultures from anaerobic sludge. *Enzyme and Microbial Technology*, 40(4), 947-953.

Muchie, M. and Baskaran, A. (2012). Creating systems of innovation in Africa: country case studies: *African Books Collective*.

Muñoz, R., Meier, L., Diaz, I. and Jeison, D. (2015). A review on the state-of-the-art of physical/chemical and biological technologies for biogas upgrading. *Reviews in Environmental Science and Bio/Technology*, 14(4), 727-759.

Muritala, I. K., Guban, D., Roeb, M. and Sattler, C. (2019). High-temperature production of hydrogen: Assessment of non-renewable resources technologies and emerging trends. *International Journal of Hydrogen Energy*.

Mustafa, A. M., Poulsen, T. G. and Sheng, K. (2016). Fungal pre-treatment of rice straw with *Pleurotus ostreatus* and *Trichoderma reesei* to enhance methane production under solid-state anaerobic digestion. *Applied energy*, 180, 661-671.

Nanda, S., Mohanty, P., Pant, K. K. Naik, S. Kozinski, J. A. and Dalai, A. K. (2013). Characterisation of North American Lignocellulosic Biomass and Biochars in Terms of their Candidacy for Alternate Renewable Fuels. *Bioenerg. Res.* 6: 663 – 677.

Nandiyanto, A. B. D., Ragadhita, R. and Istadi, I. (2020). Techno-economic Analysis for the Production of Silica Particles from Agricultural Wastes. *Moroccan Journal of Chemistry*, 8 (4), 8-4.

Nan-Qi, R., Lei Z., Chuam, C., Wan-Qian, G. and Guang-Li C. (2016). A review on bioconversion of lignocellulosic biomass to Hydrogen: Key challenges and new insights. *Bioresource Technology* 215: 92 - 99.

Nasir, I. M., Mohd Ghazi, T. I. and Omar, R. (2012) Anaerobic digestion technology in livestock manure treatment for biogas production: A review. *Engineering in Life Sciences*, 12(3): 258-269.

Nath, K. and Das, D. (2004). Biohydrogen production as a potential energy resource–Present state-of-art. *Journal of Scientific and Industrial Research* 63: 729-738.

Nathao, C., Sirisukpoka, U. and Pisutpaisal, N. (2013) Production of hydrogen and methane by one and two-stage fermentation of food waste. *Int. J. Hydrog. Energy* 38: 15764 – 15769.

Neshat, S. A., Mohammadi, M., Najafpour, G. D. and Lahijani, P. (2017) Anaerobic co-digestion of animal manures and lignocellulosic residues as a potent approach for sustainable biogas production. *Renewable and Sustainable Energy Reviews*, 79: 308-322.

Newsom, C. (2012). Low-carbon approaches to tackling Nigeria's energy poverty. Renewable energy potential in Nigeria. International Institute for Environment and Development.

Nguyen, V. H., Topno, S., Balingbing, C., Nguyen, V. C. N., Röder, M., Quilty, J., ... and Gummert, M. (2016). Generating a positive energy balance from using rice straw for anaerobic digestion. *Energy Reports*, 2, 117-122.

Nielsen, S. S. (2017). *Food Analysis*: Springer International Publishing.

Nigeria Energy Market Report (2021). <https://www.enerdata.net/estore/country-profiles/nigeria.html>. (Accessed on the 20<sup>th</sup> January 2022)

Nigerian Electricity Regulatory Commission (NERC). NERC Third Quarter Report. (2018). <https://nerc.gov.ng/index.php/library/documents/NERC-Reports/NERC-Quarterly-Reports/NERC-Third-Quarter-Report-2018/>. (accessed 15<sup>th</sup> July 2020).

Nigerian Electricity Supply Industry (NESI) (2020). Electricity supply statistics <http://www.nesistats.org> (accessed 16<sup>th</sup> July 2020).

Nigerian Energy Support Programme (NESP), (2015). The Nigerian Energy Sector. An Overview with special emphasis on renewable energy, energy efficiency and rural electrification. Second edition.

Nigerian National Petroleum Corporation (NNPC) (2016). Annual statistical bulletin.

Nilsson, D. (1997). Energy, exergy and emergy analysis of using straw as fuel in district heating plants. *Biomass and Bioenergy*, 13(1-2), 63-73.

Nilsson, M., Linné, M., Dahl, A. and Biomil, AB (2001). *Life cycle inventory for biogas as a vehicle fuel*. SGC.

Ntaikou, I., Antonopoulou, G. and Lyberatos, G. (2010). Biohydrogen production from biomass and wastes via dark fermentation: a review. *Waste and Biomass Valorisation* 1(1): 21-39.

Oh, S. E., Van Ginkel, S. and Logan, B. E. (2003). Effects of thermophilic heat pretreatment of mixed inoculum on biohydrogen production from synthetic and sugarcane mill wastewaters. *Environ. Sci. Technol.* 37(22): 5186 – 5190.

Oksanen, J., Kindt, R., Legendre, P., O'Hara, B., Stevens, M. H. H., Oksanen, M. J. and Suggests, M. A. S. S. (2007). The vegan package. *Community ecology package*, 10(631-637), 719.

Okunade, D. A. and Adekalu, K. O. (2013). "Physiochemical Analysis of Contaminated Water Resources Due to Cassava Wastewater Effluent Disposal" *European International Journal of Science and Technology Vol. 2 No. 6* pp 75-85.

Olugasa, T. T., Odesola, I. F. and Oyewola, M. O. (2014). Energy production from biogas: A conceptual review for use in Nigeria. *Renewable and Sustainable Energy Reviews*, 32, 770-776.

Oreopoulou, V. and Russ, W. (2006). *Utilisation of By-Products and Treatment of Waste in the Food Industry*: Springer US.

O-Thong, S., Hniman, A., Prasertsan, P. and Imai, T. (2011). Biohydrogen production from cassava starch processing wastewater by thermophilic mixed cultures. *International Journal of Hydrogen Energy* 36: 3409 - 3416.

O-Thong, S., Prasertsan, P. and Birkeland, N. K. (2009). Evaluation of methods for preparing hydrogen-producing seed inocula under thermophilic condition by process performance and microbial *Bioresource Technology* 100: 909 – 918.

Oyedepo, S. O., Babalola, O. P., Nwanya, S. C., Kilanko, O., Leramo, R. O., Aworinde, A. K., ... and Agbereggha, O. L. (2018). Towards a Sustainable Electricity Supply in Nigeria: The Role of Decentralised Renewable Energy System. *European Journal of Sustainable Development Research*, 2(4), 40.

- Oyeyinka, S. A., Adegoke, R., Oyeyinka, A. T., Salami, K. O., Olagunju, O. F., Kolawole, F. L. ... and Bolarinwa, I. F. (2018). Effect of annealing on the functionality of Bambara groundnut (*Vigna subterranea*) starch–palmitic acid complex. *International Journal of Food Science & Technology*, 53(2), 549-555.
- Oyeyinka, S. A., Adeloye, A. A., Olaomo, O. O. and Kayitesi, E. (2020). Effect of fermentation time on physicochemical properties of starch extracted from cassava root. *Food Bioscience*, 33, 100485.
- Pachapur, V. L., Sarma, S. J., Brar, S. K., Le Bihan, Y., Soccol, C. R., Buelna, G. and Verma, M. (2015). Co-culture strategies for increased biohydrogen production. *Int. J. Energy Res.* 39(11): 1479 – 1504.
- Palmqvist, E. and Hahn-Hägerdal, B. (2000). Fermentation of lignocellulosic hydrolysates. II: inhibitors and mechanisms of inhibition. *Bioresource Technology*, 74(1), 25-33.
- Pan, C. M., Ma, H. C., Fan, Y. T. and Hou, H. W. (2011). Bioaugmented cellulosic hydrogen production from cornstalk by integrating dilute acid-enzyme hydrolysis and dark fermentation. *International Journal of hydrogen energy*, 36(8), 4852-4862.
- Parawira, W., Murto, M., Zvauya, R. and Mattiasson, B. (2004). Anaerobic batch digestion of solid potato waste alone and in combination with sugar beet leaves. *Renewable Energy*, 29(11), 1811-1823.
- Patel, K. G., Shettigar, R. R. and Misra, N. M. (2017). Recent Advance in Silica Production Technologies from Agricultural Waste Stream. *Journal of Advanced Agricultural Technologies* 4 (3).
- Patel, S. K., Kumar, P., Mehariya, S., Purohit, H. J., Lee, J. K. and Kalia, V. C. (2014). Enhancement in hydrogen production by co-cultures of *Bacillus* and *Enterobacter*. *International Journal of Hydrogen Energy*, 39(27), 14663-14668.
- Patterson, T., Esteves, S., Dinsdale, R., and Guwy, A. (2011). An evaluation of the policy and techno-economic factors affecting the potential for biogas upgrading for transport fuel use in the UK. *Energy Policy*, 39 (3), 1806-1816.
- Peacock, A. D. and Newborough, M. (2008). Effect of heat-saving measures on the CO<sub>2</sub> savings attributable to micro-combined heat and power ( $\mu$ CHP) systems in UK dwellings. *Energy*, 33(4), 601-612.
- Pellegrini, L. A., De Guido, G., Consonni, S., Bortoluzzi, G. and Gatti, M. (2015). From biogas to biomethane: how the biogas source influences the purification costs. In *ICheaP12 International Conference on Chemical & Process Engineering* (pp. 409-414). Italian Association of Chemical Engineering-AIDIC.
- Perez, J., Munoz-Dorado, J. de la Rubia, T. and Martinez, J. (2002). Biodegradation and biological treatment of cellulose, hemicellulose and lignin: an overview. *International Microbiology* 5 (2): 53 -63.

Peña Muñoz, K. and Steinmetz, H. (2012) Evaluation of pre-treatment on the first stage of an anaerobic digester for enhancing bio-hydrogen production and its associated energy balance. *Energy Procedia*, 29, pp. 469-479.

Pendyala, B., Chaganti, S. R., Lalman, J. A., Shanmugam, S. R., Heath, D. D. and Lau, P. C. (2012). Pretreating mixed anaerobic communities from different sources: correlating the hydrogen yield with hydrogenase activity and microbial diversity. *International journal of hydrogen energy*, 37(17): 12175-12186.

Permatasari, N. Sucahya, T. N. and Nandiyanto, A. B. D. (2016). Review: Agricultural waste as a source of silica materials. *Indonesian Journal of Science and Technology* 1(1); 82 – 106.

Piera, M. (2006). Safety issues of nuclear production of hydrogen. *Energy Convers Manag* 47(17): 2732 – 2739.

Pilavachi, P. A. (2002). Mini-and micro-gas turbines for combined heat and power. *Applied thermal engineering*, 22(18), 2003-2014.

Pinto, F. A. L., Troshina, O. and Lindblad, P. (2002). A brief look at three decades of research on cyanobacterial hydrogen evolution. *International journal of hydrogen energy*, 27(11-12), 1209-1215.

Poltronieri, P. and D'urso, O. F. . (2016). Biotransformation of Agricultural Waste and By-products: The Food, Feed, Fibre, Fuel (4F) Economy. (Eds.). Elsevier.

Pöschl, M., Ward, S. and Owende, P. (2010). Evaluation of energy efficiency of various biogas production and utilisation pathways. *Applied Energy*, 87(11), 3305-3321.

Präger, F., Paczkowski, S., Sailer, G., Derkyi, N. S. A. and Pelz, S. (2019). Biomass sources for a sustainable energy supply in Ghana—A case study for Sunyani. *Renewable and Sustainable Energy Reviews*, 107, 413-424.

Prakasham, R. S., Satish, T. and Brahmaiah, P. (2010). Biohydrogen production process optimisation using anaerobic mixed consortia: a prelude study for the use of agro-industrial material hydrolysate as substrate. *Bioresource Technology* 101: 5708 – 5711.

Qian, D. K., Geng, Z. Q., Sun, T., Dai, K., Zhang, W., Zeng, R. J. and Zhang, F. (2020). Caproate production from xylose by mesophilic mixed culture fermentation. *Bioresource technology*, 308, 123318.

Quéméneur, M., Bittel, M., Trably, E., Dumas, C., Fourage, L., Ravot, G., ... and Carrère, H. (2012a). Effect of enzyme addition on fermentative hydrogen production from wheat straw. *International journal of hydrogen energy*, 37(14), 10639-10647.

Quéméneur, M., Hamelin, J., Barakat, A., Steyer, J. P., Carrère, H. and Trably, E. (2012b). Inhibition of fermentative hydrogen production by lignocellulose-derived compounds in mixed cultures. *International journal of hydrogen energy*, 37(4), 3150-3159.

- Qyyum, M. A., Haider, J., Qadeer, K., Valentina, V., Khan, A., Yasin, M., ... and Lee, M. (2020). Biogas to liquefied biomethane: Assessment of 3P's—Production, processing, and prospects. *Renewable and Sustainable Energy Reviews*, 119, 109561.
- Rabiu, A. M., Dlangamandla, N. and Ulleberg, Ø. (2012). Novel heat integration in a methane reformer and high-temperature PEM fuel cell-based mCHP system. *APCBEE Procedia*, 3, 17-22.
- Rafiee, E., Shahebrahimi, S., Feyzi, M. and Shaterzadeh, M. (2012). Optimisation of synthesis and characterisation of nanosilica produced from rice husk (a common waste material). *International Nano Letters* 2 (1): 1 – 8.
- Rajagopal, R., Massé, D. I. and Singh, G. (2013). A critical review on inhibition of anaerobic digestion process by excess ammonia. *Bioresource Technology*, 143: 632-641.
- Ren, N., Cao, G., Wang, A., Lee, D. J., Guo, W. and Zhu, Y. (2008). Dark fermentation of xylose and glucose mix using isolated *Thermoanaerobacterium thermosaccharolyticum* W16. *International journal of hydrogen energy* 33(21): 6124-6132.
- Ren, N. Q., Cao, G. L., Guo, W. Q., Wang, A. J., Zhu, Y. H., Liu, B. and Xu, J. F. (2010). Biological hydrogen production from corn stover by moderately thermophile *Thermoanaerobacterium thermosaccharolyticum* W16. *Int. J. Hydrogen Energy* 35: 2708 – 2712.
- Ren, N. Q., Guo, W. Q., Wang, X. J., Xiang, W. S., Liu, B. F., Wang, X. Z., ... and Chen, Z. B. (2008). Effects of different pretreatment methods on fermentation types and dominant bacteria for hydrogen production. *International Journal of Hydrogen Energy*, 33(16), 4318-4324.
- Rodríguez, A., Moral, A., Serrano, L., Labidi, J. and Jiménez, L. (2008). Rice straw pulp was obtained by using various methods. *Bioresour. Technol.* 99: 2881-2886.
- Rodriguez, C., Alaswad, A., Benyounis, K. Y. and Olabi, A. G. (2017) Pretreatment techniques used in biogas production from grass. *Renewable and Sustainable Energy Reviews*, 68. 1193-1204.
- Rognes, T., Flouri, T., Nichols, B., Quince, C. and Mahé, F. (2016). VSEARCH: a versatile open-source tool for metagenomics. *PeerJ*, 4, e2584.
- Rohatgi, K., Prasad, S. V., and Rohatgi, P. K. (1987). Release of silica-rich particles from rice husk by microbial fermentation. *Journal of Materials Science Letters*, 6 (7), 829-831
- Rosa, L. and Mazzotti, M. (2022). Potential for hydrogen production from sustainable biomass with carbon capture and storage. *Renewable and Sustainable Energy Reviews*, 157, 112123.
- Rouches, E., Herpoël-Gimbert, I., Steyer, J. P. and Carrere, H. (2016) Improvement of anaerobic degradation by white-rot fungi pretreatment of lignocellulosic biomass: A review. *Renewable and Sustainable Energy Reviews*, 59, pp. 179-198.

Roy, S., Schievano, A. and Pant, D. (2016). Electro-stimulated microbial factory for value-added product synthesis. *Bioresource technology*, 213, 129-139.

Ryckebosch, E., Drouillon, M. and Vervaeren, H. (2011). Techniques for transformation of biogas to biomethane. *Biomass and bioenergy*, 35(5), 1633-1645.

Saady, N. M. C. (2013). Homoacetogenesis during hydrogen production by mixed cultures dark fermentation: unresolved challenge. *International Journal of Hydrogen Energy* 38(30): 13172-13191.

Salakkam, A., Plangklang, P., Sittijunda, S., Kongkeitkajorn, M. B., Lunprom, S. and Reungsang, A. (2019). Bio-hydrogen and Methane Production from Lignocellulosic Materials. In *Biomass for Bioenergy-Recent Trends and Future Challenges*.

Salerno, M. B., Park, W., Zuo, Y. and Logan, B. E. (2006). Inhibition of biohydrogen production by ammonia. *Water Research* 40(6): 1167-1172.

Sambo, A. S. (2018), Energy Crisis in Nigeria: Engineers' Proactive Steps towards Energy Self-Sufficiency. Lecture as the First in the Series of the Distinguished Lectures in honour of Engr. Dr. E. J. S. Uujamhan, at the University of Benin, Benin City, on the 6th Day of April 2018, 1-27.

Sambusiti, C., Ficara, E., Malpei, F., Steyer, J. P. and Carrère, H. (2013). The benefit of sodium hydroxide pre-treatment of ensiled sorghum forage on the anaerobic reactor stability and methane production. *Bioresource technology*, 144, 149-155.

Sangnark, A. and Noomhorm, A. (2004). Chemical, physical and baking properties of dietary fibre prepared from rice straw. *Food Res. Inter.* 37. 66.

Sapawe, N., Osman, N. S., Zakaria, M. Z., Fikry, S. A. S. S. M. and Aris, M. A. M. (2018). Materials Today: *Proceedings* 5 (10): 21861-21866

Sattar, A., Arslan, C., Ji, C., Chen, K., Nasir, A., Fang, H. and Umair, M. (2016a). Optimising the physical parameters for bio-hydrogen production from food waste co-digested with mixed consortia of clostridium. *Journal of Renewable and Sustainable Energy*, 8: 013107.

Sattar, A., Arslan, C., Ji, C., Sattar, S., Mari, I. A., Rashid, H. and Ilyas, F. (2016b). Comparing the bio-hydrogen production potential of pre-treated rice straw co-digested with seeded sludge using an anaerobic bioreactor under mesophilic, thermophilic conditions. *Energies* 9: 198.

Schön, M. (2010). Numerical Modelling of Anaerobic Digestion Processes in Agricultural Biogas Plants: Innsbruck University Press.

Schroyen, M., Vervaeren, H., Vandepitte, H., Stijn W.H. Van-Hulle, S. W. H. and Raes, K. (2015). Effect of enzymatic pretreatment of various lignocellulosic substrates on the production of phenolic compounds and biomethane potential. *Bioresource Technology* 192: 696–702.

Shah, F. A., Mahmood, Q., Rashid, N., Pervez, A., Raja, I. A. and Shah, M. M. (2015) Codigestion, pretreatment and digester design for enhanced methanogenesis. *Renewable and Sustainable Energy Reviews*, 42: 627-642.

Sharma, V. K., Zboril, R. and Varma, R. S. (2015). Ferrates: greener oxidants with multimodal action in water treatment technologies. *Accounts of chemical research*, 48(2), 182-191.

Sharmila, V. G., Tamilarasan, K., Kumar, M. D., Kumar, G., Varjani, S., Kumar, S. A. and Banu, J. R. (2022). Trends in dark biohydrogen production strategy and linkages with transition towards low carbon economy: An outlook, cost-effectiveness, bottlenecks and future scope. *International Journal of Hydrogen Energy*.

Shim, J., Velmurugan, P., and Oh, B. T. (2015). Extraction and physical characterisation of amorphous silica made from corn cob ash at variable pH conditions via sol-gel processing. *Journal of industrial and Engineering Chemistry*, 30, 249-253.

Shin, H. S., Youn, J. H. and Kim, S. H. (2004). Hydrogen Production from food waste in anaerobic mesophilic and thermophilic acidogenesis. *Int J Hydrogen Energy* 29: 1355 – 1363.

Show, K. Y., Zhang, Z. P., Tay, J. H., Liang, D. T., Lee, D. J. and Jiang, W. J. (2007). Production of hydrogen in a granular sludge-based anaerobic continuous stirred tank reactor. *International Journal of Hydrogen Energy*, 32(18), 4744-4753.

Sikkema, R., Junginger, M., Pichler, W., Hayes, S. and Faaij, A. P. (2010). The international logistics of wood pellets for heating and power production in Europe: Costs, energy-input and greenhouse gas balances of pellet consumption in Italy, Sweden and the Netherlands. *Biofuels, Bioproducts and Biorefining*, 4(2), 132-153.

Sikora, A., Błaszczuk, M., Jurkowski, M. and Zielenkiewicz, U. (2013). *Lactic acid bacteria in hydrogen-producing consortia: on purpose or by coincidence?* (pp. 488-514). INTECH open science open minds.

Sindhu, R., Binod, P. and Pandey, A. (2016). Biological pretreatment of lignocellulosic biomass – an overview. *Bioresour. Technol.* 199: 76–82.

Singh, L. and Wahid, Z. A. (2015). Methods for enhancing bio-hydrogen production from the biological process: a review. *Journal of Industrial and Engineering Chemistry*, 21, 70-80.

Singh, P., Sulaiman, O., Hashim, R., Rupani P. F. and Peng, L. C. (2010). Biopulping of lignocellulosic material using different fungal species: a review. *Rev Environ Sci Bio* 9: 141 – 151.

Sinha, P. and Pandey, A. (2011). An evaluative report and challenges for fermentative biohydrogen production *Int. J. Hydrogen Energy* 36 (13): 7460–7478.

Sipilä, K. (2016). Cogeneration, biomass, waste to energy and industrial waste heat for district heating. In *Advanced District Heating and Cooling (DHC) Systems* (pp. 45-73). Woodhead Publishing



- Sircar, S. (2002). Pressure swing adsorption. *Industrial & engineering chemistry research*, 41(6), 1389-1392.
- Siriwongrungson, V., Zeng, R. J. and Angelidaki, I. (2007). Homoacetogenesis as the alternative pathway for H<sub>2</sub> sink during thermophilic anaerobic degradation of butyrate under suppressed methanogenesis. *Water Research* 41(18): 4204-4210.
- Skov, I. R., Nielsen, S., Nørholm, M. S. and Vestergaard, J. P. (2019). Screening of biogas methanation in Denmark: Resources, technologies and renewable energy integration.
- Soltani, N., Bahrami, A., Pech-Canul., M. I. and Gonzalez, L. A. (2015). Review on the physicochemical treatments of rice husk for production of advanced materials. *Chemical Engineering Journal* 264: 899 – 935.
- Sonesson, U. (1996). Modelling of the compost and transport process in the ORWARE simulation model.
- Soto, M., Méndez, R. and Lema, J. M. (1993). Methanogenic and non-methanogenic activity tests. Theoretical basis and experimental set-up. *Water Research* 27(8): 1361-1376.
- Srikanth, S. and Mohan, S. V. (2014). Regulating feedback inhibition caused by the accumulated acid intermediates during acidogenic hydrogen production through feed replacement. *International journal of hydrogen energy* 39(19): 10028-10040.
- Srivastava, N., Srivastava, M., Abd\_Allah, E. F., Singh, R., Hashem, A. and Gupta, V. K. (2021). Biohydrogen production using kitchen waste as the potential substrate: A sustainable approach. *Chemosphere*, 271, 129537.
- Ssekagiri, A., Sloan, W., and Ijaz, U. Z. (2017). MicrobiomeSeq: An R package for analysis of microbial communities in an environmental context. In *ISCB Africa ASBCB Conference, Kumasi, Ghana*. <https://github.com/umerijaz/microbiomeSeq> (Vol. 10).
- Steven, R. H., Byung, Y. Y., David, V., Kurt, K. and Rex M. (1996). Composition of Corn Steep Water during Steeping. *J. Agric. Food Chem.* 44: 1857 – 1863.
- Su, B., Han, W., Chen, Y., Wang, Z., Qu, W. and Jin, H. (2018). Performance optimization of a solar assisted CCHP based on biogas reforming. *Energy Conversion and Management*, 171, 604-617.
- Sukumaran, R. K., Singhanian, R. R. and Pandey, A. (2005). Microbial cellulases-production, applications and challenges. *J Sci Ind Res* 64: 832 – 844.
- Sun, J., Fu, L. and Zhang, S. (2012). A review of working fluids of absorption cycles. *Renewable and Sustainable Energy Reviews*, 16(4), 1899-1906.

Sun, L., Liu, T., Müller, B. and Schnürer, A. (2016) The microbial community structure in industrial biogas plants influences the degradation rate of straw and cellulose in batch tests. *Biotechnology for Biofuels*, 9(1), p. 128

Sun, Q., Li, H., Yan, J., Liu, L., Yu, Z. and Yu, X. (2015). Selection of appropriate biogas upgrading technology-a review of biogas cleaning, upgrading and utilisation. *Renewable and Sustainable Energy Reviews*, 51, 521-532.

Suominen, S., van Vliet, D. M., Sánchez-Andrea, I., van der Meer, M. T., Sinninghe Damste, J. S and Villanueva, L. (2021). Organic matter type defines the composition of active microbial communities originating from anoxic Baltic Sea sediments. *Frontiers in microbiology*, 12, 978.

Surendra, K.C., Takara, D., Hashimoto, A. D. and Khanal, S. K. (2014). Biogas as a sustainable energy source for developing countries: Opportunities and challenges. *Renewable and Sustainable Energy Reviews* 31: 846–859.

Swedish Gas Technology Centre Ltd (SGC) (2012). Basic Data on Biogas <http://www.sgc.se/ckfinder/userfiles/files/BasicDataonBiogas2012.pdf> (accessed on February, 14<sup>th</sup> 2020).

Tabraiz, S., Petropoulos, E., Shamurad, B., Quintela-Baluja, M., Mohapatra, S., Acharya, K., ... and Sallis, P. J. (2021). Temperature and immigration effects on quorum sensing in the biofilms of anaerobic membrane bioreactors. *Journal of Environmental Management*, 293, 112947.

Takaichi, S., Maoka, T., Takasaki, K. and Hanada, S. (2010). Carotenoids of *Gemmatimonas aurantiaca* (*Gemmatimonadetes*): identification of a novel carotenoid, deoxyoscillol 2-rhamnoside, and proposed biosynthetic pathway of oscillol 2, 2'-dirhamnoside. *Microbiology*, 156(3), 757-763.

Tambone, F., Genevini, P., D'Imporzano, G. and Adani, F. (2009). Assessing amendment properties of digestate by studying the organic matter composition and the degree of biological stability during the anaerobic digestion of the organic fraction of MSW. *Bioresource Technology*, 100(12), 3140-3142.

Temudo, M. F., Kleerebezem, R. and Loosdrecht, M. V. (2007). Influence of the pH on (open) mixed culture fermentation of glucose: a chemostat study. *Biotechnol Bioeng* 98(1): 69 - 79.

Thao, N. T. N. L., Chiang, K. Y., Wan, H. P., Hung, W. C. and Liu, C. F. (2019). Enhanced trace pollutants removal efficiency and hydrogen production in rice straw gasification using a hot gas cleaning system. *International Journal of Hydrogen Energy*, 44(6), 3363-3372.

Tirunehe, G. and Norddahl, B. (2016). The influence of polymeric membrane gas spargers on hydrodynamics and mass transfer in bubble column bioreactors. *Bioprocess and biosystems engineering*, 39(4), 613-626.

Toledo-Cervantes, A., Serejo, M. L., Blanco, S., Pérez, R., Lebrero, R. and Muñoz, R. (2016). Photosynthetic biogas upgrading to bio-methane: Boosting nutrient recovery via biomass productivity control. *Algal Research*, 17, 46-52.

Triolo, J. M., Ward, A. J., Pedersen, L. and Sommer, S. G. (2013). Characteristics of animal slurry as key biomass for biogas production in Denmark. *Biomass Now-Sustainable Growth and Use*, 307-326.

Tsavkelova, E. A and Netrusov, A. I (2012) Biogas production from cellulose-containing substrates: a review. *Appl Biochem Microbiol* 48: 421–433.

Türker, L., Gümüş, S. and Tapan, A. (2008). Biohydrogen production: molecular aspects. *Journal of Scientific and Industrial Research* 67: 994-1016.

Tye, Y. Y., Lee, K. T., Wan Abdullah, W. N. and Leh, C. P. (2011). Second generation bioethanol as a sustainable energy source in Malaysia transportation sector: status, potential and future prospects. *Renew Sustain Energy Rev* 15(9):4521 – 4536.

Udoetok, I. A. (2012). Characterisation of ash made from oil palm empty fruit bunches (oEPFB). *International Journal of Environmental Sciences*, 3(1), 518-524.

Ueno, Y., Fukui, H. and Goto, M. (2007). Operation of a two-stage fermentation process producing hydrogen and methane from organic waste. *Environ. Sci. Technol.*, 41: 1413 – 1419

Ugwoke, B., Gershon, O., Becchio, C., Corgnati, S. P. and Leone, P. (2020). A review of Nigerian energy access studies: The story told so far. *Renewable and Sustainable Energy Reviews*, 120, 109646.

UK Energy in Brief (2021). [https://assets.publishing.service.gov.uk/government/uploads/system/uploads/attachment\\_data/file/1032260/UK Energy in Brief 2021.pdf](https://assets.publishing.service.gov.uk/government/uploads/system/uploads/attachment_data/file/1032260/UK_Energy_in_Brief_2021.pdf). Accessed on the 22<sup>nd</sup> January 2022

Umeda, J. and Kondoh, k. (2008). High-purity amorphous silica originated in rice husks via the carboxylic acid leaching process. *Journal of Materials Science* 43(22): 7084 – 7090.

Umeda, J. and Kondoh, k. (2010). High-purification of amorphous silica originated from rice husks by a combination of polysaccharides hydrolysis and metallic impurities removal. *Industrial Crops and Products* 32 (3): 538 – 544.

US Department of Energy (2017) <https://www.energy.gov/sites/prod/files/2017/06/f35/CHP-Absorption%20Chiller-compliant.pdf> (accessed on 8<sup>th</sup> December 2019)

Usman, Z. G. and Abbasoglu, S. (2015). An Overview of Power Sector Laws, Policies and Reforms in Nigeria. *Asian Transactions on Engineering*, 4(2), 6-12

Vaibhav, V., Vijayalakshmi, U., and Roopan, S. M. (2015). Agricultural waste as a source for the production of silica nano-particles. *Spectrochimica acta part a; Molecular and biomolecular spectroscopy* 139: 515 – 520.

Vaňáčová, Š., Rasoloson, D., Rázga, J., Hrdý, I., Kulda, J. and Tachezy, J. (2001). Iron-induced changes in pyruvate metabolism of *Tritrichomonas foetus* and involvement of iron in the expression of hydrogenosomal proteins. *Microbiology* 147(1): 53-62.

Van-Dyk, J. S. and Pletschke, B. I. (2012). A review of lignocellulose bioconversion using enzymatic hydrolysis and synergistic cooperation between enzymes—Factors affecting enzymes, conversion and synergy. *Biotechnology Advances* 30: 1458 – 1480.

Van-Ginkel, S. and Logan, B. E. (2005). Inhibition of biohydrogen production by undissociated acetic and butyric acids. *Environ Sci Technol* 39:9351–9356.

Van-Ginkel, S. and Sung, S. (2001). Biohydrogen production as a function of pH and substrate concentration. *Environ Sci Technol* 35(24): 4726 – 4730.

Van Haandel, A. and Van Der Lubbe, J. (2007). *Handbook biological waste water treatment-design and optimisation of activated sludge systems*. Webshop Wastewater Handbook.

Van-Soest, P. J. (2006). Rice straw, the role of silica and treatments to improve quality Anim. Feed Sci. Technol. (130): 137-171.

Vanwonterghem, I., Evans, P. N., Parks, D. H., Jensen, P. D., Woodcroft, B. J., Hugenholtz, P. and Tyson, G. W. (2016). Methylophilic methanogenesis was discovered in the archaeal phylum Verstraetearchaeota. *Nature microbiology*, 1(12), 1-9.

Velmurugan, P., Shim, J., Lee, K. J., Cho, M., Lim, S. S., Seo, S. K., Cho, K. M., Bang, S. K., and Oh, B. T. (2015). Extraction, characterisation, and catalytic potential of amorphous silica from corn cobs by sol-gel method. *Journal of Industrial and Engineering Chemistry*, 29, 298-303.

Vera, L., Sun, W., Iftikhar, M. and Liu, J. (2015). LCA based comparative study of a microbial oil production starch wastewater treatment plant and its improvements with the combination of CHP system in Shandong, China. *Resour. Conserv. Recycl.* 96: 1 – 10.

Verein Deutscher Ingenieure (VDI) 4630 (2006). Fermentation of organic materials. Characterisation of the substrates, sampling, collection of material data, fermentation test.

Vijayaraghavan, K and Soom, M. A. M. (2006). Trends in biological hydrogen production—a review. *Environ Sci* 3(4):255–71

Von Sperling, M. and De Lemos Chernicharo, C. A. (2005). *Biological Wastewater Treatment in Warm Climate Regions*: IWA Publishing.

Walla, C. and Schneeberger, W. (2008). The optimal size for biogas plants. *Biomass and bioenergy*, 32(6), 551-557.

Wan, C. X. and Li, Y. B. (2012). Fungal pretreatment of lignocellulosic biomass. *Biotechnol. Adv.* 30: 1447 – 1457.

Wang, B., Wan, W. and Wang, J. (2008). Inhibitory effect of ethanol, acetic acid, propionic acid and butyric acid on fermentative hydrogen production. *International Journal of Hydrogen Energy* 33(23): 7013-7019.

Wang, C. C., Chang, C. W., Chu, C. P., Lee, D. J., Chang, B. V., and Liao, C. S. (2003). Producing hydrogen from wastewater sludge by *Clostridium bifermentans*. *J Biotechnol*, 102: 83 – 92.

Wang, H., Fang, M., Fang, Z. and Bu, H. (2010). Effects of sludge pre-treatments and organic acids on hydrogen production by anaerobic fermentation. *Bioresource technology* 101(22): 8731-8735.

Wang, J. and Wan, W. (2008a). Comparison of different pretreatment methods for enriching hydrogen-producing bacteria from digested sludge. *Int. J Hydrogen Energy* 33: 2934 – 2941.

Wang, J. and Wan, W. (2008b). Effect of temperature on fermentative hydrogen production by mixed cultures. *International Journal of hydrogen energy* 33(20): 5392-5397.

Wang, J. J., Yang, K., Xu, Z. L. and Fu, C. (2015). Energy and exergy analyses of an integrated CCHP system with biomass air gasification. *Applied energy*, 142, 317-327.

Wang, S., Zhang, T. and Su, H. (2016). Enhanced hydrogen production from corn starch wastewater as a nitrogen source by mixed cultures. *Renewable Energy*, 96: 1135 – 1141.

Wang, X. and Zhao, Y. C. (2009). A bench-scale study of fermentative hydrogen and methane production from food waste in an integrated two-stage process. *International Journal of Hydrogen Energy* 34(1): 245-254

Wang, X. J., Ren, N. Q., Xiang, W. S. and Guo, W. Q. (2007). Influence of gaseous end-products inhibition and nutrient limitations on the growth and hydrogen production by hydrogen-producing fermentative bacterial B49. *International journal of hydrogen energy* 32(6): 748-754.

Ward, A. J., Hobbs, P. J., Holliman, P. J. and Jones, D. L. (2008). Optimisation of the anaerobic digestion of agricultural resources. *Bioresource Technology*, 99(17): 7928-7940.

Wattanasiriwech, S., Wattanasiriwech, D. and Svasti, J. (2010). Production of amorphous silica nanoparticles from rice straw with microbial hydrolysis pretreatment. *Journal of Non-Crystalline solids* 356: 1228 – 1232.

Wei, S. (2016). The application of biotechnology on the enhancing of biogas production from lignocellulosic waste. *Applied Microbiology and Biotechnology*, 100(23), pp. 9821-9836.

Wei, S., Zhang, H., Cai, X., Xu, J., Fang, J. and Liu, H. (2014) Psychrophilic anaerobic co-digestion of highland barley straw with two animal manures at high altitude for enhancing biogas production. *Energ Convers Manag* 88: 40–48.

Weiland, P. (2010) Biogas production: current state and perspectives. *Applied Microbiology and Biotechnology*, 85(4), pp. 849-60.

Westerholm, M., Hansson, M. and Schnurer, A. (2012) Improved biogas production from whole stillage by co-digestion with cattle manure. *Bioresource Technology*, 114: 314-319.

Westerholm, M., Moestedt, J. and Schnürer, A. (2016) Biogas production through syntrophic acetate oxidation and deliberate operating strategies for improved digester performance. *Applied Energy*, 179 124-135.

White, D. (2000). *The Physiology and Biochemistry of Prokaryotes*. Oxford University Press, Oxford, UK.

Wilson, D. B. (2011). Microbial diversity of cellulose hydrolysis. *Cur. Opin. Microbiol.* 14: 259 – 263.

Winkler, M., Heil, B., Heil, B. and Happe, T. (2002). Isolation and molecular characterisation of the [Fe]-hydrogenase from the unicellular green alga *Chlorella fusca* *Biochim Biophys Acta (BBA): Gene Struct Express* 1576: 330 – 334.

Winter, C. J. (2005). Into the hydrogen energy economy-milestones. *Int J Hydrogen Energy*, 30: 681-685.

Wong, Y. M., Wu, T. Y. and Juan, J. C. (2014). A review of sustainable hydrogen production using seed sludge via dark fermentation. *Renewable and Sustainable Energy Reviews*, 34: 471-482.

World Energy Council. World Energy Resources, (2016). Available from: [https://www.worldenergy.org/wp-content/uploads/2017/03/WEResources\\_Bioenergy\\_2016.pdf](https://www.worldenergy.org/wp-content/uploads/2017/03/WEResources_Bioenergy_2016.pdf) [Accessed: Dec 16, 2018]

World Population Review. Total population by country, 2020. <https://worldpopulationreview.com/countries> (accessed 16<sup>th</sup> July, 2020).

Xie, G. J., Feng, L. B., Ren, N.Q., Ding, J., Liu, C., Xing, D.F., Qian, G. W. and Ren, H. Y. (2010). Effect of carbon sources on the aggregation of photo fermentative bacteria induced by L-cysteine for enhancing hydrogen production. *Int. J. Hydrogen Energy* 35(5): 1929 – 1935.

Yan, B. H., Selvam, A. and Wong, J. W. (2020). Bio-hydrogen and methane production from two-phase anaerobic digestion of food waste under the scheme of acidogenic off-gas reuse. *Bioresource technology*, 297, 122400.

Yang, J., Liu, X., Liu, X., Xu, Q., Wang, W., Wang, D., ... and Ni, B. J. (2020). Enhanced dark fermentative hydrogen production from waste activated sludge by combining potassium ferrate with alkaline pretreatment. *Science of The Total Environment*, 707, 136105.

Yasin, N. H. M., Man, H. C., Yusoff, M. Z. M. and Hassan, M. A. (2011). Microbial characterisation of hydrogen-producing bacteria in fermented food waste at different pH values. *Int. J. Hydrogen Energy* 36(16): 9571 – 9580.

Yousef, S., Šereika, J., Tonkonogovas, A., Hashem, T. and Mohamed, A. (2021). CO<sub>2</sub>/N<sub>2</sub>, CO<sub>2</sub>/H<sub>2</sub> and CO<sub>2</sub>/CH<sub>4</sub> selectivity performance of PES membranes under high pressure and temperature for biogas upgrading systems. *Environmental Technology & Innovation*, 21, 101339.

Yu, H., Zhu, Z., Hu, W. and Zhang, H. (2002). Hydrogen production from rice winery wastewater in an up-flow anaerobic reactor by using mixed anaerobic cultures. *International journal of hydrogen energy* 27(11-12): 1359-1365.

Yu, G., Yano, S., Inoue, H., Inoue, S., Endo, T. and Sawayama, S. (2010). Pretreatment of rice straw by a hot-compressed water process for enzymatic hydrolysis. *Appl Biochem Biotechnol* 160: 539 - 551.

Yu, Z. and Schanbacher, F. L. (2010). Production of methane biogas as fuel through anaerobic digestion. In: *Sustainable biotechnology*. pp. 105-127. Springer, Dordrecht.

Yuan, Z., Wu, C., Huang, H. and Lin, G. (2002). Research and development on biomass energy in China. *Int. J. Energy Technol. Policy* 1: 108 – 144.

Yusoff, S. (2006). Renewable energy from palm oil e innovation on effective utilisation of waste. *Journal of Cleaner Production* 14: 87 - 93

Zaky, R. R., Hessien, M. M., El-Midany, A. A., Khedr, M. H., Abdel-Aal, E. A. and El-Barawy, K. A. (2008). Preparation of silica nano-particles from semi-burned rice straw ash. *Powder Technol.* 185: 31.

Zhang, M. L., Fan, Y. T., Xing, Y., Pan, C. M., Zhang, G. S. and Lay, J. J. (2007). Enhanced biohydrogen production from cornstalk wastes with acidification pretreatment by mixed anaerobic cultures. *Biomass and Bioenergy* 31(4): 250 - 254.

Zhang, Q. and Cai, W. (2008). Enzymatic hydrolysis of alkali-pretreated rice straw by *Trichoderma reesei* ZM4-F3. *Biomass and Bioenergy*, 32(12), 1130-1135.

Zhang, T., Jiang, D., Zhang, H., Lee, D. J., Zhang, Z., Zhang, Q., ... and Xia, C. (2020). Effects of different pretreatment methods on the structural characteristics, enzymatic saccharification and photo-fermentative bio-hydrogen production performance of corn straw. *Bioresource technology*, 304, 122999.

Zhang, T., Liu, H. and Fang, H. H. P. (2003). Biohydrogen production from starch in wastewater under thermophilic conditions. *J Environ Manag*, 69: 149 – 156.

Zhang, Y., Hu, R., Tian, J. and Li, T. (2018). Disintegration of waste activated sludge with composite ferrate solution: Sludge reduction and settleability. *Bioresource technology*, 267, 126-132.

Zhao, R., Zhang, Z., Zhang, R., Li, M. , Lei, Z. F., Utsumi, M. and Sugiura, N. (2010). Methane production from rice straw pretreated by a mixture of acetic–propionic acid. *Bioresource Technology*, 101 (3): 990 – 994.

Zhi, Z. and Wang, H. (2014). White-rot fungal pre-treatment of wheat straw with *Phanerochaete chrysosporium* for biohydrogen production: simultaneous saccharification and fermentation. *Bioprocess and biosystems engineering*, 37(7), 1447-1458.

Zhou, P., Elbeshbishy, E. and Nakhla, G. (2013). Optimisation of biological hydrogen production for anaerobic co-digestion of food waste and wastewater biosolids. *Bioresource technology* 130, 710-718.

Zhu, H., and Beland, M. (2006). Evaluation of alternative methods of preparing hydrogen-producing seeds from digested wastewater sludge." *International Journal of Hydrogen Energy* 31 (14): 1980-1988.

Zhu, H., Parker, W., Basnarc, R., Prorackic, A., Falletta, P. Be'land, M. and Seto, P. (2008). Biohydrogen production by anaerobic co-digestion of municipal food waste and sewage sludges. *International Journal of Hydrogen Energy* 33: 3651 – 3659

Ziemiński, K. and Frąc, M. (2012). Methane fermentation process as anaerobic digestion of biomass: Transformations, stages and microorganisms. *African Journal of Biotechnology*, 11(18), 4127-4139.

Zubairu, G. U., Serkan, A., Neyre, T. E. and Murat, F. (2015). Transforming the Nigerian Power Sector for Sustainable Development. *Energy Policy*, 87: 429–437.